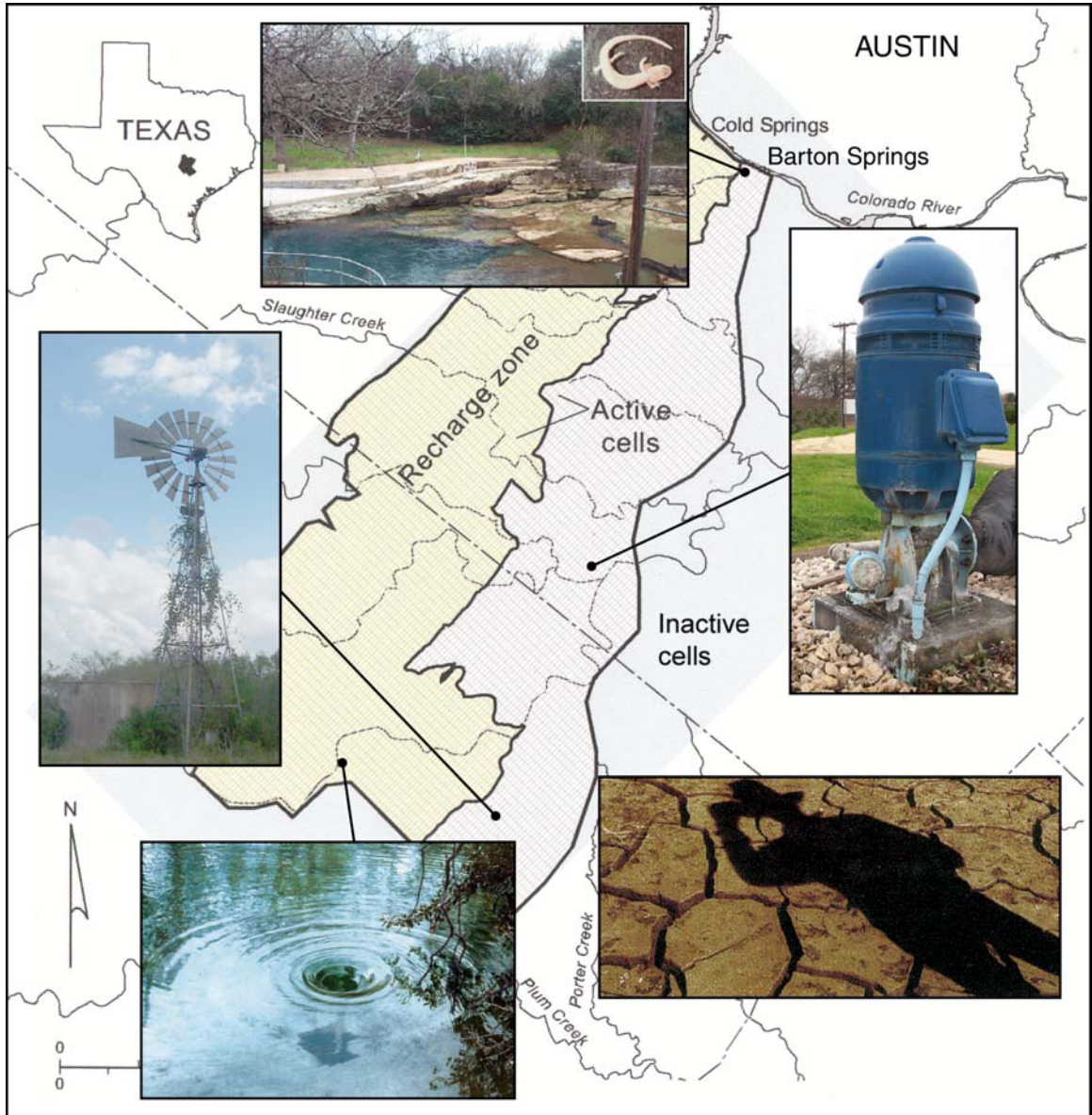


**EVALUATION OF SUSTAINABLE YIELD OF THE
BARTON SPRINGS SEGMENT OF THE EDWARDS AQUIFER,
HAYS AND TRAVIS COUNTIES, CENTRAL TEXAS**



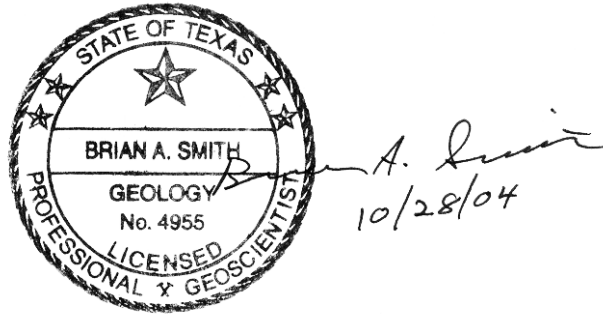
Barton Springs/Edwards Aquifer Conservation District

October 2004

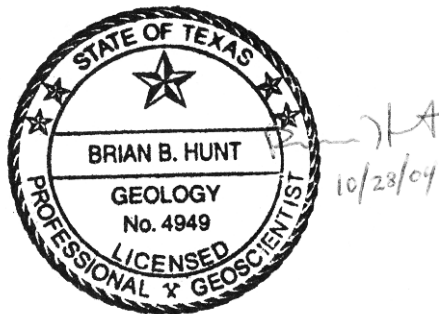
Cover Illustration

Background image of the numerical model area was modified from Scanlon et al. (2001). Photographs (clockwise from the top) include: Barton Springs Pool with low water level during cleaning and image of the endangered Barton Springs Salamander, photograph of spring by Brian A. Smith; turbine pump in the Creedmoor-Maha well field, photograph by Brian B. Hunt; mudcracks and farmer's shadow during a drought, photograph by Mike Rayner ('The Age'); whirlpool formed above Cripple Crawfish Cave in Onion Creek, photograph by David Johns; windmill that serves as the District's Mountain City observation well for drought declaration, photograph by Brian B. Hunt. Cover illustration arranged by Brian B. Hunt.

**EVALUATION OF SUSTAINABLE YIELD OF THE
BARTON SPRINGS SEGMENT OF THE EDWARDS AQUIFER,
HAYS AND TRAVIS COUNTIES, CENTRAL TEXAS**



Brian A. Smith, Ph.D., P.G.
Senior Hydrogeologist, Assessment Program Manager



Brian B. Hunt, P.G.
Hydrogeologist

Barton Springs/Edwards Aquifer Conservation District
October 2004

**EVALUATION OF SUSTAINABLE YIELD OF THE
BARTON SPRINGS SEGMENT OF THE EDWARDS AQUIFER,
HAYS AND TRAVIS COUNTIES, CENTRAL TEXAS**

Barton Springs/Edwards Aquifer Conservation District
1124 Regal Row
Austin, Texas 78748
(512) 282-8441

Dana Wilson, Interim General Manager

Board of Directors

Dr. Robert D. Larsen- President
Precinct 3

Jack Goodman- Vice President
Precinct 4

Craig Smith- Secretary
Precinct 5

Dr. David R. Carpenter
Precinct 2

Chuck Murphy
Precinct 1

Edited by Board Subcommittee on Sustainable Yield

Dr. Robert D. Larsen
Dr. David R. Carpenter

Technical Editing

Lana Dieterich, Bureau of Economic Geology, The University of Texas at Austin

October 2004

STATE OF TEXAS

§

RESOLUTION # 102804-01

COUNTY OF TRAVIS

§

§

A RESOLUTION OF THE BOARD OF DIRECTORS, BARTON SPRINGS EDWARDS AQUIFER CONSERVATION DISTRICT, ACCEPTING AND ENDORSING THE REPORT ENTITLED *EVALUATION OF SUSTAINABLE YIELD OF THE BARTON SPRINGS SEGMENT OF THE EDWARDS AQUIFER, HAYS AND TRAVIS COUNTIES, CENTRAL TEXAS, BEING A SCIENTIFIC STUDY PREPARED BY DISTRICT STAFF*

WHEREAS, the Barton Springs Edwards Aquifer Conservation District (the District) is a Groundwater Conservation District created by an act of the 70th Legislature and subject to various requirements of State Law governing groundwater districts, including Texas Water Code Chapter 36; and

WHEREAS, the District was established for the purpose of providing for the conservation, preservation, protection, recharging and prevention of waste of groundwater and of groundwater reservoirs in the Barton Springs segment of the Edwards Aquifer (Aquifer), and to control subsidence caused by withdrawal of groundwater from those groundwater reservoirs or their subdivisions; and

WHEREAS, the Aquifer is either a sole source or primary source of drinking water for approximately 44,000 people living and working in the central part of this state, and is a vital resource to the general economy and welfare of the State of Texas; and

WHEREAS, the District’s Management Plan defines sustainable yield as the amount of water that can be pumped for beneficial use from the Aquifer under a reoccurrence of the drought of record conditions, after considering adequate water levels in water wells and degradation of water quality that could result from low water levels and low spring discharge; and

WHEREAS, the Board of Directors in 2003 instructed staff to develop and conduct a scientific investigation relative to determining the sustainable yield of the Aquifer and revising the Texas Water Development Board’s currently approved Groundwater Availability Model for the Aquifer; and

WHEREAS, staff has developed and completed a report responsive to all charges assigned by the Board of Directors; and

WHEREAS, the report was subjected to an independent peer-review process by members of the Groundwater Model Advisory Team, who included, Renee Barker, Senior Hydrogeologist, United States Geological Survey; Nico Hauwert, Hydrogeologist, City of Austin and Doctoral Candidate, University of Texas at Austin; David Johns, Senior Hydrogeologist, City of Austin; Dr. Robert Mace, Director Groundwater

Resources Division, Texas Water Development Board; Dr. Bridget Scanlon, Senior Research Scientist, Bureau of Economic Geology, University of Texas at Austin; Dr. Jack Sharp, Chevron Centennial Professor in Geology, University of Texas at Austin; Raymond Slade, United States Geological Survey (retired) and Consulting Hydrologist; Eric Strom, Assistant District Chief, United States Geological Survey;

NOW, THEREFORE BE IT RESOLVED by the Board of Directors of the Barton Springs Edwards Aquifer Conservation District, that:

SECTION I

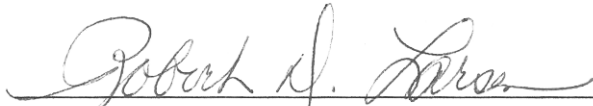
The Board of Directors accepts and endorses the report prepared by staff entitled, *Evaluation of Sustainable Yield of the Barton Springs Segment of the Edwards Aquifer, Hays and Travis Counties, Central Texas.*

SECTION II

Furthermore, the Board of Directors declares that the information presented in the report is the best science and information currently available for evaluating the sustainable yield of the Barton Springs segment of the Edwards Aquifer.

The motion passed with 5 ayes, and 0 nays.

PASSED AND APPROVED THIS THE 28th DAY OF OCTOBER, 2004.



Dr. Robert D. Larsen, Board President



Jack Goodman, Board Vice-President



David Carpenter, Board Member



Chuck Murphy, Board Member

ATTEST:



Craig Smith, Board Secretary

CONTENTS

	PREFACE.....	xi
	EXECUTIVE SUMMARY.....	xiii
1.0	INTRODUCTION.....	1
1.1	Purpose and Approach.....	2
1.2	Concepts and Definitions of Sustainable Yield.....	3
2.0	SETTING.....	4
2.1	Study Area.....	4
2.2	Previous Aquifer Studies.....	4
2.3	Geology.....	6
2.4	Hydrogeology.....	7
2.4.1	Aquifer Boundaries.....	7
2.4.2	Recharge.....	8
2.4.2.1	Surface Recharge.....	8
2.4.2.2	Subsurface Recharge.....	8
2.4.3	Discharge.....	9
2.4.3.1	Spring Flow.....	9
2.4.3.2	Pumpage.....	10
2.4.4	Groundwater Storage and Flow.....	11
2.4.5	1950's Drought.....	12
2.4.6	Trinity Aquifer.....	12
3.0	NUMERICAL GROUNDWATER MODELING.....	13
3.1	Purpose and Approach of Modeling.....	13
3.2	Previous Work: 2001 GAM.....	14
3.2.1	2001 GAM Simulations.....	16
3.3	Transient-Model Recalibration.....	16
3.3.1	Water Levels.....	17
3.3.2	Spring flow.....	18
3.3.3	Sensitivity Analyses.....	19
3.4	Predictions.....	19

3.4.1	Pumping.....	19
3.4.2	Impacts to Spring Flow and Water Levels.....	20
3.5	Qualifications and Data Needs.....	21
3.6	Major Findings.....	24
4.0	IMPACTS TO WATER LEVELS AND WATER-SUPPLY WELLS FROM 1950’S DROUGHT CONDITIONS AND PUMPING.....	25
4.1	Methods.....	25
4.1.1	Data Sets.....	26
4.1.1.1	Structure-Contour Maps.....	26
4.1.1.2	Potentiometric Maps.....	27
4.1.1.3	Simulated Drawdown.....	28
4.1.1.4	Well Data.....	28
4.1.2	Saturated Aquifer Thickness Analysis.....	29
4.1.3	Saturated Borehole Thickness Analysis.....	30
4.2	Results.....	31
4.3	Discussion.....	32
4.4	Major Findings.....	35
5.0	CONCLUSIONS.....	36
5.1	Acknowledgments.....	36
6.0	REFERENCES.....	38
7.0	GLOSSARY OF HYDROGEOLOGIC TERMS.....	44

TABLES

- 3-1. Comparison of measured and simulated water-level values and residuals from the 2001 GAM and recalibrated model
- 3-2. Comparison of hydraulic conductivity for the 2001 GAM and recalibrated GAM
- 4-1. Composite potentiometric data
- 4-2. Simulated drawdown in wells under 1950’s drought conditions and various pumping scenarios

- 4-3. Saturated aquifer thickness analysis under 1950's drought conditions and various rates of pumping
- 4-4. Saturated borehole analysis under 1950's drought conditions and various rates of pumping
- 4-5. Total impact to wells under 1950's drought conditions and various rates of pumping

FIGURES

- 2-1. Location map of study area
- 2-2. Cross section of Barton Springs and Trinity Aquifers in Hays County
- 2-3. Histogram of permitted and actual pumping
- 3-1. Hydrograph of simulated and measured spring flow from 1950's drought
- 3-2. Map of zonal distribution of hydraulic conductivity in the recalibrated GAM
- 3-3. Scatter plot of simulated results from 2001 GAM and recalibrated GAM plotted against measured low-flow 1950's water levels
- 3-4. Comparison of simulated and measured water-level elevation hydrographs of the study area
- 3-5. Scatter plot of spring-flow simulations from the 2001 GAM and recalibrated GAM and mean of measured spring-flow values for all flow conditions and low-flow conditions
- 3-6. Sensitivity of transient simulated spring discharge to recharge, specific yield, and specific storage
- 3-7. Sensitivity of transient calibration water levels to specific storage
- 3-8. Sensitivity of transient calibration water levels to specific yield
- 3-9. Sensitivity of transient calibration water levels to recharge
- 3-10. Hydrograph of simulated spring flow under 1950's drought conditions and 0.66, 10, and 15 cfs pumping rates
- 3-11. Simulated potentiometric surface contour map under average conditions and 19 cfs of pumping and drought conditions with 19 cfs pumping
- 4-1. Structure contour of the elevation of the bottom of the Edwards Aquifer
- 4-2. Isopach map of the Edwards Aquifer
- 4-3. Potentiometric map of the Edwards Aquifer under 1950's drought conditions

- 4-4. Simulated drawdown from pumping 10 cfs at the end of the 10-yr simulation
- 4-5. Potentiometric map of 1950's drought conditions and 10 cfs pumping
- 4-6. Histogram of specific-capacity values from the unconfined portion of the Edwards Aquifer and distribution and classed values of specific-capacity data
- 4-7. Saturated-thickness contour map of the Edwards Aquifer under 1950's drought conditions with minimal pumping
- 4-8. Composite of 100-ft saturated aquifer thickness contour lines under 1950's drought conditions with 0.66, 5, 10, 15, and 19 cfs of pumping
- 4-9. Chart summarizing number of wells impacted under 1950's drought conditions and various pumping rates

APPENDICES

- A.** Groundwater Availability of the Barton Springs Segment of the Edwards Aquifer, Texas: Numerical Simulations through 2050
- B.** Sensitivity Analysis of Southern Groundwater Divide
- C.** List of participants and affiliations at sustainable yield meetings at the BSEACD: September 10, 2003 and March 24, 2004

PREFACE

A statutory mandate charges the Barton Springs/Edwards Aquifer Conservation District (District) with the responsibility of conserving, protecting, and enhancing groundwater resources of the Barton Springs segment of the Edwards Aquifer. Part of this responsibility is to determine the amount of groundwater available for use in the aquifer. The District considers the amount of groundwater available for use as the “sustainable yield” that is defined in Section 1.2 (Concepts and Definitions of Sustainable Yield). So that this amount may be readily determined, Texas Water Code (§ 36.1071(h)) requires the District to use results of a groundwater availability model (GAM) in conjunction with other studies or information of the aquifer. Additionally, to ensure that future water needs are met during times of severe drought, the regional water planning process (§ 16.053(a)) requires water planning to be based on drought-of-record conditions.

To fulfill these mandates, at the May 22, 2003, board meeting, the District’s Board of Directors charged the Assessment Program staff with conducting an evaluation of sustainable yield of the Barton Springs segment of the Edwards Aquifer. Assessment Program staff made 11 presentations to the District’s board and 2 board workshops were held during the evaluation process. Results of the evaluation were presented to the board on February 5, 2004. The purpose of this report is to present the results of that evaluation and to provide a scientific foundation for establishing sustainable-yield policies by the District for resource management.

This report is based on research conducted by many scientists and represents decades of work. Numerical modeling presented herein expands on that knowledge, specifically building on the research and modeling of Slade et al. (1985), Wanakule (1989), Barrett and Charbeneau (1996), and Scanlon et al. (2001). To assist in the evaluation of sustainable yield, the District’s Assessment Program staff assembled a Groundwater Model Advisory Team (GMAT) consisting of expert scientists from the Austin area. GMAT met monthly between September 2003 and February 2004 and provided critical input and comments throughout the modeling and sustainable-yield evaluation process. GMAT is made up of:

Rene Barker, Senior Hydrogeologist, U.S. Geological Survey

Nico Hauwert, Hydrogeologist, City of Austin; Ph.D. candidate, The University of Texas at Austin

David Johns, Senior Hydrogeologist, City of Austin

Dr. Robert Mace, Director, Groundwater Resources Division, Texas Water Development Board

Dr. Bridget Scanlon, Senior Research Scientist, Bureau of Economic Geology, The University of Texas at Austin

Dr. Jack Sharp, Chevron Centennial Professor in Geology, The University of Texas at Austin

Raymond Slade, U.S. Geological Survey, retired, and Consulting Hydrologist

Eric Strom, Assistant District Chief, U.S. Geological Survey

Technical meetings were held on September 10, 2003, and March 24, 2004, for the District to receive input from a broad group of technical specialists (Appendix C). From March through April 2004 results of these studies were presented to various stakeholder groups, including the Lower Colorado River Authority (LCRA), U.S. Fish and Wildlife Service (USFWS), District permittees, news media, environmental groups, and representatives from the City of Kyle.

It is the authors' professional opinion, and the consensus of GMAT members, that the information presented herein is the best science and information currently available for evaluating sustainable yield of the Barton Springs segment of the Edwards Aquifer.

EVALUATION OF SUSTAINABLE YIELD OF THE BARTON SPRINGS SEGMENT OF THE EDWARDS AQUIFER, HAYS AND TRAVIS COUNTIES, CENTRAL TEXAS

Brian A. Smith, Ph.D., P.G. and Brian B. Hunt, P.G.

EXECUTIVE SUMMARY

The combined effects of drought and substantial pumping can result in a decline in water levels and spring flow in an aquifer. This report evaluates potential impacts on groundwater availability in the Barton Springs segment of the Edwards Aquifer (Barton Springs aquifer) during a recurrence of drought-of-record (1950's) conditions and various rates of pumping. A numerical groundwater model and hydrogeologic data were the primary tools used in this evaluation.

The Barton Springs aquifer is an important groundwater resource for municipal, industrial, domestic, recreational, and ecological needs. Approximately 50,000 people depend on water from the Barton Springs aquifer as their sole source of drinking water. Additionally, various spring outlets at Barton Springs are the only known habitats of the endangered Barton Springs salamander. The amount of groundwater available to meet current and future needs is limited, however.

A statutory mandate charges the Barton Springs/Edwards Aquifer Conservation District (District) with the responsibility of conserving, protecting, and enhancing groundwater resources of the Barton Springs aquifer. Part of this responsibility is to determine the amount of groundwater available for use in the aquifer, referred to as "sustainable yield" by the District. State law requires water planning for drought conditions and use of groundwater modeling information in conjunction with other studies or data about the aquifer. The purpose of this report is to provide scientific foundation and documentation for policy makers' use so that future water needs are met during times of severe drought.

The Barton Springs aquifer is located within parts of Travis and Hays Counties in Central Texas. It lies along the Balcones Fault Zone and is generally bounded to the north by the Colorado River, to the south by the southern groundwater divide near the City of

Kyle, to the east by the interface between the fresh- and saline-water zones, and to the west by the Balcones Fault.

A numerical model was developed for the Barton Springs aquifer (Scanlon et al., 2001; Appendix A). However, the model was constructed to match water levels and spring flow from a period wetter than that of the 1950's drought. Because the model was calibrated to a relatively wet period, it overestimates spring flow and underpredicts water-level elevations compared with measurements taken during the 1950's drought of record. The model was recalibrated so that simulated and measured spring-flow and water-level data from the 1950's drought matched better. The recalibrated model was then used to predict spring-flow and water-level declines under 1950's drought conditions and various future pumping scenarios. Hydrogeological data, such as saturated-thickness maps, potentiometric-surface maps, and well-construction and yield data, were evaluated alongside the model results so that impacts to water-supply wells under 1950's drought conditions and various rates of pumping could be estimated.

Results of the evaluations indicate that water levels and spring flow are significantly impacted by 1950's drought conditions and projected pumping. The model indicates that 10 cubic feet per second (cfs) of pumping, combined with 1950's drought conditions, produces a mean monthly spring flow of about 1 cfs. According to a minimum daily discharge of 9.6 cfs, such as that measured in 1956, spring flow could temporarily cease for periods less than 1 month. At 15 cfs of pumping, spring flow would cease for at least 4 months. Simulations indicate that a given pumping rate applied under 1950's drought conditions would diminish Barton Springs spring flow by an amount equivalent to the pumping rate. As many as 19% of all water-supply wells in the District may be negatively impacted under 1950's drought conditions and a pumping rate of 10 cfs. Negative impacts might include wells going dry, water levels dropping below pumps, or intermittent yield due to low water levels. Finally, under 1950's drought conditions and high rates of pumping, potential for saline water to flow from the saline-water zone into the freshwater aquifer would increase, impacting water-supply wells and endangered species.

Information presented herein is based on the best science and information currently available for evaluating sustainable yield of the Barton Springs segment of the

Edwards Aquifer. Results of this sustainable-yield evaluation will be considered in District sustainable-yield policies for resource management.

1.0 INTRODUCTION

The Barton Springs segment of the Edwards Aquifer (Barton Springs aquifer) is a part of a prolific karst aquifer on which approximately 50,000 people depend as their sole source of drinking water. As part of the Barton Springs/Edwards Aquifer Conservation District's (District's) role of managing groundwater extraction from the Barton Springs aquifer, the District has conducted groundwater modeling of the aquifer to help determine the amount of groundwater available for pumping from the aquifer. The principal tool for this evaluation has been a groundwater availability model developed for the Lower Colorado Regional Water Planning Group (LCRWPG) and the Texas Water Development Board (TWDB). Modifications were made to the model to evaluate the amount of spring flow at Barton Springs and potential impacts to water-supply wells during a recurrence of 1950's drought-of-record conditions using various rates of projected pumping. Aquifer conditions from the 1950's were used in this evaluation because the regional water-planning process ((Texas Water Code, § 16.053(a)) requires that water planning be based on drought-of-record conditions.

The model indicates that under 1950's drought conditions and current (2004) pumping rates of about 10 cubic feet per second (cfs), flow from Barton Springs would decrease to less than 1 cfs or cease altogether. Low flows or a lack of flow from the springs is likely to have a negative impact on Barton Springs as a recreational resource and on the endangered salamanders that live in the springs. An analysis of hydrogeologic data and model-simulated water-level drawdown due to pumping shows that, under 1950's drought conditions and current (2004), permitted pumping rates, as many as 19% of the water-supply wells in the District would be dry or experience a reduction in yield. Results of these model simulations will be used by the District to establish policies with the objective of minimizing impacts of high rates of pumping during a recurrence of 1950's drought conditions.

1.1 Purpose and Approach

The purpose of this study was to evaluate impacts of pumping and 1950's drought conditions on spring flow and water levels in wells in the Barton Springs aquifer. The evaluation was based on modification of a Groundwater Availability Model (GAM) developed for the Barton Springs aquifer by Scanlon et al. (2001) (hereafter referred to as the 2001 GAM). That model evaluated long-term groundwater availability in response to future pumping and potential future droughts. A GAM first developed in 2000 established the model framework (Scanlon et al., 2000). Modifications were made to the 2000 GAM to meet standards set by TWDB for the Barton Springs GAM. The 2001 GAM, the foundation for numerical modeling in this study, was recalibrated to better simulate 1950's drought conditions.

The approach to evaluating sustainable yield of the Barton Springs aquifer consisted of:

I. Numerical Modeling (Section 2)

- The 2001 GAM was recalibrated (hereafter referred to as the *recalibrated GAM*) by changing hydraulic conductivity and storage values to better match spring-flow and water-level data from the 1950's drought;
- The recalibrated GAM was then used to predict spring-flow and water-level declines under 1950's drought conditions and various rates of projected future pumping.

II. Water-Supply-Well Impacts (Section 3)

- A potentiometric map of water levels measured during the 1950's drought was superimposed on simulated drawdown maps for various rates of pumping to create a series of saturated-thickness maps.
- Well yield and construction data were evaluated using the potentiometric and saturated thickness maps to estimate the number of wells that might be negatively impacted under various simulated pumping rates. Negative impacts might include wells going dry, water levels dropping below the pumps, or intermittent yield due to low water levels.

1.2 Concepts and Definitions of Sustainable Yield

One commonly used definition of safe yield of an aquifer is “the amount of water which can be withdrawn from it [the aquifer] annually without producing an undesired result” (Todd, 1959). The potential for “undesired results” from excessive pumping of an aquifer is an important concept that the District considers in its role of protecting and enhancing groundwater resources of the Barton Springs aquifer. The term *sustainable yield* is used more commonly today to acknowledge limits to aquifer pumping that need to be considered in the management of an aquifer in order to minimize or eliminate undesired results (Sophocleous, 1997). The District’s task is to determine quantitatively the undesired results and what policies can be developed to minimize them.

The District defines sustainable yield as: *the amount of water that can be pumped for beneficial use from the aquifer under drought-of-record conditions after considering adequate water levels in water-supply wells and degradation of water quality that could result from low water levels and low spring discharge* (Barton Springs/Edwards Aquifer Conservation District, 2003). During periods of severe drought the District is concerned about sufficient yield from water-supply wells, quality of groundwater, and quantity and quality of groundwater discharging from Barton Springs. Low-water-level conditions brought about by 1950’s drought conditions combined with high rates of future pumping could cause Barton Springs and some water-supply wells to undergo water-quality degradation because of migration of saline water from the saline-water zone into the freshwater part of the aquifer.

2.0 SETTING

The Barton Springs aquifer is an important groundwater resource for municipal, industrial, domestic, recreational, and ecological needs. Approximately 50,000 people depend on water from the Barton Springs aquifer as their sole source of drinking water, and the various spring outlets at Barton Springs are the only known habitats for the endangered Barton Springs salamander. The following sections provide the geologic and hydrogeologic framework needed for evaluating sustainable yield.

2.1 Study Area

The Barton Springs aquifer constitutes the study area. Located within parts of Travis and Hays Counties in Central Texas, the aquifer lies within the Balcones Fault Zone and is generally bounded to the north by the Colorado River, to the south by the southern groundwater divide near the City of Kyle, to the east by the interface between the fresh- and saline-water zones, and to the west by the Balcones Fault (Figure 2-1).

2.2 Previous Aquifer Studies

Previous investigations in the Barton Springs aquifer have concentrated primarily on characterizing the geology and hydrogeology of the Edwards Aquifer system. Brune and Duffin (1983) discussed the availability of groundwater during a drought in terms of spring flow and recognized that withdrawals (pumping) equal to, or greater than, the lowest recorded spring-flow measurement of 9.6 cfs (March 29, 1956) would dry up all spring flow at Barton Springs. Similarly, Guyton and Associates (1979) reported a one-to-one relationship of pumping to spring flow at Comal and San Marcos Springs in the San Antonio segment of the Edwards Aquifer (San Antonio aquifer). Senger and Kreitler (1984) discussed the hydrogeology and hydrochemistry of the aquifer.

Slade et al. (1986) presented a series of potentiometric maps, including two that represented drought conditions from 1956 and 1978. Slade et al. (1985) used a numerical groundwater-flow model calibrated to average aquifer conditions in order to simulate the effects of pumping on groundwater availability. Transient-model simulations were calibrated to a limited period (164 days) under average flow conditions and did not focus on 1950's drought conditions or the effects on spring flow. Results of their future

simulations, with increased projected demand (pumping of 12.3 cfs), indicate that water levels would decline more than 100 ft in the vicinity of Kyle and that significant portions of the western aquifer would be completely dewatered.

A groundwater-flow model was developed by Wanakule (1989) to be used as an aquifer-management tool for the Barton Springs aquifer. This study identified dewatering of parts of the aquifer and decreasing spring flow as major issues to be considered in any aquifer-management scenarios.

Barrett and Charbeneau (1996) developed a lumped-parameter model of the Barton Springs aquifer that divided the aquifer into five cells, each representing a surface drainage basin associated with creeks flowing across the recharge zone. The lumped-parameter model was calibrated to 1989 through 1994 conditions. Although this model was more simplistic than the finite-difference model prepared by Slade et al. (1985), it did not simulate water levels, but showed a good match between simulated and measured spring flow for the period of simulation of 1989 through 1998. However, the lumped-parameter model appears to overpredict spring flow slightly during the 1996 drought period, when compared with measured values.

Sharp and Banner (1997) discussed hydrogeology and critical issues with regard to the Edwards Aquifer as a resource, such as endangered species and legal, political, and economic management problems. Sharp and Banner pointed out that demand on groundwater in 1996 exceeded historical availability during the droughts between 1947 and 1956 and that continued demand at or above this level would cause considerable hardship on the region when severe drought conditions recur.

The 2000 and 2001 GAMs were developed to evaluate groundwater availability and predict water levels and spring flow in response to increased pumpage and 1950's drought conditions (Scanlon et al., 2000, 2001). The 2001 GAM reduced a bias in the 2000 GAM that overpredicted spring flow during 1950's drought conditions by about 10 cfs. Good agreement was found between measured and simulated flow at Barton Springs and between measured and simulated water levels (Scanlon et al., 2001). Results of the simulations indicated that under average recharge conditions, with future pumpage conditions of 19 cfs., water-level drawdown is small (less than 35 ft). Water-level declines are large (up to 270 ft) under future pumpage (19 cfs) and drought conditions.

The 2001 GAM predicts that spring flow would cease at a pumping rate of 15 cfs under drought-of-record conditions. However, both the 2000 and 2001 GAMs were calibrated to data from the 1990's, a period wetter than that of the 1950's drought. Because the model was calibrated to a wetter period, the 2001 GAM overestimated spring flow and generally underpredicted head elevations compared with those of measured 1950's drought conditions (Smith and Hunt, 2004). Results of the 2000 GAM, corrected for an apparent 10 cfs bias during 1950's drought conditions, predicts that spring flow will decline to rates of 4 cfs at a pumping rate of 6.3 cfs under drought-of-record conditions. The 2001 GAM model, uncorrected for an estimated bias of 2 cfs (Section 3.1—Purpose and Approach of Modeling), showed drying of Barton Springs at 15 cfs of pumpage combined with 1950's drought conditions. Both models indicate that during drought conditions, spring flow declined in direct proportion to increases in pumpage. Therefore, when corrected for estimated bias, both models indicate that under 1950's drought conditions, Barton Springs begins to experience drying at pumping rates of about 10 to 11 cfs.

Scanlon et al. (2003) demonstrated that equivalent porous media models are capable of simulating regional groundwater flow and spring discharge in a karst aquifer.

2.3 Geology

The Edwards Aquifer is composed of the Cretaceous-age Edwards Group (Kainer and Person Formations) and the Georgetown Formation (Figure 2-2; Figures 6 and 7 in Appendix A). Sediments making up the Edwards Group accumulated on the Comanche Shelf as shallow marine, intertidal, and supratidal deposits. The Georgetown Formation, disconformably overlying the Edwards Group, was deposited in a more openly circulated, shallow-marine environment (Rose, 1972).

The prolific Edwards Aquifer evolved over millions of years as the result of numerous geologic processes such as deposition, tectonism, erosion, and diagenesis. The formation of the aquifer was influenced significantly by fracturing and faulting associated with the Balcones Fault Zone (BFZ) and dissolution of limestone and dolomite units by infiltrating meteoric water (Sharp, 1990; Barker et al., 1994; Sharp and Banner, 1997).

Mapping of the Barton Springs aquifer has delineated geologic faults and several informal stratigraphic members of the Kainer and Person Formations of the Edwards Group (Rose, 1972), each having distinctive hydrogeologic characteristics (Small et al., 1996; Barton Springs/Edwards Aquifer Conservation District, 2002). The limestone units generally step down to the east, primarily because of faulting. Most faults trend to the northeast and are downthrown to the southeast, with total offset of about 1,100 ft across the study area. As a result of faulting and erosion, the aquifer ranges from about 450 ft at its thickest along the east side, to 0 ft along the west side of the recharge zone (Slade et al., 1986).

2.4 Hydrogeology

2.4.1 Aquifer Boundaries

The areal extent of the Barton Springs aquifer is about 155 mi². Approximately 80% of the aquifer is unconfined; the remainder is confined (Slade et al., 1985). The aquifer is bounded on the north by the Colorado River, the regional base level and location of spring discharge (Slade et al., 1986) (Figure 2-1). The east boundary is the interface between the fresh-water zone and the saline-water or “bad-water” zone of the aquifer, characterized by a sharp increase in dissolved constituents (more than 1,000 mg/L total dissolved solids) and a decrease in permeability (Flores, 1990). The west boundary of the aquifer is defined by the western limit of Edwards Aquifer hydrogeologic units and the BFZ (Slagle et al., 1986; Small et al., 1996) and is limited locally by saturated thickness of the aquifer.

The southern hydrologic divide between the Barton Springs aquifer and the San Antonio segment of the Edwards Aquifer (San Antonio aquifer) is estimated to occur between Onion Creek and the Blanco River, according to potentiometric-surface elevations and recent dye-tracing information (LBG-Guyton Associates, 1994; Hauwert et. al, 2004).

2.4.2 Recharge

2.4.2.1 Surface Recharge

Estimates of recharge based primarily on 3 years of continuous flow data from five of the six major creeks show that as much as 85% of the water that recharges the Barton Springs aquifer occurs within six major creek channels (Slade et al., 1986). The remaining recharge is attributed to upland areas, which include tributary streams. Recent investigations have demonstrated that most recharge infiltrates via discrete features, such as caves, sinkholes, fractures, and solution cavities within stream channels (Barton Springs/Edwards Aquifer Conservation District and City of Austin, 2001). Additional flow and recharge data are currently being collected by the USGS, City of Austin, the District, and The University of Texas at Austin to verify and further refine quantification of sources of recharge to the Barton Springs aquifer. The recharge zone is about 90 mi². East of the recharge zone, the aquifer is overlain by less permeable clay and limestone units, which hydraulically confine the aquifer farther east in the confined, or artesian, zone (Figure 2-1).

2.4.2.2 Subsurface Recharge

The amount of subsurface recharge occurring through adjacent aquifers is unknown, although it is thought to be relatively small on the basis of water-budget analysis for surface recharge and surface discharge (Slade et al., 1985). Leakage from the saline-water zone is probably minimal, although the leakage does influence water quality at Barton Springs during low-spring-flow conditions (Senger and Kreitler, 1984; Slade et al., 1986). On the basis of a geochemical evaluation, Hauwert et al. (2004) found that the contribution to spring flow from the saline-water zone to Barton Springs under low-flow conditions could be about 3.5% of the discharge.

Subsurface flow into the Barton Springs aquifer from adjacent aquifers such as the San Antonio aquifer and the Trinity Aquifer is limited when compared with surface recharge (Slade et al., 1985). Hauwert et al. (2004) indicated that flow across the south boundary is probably insignificant under the conditions tested. However, the potential exists for such leakage during severe drought conditions, which was not tested in that study. As part of the sustainable-yield evaluation, an analysis of the southern

groundwater divide was conducted to evaluate the potential for flow across that boundary (Appendix B).

Flow (or leakage) from the Trinity Aquifer into the Barton Springs aquifer is thought to be relatively insignificant. In fact, estimates based on water quality at Barton Springs suggest that less than 1% of flow to the springs is from the Trinity Aquifer (Hauwert et al., 2004). Although leakage from the Trinity Aquifer is thought to be insignificant compared with total recharge rates, leakage may nevertheless locally impact water quality and influence water levels (Slade et al., 1986). A groundwater model of the Trinity Aquifer includes lateral groundwater leakage into the Edwards Aquifer in the San Antonio area in order for the model to simulate observed hydrogeologic conditions (Mace et al., 2000). However, where the Trinity Aquifer is in contact with the Barton Springs aquifer, the Trinity model indicates little or no lateral flow into the Barton Springs aquifer. Upward “leakage” from the Trinity Aquifer into the Edwards Aquifer is also thought to be limited and to occur locally along high-permeability fault zones (Slade et al., 1986). The District investigated the local vertical flow potential between the Edwards and (upper-middle) Trinity Aquifers using a nested well pair in the west part of the recharge zone. Results of that local investigation support the idea of limited vertical leakage from the Trinity to the Edwards Aquifer, demonstrating that actual potential for vertical flow is from the Edwards to the Trinity in the vicinity of the nested wells.

2.4.3 Discharge

Discharge from the aquifer is primarily from spring flow and pumpage from wells in the study area. Amount of subsurface discharge occurring through adjacent aquifers is unknown, although it is thought to be relatively small on the basis of a water-budget analysis for surface recharge and surface discharge (Slade et al., 1985).

2.4.3.1 Spring Flow

The largest natural discharge point of the Barton Springs aquifer is Barton Springs, located in Barton Creek about ¼ mi upstream of its confluence with the Colorado River (Figure 2-1). Barton Springs consists of four major outlets, the largest discharging directly into Barton Springs pool, a major recreational attraction of the City of Austin.

Long-term mean discharge from Barton Springs is 53 cfs (Figure 26 in Appendix A). The lowest instantaneous spring-flow measurement of 9.6 cfs was made on March 29, 1956 (Baker et al., 1986; Brune, 2002). The lowest monthly mean spring flow of 11 cfs was reported at the end of the 7-yr drought-of-record (1950's drought) during July and August of 1956 (Slade et al., 1986). Comal Springs in the San Antonio aquifer ceased flowing for about 4 months in 1956 during that drought.

Additional springs with small discharge are present along Town Lake. The largest of these is Cold Springs, which is located on the south bank of the Colorado River about 1.5 mi upstream of the mouth of Barton Creek. Measurements of spring flow from Cold Springs are limited and imprecise but range from 2.6 to 6.8 cfs (Brune, 2002; Hauwert et al., in press).

The aqueous chemistry of groundwater discharging from the springs varies with aquifer conditions, the most substantial decrease in water quality occurring under low-flow conditions. Increases in chloride, sodium, sulfate, and strontium concentrations are reported for low-flow conditions that result from an influx from the saline-water zone and the underlying Trinity Aquifer (Senger and Kreitler, 1984). Additionally, under low-flow conditions, nutrients (primarily nitrates) increase in concentration (City of Austin, 1997).

2.4.3.2 Pumpage

Water-supply wells in the Barton Springs aquifer include about 970 active wells that pump water for public, domestic, industrial, commercial, irrigation, and agricultural uses. About 10% of these wells have annual pumping permits issued by the District, which have so far totaled about 2.3 billion gallons (7,060 acre-ft per year, 9.75 cfs) of water in 2004. Most permitted pumpage is for public-supply and industrial purposes. Nonpermitted pumpage, such as agricultural and domestic supply, is estimated to be less than 10% of the permitted pumpage volume, or about 200 million gallons per year. The most significant volumes of permitted pumping occur in the southeast part of the aquifer (Figure 28 in Appendix A). Combined, these pumping volumes are about 2.5 billion gallons per year (7,818 acre-ft per year) and equate to a mean pumping rate of about 10.8 cfs for 2004 (Figure 2-3).

Scanlon et al. (2001) estimated that pumping would increase linearly from 9.3 cfs in 2000 to 19.6 cfs by the year 2050. Future pumping projections are described in Appendix A (Scanlon et al., 2001). These rates are rough estimates that are based on projections from LCRWPG and the Capital Area Metropolitan Planning Organization (CAMPO).

2.4.4 Groundwater Storage and Flow

The Edwards Aquifer is geologically and hydraulically heterogeneous and anisotropic, both of which strongly influence groundwater flow and storage (Slade et al., 1985; Maclay and Small, 1986; Hovorka et al., 1996; Hovorka et al., 1998). Karst aquifers, such as the Barton Springs aquifer, are commonly described as triple porosity (and permeability) systems consisting of matrix, fracture, and conduit porosity (Ford and Williams, 1992; Quinlan et al., 1996; Palmer et al., 1999). Most storage of water in the Edwards Aquifer is within the matrix porosity (Hovorka et al., 1998); therefore, volumetrically, flow through the aquifer is dominantly diffuse. However, groundwater dye-tracing studies demonstrate that significant components of groundwater flow are rapid and influenced by conduits (Hauwert et al., 2002). Hydraulic conductivity values from aquifer tests range from 0.40 to 75.3 ft/day and are log-normally distributed (Figure 27 in Appendix A). Storativity values range from 0.05 to 0.00078, reflecting unconfined to confined aquifer conditions, respectively (Scanlon et al., 2001). Heterogeneity of the aquifer is further expressed in terms of well yields, which range from less than 10 gallons per minute (gpm) to greater than 1,000 gpm. Well yields in the confined part of the Edwards Aquifer are often limited more by pump size than by aquifer properties (Schindel et al., 2004). Pump setting and well depth can also limit well yields.

The Edwards Aquifer is dynamic, with rapid fluctuations in spring flow, water levels (Figures 14 and 15 in Appendix A), and storage, reflecting changes in recharge (climatic conditions) and pumpage (demand). Water-level measurements and groundwater dye-tracing studies provide insight into groundwater-flow paths from source areas (recharge locations) to wells and springs. Groundwater generally flows west to east across the recharge zone, converging with preferential groundwater-flow paths subparallel to major faulting, and then flowing north toward Barton Springs. Although regional groundwater flow in the aquifer occurs largely under diffuse conditions, preferential flow paths were

traced along troughs in the potentiometric surface, indicating zones of high permeability. Rates of groundwater flow along preferential flow paths, determined from dye tracing, can be as fast as 4 to 7 mi/day under high-flow conditions or about 1 mi/day under low-flow conditions (Hauwert et al., 2002).

2.4.5 1950's Drought

The worst drought on record for central and other parts of Texas occurred from 1950 through 1956 and is referred to as the “1950's drought” (Lowry, 1959). The mean annual precipitation of 23.1 inches during the 7-yr drought was about two-thirds of the long-term annual precipitation of 33.5 inches (Figure 4a in Appendix A). Mean annual precipitation during the last 3 years of the drought was 16.5 inches, about half the long-term average precipitation (Scanlon et al., 2001). During the 1950's drought, spring flow reached historic lows at Barton Springs and ceased at Comal Springs.

2.4.6 Trinity Aquifer

The Edwards Aquifer overlies the Trinity Aquifer system in the BFZ (Figure 2-2). Along the west part of the study area, where the Edwards Aquifer is thin, water-supply wells commonly penetrate the lower Edwards units and are completed in the Upper Trinity Aquifer. The Upper Trinity Aquifer comprises the Upper Glen Rose Formation, which satisfies, almost exclusively, domestic and livestock needs with very small (less than 5 gpm) to small (5–20 gpm) yields of highly mineralized water (relative to the Edwards Aquifer) in the Central Texas Hill Country west of the BFZ (DeCook, 1960; Ashworth, 1983; Muller and McCoy, 1987). The Upper Trinity Aquifer, consistently about 350 to 400 ft thick in Hays County, has hydraulic properties (storage and hydraulic conductivity) substantially lower than those of the Edwards Aquifer (Ashworth, 1983; Barker et al., 1994). Seasonal variations in heads in the Upper Trinity Aquifer are most dramatic in wells less than 250 ft deep. These aspects make the Upper Trinity Aquifer more susceptible than the Edwards Aquifer to the effects of drought (Barker et al., 1994).

3.0 NUMERICAL GROUNDWATER MODELING

A numerical model was developed for the Barton Springs aquifer (Scanlon et al., 2001; Appendix A) as an aquifer-management tool to help evaluate the effects of pumping on the aquifer. The numerical model was developed by The University of Texas at Austin, Bureau of Economic Geology, and the District for the Groundwater Availability Model (GAM) initiative of TWDB. GAM models are part of an effort to develop state-of-the-art, publicly available, numerical groundwater-flow models for major and minor aquifers in Texas. The 2001 GAM was recalibrated to better match spring-flow and water-level data from the 1950's drought and was used to predict spring-flow and water-level declines under 1950's drought conditions and various rates of pumping.

3.1 Purpose and Approach of Modeling

The District reviewed the 2001 GAM (Scanlon et al., 2001) to evaluate its effectiveness as a tool for helping determine groundwater availability during conditions similar to those of the 1950's drought. The District conducted extensive reviews and analyses of hydrogeologic data collected by numerous individuals and organizations over many years. The Groundwater Model Advisory Team (see Preface), a team of scientists from the Austin area, assisted the District in reviewing the data and the model.

After reviewing the results of the 2001 GAM, the team decided that the model could not simulate spring-flow or water-level conditions of the 1950's drought as well as it could simulate conditions of the 1990's. The 2001 GAM indicated that monthly mean spring flow under 1950's drought conditions with no pumping would be 13.7 cfs. The lowest monthly mean measured flow from the springs was 11 cfs in July and August 1956 (Slade et al., 1986). Subtracting a pumping rate of 0.66 cfs from 13.7 cfs gives a discrepancy of about 2 cfs between the 2001 GAM simulated results and mean measured values of spring flow. Because the 2001 and recalibrated GAMs are based on stress periods of 1 month, they may not be able to simulate conditions equivalent to those represented by instantaneous spring-flow measurements. This limitation of resolution of

the models precludes a direct comparison of the model results for lowest spring flow with the lowest instantaneous measurements at Barton Springs of 9.6 cfs (Figure 3-1).

The 2001 GAM underpredicted water levels by as much as 150 ft in some parts of the aquifer relative to actual water-level measurements from the 1950's. Table 3-1 shows data representing the lowest water levels measured in nine wells during the 1950's drought and the amount of water-level adjustments necessary for model results to match measured water levels. Because of the discrepancy between measured and simulated values for spring flow and water levels of 1950's drought conditions, the District decided to recalibrate the 2001 GAM to emphasize conditions during the 1950's drought. The recalibrated model is hereafter referred to as the recalibrated GAM. The following approaches were taken in recalibrating the model:

- Hydraulic conductivity and storage values were modified from values used in the 2001 GAM to provide a better match between simulated and measured heads and simulated and measured spring flow. All other model parameters were unchanged.
- Pumping rates were set at 0.66, 10, 15, and 19 cfs for each simulation to represent 1950's pumping, current pumping, and two future-pumping scenarios, respectively.

3.2 Previous Work: 2001 GAM

A GAM was developed for the Barton Springs segment of the Edwards Aquifer by The University of Texas at Austin, Bureau of Economic Geology (BEG), and the District on behalf of the LCRWPG and TWDB (Scanlon et al., 2001). The conceptual model, design, and boundaries are described in Appendix A (Scanlon et al., 2001), and parts of the report are described only briefly here.

The GAM is a two-dimensional (one-layer), finite-difference model based on the U.S. Geological Survey's (USGS's) MODFLOW code (Harbaugh and McDonald, 1996). Processing MODFLOW for Windows (PMWIN) v. 5.1.7 was used as a pre- and postprocessor for running MODFLOW (Chiang and Kinzelbach, 2001). The model consists of a single layer with 120 rows, 120 columns, and 7,043 active rectangular cells 1,000 ft long and 500 ft wide (Figure 29 in Appendix A).

The north boundary of the model is the Colorado River, which is the regional base level (Slade et al., 1986). The east boundary is the bad-water line that is thought to have minimal contribution via leakage (Senger and Kreitler, 1984; Slade et al., 1986; Hauwert et al., 2004). The south boundary is a hydrologic divide along Onion Creek in the recharge zone and between the cities of Buda and Kyle in the confined part of the aquifer (LBG-Guyton Associates, 1994). The west boundary is the Mount Bonnell fault, which acts as a hydrologic barrier to flow (Senger and Kreitler, 1984). All boundaries are simulated as no-flow boundaries in the model, as described earlier in Section 2.4.2.2 (Subsurface Recharge).

Ten zones of hydraulic conductivity resulted from steady-state calibration, with values ranging from 1 to 1,236 ft/day (Figure 30 in Appendix A). Recharge values were distributed to stream cells across the recharge zone on the basis of recharge estimates from flow-loss studies. Interstream recharge was set at 15% of the total recharge (Slade et al., 1986). For 7-yr drought-of-record simulations, recharge was assumed to equal discharge (1950 through 1956).

As required by TWDB for its GAM contracts, the model was run in five 10-yr periods to simulate aquifer conditions from 2001 through 2050. Each 10-yr period simulated 3 years of average flow conditions, followed by 7 years of drought conditions, which mimicked the drought of the 1950's. Monthly stress periods were used for transient simulations, resulting in a total of 120 stress periods for a 10-yr simulation. Recharge and pumpage were set for each stress period. Pumping rates were increased linearly over that period, with pumping at the end of 2050 (19 cfs) representing 2.1 times the pumping rate at the beginning of 2001.

Transient simulations of the 2001 GAM were calibrated to conditions from 1989 through 1998. Simulated values for spring flow during this period, plotted with measured spring-flow values, are shown in Figure 36 in Appendix A. Spring flows ranged from 17 cfs in August 1997 to about 123 cfs in 1992. For this calibration period, peak spring-flow values might have been higher than those shown in Figure 36 in Appendix A for 1992 because floodwaters overtopping the upstream pool dam may have distorted accurate measurement of spring flow.

Pumping from permitted wells was assigned to cells on the basis of pumping records at the District. Estimates of exempt well pumping were calculated from countywide estimates and assigned equally to all active cells. During each simulation, pumping rates changed monthly as a result of seasonal demand.

The Drain package of MODFLOW represents Barton Springs and Cold Springs, with a high drain-conductance value to allow unrestricted discharge. To estimate spring flow from Barton Springs, spring flow output from the model was reduced 6% to account for flow discharging from Cold Springs.

3.2.1 2001 GAM Simulations

Good agreement was found in the 2001 GAM between measured and simulated flow at Barton Springs and between measured and simulated water levels (Scanlon et al., 2001). The root mean square (RMS) error between measured and simulated discharge for the transient model is 12 cfs, which represents 11% of the range in discharge measured at Barton Springs (1989 through 1998). Spring flow during periods of high flow (more than 100 cfs of spring flow) is overpredicted by the 2001 GAM (Figure 36 in Appendix A). The 2001 GAM generally reproduced water levels monitored continuously in wells throughout the study area (Figures 38 and 39 in Appendix A). The RMS error of 29 ft represents 11% of the water-level drop in the model area during low-flow conditions (March and April 1994) (Figure 40 in Appendix A).

Results of the simulations indicated that under average recharge and future pumpage conditions (19 cfs) water-level drawdown is small (less than 35 ft). Water-level declines are large (as much as 270 ft) under future pumpage (19 cfs) and when combined with 1950's drought conditions. Predicted spring flow is 0 cfs in response to pumping 19 cfs under 1950's drought conditions.

3.3 Transient-Model Recalibration

Incremental changes were made through trial and error to specific yield, specific storage, and hydraulic conductivity values to recalibrate the transient portion of the 2001 GAM to 1950's drought conditions. The recalibrated GAM was run with the adjusted parameters, and model output was reviewed for spring-flow and water-level responses to

parameter changes. Between model runs, changes were made to one parameter at a time. Further adjustments were made to parameters until simulated spring flow and water-level values were deemed to agree adequately with measured values from the 1950's drought.

By the end of recalibration, specific yield was decreased from 0.005 to 0.0021, and specific storage was decreased from 1.0×10^{-6} to 5.0×10^{-7} . Revised hydraulic conductivity values range from 0.3 to 740 ft/day (Table 3-2 and Figure 3-2), compared with a range of 1 to 1,236 ft/day in the 2001 GAM. Hydraulic conductivity and storage values for the aquifer under 1950's drought conditions were expected to be lower because of differences between the shallow part of the aquifer, where dissolution of the limestone and conduit development would be greater than at greater depths in the aquifer (Ogden et al., 1986; Maclay, 1995; Small et al., 1996). Additionally, specific-capacity tests have been performed in one well in the Barton Springs aquifer during high- and low-flow conditions. Results indicated that hydraulic parameters were lower under low-flow conditions (Raymond Slade, personal communication).

3.3.1 Water Levels

Nine wells were identified as having an adequate number of water-level measurements from the 1950's to recalibrate the 2001 GAM to low-flow conditions. An additional well measurement from the 1978 drought was added to this data set for better geographic coverage. Table 3-1 shows the lowest measured values for water levels in 10 wells with 1950's water-level data, plus simulated water-level values from the 2001 GAM and from the recalibrated GAM. The RMS error between measured water levels and simulated water levels in the 10 wells was improved to 6% using the recalibrated GAM, compared with 25% using the 2001 GAM. TWDB contract requirements request less than a 10% RMS error in water levels for the steady-state model. Water levels from the end of simulated 1950's drought conditions are plotted against measured values from the 1950's drought in Figure 3-3. In addition to a lower RMS error for results of the recalibrated model, the coefficient of determination (R^2) value of 0.94, using linear regression procedures, indicates a good match between simulated and measured values. The R^2 value for a perfect fit between data sets would be 1.0. For this same time period, R^2 value of the 2001 GAM results is 0.64.

The recalibrated GAM provides a good match between simulated water levels and measured water levels during periods of lowest flow, particularly during July and August 1956 (Figure 3-4). The simulation of 1950's drought conditions includes periods when recharge increases to near-average conditions, such as in 1953, which brought the aquifer briefly out of severe drought. During these periods, simulated water-level elevations in the recalibrated GAM are overpredicted when compared with measured values. This overprediction of water levels during these periods may be due to the inability of the model to simulate high rates of conduit flow during high water-level conditions. However, the recalibrated GAM succeeds in adequately simulating periods of low flow, such as during 1952 and 1954 through 1956 (Figure 3-4).

3.3.2 Spring Flow

Simulated and measured monthly mean spring-discharge values from the 1950's drought show good agreement in both the 2001 and recalibrated GAMs (Figure 3-5a), with very good agreement for periods when spring flow is below 20 cfs in the recalibrated GAM (Figure 3-5b). In the recalibrated GAM, RMS error between measured and simulated discharge for the entire 1950's drought is 13.8 cfs, which represents 23% of the range of measured discharge fluctuations. The 2001 GAM data set has an RMS error of 12.4 cfs, which represents 21% of the range of measured discharge for the same period. However, for periods of low flow below 18 cfs, the recalibrated GAM data set has a better match to measured values than the 2001 GAM, achieving an RMS of 6.0 cfs, or 10% of the range of measured discharge. The 2001 GAM achieves an RMS of 9.7 cfs, or 16% of the range of measured discharge for the same low flow period.

Amount of pumping estimated for the 1950's of 0.66 cfs (an annual rate of 478 acre-ft/yr) was incorporated into the recalibrated GAM (Brune and Duffin, 1983). The 2001 GAM indicated that spring flow under 1950's drought conditions with no pumping would be 13.7 cfs. The lowest monthly mean flow from the springs was 11 cfs from four flow measurements in July and August 1956 (Slade et al., 1986). The lowest daily flow measurement ever recorded was 9.6 cfs, which occurred on March 29, 1956 (Brune, 2002). Subtracting a pumping rate of 0.66 cfs from 13.7 cfs gives a discrepancy of about 2 cfs between 2001 GAM simulated results and measured values of spring flow. The

recalibrated GAM was able to produce a spring-flow value of 11 cfs, matching the lowest monthly mean for measured spring flow.

3.3.3 Sensitivity Analyses

Following TWDB requirements for GAM contracts, sensitivity analyses were conducted on the recalibrated GAM to assess the impact of varying certain aquifer parameters, such as recharge, specific yield, and specific storage, on simulated spring flow and water levels in various wells. Because of convergence problems with the 2001 GAM for adjustments of some parameters, only those analyses that were reported in the 2001 GAM report (Scanlon et al., 2001) were tested during evaluation of the recalibrated model. Results of these sensitivity analyses are presented in Figures 3-6 through 3-9. Sensitivity analyses were not conducted to test responses to variations in pumping because the scenarios for future conditions use various pumping rates. Of the parameters tested, changes in recharge had the most significant impacts on spring flow and water levels. Changes to specific yield and specific storage had similar impacts on spring flow, although water levels are more sensitive to changes in specific storage than specific yield. By changing specific storage from 5.0×10^{-7} to 5.0×10^{-6} , range of simulated water levels was reduced considerably. Spring flows were not impacted significantly by increasing specific storage and specific yield by a factor of 10, but lower end spring-flow values increased slightly. Because concerns about the aquifer are primarily for low-flow conditions, small changes in spring flow under these conditions are significant.

3.4 Predictions

3.4.1 Pumping

Pumping data for each simulation incorporated changes in pumping due to seasonal demand, as originally constructed in the 2001 GAM. The 2001 GAM considered impacts to spring flow and water levels over a 50-yr period, with steadily increasing pumpage. Because a drought similar to that of the 1950's could occur at any time in the future, the recalibrated GAM simulates 1950's drought conditions under pumping rates mentioned earlier. The purpose of this approach is to avoid any implication that any particular set of aquifer conditions or impacts might occur at a particular future date.

3.4.2 Impacts to Spring Flow and Water Levels

For effects of specific pumping rates on water levels and spring flow under 1950's drought conditions to be determined, pumping rates of 0.66, 5, 10, 15, and 19 cfs were evaluated in the recalibrated GAM. At a pumping rate of 0.66 cfs, the model predicts flow at Barton Springs to be 11 cfs, which is the same as the measured monthly mean flow (Figure 3-10), but 1.4 cfs more than an instantaneous flow measurement of 9.6 cfs reported for March 29, 1956. At 5 cfs of pumping (not shown in Figure 3-10), simulated spring flow decreases to a monthly mean of about 6.5 cfs. At 10 cfs of pumping, which is the estimated amount of pumpage in 2004, the model predicts that spring flow will be about 1 cfs averaged over 1 month. According to a minimum daily discharge of 9.6 cfs measured in 1956, spring flow may temporarily cease for periods less than 1 month. At a pumping rate of 15 cfs, simulated spring flow will be 0 for at least 4 months. Model simulations suggest a nearly one-to-one relationship between pumpage and spring flow. This relationship is in agreement with the conceptual model of previous investigators (Brune and Duffin, 1983) and historical water-balance analysis (Sharp and Banner, 1997).

To illustrate the impacts to spring flow from the combined effects of 1950's drought conditions and pumping, two potentiometric surface maps were prepared comparing the effects of 19 cfs pumping during both average flow conditions and 1950's drought conditions (Figure 3-11). The equipotential lines for average flow conditions with 19 cfs of pumping show that groundwater flow in the west part of the aquifer is primarily from west to east. Near the boundary between recharge and confined zones, flow turns to the northeast, toward the springs. This pattern of flow matches well with potentiometric surface maps prepared from measured water levels in as many as 175 wells across the aquifer. Under 1950's drought conditions with 19 cfs of pumping, flow in the west part of the aquifer is again from west to east. However, near the boundary between the recharge and confined zones, flow is to the southeast. This is the area in which primary pumping wells are concentrated (Figure 28 in Scanlon et al., 2001). Potentiometric surface lines show that flow is converging on a broad area north and south of Buda. Under these conditions there is no flow from the springs, and water levels are about 18 ft below the

elevation of Barton Springs. Section 4.0 (Impacts to Water Levels and Water-Supply Wells from 1950's Drought Conditions and Pumping) discusses in detail potential impacts to water-supply wells due to pumping at various rates under 1950's drought conditions.

Under low-flow conditions, additional gains and losses of groundwater could affect availability of usable groundwater for wells and flow at Barton Springs. Other potential sources include the Trinity Aquifer, part of the Edwards Aquifer south of the southern groundwater divide, the saline-water zone, cross-aquifer flow via poorly constructed wells, and urban leakage (water and wastewater). The volume of contributing flows from Trinity leakage, the saline-water zone, and gains and losses in groundwater from the San Antonio aquifer appears to be less than 1% of the total spring flow during droughts (Hauwert et al., 2004). Additionally, during periods of drought, water levels in the Trinity and San Antonio aquifers will also be low, with a low potential for substantial flow from these sources. However, the quality of water from the saline-water zone, the Trinity Aquifer, or infrastructure leakage may be poor and significantly degrade water in the Barton Springs aquifer, potentially rendering it unsuitable for drinking or for endangered species. Future studies are required to quantify these influences.

Although these factors that could potentially affect spring flow were not specifically simulated in the 2001 and recalibrated GAMs, simulation results can be compared with historic measured values of Barton Springs flow to examine whether the sum of recharge sources was accurately assessed. Because discharge is assumed to equal recharge for the 1950's drought, the 2001 and recalibrated GAMs indirectly account for these potential additions of water at spring-flow rates as low as 11 cfs. Furthermore, pumpage increases within the Trinity Aquifer source area west of the Barton Springs aquifer can be expected to reduce contributions that were experienced in the 1950's.

3.5 Qualifications and Data Needs

All models have limitations on how they simulate a real system. Because this model simulates a karst aquifer that consists of diffuse, fracture, and conduit flow of groundwater, its limitations are associated primarily with its ability to simulate conduit flow. The 2001 and recalibrated GAMs use zones of high hydraulic conductivity near the

springs to approximate conduit flow. This works well for simulating potentiometric maps, spring flow, and regional groundwater flow, but it is unsuitable for simulating travel times (Scanlon et al., 2003).

The 1950's simulation period contains times when rainfall and recharge increase to near-average conditions, such as in 1953, bringing the aquifer briefly out of severe drought. During these periods, simulated water-level elevations are overpredicted when compared with measured values, owing to the dynamic nature of the karst system and the inability of MODFLOW to explicitly simulate conduit flow. It is recommended that the District evaluate the potential of new groundwater models, as they become available, that can incorporate conduit flow. In the future, a karst groundwater modeling initiative at the Southwest Research Institute may provide such a model (Ron Green, personal communication). Another option may be a revision to the modeling pre- and postprocessor, Groundwater Vistas, which will allow for variable hydraulic conductivities as a function of saturated thickness (Robert Mace, personal communication).

Any future groundwater model in the Barton Springs aquifer will be limited by the number of surface and subsurface recharge data available. The 2001 GAM uses stream-flow and stream-loss data to estimate surface recharge for the transient period of 1989 through 1998. Future scenarios were based on 1950's drought conditions for which no recharge data are available. To estimate recharge, the 2001 GAM had spring discharge equal to recharge, and the recalibrated GAM incorporates this same assumption. Recharge may be slightly overestimated during low recharge periods because some of the water being discharged may be coming from aquifer storage rather than directly from recharge (Scanlon et al., 2001). The District, City of Austin, and the Texas Commission on Environmental Quality (TCEQ) are currently funding USGS flow stations on all major upstream and downstream locations of the recharge zone in order to gauge recharge.

Additional studies are needed to better characterize the potential for flow in or out of the aquifer at its boundaries. These areas include:

- (1) *Southern groundwater divide*. The groundwater model currently being developed for the San Antonio aquifer could be used to quantify the amount of water that might flow between Barton Springs and San Antonio aquifers under various

aquifer conditions. This model incorporates the Barton Springs aquifer within the model area. A water flux could be determined for a line of cells near the groundwater divide. Simulated water levels from the San Antonio model could be used to establish a time-varying specified-head boundary for the Barton Springs model (Appendix B). Additional groundwater dye tracing coupled with detailed potentiometric map studies may also provide further insight into flow along the boundaries.

- (2) *Edwards-Trinity connection.* Additional monitor well pairs could be installed to measure head differences between Edwards and Trinity Aquifers. An effective method for determining vertical hydraulic gradients between aquifers would be to install one or more multiport monitoring wells. Such a well would be completed with multiple zones in both the Edwards and Trinity Aquifers that could indicate the potential for flow between different hydrogeologic units. Synoptic water-level data could be collected from wells in areas for which both Edwards and Trinity wells are available to compare potentiometric surfaces between aquifers. Potential impacts on water quality at Barton Springs and in water-supply wells due to flow from the Trinity into the Edwards Aquifer are poorly understood. Losses and gains of water via interaquifer flow due to poorly constructed wells are also unknown.
- (3) *Saline-water line.* Additional studies are needed to determine potential for migration of saline water into the freshwater part of the aquifer and potential impacts on water quality at Barton Springs and in water-supply wells near the saline-water line.
- (4) *Influence of urban recharge.* Studies currently being conducted at The University of Texas at Austin suggest that a significant amount of subsurface recharge due to losses from water-supply, storm-water, and sewer lines could be occurring. During periods of severe drought (1950's drought conditions), the amount of water available from urban recharge might make up a significant part of recharge to the aquifer. Potential impacts on water quality at Barton Springs and in water-supply wells from urban recharge are poorly understood. As those studies are completed, results could be incorporated in the District's modeling.

3.6 Major Findings

- The recalibrated GAM provides a better match between simulated and measured spring-flow and water-level values under 1950's drought conditions than does the 2001 GAM.
- Recalibrated GAM simulations indicate that for each 1 cfs of groundwater pumped from the aquifer under 1950's drought conditions, discharge from Barton Springs will diminish by about 1 cfs.
- The recalibrated GAM simulates a mean monthly spring flow of about 1 cfs, with the present (2004) pumping rate of 10 cfs under 1950's drought conditions. According to a minimum daily discharge of 9.6 cfs measured in 1956, spring flow may temporarily cease for periods of less than 1 month. At 15 cfs of pumping, spring flow will cease for at least 4 months.
- Simulations of 1950's drought conditions with present (2004) and future rates of pumping indicate that significantly lower water levels will occur in most parts of the aquifer, resulting in an increased potential for flow from sources with poor water quality, such as the saline-water zone.

4.0 IMPACTS TO WATER LEVELS AND WATER-SUPPLY WELLS FROM 1950'S DROUGHT CONDITIONS AND PUMPING

The combined effects of drought and significant pumping can result in a decline in water levels and spring flow in an aquifer. Municipal water supplies in some areas of Texas declined or were exhausted completely during the 1950's drought (Lowry, 1959). Declining water levels due to drought and pumping will have negative effects on water-supply wells in a variety of ways, including increased energy costs, deterioration of water quality, water levels declining below pumps or well bores, and well yields that decline below usable rates (Bartolino and Cunningham, 2003). For the Barton Springs aquifer, these effects will profoundly impact wells that partly penetrate the aquifer and where dewatering of the aquifer occurs. Earlier discussion stated that current demand on groundwater in the Edwards Aquifer may exceed the historical availability during the 1950's drought and would cause considerable hardship on the region when severe drought conditions recur (Sharp and Banner, 1997).

To assess these potential hardships, this section describes methods used to characterize and quantify impacts to water-supply wells under 1950's drought conditions with increasing demand on groundwater. Hydrogeological, structural, and well data were used, along with results from the recalibrated GAM to estimate potential impacts to water-supply wells due to 1950's drought conditions and increasing rates of pumping. Results of this study indicate that water levels are significantly impacted by 1950's drought conditions alone and that even greater impact occurs when effects of pumping are combined with 1950's drought conditions.

4.1 Methods

About 970 active water-supply wells are in the District that pump water from the Barton Springs aquifer for public, domestic, industrial, commercial, irrigation, and agricultural purposes. Pumping from the Barton Springs aquifer under 1950's drought conditions could negatively impact many of these wells. In general terms, *negative impacts* to wells occur when instantaneous demand from a well is not met. The number of wells that could be negatively impacted by low water levels was evaluated using two methods:

- Saturated aquifer thickness analysis: assessing the number of wells having low specific capacity that are located in areas having less than 100 ft of saturated aquifer thickness in the unconfined zone and
- Saturated borehole thickness analysis: assessing the total number of wells throughout the study area that partly penetrate the aquifer, resulting in less than 25 ft of saturated borehole.

Each of these methods requires evaluation of changes in saturation of the aquifer and well boreholes using measured and model-simulated data. Data sets used in the evaluation, including structure-contour maps, potentiometric maps, simulated drawdown, and well information, are described in the subsections following.

A small number of the same wells may be included within each evaluation. However, attempts to eliminate duplicate counts of wells do not appear possible because one is a broad, percentage-based evaluation and the other is a well-by-well evaluation.

4.1.1 Data Sets

An evaluation of saturated aquifer thickness and saturated borehole thickness relies heavily on several key data sets and maps described in the subsections following. Contouring of all surfaces was done using the grid-based graphics program Surfer[®] in the UTM-feet coordinate system (NAD 83). Kriging was used for generating contour surfaces because it produced the most realistic contours. Grid size of cells was about 1,200 × 1,500 ft, according to distribution and density of data sets within Surfer[®].

4.1.1.1 Structure-Contour Maps

The primary data set (245 wells) for the structure-contour surface of the bottom of the aquifer was derived from driller's descriptions, geophysical logs, geotechnical logs, and core data (Figure 4-1). Geologic contacts and geologic maps (Small et al., 1996) were also used for control. Faulting was not incorporated into the gridding process; limited faulting incorporated into the gridding process did not appear to have a profound effect on contour shapes owing to the relatively high density of data. The top of the basal nodular member of the Kainer Formation was used as the effective bottom of the aquifer in this study. This member is about 50 ft thick in the study area and, despite localized

karst development where exposed at the surface, it appears to have low permeability and storage compared with that of the rest of the Edwards Group (Small et al., 1996). These hydraulic characteristics of the basal nodular are evident from a few widely spaced well-drilling observations. In contrast, at many localities where the basal nodular is exposed at the surface, the unit characteristically contains light-toned, recrystallized rock having abundant springs and solution cavities that suggest a high permeability. Furthermore, in many driller's and geophysical logs, the top of the basal nodular member can be distinguished more readily than the top of the Glen Rose Formation. For the purposes of estimating the bottom of the aquifer, the top of the basal nodular was assumed to be the base of the Edwards Aquifer, even though the basal nodular is clearly a part of the Edwards Aquifer. In many areas elevation of the bottom of the aquifer was derived by applying known total aquifer thickness and unit thicknesses from well-defined, stratigraphic control points.

To characterize change in thickness of the aquifer as it relates to groundwater availability, an isopach (thickness) map of the lithologic units in the recharge and confined zones was created (Figure 4-2).

4.1.1.2 Potentiometric Maps

For a potentiometric map representing 1950's drought conditions to be constructed, water-level data since 1937 were collected from the TWDB database and reports and USGS reports (Follet, 1956; DeCook, 1960; Slade et al., 1986). Limited water-level data from the 1950 through 1957 drought period exist. A composite potentiometric-surface map was constructed using July and August 1956 water-level data as the base data set. Additional 1950's water-level data were adjusted in elevation to better match the July and August 1956 period when possible, and additional water-level data from low-spring-flow periods were used. The final data set used to construct the composite potentiometric-surface map representing 1950's drought conditions has about 50 control points within the District boundaries (Table 4-1; Figure 4-3).

The composite potentiometric-surface map generally contains a steep west-east gradient along the west (unconfined) part of the aquifer. The gradient decreases toward the confined part of the aquifer, and direction of flow changes from W-E to SW-NE,

which is similar to other potentiometric-surface maps that were constructed with many more data points. The composite potentiometric-surface map created by these procedures is similar in shape, gradient, and elevation to the 1950's map in Slade et al. (1986). However, most significant differences in the maps occur in the area of interest along the western Edwards Aquifer, with some elevations being more than 50 ft higher in elevation in the Slade et al. (1986) map. The map constructed in this study contains more control data in this area, which may account for these differences.

4.1.1.3 Simulated Drawdown

The recalibrated GAM was used to simulate drawdown in 41 wells at pumping rates of 5, 10, 15, and 19 cfs (Table 4-2). Some of these wells also have historical water-level data. Simulated drawdown was calculated as the difference in water levels between simulated 1950's drought conditions (with 0.66 cfs pumping) and simulated 1950's drought conditions for each pumping scenario listed earlier. Data were gridded and contoured to create drawdown surfaces. Figure 4-4 is an example of the drawdown contour map with 10 cfs pumping. Each of these simulated drawdown surfaces was subtracted from the potentiometric map representing measured 1950's drought conditions. Resulting potentiometric maps were created to quantify impacts under drought with pumping scenarios described earlier. Figure 4-5 is an example of a potentiometric map representing combined effects of 1950's drought and 10 cfs of pumping.

4.1.1.4 Well Data

Specific capacity is defined as well production per unit decline in head and is a function of the aquifer and well setting and pumping rate and duration (Mace et al., 2000). In this study, specific-capacity data throughout the aquifer were used to characterize the percentage and magnitude of drawdown in wells from pumping. Specific-capacity data were assembled from well schedules and pumping-test reports and reviewed to improve data quality. A total of 168 measurements were compiled from various hydrologic conditions, 29 of which are from long-term aquifer pumping tests, and they have a broad distribution of values. No attempts were made to normalize the

specific-capacity data to aquifer thickness (unit specific capacity). The data show heterogeneity distributed across the aquifer; however, the lowest values are located primarily within the western, unconfined area of the aquifer and along the saline-water zone on the east side of the aquifer (Figure 4-6a and 4-6b).

Wells drilled to produce water in the Edwards Aquifer range in depth from 40 to 800 ft, with an average well depth of about 400 ft. Distribution of well depths is not systematic across the aquifer. A District review of wells reported to have “gone dry” or that had yield problems during a drought revealed that cable-tool drilling, a drilling technology largely unused today, was responsible for many shallow-penetrating wells.

4.1.2 Saturated Aquifer Thickness Analysis

Maps of saturated aquifer thickness were created from three types of data: (1) the structure contour of the bottom of the aquifer, (2) potentiometric maps representing measured 1950’s drought conditions, and (3) simulated drawdown for various pumping rates. Saturated-thickness maps in the unconfined zone were created using the following mathematical relationship at each grid node:

$$b_{wt} = (H_t - s) - A_b \tag{1}$$

where b_{wt} is saturated thickness of the water-table aquifer (in feet), H_t is the total measured hydraulic head representing 1950’s drought conditions in feet above mean sea level (msl), s is the hydraulic head loss due to pumping (in feet), and A_b is the elevation of the bottom of the aquifer in feet above msl.

For purposes of this evaluation, 100 ft of saturated aquifer thickness was defined as sufficient to derive adequate water supplies for wells in the unconfined aquifer. This number is a reasonable thickness based on distribution of wells on nondrought saturated-thickness maps and amount of drawdown that occurs for low-yield wells along the west part of the aquifer. Specific-capacity data were compiled and mapped to determine range and distribution of well yields in the unconfined aquifer (Figure 4-6a and 4-1b). In the unconfined zone, 13% of 113 specific-capacity values were less than or equal to 0.17 gallons per minute per foot (gpm/ft). These wells have more than 100 ft of drawdown for a constant pumping rate of 15.9 gallons per minute (gpm). From 184 measurements, average pumping rate for domestic supply wells was determined to be 15.9 gpm.

According to this general approach, those wells will most likely experience problems producing water because drawdown in the borehole will exceed the saturated thickness of the aquifer under these conditions. For example, under 1950's drought conditions with minimal pumping (0.66 cfs), it is estimated that 230 wells may have less than 100 ft of saturated aquifer thickness, and it is estimated that of that total number, 13%, or 30 wells, will experience yield problems. It is assumed that all wells in this analysis penetrate the entire thickness of the aquifer because these wells are generally in the thinnest part of the aquifer.

4.1.3 Saturated Borehole Thickness Analysis

Quantification of the number of wells that would be impacted by combined effects of lower head and partial penetration of the aquifer by a well requires three types of data: (1) location and elevation of the bottom of the well borehole, (2) a corresponding potentiometric surface elevation representing 1950's drought conditions, and (3) drawdown from pumping scenarios. The saturated borehole for each well was determined using the following mathematical relationship:

$$b_s = H_t - W_b \quad (2)$$

where b_s is saturated borehole thickness (in feet), H_t is total hydraulic head (in feet above msl), and W_b is elevation of the bottom of the borehole (in feet above msl). Hydraulic head for each well having sufficient depth and location information (614 wells) was determined from residuals on potentiometric surface maps in Surfer[®].

As in the saturated-thickness evaluation, it is recognized that a negative impact to a well would likely occur before the saturated thickness of a well borehole reached 0 from drought and regional pumping. For this part of the evaluation, 25 ft of saturated borehole was defined as sufficient for deriving adequate water supplies. This number results from recognition that well pumps are generally not set at the bottom of the borehole and the confined part of the aquifer generally has specific-capacity values that are higher than those of the unconfined zone. Therefore, wells in this area would experience less drawdown. For example, under 1950's drought conditions with minimal pumping (0.66 cfs), it is estimated that 43 of the 970 water-supply wells in the District

may have less than 25 ft saturated borehole thickness and will therefore have problems with yield.

4.2 Results

The saturated thickness of the aquifer is shown in Figure 4-7 under 1950's drought conditions and minimal pumping (0.66 cfs). The cross-sectional expression of this surface is shown in Figure 2-2. A significant part of the unconfined aquifer in the recharge zone is likely to have little to no water available for water-supply wells under 1950's drought conditions. Figure 4-8 is a composite map of the 100-ft saturated-thickness contour lines under 1950's drought conditions with various pumping scenarios (0.66, 5, 10, 15, and 19 cfs). This figure shows effective drawdown of the aquifer with each scenario of increased pumping under 1950's drought conditions as the 100-ft saturated-thickness contour line moves east with higher rates of pumping. The most significant decrease in saturated thickness occurs along the southwest part of the unconfined aquifer, with the greatest shift in contours between high flow and 1950's drought conditions (Figure 4-8). Drawdown of water levels is small in the north part of the aquifer near the springs and the Colorado River, although even small changes in water levels in this area are associated with significant changes in spring flow. Table 4-3 lists the number of wells located west of the saturated aquifer contour line, which indicates that they have less than 100 ft of saturated aquifer thickness available. For given demand (15.9 gpm) and well yield ($S_c = 0.17$ gpm/ft), these wells will most likely have insufficient yield as a result of drawdown of the aquifer from 1950's drought conditions and increased pumping. Under 1950's drought conditions and minimal pumping (0.66 cfs), it is estimated that 230 wells may have less than 100 ft of saturated aquifer thickness, and it is estimated that of that total number, 13%, or 30 wells, will experience yield problems.

Under 1950's drought conditions and increased demand, water levels in the confined zone decrease. Although saturated thickness of the aquifer is not severely impacted in the confined zone under these scenarios, decreases in water levels under 1950's drought conditions and increased pumping shift the boundary of unconfined to confined

conditions to the east (Figure 2-2). Under 1950's drought conditions and 19 cfs of pumping, nearly the entire aquifer is hydraulically unconfined.

Water-level decreases will leave some wells with less than 25 ft of saturated borehole (Table 4-4). These wells will most likely have insufficient yield owing to the dewatering of the well borehole primarily because of lower water-level values and partial penetration of the aquifer by the borehole. Under 1950's drought conditions with minimal pumping (0.66 cfs), it is estimated that 43 of the 970 water-supply wells in the District may have less than 25 ft of saturated borehole thickness and will therefore have problems with yield.

Total number of wells estimated to be impacted by drawdown of water levels is shown in Table 4-5 and in Figure 4-9. Public water-supply systems in operation in the District at the time this report was generated were evaluated to determine whether there was likely to be any impact under 1950's drought conditions and various rates of pumping. Only two public water-supply systems in the southwest part of the aquifer were found to have insufficient aquifer saturation under 1950's drought conditions alone. Those two systems serve areas of Oak Forest and Ruby Ranch Subdivisions. Most other public water-supply systems are located in the highly transmissive, confined part of the aquifer and penetrate most of the aquifer thickness. Some small public-supply systems rely primarily on the Trinity Aquifer. Effects of drought and pumping on the Trinity Aquifer are beyond the scope of this investigation.

4.3 Discussion

Hydraulic properties of this karst aquifer are heterogeneous and anisotropic. Wells in the unconfined zone have lower and more variable specific-capacity values than those of the confined zone (Figure 4-6b) and are more susceptible to variations in saturated thickness (Figure 2-2). In the unconfined zone we expect transmissivity and, therefore, specific-capacity values to be lower under lower water-level conditions (drought). Therefore, the percentage of wells with more than 100 ft of drawdown would most likely increase during drought. Accordingly, results presented should represent a minimum estimate of negative impacts to wells from drought and various pumping rates that were evaluated.

Wells in the confined zone are negatively impacted by the combination of decreases in hydraulic head and partial penetration of wells into the aquifer. Many shallow wells were drilled using cable-tool technology before rotary drilling became commonplace.

A significant decrease in hydraulic head in the freshwater zone will increase the potential for flow from the bad-water zone into the freshwater zone (as shown in Figure 2-2), resulting in potential water-quality implications for water-supply wells and Barton Springs. More investigations are needed to characterize this potential.

The compounded effects of drought and significant pumping have been characterized as “negative impacts” in this report. Negative impacts do not necessarily mean that wells will “go dry.” If water levels drop below the pump or bottom of the borehole, air would enter the system, causing the well to cease production.

Potential remedies to these negative impacts could include deepening the well farther into the Edwards Aquifer or into the Middle Trinity Aquifer, lowering the pump, setting a lower pumping rate, and obtaining more storage capacity. Other solutions for municipalities or large public-supply corporations include conservation; cross connections to other water sources, such as surface-water lines; desalination of saline water; or an aquifer storage and recovery facility.

Most public-supply wells are drilled to sufficient depth, are located in the confined part of the aquifer, and will not likely be impacted negatively. Generally speaking, public water-supply systems are more capable of mitigating impacts during a drought owing to their ability to control pumping rates, store water, and to cross connect with other water-supply sources.

In the unconfined zone it is common for wells to penetrate into the underlying Upper Trinity Aquifer, as illustrated by wells 5857204 and 5857609 in Figure 2-2. In general these wells penetrate less than 250 ft into the Upper Glen Rose and most likely derive their water from both the Edwards and Upper Trinity Aquifers. The Upper Trinity has negligible contribution to these hybrid wells compared with the Edwards, according to the literature (Barker et al., 1994). However, during drought conditions with high rates of pumping, the Upper Trinity may locally provide sufficient supplies to wells that penetrate through the Edwards. Accordingly, this analysis overestimates impacts on such hybrid

wells. Further investigations are needed for us to understand the Trinity Aquifer system's hydraulic connection to the Edwards and its potential as a source of water.

Although the District has the most complete and comprehensive database for the study area, many wells are likely to remain undocumented. In general, these wells predate the existence of the District (pre-1987) and could represent a higher number of wells that partly penetrate the aquifer. Accordingly, our estimates would underestimate impacts of these additional wells during drought conditions and with the various pumping rates evaluated in this report.

The heterogeneity of the karst aquifer system necessitated some assumptions to quantify an "impact" to wells. Primary assumptions that have a direct bearing on the number of wells impacted include specific definitions of impact (e.g., how much saturated aquifer and borehole are sufficient for supplies?). For this study we chose 100 ft of saturated aquifer and 25 ft of saturated borehole, generally corresponding to the recharge and confined zone, respectively. We think that this approach gives a reasonable qualitative and quantitative evaluation of potential impacts. Although all measured data sets (structure, water level, specific capacity) and contour surfaces have implicit assumptions, the results of this study rely heavily on measured data for the impacts of a recurrence of 1950's drought conditions to be assessed. The only data set that uses model-simulated results is effects of pumping on drawdown.

As discussed in Section 3.0, other sources of water may not be accounted for in drawdown simulations, which might overpredict drawdown, such as influx from the saline-water zone, San Antonio and Trinity Aquifers, or recharge from urban infrastructure, such as leaking water and sewer lines. These evaluations may also underpredict drawdown by not accurately estimating pumping from exempt wells, overpumping from permitted wells, or water discharging from the Edwards into the Trinity owing to poor well construction. However, these gains and losses of water from various sources are thought to be small (Hauwert et al., 2004) and may have only a local influence on wells or springs.

Previous studies have not quantified the impacts of drought and various pumping rates. Results of this investigation should assist in policy decision-making on aquifer management and protection of water-supply wells in the District.

4.4 Major Findings

- As many as 7% of the wells in the District, including two public water-supply systems, may be negatively impacted with insufficient yield under 1950's drought conditions alone (with minimal pumping of 0.66 cfs).
- Under 1950's drought conditions and the present pumping rate of 10 cfs, as many as 19% of the wells in the District may go dry or have reduced yields. Most of these negative impacts will be due to a combination of decreased hydraulic head and partial penetration of wells into the aquifer.
- Wells in the confined part of the aquifer that partly penetrate the aquifer are susceptible to negative impacts owing to decreases in water levels during a recurrence of 1950's drought conditions, with or without pumping from other wells.
- Because of low saturated thickness of the southwest part of the unconfined aquifer and low permeability compared with other parts of the aquifer, wells in this area are the most susceptible to negative impacts under 1950's drought conditions. As pumping rates increase, so will potential impacts in this area.
- Under 1950's drought conditions and high rates of pumping, potential for saline water to flow from the saline-water zone into the freshwater aquifer will increase.

5.0 CONCLUSIONS

Results of the sustainable-yield evaluation will be considered in District sustainable-yield policies for resource management.

- The recalibrated GAM provides a better match between simulated and measured spring-flow and water-level values under 1950's drought conditions than the 2001 GAM.
- For each 1 cfs of groundwater pumped from the aquifer under 1950's drought conditions, discharge from Barton Springs will diminish by about the same rate.
- The recalibrated GAM indicates that with the present (2004) pumping rate of 10 cfs combined with 1950's drought conditions, mean monthly spring flow will be about 1 cfs. According to a minimum daily discharge of 9.6 cfs measured in 1956, spring flow may temporarily cease on a daily basis. At 15 cfs of pumping, spring flow will cease for at least 4 months.
- Under 1950's drought conditions and the present (2004) pumping rate of 10 cfs, as many as 19% of the wells in the District may be negatively impacted. Most of those negative impacts will be due to a combination of decreased head and partial penetration of wells into the aquifer.
- Because of low saturated thickness of the southwest part of the unconfined aquifer and low permeability compared with other parts of the aquifer, wells in this area are the most susceptible to negative impacts under 1950's drought conditions. As pumping rates increase, so will potential impacts in this area.

5.1 Acknowledgments

To evaluate sustainable yield and the 2001 GAM, the District assembled a Groundwater Model Advisory Team (GMAT) composed of scientists from the Austin area. GMAT members contributed a considerable amount of time to this effort and provided critical input and comments throughout the modeling and sustainable-yield evaluation process. Those members include Rene Barker (USGS, retired), Nico Hauwert (City of Austin), David Johns (City of Austin), Dr. Robert Mace (TWDB), Dr. Bridget Scanlon (BEG), Dr. Jack Sharp (UT), Raymond Slade (USGS, retired), and Eric Strom

(USGS). Technical writing and review were by Lana Dieterich (BEG). Raymond Slade, Rene Barker, David Johns, Nico Hauwert, and Dr. Robert Mace provided final input and review of this report.

A broad group of scientists and technical experts also provided valuable input during the evaluation process (Appendix C).

In their quest for the best science available, the Board of Directors for the District are particularly acknowledged for providing impetus and support for Assessment Program staff and research activities presented in this report. Those members include Dr. Bob Larsen (President), Jack Goodman (Vice-President), Craig Smith (Secretary), Dr. David Carpenter, and Chuck Murphy. Dr. Larsen and Dr. Carpenter provided additional Board direction and input. Special thanks also go to Jim Camp for his initiation and support of these efforts during his tenure as District President.

Other District staff contributors include Joe Beery, who assisted with many of the sensitivity analyses, and Shu Liang, who developed the District's well database. Assessment interns Anne Christian and Lindsay Reeve investigated reports of dry wells and helped update data in the District's well database, respectively. Brian B. Hunt drafted the figures for this report.

6.0 REFERENCES

- Ashworth, J. B., 1983, Ground-Water Availability of the Lower Cretaceous Formations in the Hill Country of South-Central Texas: Texas Department of Water Resources, Report 273, 172 p.
- Baker, E. T., Slade, R. M., Dorsey, M. E., Ruiz, L. M., and Duffin, G. L., 1986, Geohydrology of the Edwards Aquifer in the Austin Area, Texas: Texas Water Development Board, Report 293, 216 p.
- Barker, R. A., Bush, P. W., and Baker, E. T., Jr., 1994, Geologic History and Hydrogeologic Setting of the Edwards-Trinity Aquifer System, West-Central Texas: U.S. Geological Survey, Water-Resource Investigations Report 94-4039, 51 p.
- Barrett, M. E., and Charbeneau, R. J., 1996, A Parsimonious Model for Simulation of Flow and Transport in a Karst Aquifer: Technical Report Center for Research in Water Resources, Report No. 269, 149 p.
- Bartolino, J. R. and Cunningham, W. L., 2003, Ground-Water Depletion across the Nation: U.S. Geological Survey Fact Sheet 103-03, 4 p.
- Barton Springs/Edwards Aquifer Conservation District and the City of Austin, 2001, Water Quality and Flow Loss Study of the Barton Springs Segment of the Edwards Aquifer: EPA-funded 319h grant report submitted to the Texas Commission on Environmental Quality (formerly TNRCC), August.
- Barton Springs/Edwards Aquifer Conservation District, 2002, Geologic Map of the Barton Springs Segment of the Edwards Aquifer: Austin, December.
- Barton Springs/Edwards Aquifer Conservation District, 2003, District Management Plan, p. 59.
- Brune, Gunnar, 2002, Springs of Texas: College Station, Texas A&M University Press, 2d ed., 566 p.
- Brune, Gunnar and Duffin, Gail, 1983, Occurrence, Availability, and Quality of Ground Water in Travis County, Texas: Texas Department of Water Resources, Report 276, 219 p.

- Chiang, W. H., and Kinzelbach, W., 2001, 3D-groundwater modeling with PMWIN: New York, Springer, 346 p.
- City of Austin (COA), 1997, The Barton Creek Report, City of Austin Drainage Utility Department Environmental Resources Management Division, Water Quality Report Series, COA-ERM/1997, 335 p.
- DeCook, K. J., 1960, Geology and Ground-Water Resources of Hays County, Texas: Texas Board of Water Engineers, Bulletin 6004, 170 p.
- Flores, R., 1990, Test Well Drilling Investigation to Delineate the Downtip Limits of Usable-Quality Groundwater in the Edwards Aquifer in the Austin Region, Texas: Texas Water Development Board, Report 325, 70 p.
- Follett, C. R., 1959, Records of Water-Level Measurements in Hays, Travis, and Williamson Counties, Texas (1937 to May 1956): Texas Board of Water Engineers, Bulletin 5612, 74 p.
- Ford, D. and P. Williams, 1992, Karst Geomorphology and Hydrology: New York, Chapman and Hall, 2d ed., 600 p.
- Harbaugh, A.W. and McDonald, M. G., 1996, User's Documentation for MODFLOW-96, An Update to the U.S. Geological Survey Modular Finite-Difference Groundwater Flow Model: U.S. Geological Survey, Open-File Report 96-485, 56 p.
- Hauwert, N., Johns, D., Hunt, B., Beery, J., and Smith, B., 2004, The flow system of the Barton Springs segment of the Edwards Aquifer interpreted from groundwater tracing and associated field studies, *in* Proceedings from the Symposium, Edwards Water Resources in Central Texas: Retrospective and Prospective, May 21.
- Hauwert, N. M., Johns, D. A., Sansom, J. W., and Aley, T. J., 2002, Groundwater Tracing of the Barton Springs Edwards Aquifer, Travis and Hays Counties, Texas: Gulf Coast Associations of Geological Societies Transactions, v. 52, p. 377–384
- Hauwert, N. M., Johns, D. A., Sansom, J. W., and Aley, T. J., in press, Groundwater tracing study of the Barton Springs segment of the Edwards Aquifer, southern Travis and northern Hays Counties, Texas: Austin, Barton Springs/Edwards

- Aquifer Conservation District and City of Austin Watershed Protection and Development Review Department.
- Hovorka, S., Dutton, A., Ruppel, S., and Yeh, J., 1996, Edwards Aquifer Ground-Water Resources: Geologic Controls on Porosity Development in Platform Carbonates, South Texas: The University of Texas at Austin, Bureau of Economic Geology, Report of Investigations No. 238, 75 p. Lowery, R. L., 1959, A Study of Droughts in Texas: Texas Board of Water Engineers, Bulletin 5914, 49 p.
- Hovorka, S., Mace, R., and Collins, E., 1998, Permeability Structure of the Edwards Aquifer, South Texas—Implications for Aquifer Management: The University of Texas at Austin, Bureau of Economic Geology, Report of Investigations No. 250, 55 p.
- LBG-Guyton Associates, 1979, Geohydrology of Comal, San Marcos, and Hueco Springs: Texas Department of Water Resources, Report 234, June, 85 p.
- LBG-Guyton Associates, 1994, Edwards Aquifer Ground-Water Divides Assessment San Antonio Region, Texas: Report 95-01 Prepared for the Edwards Underground Water District, 35 p.
- Mace, R., Chowdhury, A., Anaya, R., and Way, S., 2000, Groundwater Availability of the Trinity Aquifer, Hill Country Area, Texas: Numerical Simulations through 2050: Texas Water Development Board, 172 p.
- Maclay, R. W., 1995, Geology and Hydrology of the Edwards Aquifer in the San Antonio Area, Texas: U.S. Geological Survey, Water-Resources Investigations Report 95-4186, 64 p.
- Maclay, R. W., and Small, T. A., 1986, Carbonate Geology and Hydrogeology of the Edwards Aquifer in the San Antonio Area, Texas: Texas Water Development Board, Report 296, 90 p.
- Muller, D., and McCoy, W., 1987, Ground-Water Conditions of the Trinity Group Aquifer in Western Hays County: Texas Water Development Board, LP-205, 62 p.
- Ogden, A. E., Quick, R. A., Rothermel, S. R., and Lunsford, D. L., 1986, Hydrogeological and Hydrochemical Investigation of the Edwards Aquifer in the

- San Marcos Area, Hays County, Texas: Southwest Texas State University, Edwards Aquifer Research and Data Center, EARDC Number R1-86, 364 p.
- Palmer, A. N., Palmer, M. V., and Sasowsky, I. D., 1999, eds., *Karst Modeling: Proceedings of the Symposium Held February 24 through 27, 1999*, Charlottesville, Virginia: Karst Waters Institute, Special Publication 5, 265 p.
- Quinlan, J. F., Davies, G. J., Jones, S. W., and Huntoon, P. W., 1996, *The Applicability of Numerical Models to Adequately Characterize Groundwater Flow in Karstic and Other Triple-Porosity Aquifers*: American Society for Testing and Materials, *Subsurface Fluid-Flow (Groundwater) Modeling*, STP 1288.
- Rose, P. R., 1972, *Edwards Group, Surface and Subsurface, Central Texas*: The University of Texas at Austin, Bureau of Economic Geology Report of Investigations No. 74, 198 p.
- Scanlon, B., Mace, R., Barrett, M., and Smith, B., 2003, *Can we simulate regional groundwater flow in a karst system using equivalent porous media models? Case study, Barton Springs Edwards Aquifer, USA*: *Journal of Hydrology*, v. 276, p. 137–158.
- Scanlon, B., Mace, R., Dutton, A., and Reedy, R., 2000, *Predictions of Groundwater Levels and Spring Flow in Response to Future Pumpage and Potential Future Droughts in the Barton Springs Segment of the Edwards Aquifer*: The University of Texas at Austin, Bureau of Economic Geology, prepared for the Lower Colorado River Authority, under contract no. UTA99-0196, 42 p.
- Scanlon, B., Mace, R., Smith, B., Hovorka, S., Dutton, A., and Reedy, R., 2001, *Groundwater Availability of the Barton Springs Segment of the Edwards Aquifer, Texas—Numerical Simulations through 2050*: The University of Texas at Austin, Bureau of Economic Geology, final report prepared for the Lower Colorado River Authority, under contract no. UTA99-0, 36 p. + figs., tables, attachment.
- Schindel, G., Hoyt, J., and Johnson, S., 2004, *Edwards Aquifer, United States*, in Gunn, J., and Dearborn, Fitzroy, eds., *Encyclopedia of Caves and Karst Science*: New York, New York, p. 313–315.

- Senger, R. K. and Kreitler, C. W., 1984, Hydrogeology of the Edwards Aquifer, Austin Area, Central Texas: The University of Texas at Austin, Bureau of Economic Geology Report of Investigations No. 141, 35 p.
- Sharp, J. M., Jr., 1990, Stratigraphic, geomorphic and structural controls of the Edwards Aquifer, Texas, U.S.A., *in* Simpson, E. S., and Sharp, J. M., Jr., eds., Selected Papers on Hydrogeology: Heise, Hannover, Germany, International Association of Hydrogeologists, v. 1, p. 67–82.
- Sharp, J. M., Jr., and Banner, J. L., 1997, The Edwards Aquifer—a resource in conflict: *GSA Today*, v. 7, no. 8, p. 1–9.
- Slade, Raymond, Jr., Dorsey, Michael, and Stewart, Sheree, 1986, Hydrology and Water Quality of the Edwards Aquifer Associated with Barton Springs in the Austin Area, Texas: U.S. Geological Survey Water-Resources Investigations, Report 86-4036, 117 p.
- Slade, Raymond, Jr., Ruiz, Linda, and Slagle, Diana, 1985, Simulation of the Flow System of Barton Springs and Associated Edwards Aquifer in the Austin Area, Texas: U.S. Geological Survey, Water-Resources Investigations Report 85-4299, 49 p.
- Slagle, D. L., Ardis, A. F., and Slade, R. M., Jr., 1986, Recharge Zone of the Edwards Aquifer Hydrologically Associated with Barton Springs in the Austin Area, Texas: U. S. Geological Survey Water-Resources Investigations, Report 86-4062, Plate.
- Small, T. A., Hanson, J. A., and Hauwert, N. M., 1996, Geologic Framework and Hydrogeologic Characteristics of the Edwards Aquifer Outcrop (Barton Springs Segment), Northeastern Hays and Southwestern Travis Counties, Texas: U.S. Geological Survey Water-Resources Investigations, Report 96-4306, 15 p.
- Smith, B. A., and Hunt, B. B., 2004, Sustainable Yield of the Barton Springs Segment of the Edwards Aquifer, *in* Proceedings from the Symposium, Edwards Water Resources in Central Texas: Retrospective and Prospective, May 21, 2004, San Antonio, Texas.

Sophocleous, M. A., 1997, Managing Water Resources Systems—Why “Safe Yield” is Not Sustainable: *Groundwater*, v. 35, no. 4, p. 561

Todd, D. K., 1959, *Ground Water Hydrology*: New York, John Wiley and Sons, 336 p.

Wanakule, N., 1989, *Optimal Groundwater Management Model for the Barton Springs-Edwards Aquifer*: Southwest Texas State University, Edwards Aquifer Research and Data Center, EARDC Number R1-89, 31 p.

7.0 GLOSSARY OF HYDROGEOLOGIC TERMS

Modified from:

Sharp, J. M., Jr., 1999, A Glossary of Hydrogeological Terms: The University of Texas at Austin, Department of Geological Sciences, 35 p.

Anisotropy – variation of a property at a point with direction.

Aquifer – consolidated or unconsolidated geologic unit (material, stratum, or formation) or set of connected units that yields a significant quantity of water of suitable quality to wells or springs in economically usable amounts.

Confined (or artesian) – an aquifer that is immediately overlain by a low-permeability unit (confining layer). A confined aquifer does not have a water table.

Unconfined (or water-table) – the upper surface of the aquifer is the water table. Water-table aquifers are directly overlain by an unsaturated zone.

Aquifer system – intercalated permeable and poorly permeable materials that comprise two or more permeable units separated by aquitards that impede vertical groundwater movement but do not affect the regional hydraulic continuity of the system.

Artesian – hydrostratigraphically confined. In the common usage, it implies the existence of flowing wells, but all flowing wells are not artesian nor do all artesian wells flow.

Attributes – nonspatial, usually alphanumeric, data that are linked to a spatial element (e.g., points depicting well locations may be linked to attribute files containing data on stratigraphy, water levels, water chemistry, etc.).

bad water line- eastern boundary of Edwards Aquifer water in the Barton Springs aquifer of the Edwards Aquifer characterized by having more than 1,000 milligrams per liter (mg/L) of total dissolved solids (Barton Springs/Edwards Aquifer Conservation District, 2003).

Baseflow – groundwater flow to a surface-water body (lake, swamp, or stream).

Bedrock – consolidated rock at various depths beneath the Earth's surface.

Boundary condition – specified conditions at the edges or surfaces of a groundwater system.

Model calibration- involves changing input parameters until the model results match field (measured) observations.

Coefficient of determination (R^2) – percentage of variation of the dependent variable that is explainable by the regression line.

Conceptual model – clear, qualitative physical description of how a hydrogeological system behaves.

Conduit – high-permeability pathway most commonly associated with dissolution features.

Cross-formational flow – vertical groundwater flow from one hydrostratigraphic unit to another.

Diagenesis – process that alters sediment with its burial; temperatures are low, definitely less than metamorphic ($^{\circ}\text{C}$).

discharge – (1) volumetric flow rate [$\text{L}^3 \text{t}^{-1}$] of a stream, spring, or groundwater system; (2) water leaving a groundwater system.

Mean discharge – arithmetic mean of discharges over a given time period.

Divide – topographic high (or ridge) separating surface watersheds (catchments). A groundwater divide is an elevated area, line, or ridge of the potentiometric surface separating different groundwater flow systems.

Domestic use – water used by, and connected to, a household for personal needs or for household purposes, such as drinking, bathing, heating, cooking, sanitation or cleaning, and landscape irrigation. Ancillary use may include watering of domestic animals (Barton Springs/Edwards Aquifer Conservation District, 2003).

Double (or dual) porosity – when two porosities may be associated with a hydrogeological system. An example is a porous rock with a fracture set; such a system may then have two.

Drawdown (s) – drop in head from the initial head caused by pumping from a well or set of wells.

Drought – prolonged period of low (lower than average) rainfall. For the purposes of this study, drought corresponds to a prolonged period of low recharge, water-level elevations, and spring discharge values.

Drought of record (1950's drought) – worst drought on record for Central Texas, which occurred from 1950 through 1957.

Equipotential – line connecting points of equal hydraulic potential or hydraulic head.

Exempt well – well may be exempt if it is (Barton Springs/Edwards Aquifer Conservation District, 2003):

1. used solely to supply the domestic needs of five or fewer households, and a person who is a member of each household is either the owner of the well, a person related to the owner, or a member of the owner's household within the second degree by consanguinity, or an employee of the owner, which is drilled, completed, or equipped so that it is incapable of producing more than 10,000 gallons of groundwater a day on a tract of land larger than 10 acres; or
2. used to provide water for livestock or poultry, which is drilled, completed, or equipped so that it is incapable of producing more than 10,000 gallons of groundwater a day on a tract of land larger than 10 acres.

Fault – fracture that has experienced translation or movement of the fracture walls parallel to the plane of the fracture.

Flow path – path a molecule of water takes in its movement through a porous medium.

Formation – body of rock strata that consists of a certain lithology or combination of lithologies.

Fracture – subplanar discontinuity in a rock or soil formed by mechanical stresses.

Fresh water – water with a salinity <1,000 mg/L; drinkable or potable water is implied.

Groundwater availability modeling (GAM) – initiative by the Texas Water Development Board to develop state-of-the-art, publicly available, numerical groundwater flow models for aquifers in Texas.

Groundwater – generally all water beneath the land surface. Sometimes, it is more narrowly defined as phreatic water or water beneath the water table.

Head (h) – fluid mechanical energy per unit weight of fluid, which correlates to the elevation that water will rise to in a well [L]. Also hydraulic head.

Heterogeneity – condition in which the property of a parameter or a system varies with space.

Hydraulic conductivity (K) – volume of fluid that flows through a unit area of porous medium for a unit hydraulic gradient normal to that area.

Hydraulic head (h) – elevation in a well in reference to a specific datum; the mechanical energy per unit weight of water [L].

Hydrostratigraphic unit – formation, part of a formation, or group of formations of significant lateral extent that compose a unit of reasonably distinct (similar) hydrogeologic parameters and responses.

Isopach map – map indicating, usually by means of contour lines, the varying thickness of a designated stratigraphic unit.

Karst – geologic terrain with distinctive characteristics of relief and drainage arising primarily from dissolution of rock (or soils) by natural waters. Such terrains are underlain by rocks that have undergone significant dissolution by groundwater flow.

Kriging – geostatistical method of contouring using weighted averages of surrounding data points.

Leakage – flux of fluid from or into an aquifer or reservoir. Commonly refers to cross-formational flow.

MODFLOW – finite-difference, numerical model for groundwater flow developed by the U.S. Geological Survey.

Observation (monitor) well – well that is used to measure the elevation of the water table or the potentiometric surface.

Outcrop – point at which a formation is present at the Earth’s surface.

Parameter – (1) defined physical quantity with a numerical value or a value within a certain range; (2) characteristic of a population (e.g., the mean).

Permeability – ease with which a porous medium can transmit water or other fluids.

Permit or pumpage permit – authorization issued by the District allowing withdrawal of a specific amount of groundwater from a nonexempt well for a designated period of time, generally in the form of a specific number of gallons per District fiscal year. Under normal or nondrought conditions, this volume of water may be pumped at any time during the course of the fiscal year at the convenience of and based on the needs of the permittee. However, during times of District-declared drought, monthly pumpage target-reduction goals for specific drought stages are designated in the permittee’s UDCP. Achieving these target-reduction goals may result in a permittee pumping less than the permittee’s annual permitted pumpage volume (Barton Springs/Edwards Aquifer Conservation District, 2003).

Porosity – volume of voids divided by total volume of a porous medium.

Potential – potential energy per unit mass of fluid.

Public water supply well – well providing groundwater for public water-supply use; nonexempt well (Barton Springs/Edwards Aquifer Conservation District, 2003).

Potentiometric surface – surface of equal hydraulic heads or potentials, typically depicted by a map of equipotentials, such as a map of water-table elevations.

Precipitation – (1) water condensing from the atmosphere and falling in drops or particles (e.g., snow, hail, sleet) to the land surface; (2) formation of a solid from dissolved or suspended matter.

Pump or pumping test – one of a series of techniques to evaluate the hydraulic properties of an aquifer by observing how water levels change with space and time when water is pumped from the aquifer.

Recharge – process by which water enters the groundwater system or, more precisely, the phreatic zone.

Recharge zone – area of the aquifer in which water infiltrates the surface and enters permeable rock layers (Barton Springs/Edwards Aquifer Conservation District, 2003).

Root mean square (RMS) – statistical measure of the magnitude of a set of numbers.

Safe yield- volume of water that can be annually withdrawn from an aquifer (or groundwater basin or system) without (1) exceeding average annual recharge, (2) violating water rights, (3) creating uneconomic conditions for water use, or (4) creating undesirable side effects, such as subsidence or saline water intrusion.

Saturation – state that occurs when all pores are filled with water.

Sinkhole – closed depression in a karstic landscape.

Specific capacity – discharge of a well divided by drawdown in the well. Note that specific capacity can depend on the pumping rate.

Specific storage (S_s) – volume of water released per unit volume of aquifer for a unit decrease in hydraulic head.

Specific yield (S_y) – volume of water that a saturated porous medium can yield by gravity drainage divided by volume of the porous medium.

Spring – point(s) of natural discharge from an aquifer (Barton Springs/Edwards Aquifer Conservation District, 2003).

Storage – water contained within an aquifer or within a surface-water reservoir.

Storativity (S) – volume of water released per unit area of aquifer for a unit decline in head. In a confined aquifer, S is the specific storage (S_s) times aquifer thickness; in an unconfined aquifer, S is equal to the specific yield (S_y) or the effective porosity.

Tracer – usually a solute, suspended matter, or heat that is artificially or naturally induced to evaluate rate and direction of groundwater flow.

Transient – condition in which properties of a system vary with time.

Transmissivity (T) – discharge through a unit width of the entire saturated thickness of an aquifer for a unit hydraulic gradient normal to the unit width, sometimes termed the coefficient of transmissibility [$L^2 t^{-1}$, gpd/ft].

Transport – movement of solute, suspended matter, or heat in a porous medium, in a surface stream, or through the atmosphere.

Trinity Group aquifer – includes the Upper Member of the Glen Rose Formation, known as the Upper Trinity; the Lower Member of the Glen Rose Formation, and the Hensell Sand and Cow Creek Limestone Members of the Travis Peak Formation, known as the Middle Trinity; and the Sligo and Hosston Members of the Travis Peak Formation, known as the Lower Trinity (Barton Springs/Edwards Aquifer Conservation District, 2003).

Unconfined – refers to an aquifer that has a water table and implies direct contact from the water table to the atmosphere (through the vadose zone).

Unsaturated – condition when porosity is not completely filled with water.

Water table – a surface at or near the top of the phreatic zone (zone of saturation) where the fluid pressure is equal to atmospheric pressure. In the field this is defined by the level of water in wells that barely penetrate the phreatic (saturated) zone.

Well – any artificial excavation or borehole constructed for the purposes of exploring for or producing groundwater or for injection, monitoring, or dewatering purposes (Barton Springs/Edwards Aquifer Conservation District, 2003).

Well log – accurately kept record, made during the process of drilling, on forms prescribed by the Water Well Drillers Team, showing the depth of the well bore, thickness of the formations, and character of casing installed, together with any other data or information required by the Water Well Drillers Team; or any other special-purpose well log that may be available for a given well, such as a gamma-ray log, a temperature log, an electric log, or a caliper log (Barton Springs/Edwards Aquifer Conservation District, 2003).

Well yield – discharge of well at (nearly) steady flow [$L^3 t^{-1}$].

Yield – generically, the amount of water pumped from a well (or bore). In Australia, there is a narrower definition—maximum sustainable pumping rate such that the drawdown in a well after 24 hours does not exceed a specified percentage (typically ~2%) of the column of water above the base of the aquifer. It assumes that the well is fully penetrating and screened over all permeable intervals of the aquifer. Units of yield are volume per time [$L^3 t^{-1}$].

GLOSSARY REFERENCES

Barton Springs/Edwards Aquifer Conservation District, 2003, Rules and Bylaws of the Barton Springs Edwards Aquifer Conservation District, adopted August 2003.

Davis, S. N., and DeWiest, R. J. M., 1966, Hydrogeology: New York, John Wiley, 463 p.

Fetter, C. W., 1994, Applied Hydrogeology (3rd ed.): New York, MacMillan College Publishing Co., 691 p.

Freeze, R. A., and Cherry, J. A., 1979, Groundwater: Englewood Cliffs, Prentice-Hall, 604 p.

Lapedes, D. N., ed., 1978, Dictionary of Scientific and Technical Terms: New York, McGraw-Hill Book Co., 1771 p.

Meinzer, O. E., 1923, Outline of Ground-Water Hydrology: U.S. Geological Survey Water-Supply Paper 494, 71 p.

Morgan, S., 1995, *Ecology and Environment: The Cycles of Life*: New York, Oxford University Press, 160 p.

Pfannkuch, H. O., 1969, *Dictionary of Hydrogeology*: Amsterdam, Elsevier.

Poland, J. F., Lofgren, B. E., and Riley, F. S., 1972, *Glossary of selected terms useful in studies of the mechanics of aquifer systems and land subsidence due to fluid withdrawal*: U.S. Geological Survey Water-Supply Paper 2025, 9 p.

Soliman, M. M., LaMoreaux, P. E., Memon, B. A., Assaad, F. A., and LaMoreaux, J. W., 1998, *Environmental Hydrogeology*: Boca Raton, FCRC Press LLC, 386 p.

Stanger, G., 1994, *Dictionary of Hydrology and Water Resources*: Adelaide, Australia, Center for Groundwater Studies.

Wilson, W. E., and Moore, J. E., 1998, *Glossary of Hydrology*: Alexandria, VA, American Geological Institute, 2489 p.

TABLES

Table 3-1. Comparison of measured and simulated water-level values and residuals from the 2001 GAM and recalibrated model.

State well number	Lowest measured elevation*	Measure date	2001 GAM simulation*	Water-level residual (ft)	Recalibrated model simulation*	Water-level residual (ft)
5842911	428	Aug-56	441.7	-13.7	435	-7
5850301	459	Aug-56	443	16	453	6
5850801	521	Jul-56	445	76	519	2
5858101	561	Aug-56	473	88	583	-22
5857903	563	Aug-56	486	77	597	-34
5850502	487	Aug-56	452	35	482	5
5850702	626	Aug-56	476	150	590	36
5850412	650	Aug-78	585	65	653	-3
5857301	595	Aug-56	492	103	598	-3
5857204	643	Dec-50	513	130	624	19

*Elevation in ft above mean sea level

Table 3-2. Comparison of hydraulic conductivity (K) for the 2001 GAM and recalibrated GAM.

Original K (ft/day) 2001 GAM	Revised K (ft/day) recalibrated GAM	% Change
3	0.3	-90%
4.5	0.8	-82%
3.5	1.7	-51%
1	0.5	-50%
93	40	-57%
93	25	-73%
100	75	-25%
39	80	+105%
320	60	-81%
320	192	-40%
1236	740	-40%
39	12	-69%

Table 4-1. Composite potentiometric data.

SWN	Measurement date	Latitude	Longitude	WL elevation (feet above msl)
58-42-607	1/1/1951	30.30139	-97.77194	434.40
58-42-809	2/16/1949	30.26583	-97.80972	421.10
58-42-901	3/7/1955	30.27583	-97.77917	421.20
58-42-903	3/15/1957	30.2633	-97.77124	424.51
58-42-910	2/1/1955	30.27695	-97.78972	428.00
58-42-924	8/1/1949	30.28667	-97.76972	443.40
58-49-802	1/26/1981	30.12825	-97.92657	802.56
58-49-904	4/10/1980	30.13611	-97.88084	594.00
58-50-101	3/19/1952	30.22583	-97.86916	670.74
58-50-104	6/25/1940	30.23611	-97.84444	527.87
58-50-105	10/4/1939	30.23417	-97.85056	581.20
58-50-201	3/9/1956	30.21958	-97.79373	432.29
58-50-205	9/5/1939	30.23111	-97.80556	430.88
58-50-208	3/1/1955	30.21861	-97.82083	458.00
58-50-218	8/1/1978	30.2425	-97.79723	441.00
58-50-301	8/31/1956	30.21035	-97.78159	459.46
58-50-406	8/11/1978	30.19674	-97.84316	532.56
58-50-411	8/18/1978	30.1867	-97.85	554.95
58-50-416*	7/9/2001	30.1766	-97.86723	539.60
58-50-502	8/31/1956	30.18694	-97.81416	486.72
58-50-511	6/30/1956	30.17159	-97.82578	478.59
58-50-701	11/29/1949	30.13722	-97.84778	515.45
58-50-702	8/31/1956	30.14778	-97.87334	626.09
58-50-704	8/14/1978	30.13694	-97.85555	524.67
58-50-7DT*	7/9/2001	30.15528	-97.86182	535.55
58-50-801	8/29/1956	30.14281	-97.81076	531.14
58-50-804	2/10/1949	30.16159	-97.82873	493.86
58-50-808	6/27/1939	30.12556	-97.79972	559.49
58-50-814	3/21/1955	30.14056	-97.79694	552.60
58-50-817	1/1/1956	30.14	-97.83222	500.00
58-50-839	8/14/1978	30.12972	-97.82166	547.64
58-50-902	11/1/1954	30.14139	-97.75777	480.00
58-57-201	12/28/1982	30.10278	-97.93694	748.40
58-57-204	12/5/1950	30.08361	-97.91805	636.60
58-57-301	8/28/1956	30.09389	-97.89139	594.80
58-57-3DB	9/15/1999	30.11445	-97.91221	666.51
58-57-502	5/24/1978	30.06635	-97.94447	675.52
58-57-5JM	3/31/1952	30.04722	-97.95139	710.07
58-57-902	8/29/1956	30.00833	-97.895	567.37
58-57-903	8/28/1956	30.0385	-97.88617	560.14
58-57-905	1/3/1951	30.02667	-97.90361	559.70
58-57-9LN	3/27/1952	30.02583	-97.87833	557.10
58-58-101	8/28/1956	30.08358	-97.84264	562.03
58-58-104	10/24/1950	30.10417	-97.84861	549.10

Table 4-1 continued				
SWN	Measurement date	Latitude	Longitude	WL elevation (feet above msl)
58-58-301	8/29/1956	30.09194	-97.78917	554.39
58-58-4JH	3/27/1952	30.06694	-97.85861	570.98
58-58-4PR	11/8/1950	30.04972	-97.86777	566.33
58-58-502	1/9/1951	30.05083	-97.80722	554.40
58-58-7LN	2/26/1952	30.02972	-97.85472	551.87
67-01-3CC	3/26/1952	29.97111	-97.89222	574.50
67-01-3OG	3/26/1952	29.98228	-97.89149	574.30
67-01-3WL	8/31/1954	29.98917	-97.89139	574.00
67-01-6EN	3/26/1952	29.93083	-97.90444	570.91
67-01-807	2/2/1940	29.90083	-97.91917	570.89
67-01-809	11/14/1950	29.91195	-97.92861	574.60
67-02-101	3/26/1952	29.98139	-97.865	568.30

**Water level adjusted 34 ft from well 5850702*

Table 4-2. Simulated drawdown in wells under 1950's drought conditions and various pumping scenarios.

SWN	Water-level drawdown (ft)			
	5 cfs	10 cfs	15 cfs	19 cfs
5842914	1	2	3	16
5842915	2	5	7	21
5849802	5	11	16	20
5849935	26	29	31	30
5850211	5	12	17	26
5850212	6	13	19	34
5850215	6	13	19	33
5850216	4	9	14	28
5850222	7	17	25	40
5850301	7	15	22	38
5850406	14	31	44	56
5850408	13	27	37	45
5850412	11	23	31	38
5850413	14	28	38	46
5850501	21	47	70	96
5850502	16	35	52	74
5850511	21	47	70	95
5850520	8	18	27	43
5850701	32	75	112	151
5850702	32	55	74	87
5850704	33	76	114	151
5850801	29	67	101	135
5857201	11	23	30	35
5857204	38	84	113	128
5857301	42	97	145	187
5857502	25	43	47	49
5857602	38	82	107	114
5857903	48	115	183	246
5858101	48	113	178	241
5858102	43	101	156	211
5858104	43	100	155	209
5858123	41	96	148	200
5858406	48	115	182	246
5858704	49	115	184	245
58501NF	9	20	29	31
58502B2	4	10	15	29
58572R2	36	77	104	119
58573BW	19	41	54	64
58573JD	41	95	141	179
58573SW	16	33	44	52

Table 4-3. Saturated aquifer thickness analysis under 1950's drought conditions and various rates of pumping.

Pumping rate (cfs)	0.66*	5	10	15	19
Total number wells west of the 100-ft saturated-thickness contour	230	267	291	330	408
Number of wells with high probability of insufficient yield**	30	35	38	43	53

*1950's drought pumping;

**Based on 13% of wells with low specific capacity ($S_c=0.17$; $Q=15.9$ gpm)

Table 4-4. Saturated borehole analysis under 1950's drought conditions and various rates of pumping.

Pumping rate	0.66*	5	10	15	19
Number of wells with high probability of insufficient yield**	43	74	151	216	347

*1950's drought pumping;

**Based on wells with <25 ft saturated thickness

Table 4-5. Total impact to wells under 1950's drought and various rates of pumping.

Pumping rate	0.66*	5	10	15	19
Total number of Impacted wells	73	109	189	259	400
Percentage of total wells (n=971)	7	11	19	27	41

*1950's drought pumping

FIGURES

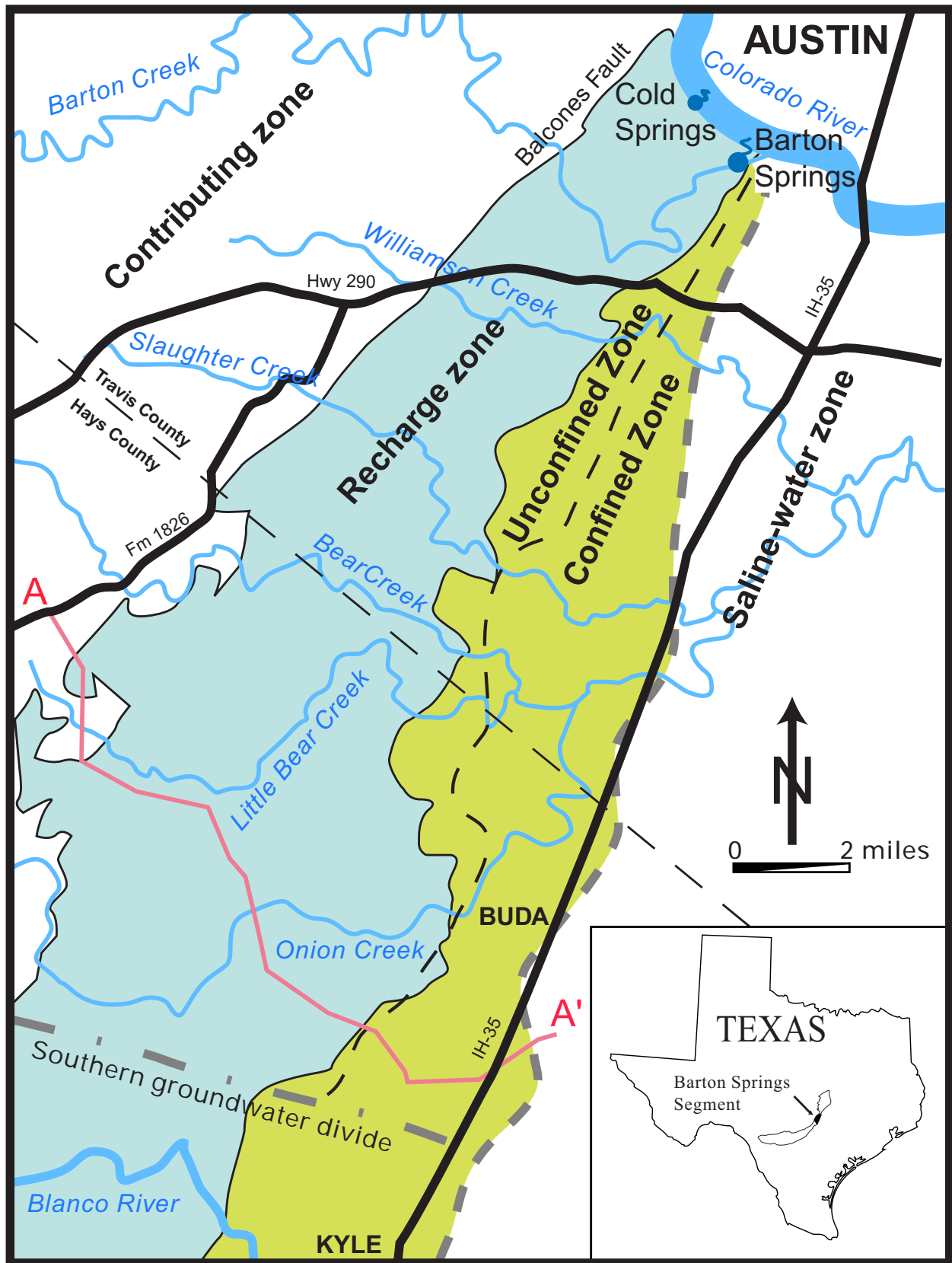


Figure 2-1. Location map of the study area. Note: shaded area is the Edwards Aquifer.

Hydrogeologic Cross Section A-A' of the Barton Springs Segment of the Edwards Aquifer, Hays County, Texas

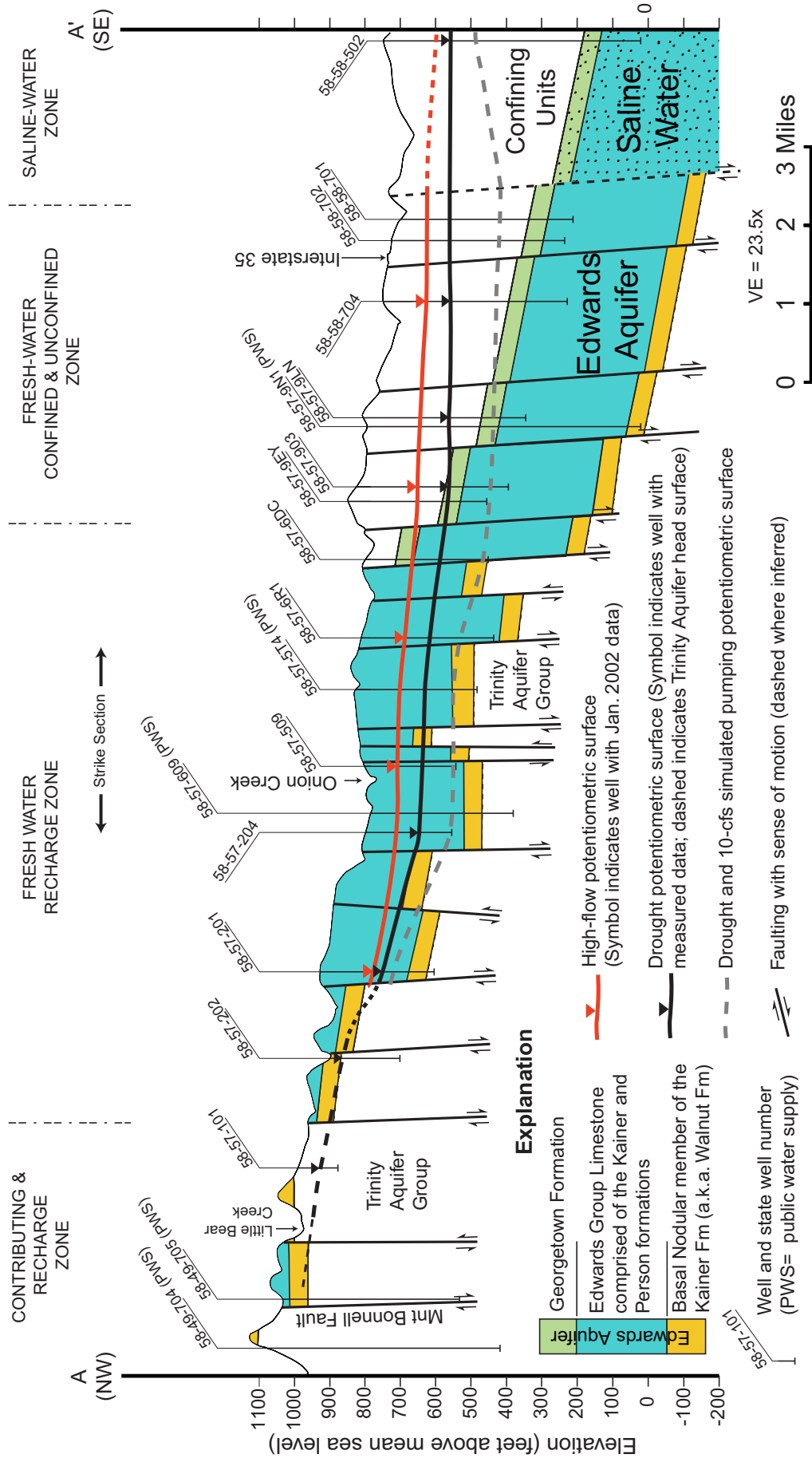


Figure 2-2. Cross section of the Barton Springs and Trinity Aquifers in Hays County (see Figure 2-1).

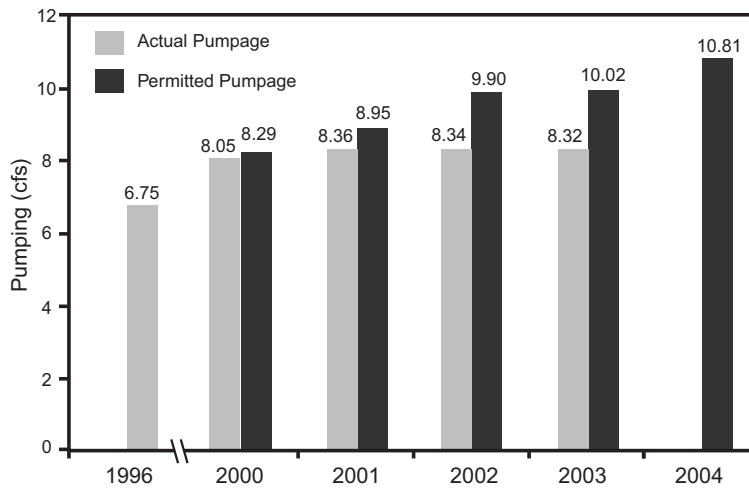


Figure 2-3. Histogram of permitted and actual pumping from the Barton Springs aquifer.

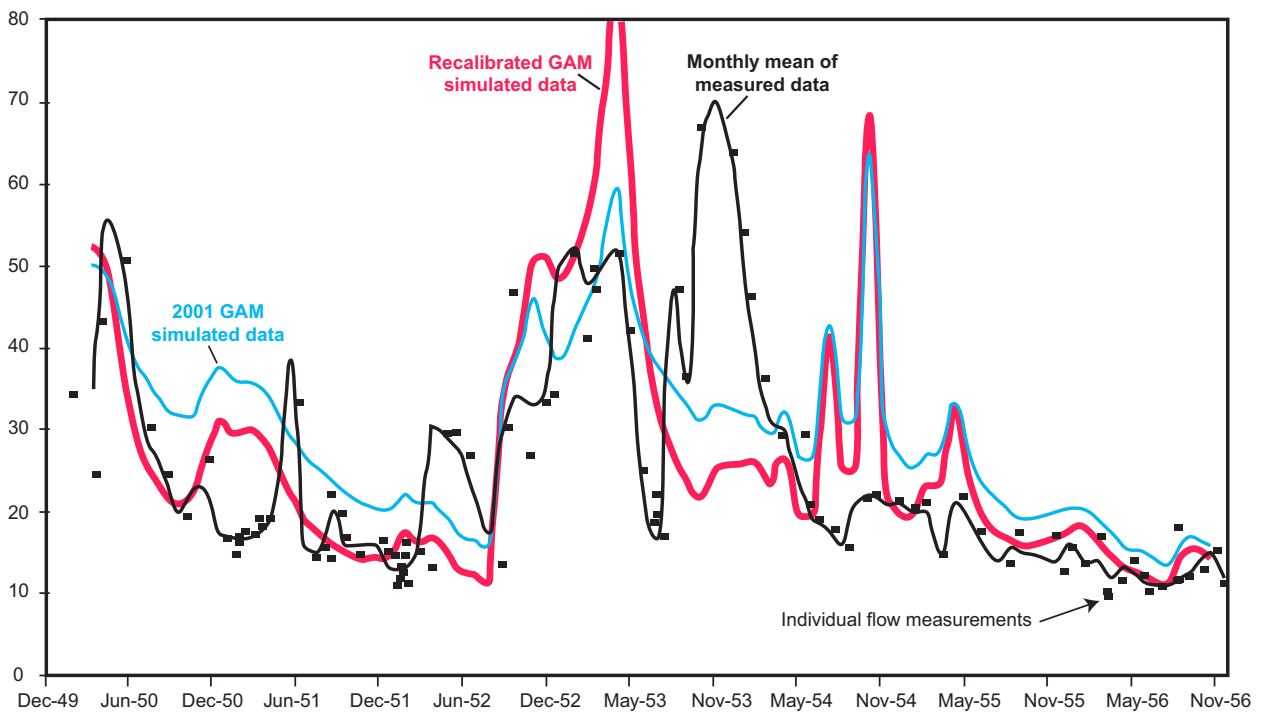


Figure 3-1. Hydrograph of simulated and measured spring flow discharge from 1950's drought. Note: lowest individual measured value (arrow) 9.6 cfs. Both simulations were run with 0.66 cfs pumping.

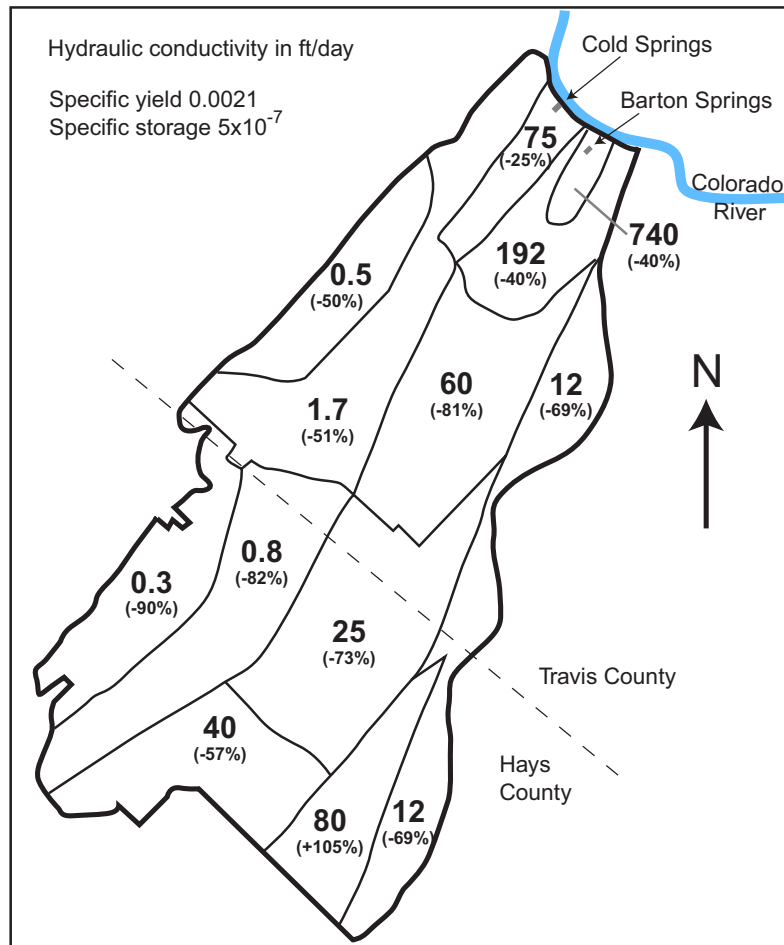


Figure 3-2. Map of zonal distribution of hydraulic conductivity (ft/day) in the recalibrated GAM model. Note: percent change from 2001 GAM values shown in parentheses (see Table 3-2).

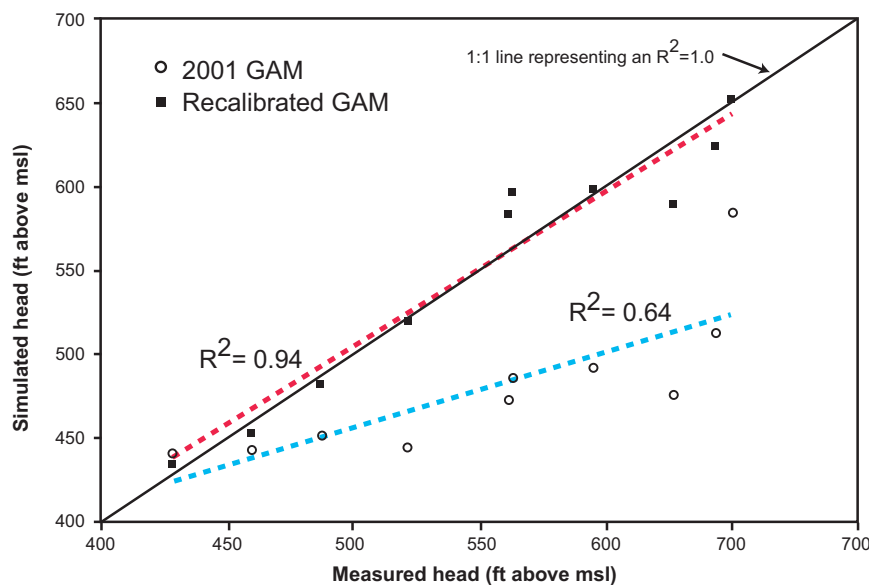


Figure 3-3. Scatter plot of the simulated results from the 2001 GAM and recalibrated GAM plotted against measured low-flow 1950's water levels. See Table 3-1.

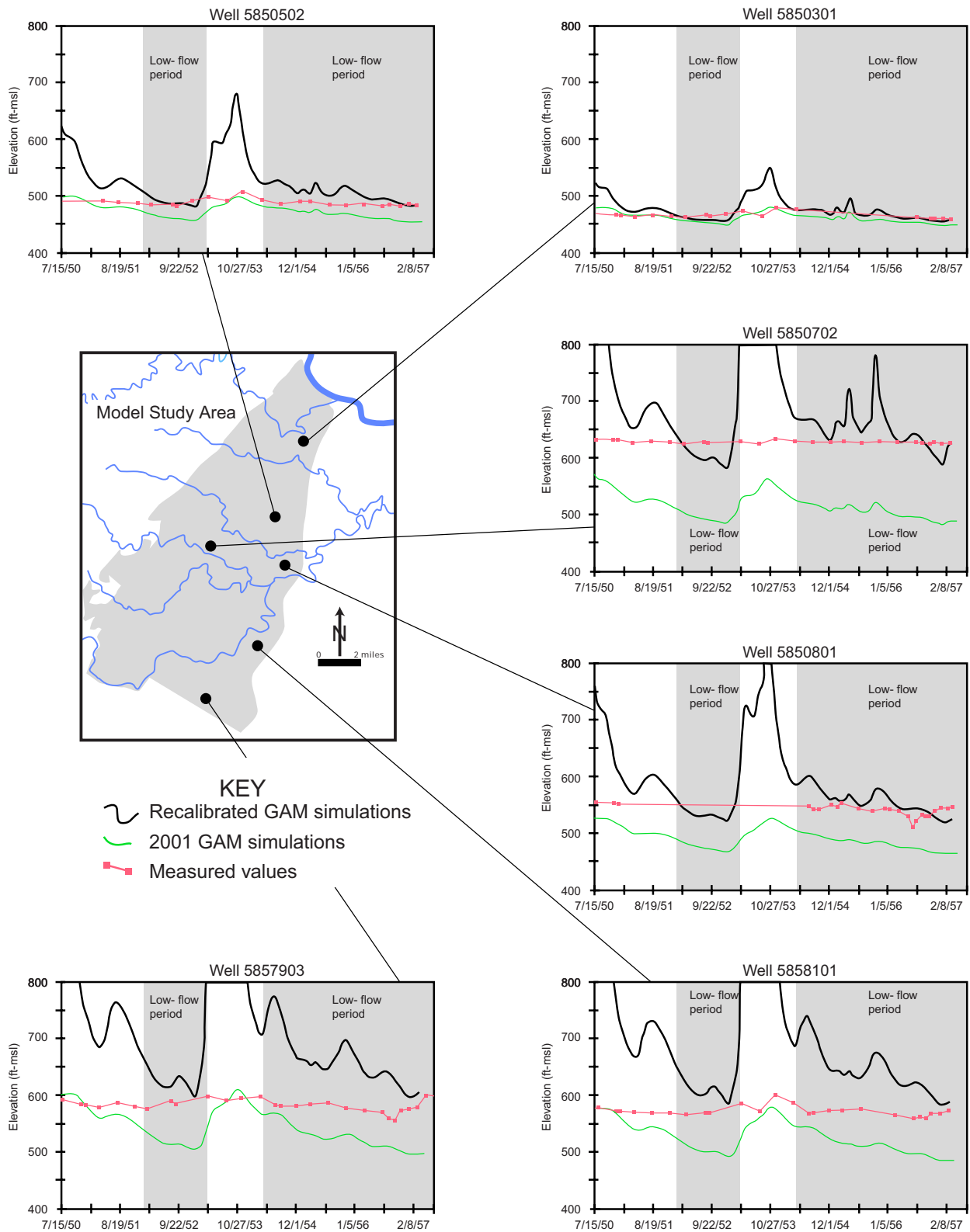


Figure 3-4. Comparison of simulated and measured water-level elevation hydrographs from the study area. Recalibration of the GAM was to the low-flow periods (shaded area) of the 1950's drought.

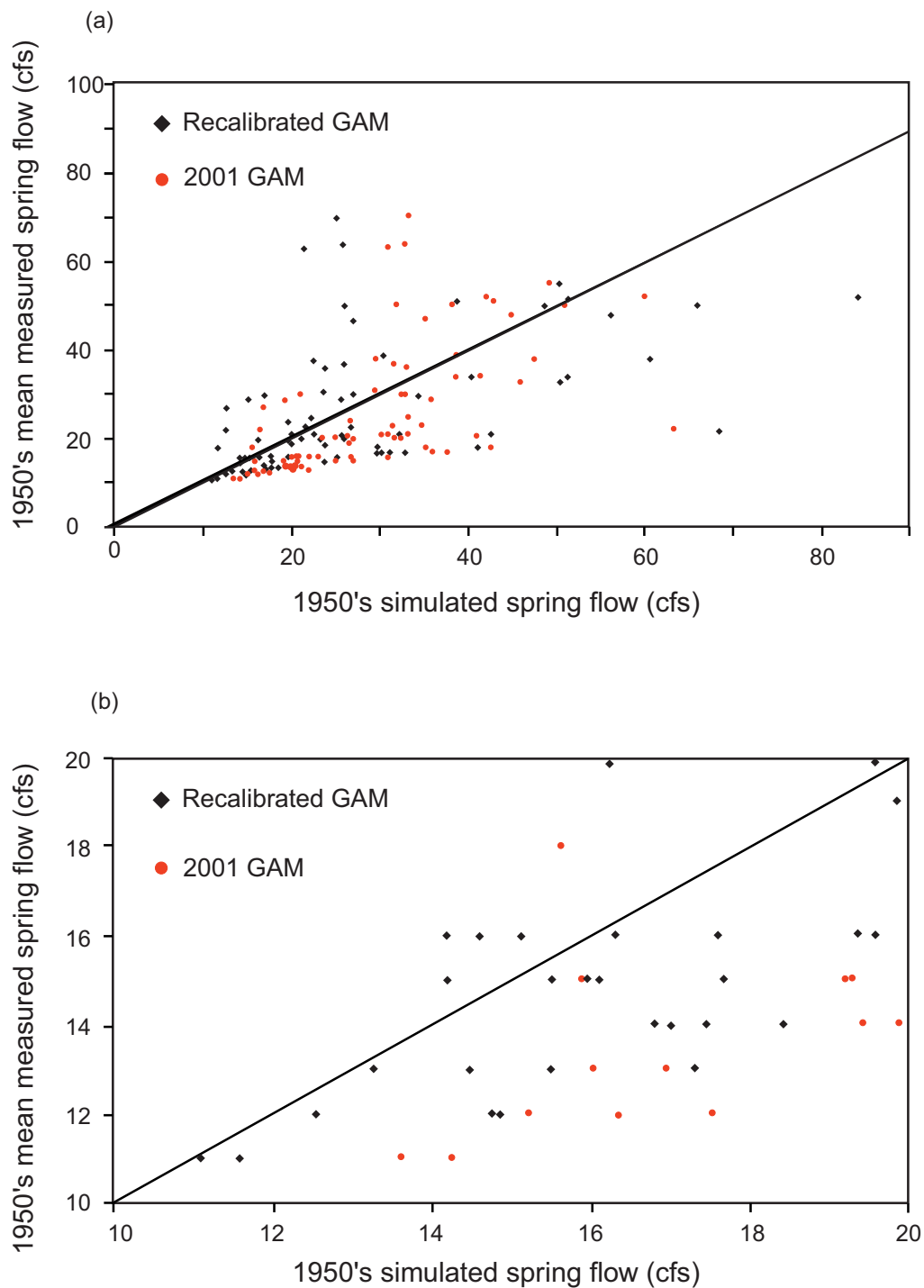


Figure 3-5. Scatter plot of spring-flow simulations from the 2001 and the recalibrated GAMs and mean of measured spring-flow values for (a) all flow conditions and (b) low-flow conditions.

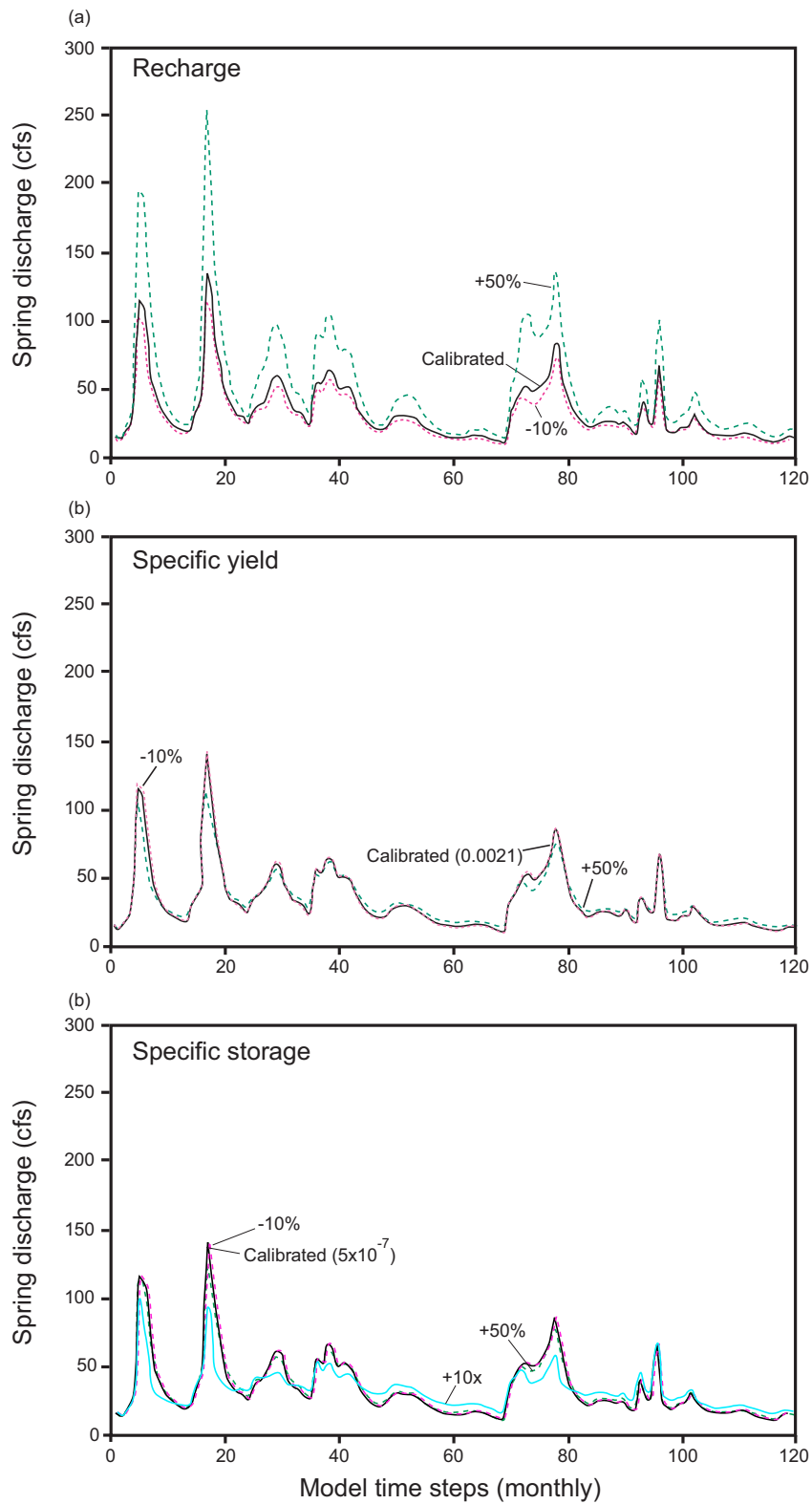


Figure 3-6. Sensitivity of transient simulated spring discharge to (a) recharge, (b) specific yield, and (c) specific storage.

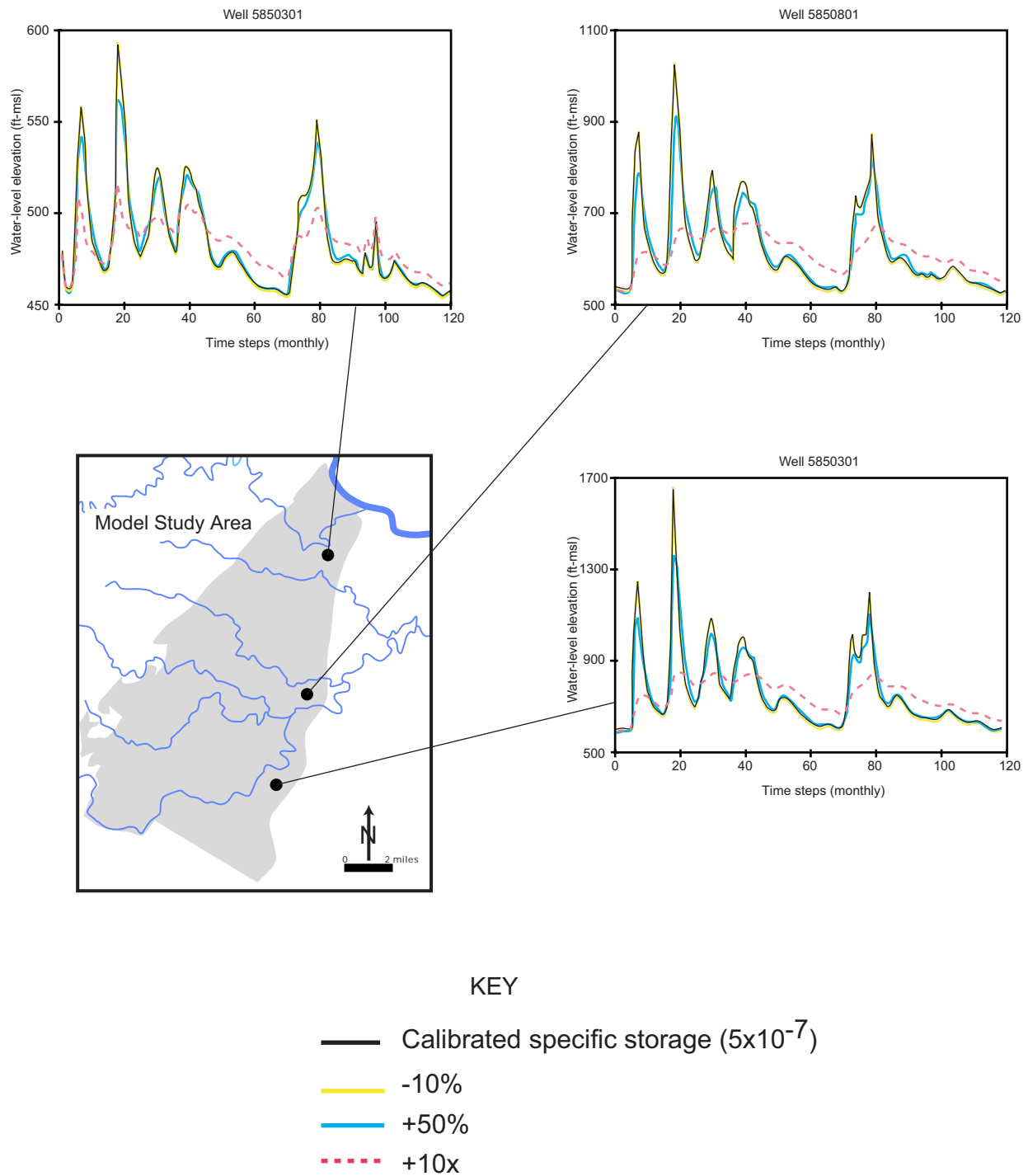


Figure 3-7. Sensitivity of transient calibration water levels to specific storage.

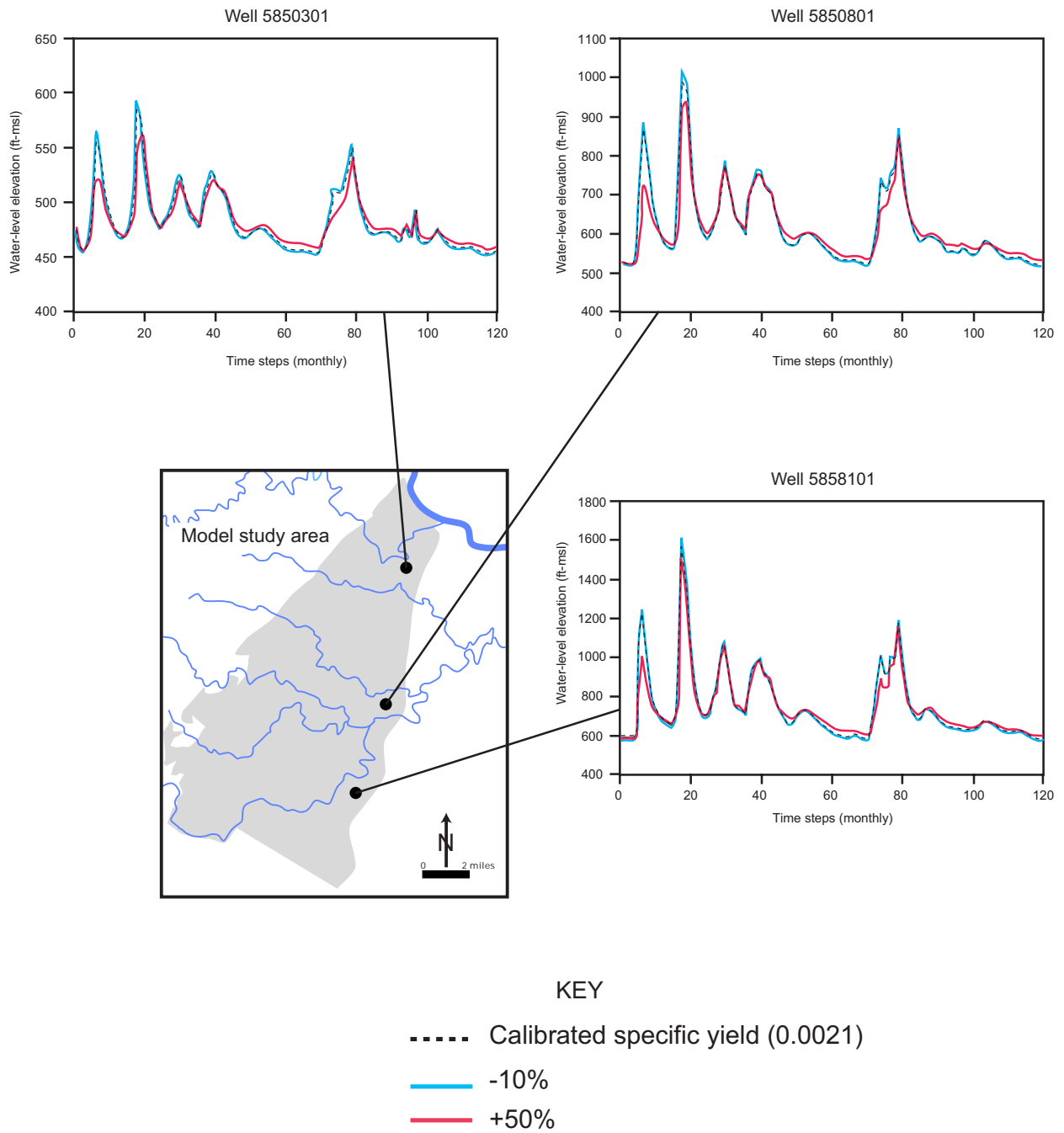


Figure 3-8. Sensitivity of transient calibration water levels to specific yield.

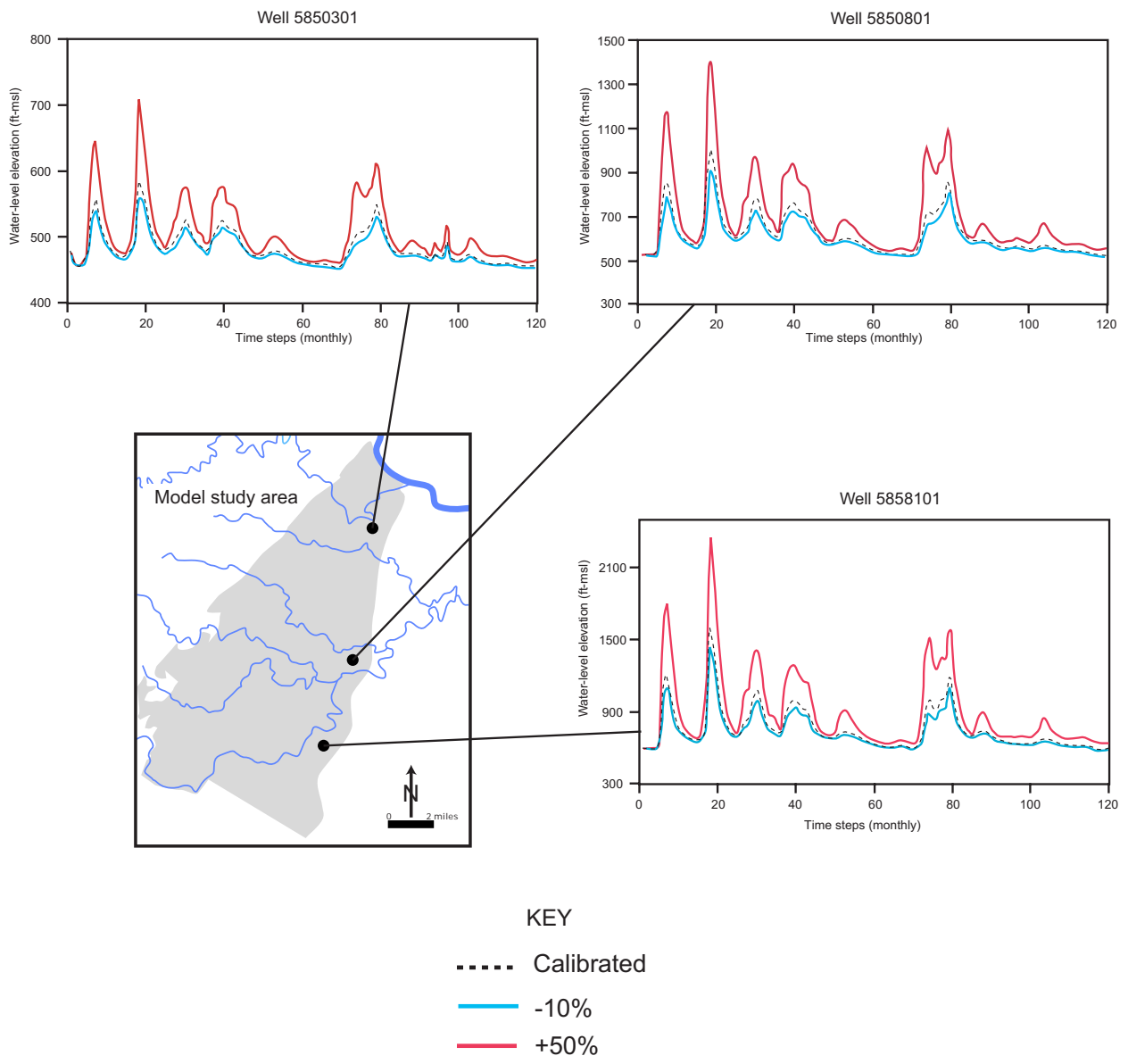


Figure 3-9. Sensitivity of transient calibration water levels to recharge.

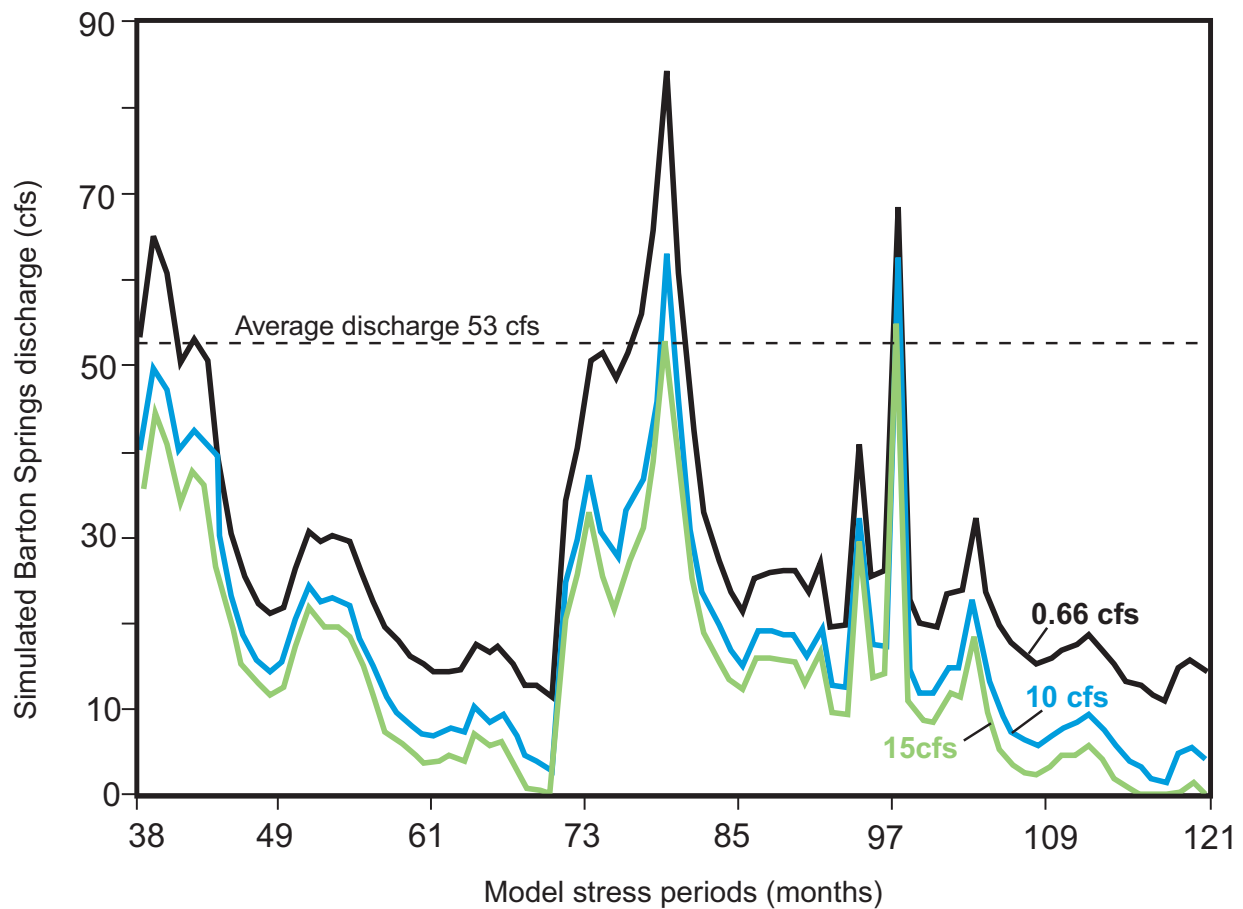


Figure 3-10. Hydrograph of simulated spring flow under 1950's drought conditions and 0.66, 10, and 15 cfs pumping rates.

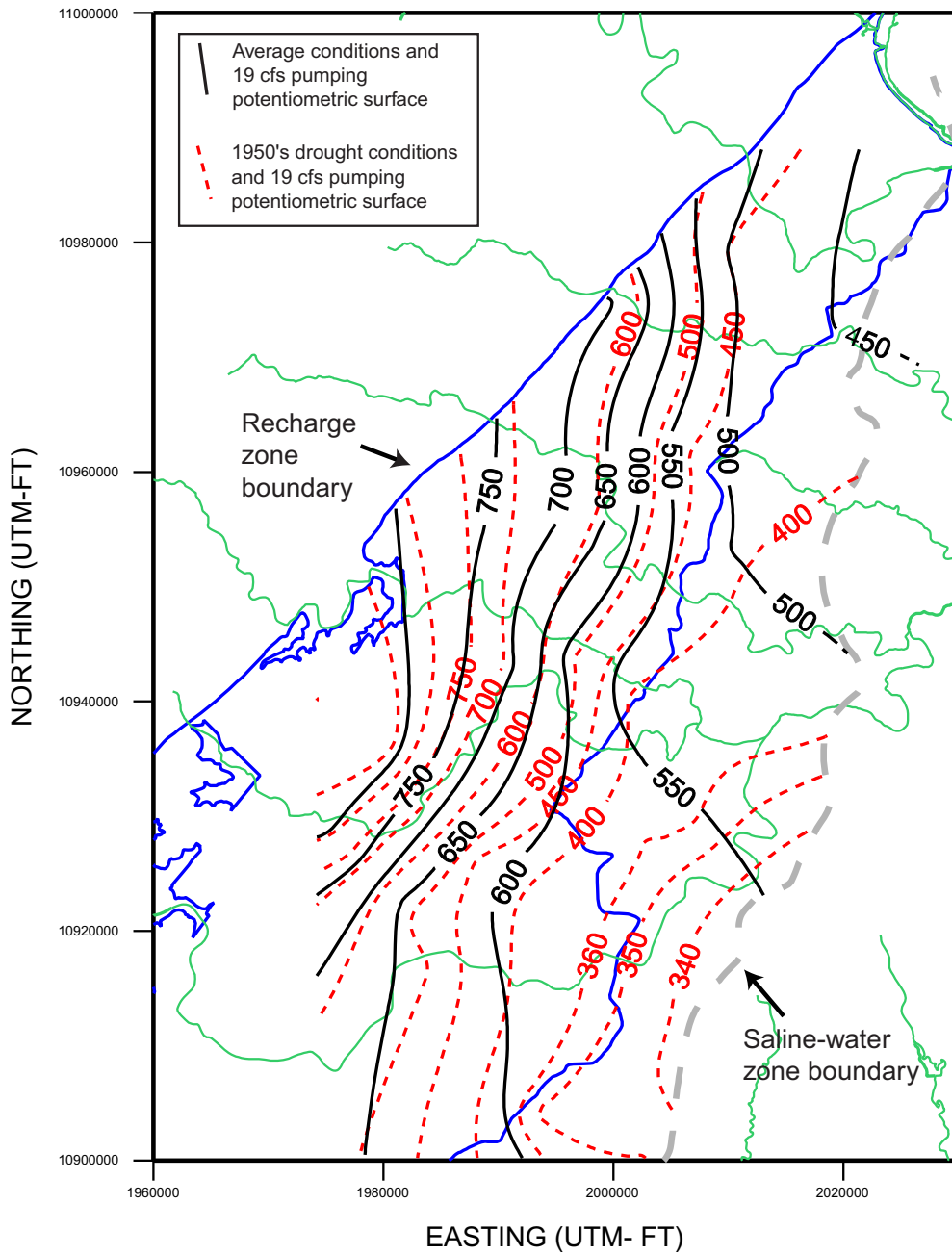


Figure. 3-11. Simulated potentiometric surface contour map under average conditions and 19 cfs of pumping (solid lines) and 1950's drought conditions with 19 cfs pumping (dashed lines). Springflow is 36 cfs and 0 cfs, respectively, at the end of simulations for each scenario .

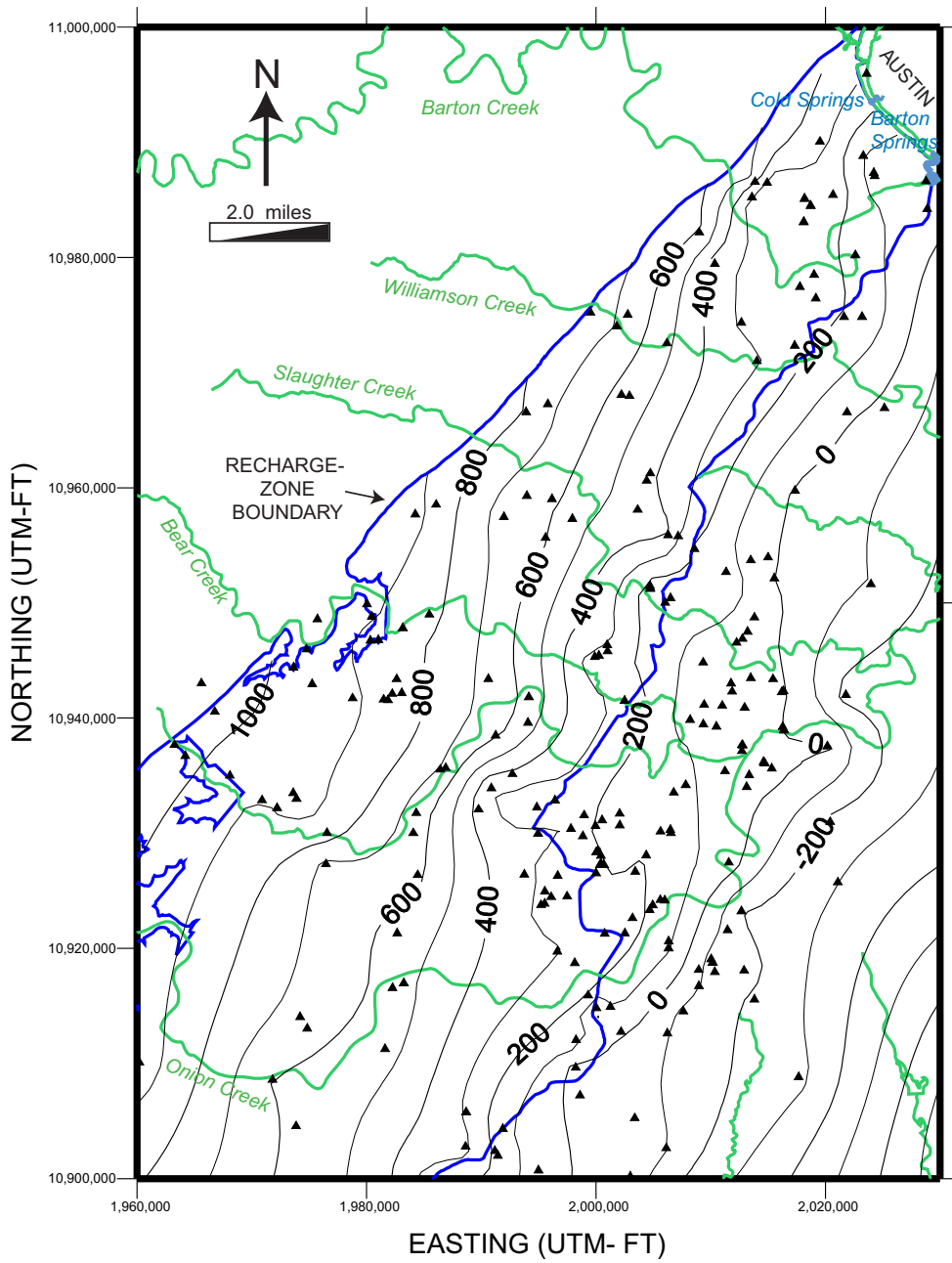


Figure 4-1. Structure contour of the elevation (ft-msl) of the bottom of the Edwards Aquifer. Note: control points shown as triangles.

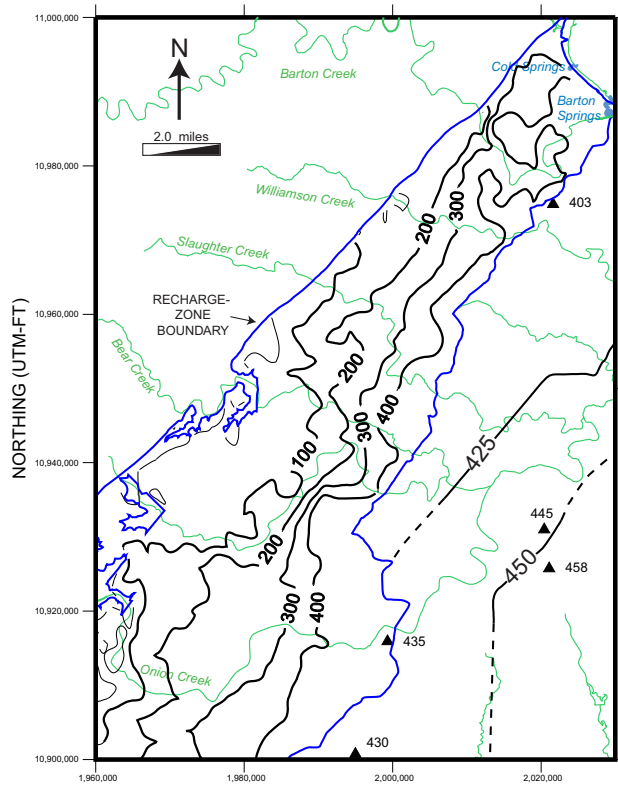


Figure 4-2. Isopach (thickness) map of the Edwards Aquifer. Note: triangles are fully-penetrating wells. Thickness contours are in ft.

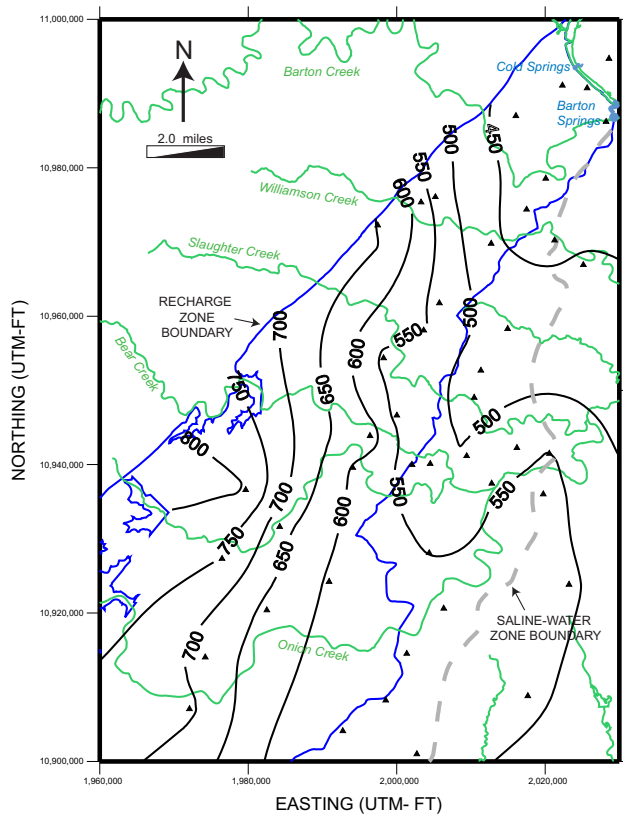


Figure 4-3. Potentiometric map of the Edwards Aquifer under 1950's drought conditions. Note: triangles indicate data locations. Contours are in ft above msl.

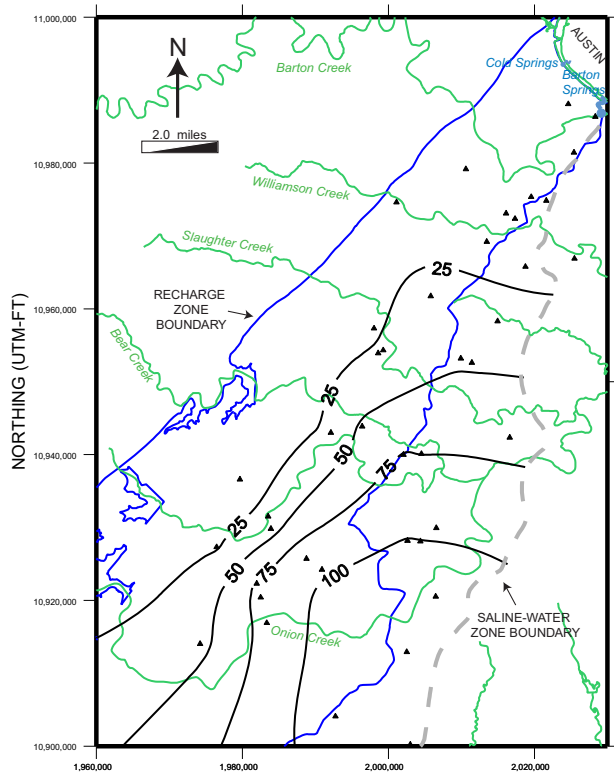


Figure 4-4. Simulated drawdown from pumping 10 cfs at the end of the 10-yr simulation. Note: contours are in ft of drawdown.

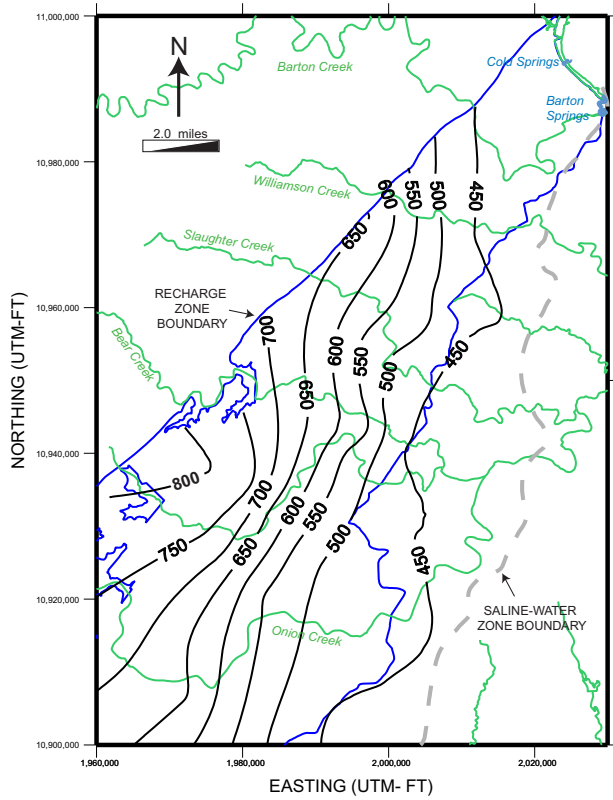


Figure 4-5. Potentiometric map of 1950's drought conditions and 10 cfs pumping. Note: contours are in ft above msl.

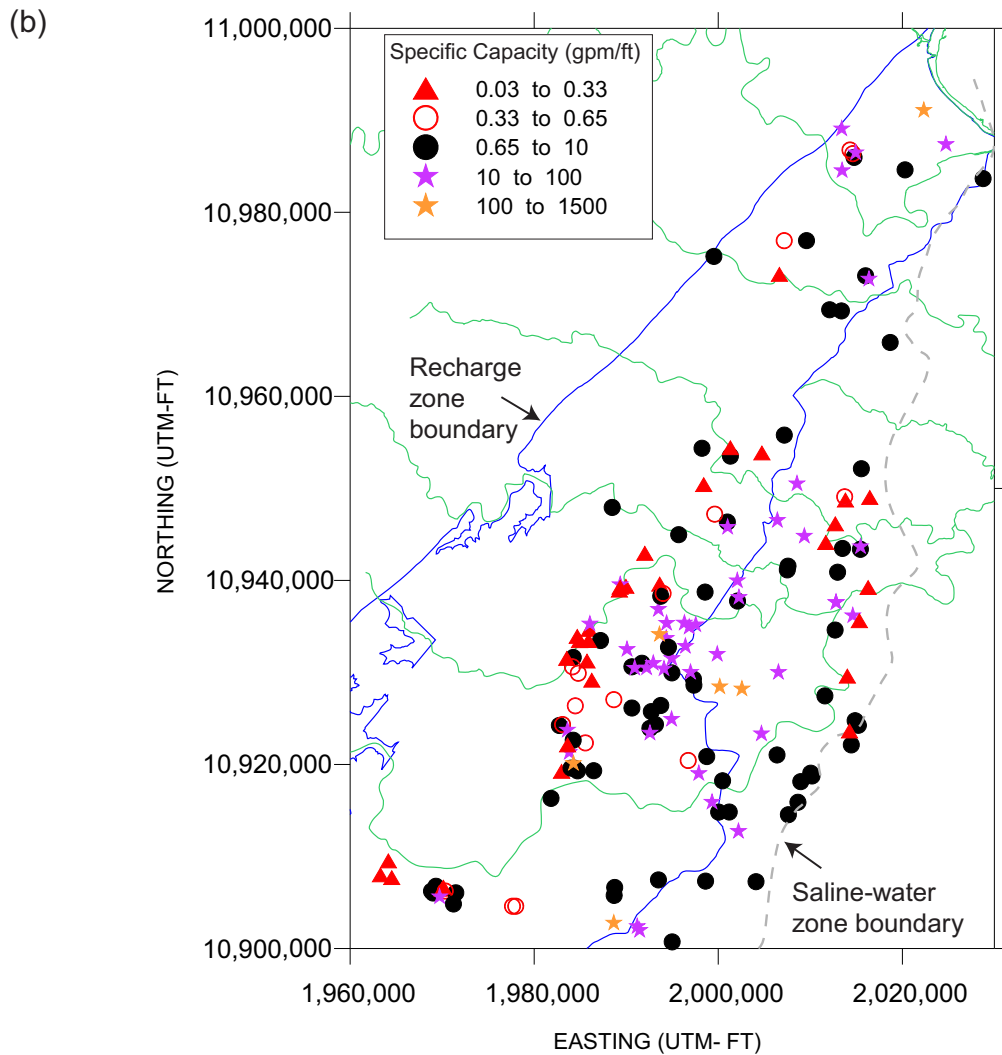
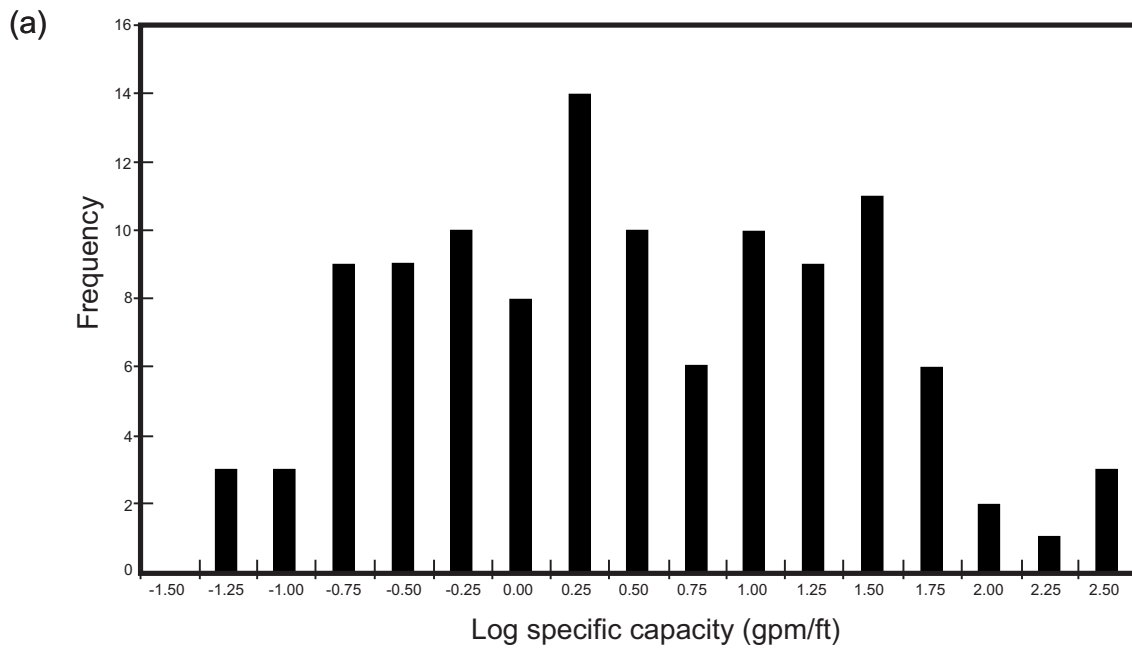


Figure 4-6. (a) Histogram of specific-capacity values from the unconfined portion of the Barton Springs aquifer (n=113). (b) Distribution and classed values of all specific capacity data (n=170).

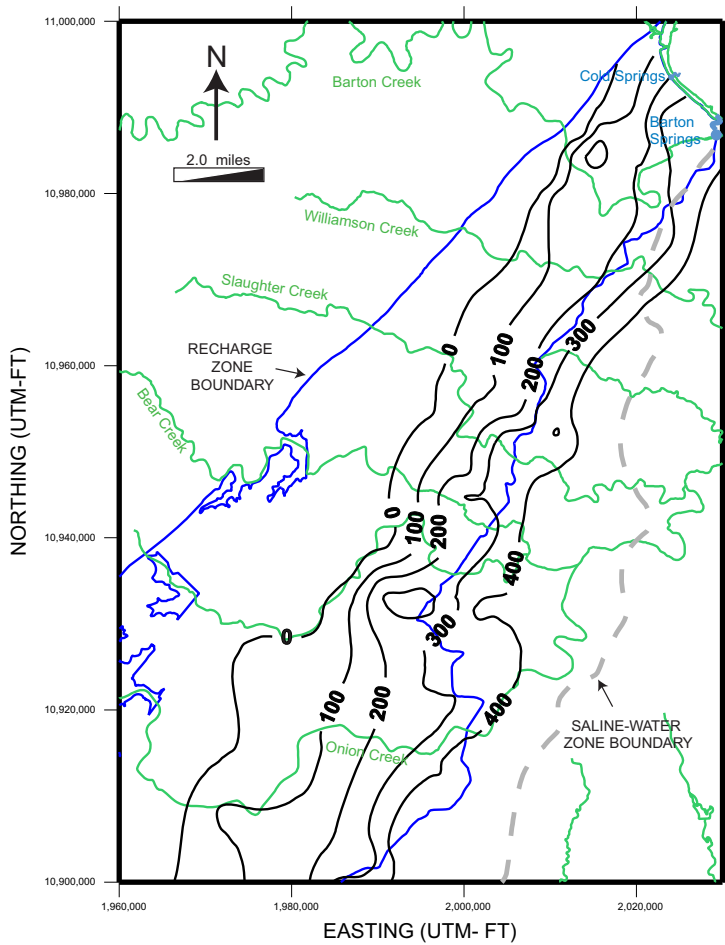


Figure 4-7. Saturated-thickness contour map of the Edwards Aquifer under 1950's drought conditions with minimal (0.66) pumping. Note: contours are in ft.

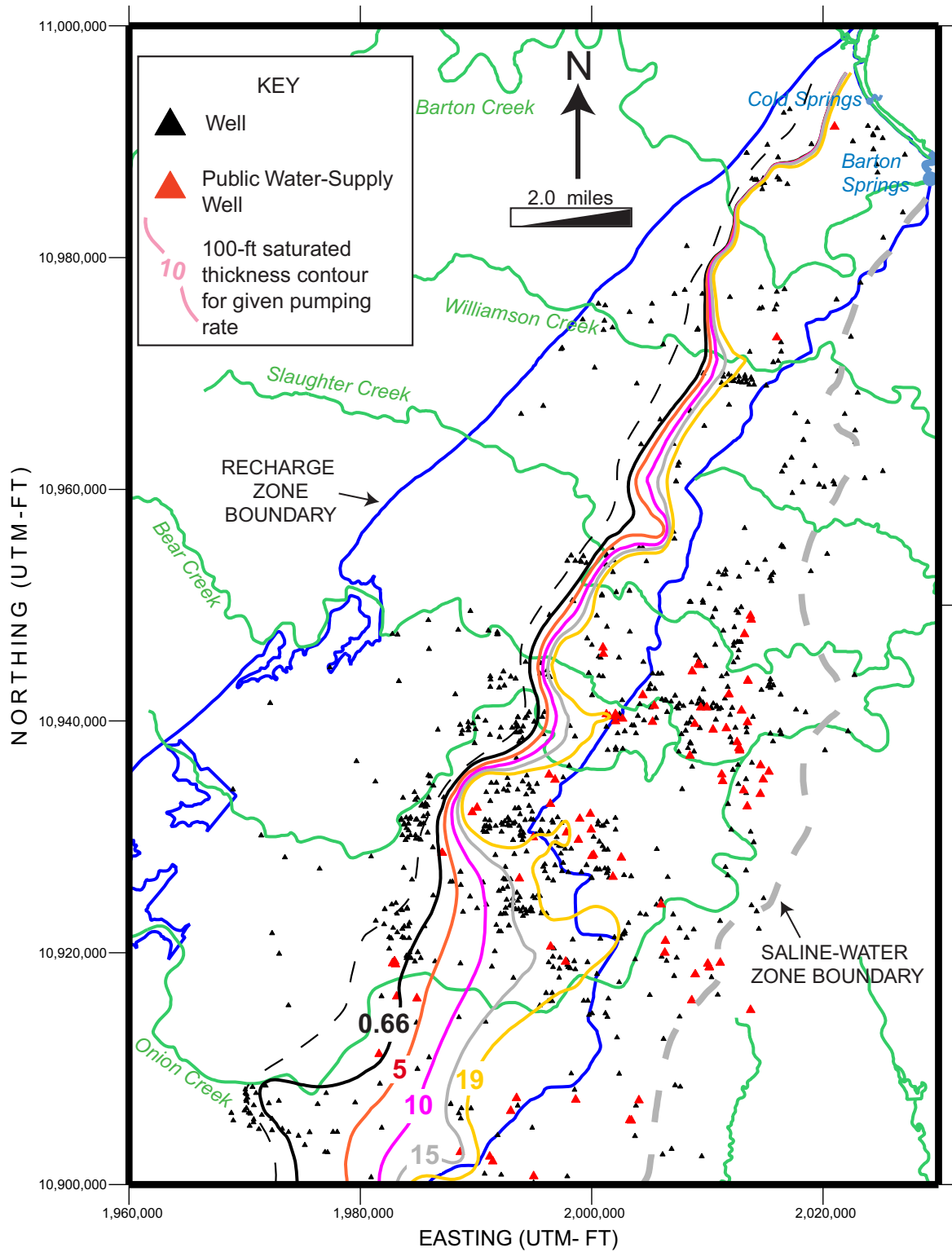


Figure 4-8. Composite of 100-ft saturated aquifer thickness contour lines under 1950's drought conditions with 0.66, 5, 10, 15, and 19 cfs of pumping. Dashed line is 100-ft saturated aquifer thickness contour under high-flow conditions.

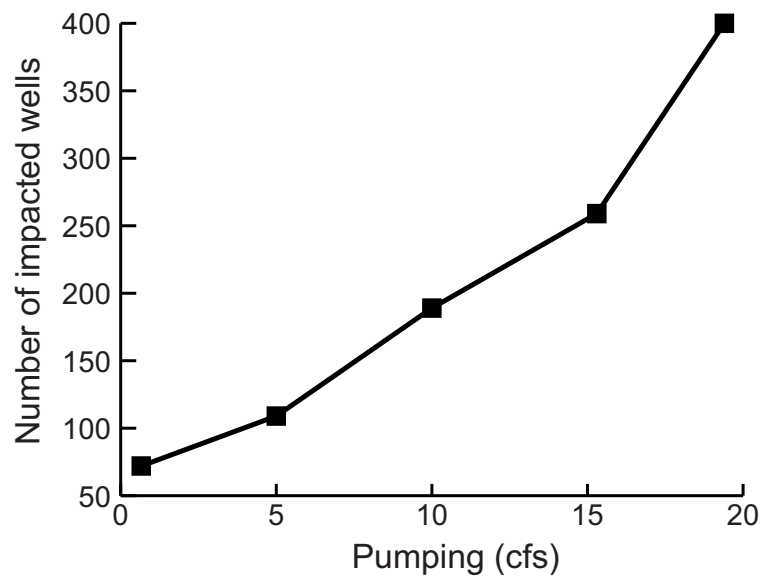


Figure 4-9. Chart summarizing number of wells impacted under 1950's drought conditions and various pumping rates.

APPENDIX A

Report:

Scanlon, B., Mace, R., Smith, B., Hovorka, S., Dutton, A., and Reedy, R., 2001, Groundwater Availability of the Barton Springs Segment of the Edwards Aquifer, Texas—Numerical Simulations through 2050: The University of Texas at Austin, Bureau of Economic Geology, final report prepared for the Lower Colorado River Authority, under contract no. UTA99-0, 36 p. + figs., tables, attachment.

GROUNDWATER AVAILABILITY OF THE BARTON SPRINGS SEGMENT OF
THE EDWARDS AQUIFER, TEXAS: NUMERICAL SIMULATIONS THROUGH
2050

by

Bridget R. Scanlon, Robert E. Mace*, Brian Smith**, Susan Hovorka, Alan R. Dutton,
and Robert Reedy

prepared for

Lower Colorado River Authority
under contract number UTA99-0

Bureau of Economic Geology
Scott W. Tinker, Director
The University of Texas at Austin
*Texas Water Development Board, Austin
**Barton Springs Edwards Aquifer Conservation District, Austin

October 2001

GROUNDWATER AVAILABILITY OF THE BARTON SPRINGS SEGMENT OF
THE EDWARDS AQUIFER, TEXAS: NUMERICAL SIMULATIONS THROUGH
2050

by

Bridget R. Scanlon, Robert E. Mace*¹, Brian Smith**, Susan Hovorka, Alan R. Dutton,
and Robert Reedy

prepared for

Lower Colorado River Authority
under contract number UTA99-0

Bureau of Economic Geology
Scott W. Tinker, Director
The University of Texas at Austin
*Texas Water Development Board, Austin
**Barton Springs Edwards Aquifer Conservation District, Austin

October 2001

¹ This study was initiated while Dr. Mace was an employee at the Bureau of Economic Geology and his involvement primarily included initial model development and calibration.

CONTENTS

ABSTRACT	1
INTRODUCTION.....	1
STUDY AREA.....	3
Physiography and Climate.....	3
Geology	4
PREVIOUS WORK	5
HYDROGEOLOGIC SETTING.....	7
Hydrostratigraphy.....	8
Structure	10
Water Levels and Regional Groundwater Flow	12
Rivers, Streams, Lakes, and Springs	13
Recharge.....	13
Hydraulic Properties.....	15
Discharge.....	15
CONCEPTUAL MODEL OF GROUNDWATER FLOW	17
MODEL DESIGN	17
Code and Processor	18
Grid.....	18
Model Parameters.....	18
MODEL BOUNDARIES	19
Modeling Approach.....	19
STEADY-STATE MODEL	21
Calibration.....	21
Sensitivity Analysis.....	23
TRANSIENT MODEL.....	24
PREDICTIONS	27
Future Pumpage.....	27
Drought of Record.....	28
Predicted Groundwater Availability.....	29
MODEL LIMITATIONS	30
CONCLUSIONS.....	31
ACKNOWLEDGMENTS.....	32
REFERENCES.....	34

Figures

1. Location of the study area relative to cities, towns, roads, and rivers.
2. Location of Groundwater Conservation Districts in the study area.
3. Land-surface elevation in the study area.
4. Historical annual precipitation for rain-gage stations at (a) Camp Mabry and Mueller Airport (NOAA station), (b) Barton Creek, (c) Slaughter Creek, and (d) Onion Creek.
5. Geologic setting of the Barton Springs segment of the Edwards aquifer.
6. Stratigraphic and hydrostratigraphic section of the study area.
7. Surface geology in the study area.
8. Geologic cross section of the study area.
9. Elevation of the top of the Edwards aquifer (which corresponds to the base of the Del Rio Formation).
10. Elevation of the base of the Edwards aquifer (which corresponds to the top Glen Rose Formation).
11. Approximate thickness of the Edwards aquifer.
12. Control points for the elevation of the top and the base of the Edwards aquifer.
13. Water-level elevations in the aquifer (include water-level measurements in July and August 1999).
14. Hydrographs for wells (a) 58-42-8TW, (b) 58-50-216, (c) 58-50-221, and (d) 58-50-301.
15. Hydrographs for wells (e) 58-50-411, (f) 58-50-801, (g) 58-58-123, and (h) 58-58-101.
16. Mean monthly streamflow for USGS gaging station 08158700 on Onion Creek near Driftwood for (a) linear and (b) logarithmic scales. Figure 25 shows the location of the stream gage.
17. Mean monthly streamflow for USGS gaging station 08158800 on Onion Creek at Buda for (a) linear and (b) logarithmic scales. Figure 25 shows the location of the stream gage.
18. Mean monthly streamflow for USGS gaging station 08158810 on Bear Creek near Driftwood for (a) linear and (b) logarithmic scales. Figure 25 shows the location of the stream gage.
19. Mean monthly streamflow for USGS gaging station 08158840 on Slaughter Creek at FM 1826 for (a) linear and (b) logarithmic scales. Figure 25 shows the location of the stream gage.
20. Mean monthly streamflow for USGS gaging station 08158922 on Williamson Creek at Brush Country Blvd., Oak Hill, for (a) linear and (b) logarithmic scales. Figure 25 shows the location of the stream gage.

21. Mean monthly streamflow for USGS gaging station 08158920 on Williamson Creek at Oak Hill for (a) linear and (b) logarithmic scales. Figure 25 shows the location of the stream gage.
22. Mean monthly streamflow for USGS gaging station 08155240 on Barton Creek at Lost Creek Blvd. for (a) linear and (b) logarithmic scales. Figure 25 shows the location of the stream gage.
23. Mean monthly streamflow for USGS gaging station 08155300 on Barton Creek at Loop 360 for (a) linear and (b) logarithmic scales. Figure 25 shows the location of the stream gage.
24. Mean monthly streamflow for USGS gaging station 08155500 at Barton Springs for (a) linear and (b) logarithmic scales. Figure 25 shows the location of the stream gage.
25. Location of the stream gages for the stream-flow hydrographs shown in figures 16 through 26.
26. Discharge at Barton Springs.
27. Histogram of hydraulic conductivity from aquifer tests.
28. Spatial distribution of pumping in the aquifer.
29. Model grid, consisting of 120 cells \times 120 cells (14,400 cells) that are 1,000 ft long \times 500 ft wide. The active zone of the model is shown by the solid line and consists of 7,043 cells.
30. Zonal distribution of hydraulic conductivity resulting from calibration of the steady-state model.
31. Comparison of simulated and measured (July/August 1999) water-level contours for the steady-state model.
32. Scatter plot of simulated and measured (July/August 1999) water levels for the steady-state model.
33. Water-level residuals (difference between measured and simulated water-level elevations) for the calibrated steady-state model.
34. Sensitivity of the numerically predicted water levels of the steady-state model to changes in model parameters at (a) calibration wells and (b) each active cell in the model.
35. (a) Monthly pumpage, (b) recharge, and (c) precipitation for the transient model (1989 through 1998).
36. Comparison of simulated and measured discharge at Barton Springs for 1989 through 1998.
37. Scatter plot of simulated versus measured spring discharge for 1989 through 1998.
38. Comparison of simulated and measured water-level elevation hydrographs in four monitoring wells, northern study area.
39. Comparison of simulated and measured water-level elevation hydrographs in four monitoring wells, central and southern study area.

40. Scatter plots of simulated versus measured water-level elevations for the transient simulations (a) March/April 1994, (b) July/August 1996, and (c) July/August 1998.
41. Sensitivity of the transient simulated spring discharge to (a) recharge, (b) pumpage, (c) specific yield, and (d) specific storage.
42. Sensitivity of the transient simulated water levels to recharge.
43. Sensitivity of the transient simulated water levels to pumpage.
44. Sensitivity of the transient simulated water levels to specific yield.
45. Sensitivity of the transient calibration water levels to specific storage.
46. Precipitation from 1860 through 2000 measured at the rainfall gaging station in Camp Mabry and Mueller Airport in Austin (NOAA), showing the drought of record during the 1950's.
47. Baseline water levels based on average recharge (55 cfs) and current pumpage at the end of a 10-yr simulation for comparison with future simulations.
48. Simulated water-level declines in 2010 using (a) average recharge conditions through 2010 and (b) average recharge conditions through 2003 and drought-of-record recharge conditions from 2004 to 2010.
49. Simulated water-level declines in 2050 using (a) average recharge conditions through 2050 and (b) average recharge conditions through 2043 and drought-of-record recharge conditions from 2043 to 2050.
50. Simulated spring discharge for 10-yr periods using (a) average recharge conditions through 2050 and (b) average recharge conditions for the first of each 10-yr period and drought of record for the last 7 yr.

Tables

1. Stream-gauge data, including location, length of record, and maximum recharge.
2. Distribution of recharge among creeks calculated from daily data from 1/1/1980 through 12/31/1998.
3. Statistical summary of hydraulic conductivity values for the Barton Springs segment of the Edwards aquifer.
4. Annual precipitation, recharge, pumpage, and number of reported users for the transient simulation (1989 through 1998) and predicted recharge for average conditions (2041 through 2043) and potential future drought (2044 through 2050) estimated from the 1950's drought for the future simulations.
5. Sensitivity of transient spring discharge to variations in recharge, pumpage, specific yield, and specific storage.
6. Water budget for the calibrated steady-state, transient, and predictive runs.

ABSTRACT

A two-dimensional, numerical groundwater-flow model was developed for the Barton Springs segment of the Edwards aquifer to evaluate groundwater availability and predict water levels and spring flow in response to increased pumpage and droughts during the period 2001 through 2050. A steady-state model was developed on the basis of average recharge for a 20-yr period (1979 through 1998) and pumpage values for 1989. Transient simulations were conducted using monthly recharge and pumping data for a 10-yr period (1989 through 1998) that includes periods of low and high water levels. Values of hydraulic conductivity were estimated by calibrating the steady-state model using trial and error and automated inverse methods. Good agreement was found between measured and simulated flow at Barton Springs (root mean square error [RMS error, average of squared differences in measured and simulated discharges] 12 cfs), between measured and simulated water levels at different times and between measured and simulated water levels in many of the monitoring wells. To assess the impact of future pumpage and potential future droughts on groundwater availability, transient simulations were conducted using extrapolated pumpage for 10-yr periods (2001 through 2050) and average recharge for a 3-yr period and recharge from the 1950's drought for the remaining 7 yr. Results of these simulations were compared with those using average recharge and future pumpage. Predicted water-level declines in response to future pumpage under average recharge conditions are small (≤ 35 ft), whereas water-level declines under future drought conditions were much greater (≤ 270 ft). Simulated spring discharge in response to future pumpage under average recharge decreased proportionally to future pumpage (2 cfs per decade), whereas spring discharge decreased to 0 cfs in response to future pumpage under drought-of-record conditions. Management of water resources under potential future drought conditions should consider enhanced recharge and conservation measures.

INTRODUCTION

This modeling study focuses on a segment of the Edwards aquifer within and adjacent to Austin, Texas, that discharges into Barton Springs and Cold Springs and is hydrologically distinct from the rest of the Edwards aquifer. This region, referred to as the Barton Springs segment of the Edwards aquifer, constitutes the sole source of water to about 45,000 residents. Barton Springs pool was created when a dam was installed immediately downstream of the

spring and it also serves as a municipal swimming pool in Zilker Park, downtown Austin. The pool was The Barton Springs salamander, listed as an endangered species, is restricted to the region immediately surrounding the spring. Increased population growth and recent droughts (1996) have focused attention on groundwater resources and sustainability of spring flow. A combination of increased pumpage and severe drought could severely impact future water resources.

A numerical groundwater flow model is a tool that can help in assessing the impacts of current and future pumpage on groundwater resources and spring discharge. A groundwater flow model numerically represents the aquifer using a computer. Information about the aquifer, such as water levels, recharge, and spring discharge, provides input to the model and helps us evaluate the reliability of the model. A calibrated groundwater model can provide a valuable tool for evaluating the impact of pumping and drought on an aquifer.

The objective of this study was to evaluate long-term groundwater availability in response to future pumpage and potential future droughts. To meet this objective, it was necessary to develop a two-dimensional numerical, finite-difference groundwater model of the Barton Springs segment of the Edwards aquifer. This model will provide (1) a management tool to the Barton Springs Edwards Aquifer Conservation District (BSEACD) and to the Regional Water Planning Group and (2) a tool for evaluating groundwater availability under drought-of-record conditions. This report describes the construction and calibration of the numerical model and the results of predictive simulations of water levels and spring discharge for the next 50 yr based on projected demands from the Regional Water Planning Group and the BSEACD.

The various components of the modeling study included (1) developing a conceptual model that included our current understanding of the geology, (2) quantifying groundwater recharge from stream-gage records, (3) calibrating a steady-state model using average recharge for a 20-yr period (1979–1998) and trial and error and automated inverse methods, (4) running a transient model for a 10-yr period (1989–1998), (5) conducting sensitivity analyses to determine the primary controls on the simulations, and (6) running predictive simulations through 2050. This report describes (1) the study area, previous work, and hydrogeologic setting used to develop the conceptual model; (2) the code, grid, and recharge assigned during model construction; (3) calibration of the steady-state model to estimate the hydraulic conductivity distribution; (4) the transient model for the 10-yr period; (5) sensitivity analysis for the steady-state and transient model; and (6) predictions of water-level changes and spring discharge under

future pumpage and drought-of-record conditions; (7) the limitations of the current model; and (8) suggestions for improvements.

The model developed in this study differs from the previous two-dimensional, finite-difference model developed by Slade and others (1985) in the grid resolution (minimum 500 ft versus a minimum of 1,500 ft) in explicitly representing the aquifer thickness in the simulation, in simulating transient flow for a long time (10 yr versus 5 mo), and in predicting groundwater availability under increased pumpage and potential future droughts for the period through 2050. The spatially distributed model developed in this study allows the effect of pumpage in different regions of the model area to be assessed, which is not possible with the lumped parameter model developed by Barrett and Charbeneau (1996). More details on these other models are provided in the Previous Work section.

STUDY AREA

The Barton Springs segment of the Edwards aquifer constitutes the study area and includes parts of Travis and Hays Counties (fig. 1). The study region is within the Lower Colorado Region (Region K) water-planning group and includes the Barton Springs/Edwards Aquifer Conservation District (fig. 2). The model boundaries are all hydrologic boundaries and include the Mount Bonnell fault to the west, which acts as a no-flow boundary (Senger and Kreitler, 1984); a groundwater divide to the south along Onion Creek (Guyton and Associates, 1958); the “bad-water” line to the east; and the Colorado River (Town Lake) to the north. Groundwater circulation in the Edwards aquifer decreases to the east and total dissolved solids (TDS) increase. The bad-water line marks the zone where TDS exceeds 1,000 mg/L, which generally coincides with Interstate 35. The groundwater divide in the south separates the Barton Springs segment from the San Antonio segment of the Edwards aquifer, which discharges into Comal and San Marcos Springs.

Physiography and Climate

Physiographically the aquifer lies on the transition between the Edwards Plateau to the west and the Blackland Prairie to the east. The topography of the area is that of the Rolling

Prairie province. Surface elevations range from about 1,050 ft in the southwest to about 250 ft along the east margin (fig. 3).

The study area is in the subtropical humid climate zone (Larkin and Bomar, 1983). Annual precipitation ranges from 11 to 65 inches (1860 through 2000), a figure which is based on records from a NOAA station located north of the study area at Camp Mabry and Mueller Airport in Austin (fig. 4a). Long-term mean annual precipitation is 33.5 inches (fig. 4a). Precipitation occurs primarily in the spring and fall, mainly as a result of mixing of cool fronts and warm, moist air from the Gulf of Mexico. Convictional thunderstorms result in small amounts of rain in the summer. Mean annual gross lake evaporation is 66 inches (Larkin and Bomar, 1983).

The Edwards aquifer is unconfined in the outcrop area where recharge occurs and in part of the section to the east, where it is overlain by the Del Rio Clay (fig. 1). Farther to the east, the aquifer is confined by the Del Rio Clay. Approximately 80 percent of the aquifer is unconfined, and the remainder is confined (Slade and others, 1985).

Geology

The Barton Springs segment of the Edwards aquifer is a hydrologically significant element within an aquifer system developed in thick and regionally extensive Lower Cretaceous carbonates that underlie large areas of Texas. The components make up the northern segment of the Edwards aquifer, the Barton Springs segment, the San Antonio segment, and the Edwards-Trinity Plateau and Trinity aquifers (fig. 5).

The sediments hosting these aquifers were deposited when a Lower Cretaceous sea-level rise flooded the North American craton. Two transgressive–regressive cyclic genetic sequences are represented by conglomerate, sandstone, shale, and limestone in the lower and middle Trinity Group (Moore, 1996). Continued transgression recorded by cyclic sedimentation resulted in deposition of two thick carbonate-dominated sequences of the Glen Rose Formation in the upper Trinity Group overlain by four sequences that comprise the Edwards aquifer and facies-equivalent limestones (fig. 6). Edwards Group and temporally equivalent limestones and marls are recognized as far north as the Texas Panhandle, where they subcrop beneath the Ogallala Formation. Water depth continued to increase cyclically through part of the Late Cretaceous, but sedimentary patterns were modified by deposition of a number of shales separated by limestone

and chalk. The first of these shale units is the Del Rio Formation, which forms the aquitard at the top of the Edwards Group over a wide area, and which is overlain by the Buda Formation (dominantly limestone) and the Eagle Ford Formation (dominantly shale). Maximum water depth is represented by deposition of the Austin Chalk over a wide area. Maximum water depth was followed by progradation, aggradation, and sea-level fall, during which clastics, including the Taylor and Navarro Formations, were the dominant deposits.

The major episode of structural deformation affecting aquifer development was uplift of the Edwards Plateau along the Balcones Fault Zone. This deformation occurred along a sinuous trend extending from Dallas through Austin and San Antonio and west toward Del Rio. Uplift of the Edwards Plateau began in the Miocene and during the creation of the regional hydraulic gradient. Normal faulting along en echelon faults and graben systems that yielded a total of 1,400 ft down-to the coast displacement across the Barton Springs segment accommodated uplift. Major faults trend north-northeast.

Uplift along the Balcones Fault Zone, followed by erosion, has resulted in stripping of younger units to expose the Glen Rose Formation to the west. This area is commonly described as the contributing zone to the Edwards aquifer. It is characterized by creeks that are maintained by spring flow. The recharge zone is the area where diverse stratigraphic units that form the Edwards aquifer crop out. The recharge zone is approximately coincident with the west edge of the Balcones Fault Zone, and structural and rock properties combine to create effective pathways for rapid recharge from streams. At the east edge of the study area, where less uplift has occurred, the aquifer is confined by younger, low-permeability units, including the Del Rio Clay, Eagle Ford Formation, Austin Chalk, Taylor, and Navarro Formations. Although faults are less easily mapped in weak and poorly exposed shales at the east edge of the study area, examination of subsurface structure shows that this area is within the Balcones Fault Zone.

PREVIOUS WORK

Numerical models of groundwater flow in the Barton Springs segment of the Edwards aquifer were previously developed by Slade and others (1985) and Barrett and Charbeneau (1996). Slade and others (1985) developed a two-dimensional numerical groundwater flow model for the part of the Edwards aquifer that discharges at Barton Springs by using a finite difference code written by Trescott and others (1976). The purpose of the modeling study was to

determine the spatial distribution of hydraulic parameters and to assess different water-management scenarios that included increased pumpage and enhanced recharge. The model grid consisted of 318 active cells, with cell spacing ranging from about 1,500 to 8,000 ft. A steady-state model was developed for mean recharge conditions that corresponded to long-term average discharge at Barton Springs (53 cfs). Recharge was estimated from stream-loss records. The model did not explicitly represent aquifer thickness, although thickness was incorporated in the transmissivity data. Calibration of the steady-state model was used to determine the spatial distribution of transmissivity, which varied from $100 \text{ ft}^2 \text{ d}^{-1}$ in the west part of the aquifer to more than 1 million $\text{ft}^2 \text{ d}^{-1}$ near Barton Springs. A transient model was developed for a 5-mo period. Calibration of the transient model yielded values of specific yield and storage coefficient for the aquifer. Predictive simulations, conducted by using projected pumpage for the year 2000, indicated that the aquifer would be dewatered in the southwest part of the study area and major declines would occur in the southeast area. However, another simulation that included use of recharge enhancement predicted a rise in potentiometric surface of about 50 ft in the southwest part of the aquifer and moderate water-level declines in the southeast zone. The model developed by Slade and others (1985) is not appropriate for regional water planning because the model was developed with a code that is no longer in use (Trescott and others, 1976), the grid cell size is large (minimum 1,500 ft), the aquifer thickness is not explicitly represented in the model, and the transient simulation period was short (5 mo).

Barrett and Charbeneau (1996) developed a new type of lumped parameter model to predict the impacts of urban development on the quantity and quality of water in the Barton Springs segment of the Edwards aquifer. The aquifer was divided into five cells corresponding to the five watersheds in the region. A single well was used to represent conditions in each cell. The model successfully reproduced measured water levels and average nitrogen concentrations in the Edwards aquifer and at Barton Springs. Increased urbanization was simulated by estimating changes in creeks that recharge the system. The results indicate that increased development will reduce spring flow and increase nitrogen concentrations in the aquifer. The resolution of the model (cells equivalent to river basins) is too coarse to evaluate the impact of more local pumpage on spring discharge; therefore, the lumped parameter model is inadequate for regional water planning.

HYDROGEOLOGIC SETTING

The hydrogeologic setting describes the aquifer and hydrologic features and hydraulic properties that influence groundwater flow in the aquifer. For this study, we built on previous surface mapping to develop two new subsurface structure maps and an isopach map.

The hydrogeologic framework developed for this model was based on previous work. An unpublished geologic map in ARC/INFO Geographic Information System (GIS) provided the interpretation of bedrock geology at the surface (figs. 7, 8) (Hauwert and others, 1997). Maps of parts of the area were published by Small and others (1996) and Hanson and Small (1995). The other major data input was an unpublished notebook of subsurface well log data and a table of depth to top of formations compiled by Nico Hauwert for BSEACD (N. Hauwert, 1998, unpublished data). Following the convention developed in the San Antonio segment of the Edwards aquifer, we consider the interval between the regionally extensive markers at the top of the Glen Rose Formation and the base of the Del Rio Formation as part of the Edwards aquifer and is the interval modeled in this study.

Other research used for subsurface interpretation for conceptual model development includes stratigraphic descriptions (Rose, 1972; Hanson and Small, 1995; Moore, 1996; and Small and others, 1996) and structural interpretations of Garner and Young (1976) and Collins and Woodruff (2001). A number of differences in interpretation among previous researchers are noted. Moore (1996) emphasized the lateral facies variation in dominant lithology and nomenclature in response to genetic sequences and paleogeography. The nomenclature derived from Rose (1972) and developed for the San Antonio segment uses a stratigraphic approach, recognizing eight named and numbered, lithologically defined hydrostratigraphic units that were applied in the Barton Springs segment by Hauwert and others (1997) and Small and others (1996).

Similarly, variations in fault interpretation are noted. The mapping of Collins and Woodruff (2001) employs a relay-ramp conceptual model (Collins, 1996; Ferrill and Morris, 2001). In this model, the vertical displacement varies laterally along each fault strand. As displacement decreases on one strand, the strain is taken up on adjacent strands. The fault strands form an en echelon pattern, with each strand dying out along strike. Between the fault strands, the rocks are folded to accommodate deformation, forming structures described as a relay ramps. The mapping of Hauwert and others (1997), Small and others (1996), and Hanson and Small

(1995) follows a conceptual model in which faults generally continue until they intersect another fault. Rather than folds commonly interpreted in the relay-ramp model, changes in elevation of formation or member contacts are commonly interpreted as the result of cross-faulting between major fault strands.

Hydrostratigraphy

The Edwards aquifer is an interval containing carbonates that have numerous intervals of intercrystalline high porosity, as well as petrophysical properties that make the carbonates subject to development of karst conduits. Underlying and, to a lesser extent, overlying stratigraphic intervals also serve as aquifers and can develop karst conduits.

Conventionally the lower boundary of the Edwards aquifer is defined as the top of the Glen Rose Formation (fig. 6). The Glen Rose Formation is the uppermost unit in the Trinity aquifer (Mace and others, 2000). In the study area, supratidal and paleosol deposits at the top of the Glen Rose Formation are overlain by marly, nodular limestones and calcareous shales (Moore, 1996, Molineux, 2001). These onlapping transgressive systems tract deposits are classified as the Walnut Formation (Rose, 1972; Moore, 1996) or the basal nodular member of the Kainer Formation, Edwards Group (Rose, 1972; Small and others 1996; Hauwert and others 1997). Irrespective of stratigraphic complexity, in many areas these units limit vertical permeability. Evidence of limited vertical permeability includes (1) numerous springs and seeps that discharge at this contact in outcrop and (2) an increase in salinity in the subsurface below the Glen Rose contact evident on resistivity logs. Regionally, however, there is cross-formational interconnection across the Edwards-Glen Rose contact. Both units are karstic limestones, and large caves that cross the contact are interpreted as evidence that cross-formational flow occurs through karst systems in at least parts of the San Antonio segment of the Edwards aquifer. Likewise, modeling of flow in the Trinity aquifer (Mace and others, 2000) concludes that cross-formational flow of significant volumes of water occurs from the Trinity into the Edwards in the San Antonio segment, illustrating connection between the aquifers.

The carbonates in the Edwards aquifer are laterally and vertically heterogeneous. This heterogeneity reflects the complex interactions among (1) paleogeography, (2) sea-level variation, (3) carbonate accumulation (productivity and transport), (4) siliciclastic transport, (5), early diagenesis, and (6) subsidence. The study area was on the north flank of a broad, low-relief

positive area known as the Texas Platform and San Marcos Arch (Rose, 1972). Stratigraphic units deposited on the platform include the Walnut Formation/basal nodular member of the Kainer Formation, and the Kainer and Person Formations. These units collectively are described as the Edwards Group (Rose, 1972). A regionally traceable transgressive unit, known as the Regional Dense Member of the Person Formation, separates the Kainer and Person. Slightly deeper water in the North Texas Basin toward the north is interpreted from facies changes. Time-equivalent units recognized in North Central Texas include the Walnut, Comanche Peak, Kiamichi, and Duck Creek Formations (Rose, 1972; Moore, 1996). Sea-level variation is reflected in regionally correlated sequences (Immenhauser and Scott, 1999) and patterns of stacked high-frequency cycles. High-frequency cycles have been described in the Walnut Formation (Moore, 1996). Inspection of outcrop and log data suggests that the same type of high-frequency upward-shoaling cyclicity recognized in the San Antonio segment (Hovorka, 1996) is a dominant pattern in the Barton Springs segment; however, no detailed stratigraphic studies have been done in units younger than the Walnut. In the San Antonio segment of the Edwards aquifer, interaction between lithologies and structure was observed to influence distribution of karst conduits (Hovorka and others, 1998). Karst conduits developed preferentially where fractures intersect subtidal dolomites. Beds of calcitized and dissolved evaporites may also focus karst dissolution. The relationship between lithofacies and structure within the Edwards aquifer of the Barton Springs segment will most likely impact flow within the aquifer similarly; however, the relationships have not been documented.

The Edwards Group is overlain by transgressive carbonates of the Georgetown Formation. The contact is at least locally unconformable, with development of pre-Georgetown karst (Rose, 1972). The Georgetown Formation is generally of a lower porosity than the Edwards Group. It is commonly included within the Edwards aquifer because (1) there is no barrier to hydrologic connection between the Edwards and Georgetown, (2) karst features are at least locally developed in the Georgetown, and (3) it is difficult to separate the carbonates of the Edwards Group consistently from the carbonates of the Georgetown using the gamma-ray logs or driller's reports commonly available from the subsurface.

The thick and regionally extensive shale of the Del Rio Formation forms a significant aquitard at the top of the Edwards aquifer. This contact can be recognized reliably on almost any type of log. Locally fracture systems may allow interconnection between the Edwards aquifer

and overlying fractured or karsted carbonates; however the high clay content and plasticity of the Del Rio suggest that in most places it will function as an effective barrier to vertical flow.

Structure

For this study, we developed three maps covering the area of the Barton Springs segment: faults and structure contour on top of the Edwards aquifer (base Del Rio) in the confined aquifer (fig. 9), faults and structure contour on the base of the Edwards aquifer (top Glen Rose) throughout the aquifer (fig. 10), and an isopach map of the Edwards aquifer (fig. 11).

The procedure for creating digital maps was designed to reduce the frequency of errors and artifacts in this structurally complex area. A table of subsurface depths to stratigraphic formation tops prepared by Nico Hauwert (unpublished digital data, 1998) was reviewed and compared with the source log data from which it was derived. Many tops were reported from driller's logs and other data sources and could not be checked. Four hydrostratigraphic units were initially isopached and the isopach maps digitized: the Georgetown, Person, and Kainer (without basal nodular member) Formations and the Walnut Formation/Basal Nodular Member. Isopachs reflect stratigraphic thickness, not a reduction in thickness as a result of normal faulting. A combination of low density of subsurface information for the lower units and apparent inconsistencies in unit identification resulted in low confidence in interpretation of isopach maps. Therefore, the digital isopachs were summed, giving a net aquifer thickness (fig. 11).

The elevation of picks (in feet, sea-level datum) was posted on a paper plot for two contacts at each subsurface data point (fig. 12). In the unconfined section, the top Glen Rose/base Edwards aquifer (Walnut/basal nodular) was mapped. In the confined section, the top Edwards aquifer (top Georgetown)/base Del Rio contact was mapped. A match line generalized from the downdip edge of the Edwards outcrop was selected to control merging of the two maps. Data density on the surface geologic map is much higher than in the subsurface. In order to increase control and assure a good match between the subsurface and surface mapping, the surface geologic mapping was used to estimate the geometry of the aquifer in the subsurface. Faults mapped at the surface were extrapolated vertically into the subsurface (fig. 7). Although we know that most Balcones faults are high angle but nonvertical, this simplification is necessary because we have little control on fault-plane dip. In addition, some refraction and possibly change in fault abundance are likely because faults intersect units with different mechanical

properties (Collins and Woodruff, 2001). Generalized isopach maps of map units were prepared. Then, within each fault block, the depth to the selected subsurface mapping horizon was calculated at several points from the elevation of the mapped contacts and the unit thickness. Because of the structural complexity, we elected to hand contour the resulting data using an irregular contour interval. This allows geologic intuition to be used to guide interpolation through areas with few data. In most fault blocks, regional dip was required to accommodate the mapped outcrop pattern and subsurface data, supporting a relay-ramp geometry, so this concept was used throughout the mapping. Integration of data and comparison of one structure map with another suggested some revision and downdip extension of the fault and outcrop patterns, which were modified to match the revised interpretation in ARC/EDIT.

The hand-contoured structure maps were digitized, attributed, and imported into ARC/INFO. The resulting contours for the top of the Edwards aquifer in the confined zone and the bottom of the Edwards aquifer in the unconfined zone were imported into GeoQuest CPS3 gridding software. This software was selected for its fault-handling capabilities. Several iterations of the grid were created until all fault blocks were completely populated with elevation data and artifacts removed.

We subtracted the gridded aquifer thickness map from the gridded top of the Edwards aquifer in the confined zone to create a grid for the base of the Edwards aquifer structure in the confined aquifer. This procedure is preferred over creation of two structure maps in structurally complex areas because it eliminates artifacts that impact the isopach used in the model. Thinning of the aquifer because of fault offset was not incorporated into the isopach. The impact of faults with greater than 250 ft of throw were represented as flow barriers in the model as discussed later in this paper. Grids for the base of the aquifer in the confined and unconfined zones were then merged along the merge line to create a base aquifer grid. The gridded top of the Edwards aquifer in the confined zone was merged with the grid for land surface in the unconfined zone to create a grid for the aquifer top.

Structure in the aquifer can be described in terms of a regional eastward dip created by faulting on north-northeast-trending normal faults and graben systems. Faulting impacts the flow in the aquifer by limiting cross-fault flow because of reduced aquifer thickness or enhancing fault-parallel flow through fracture zones associated with faults (Hovorka and others, 1998).

Water Levels and Regional Groundwater Flow

A generalized water-level map was developed for the Barton Springs segment of the Edwards aquifer by using water levels measured in July/August 1999 (fig. 13). This time period was chosen because it includes the largest compilation of synoptic water-level measurements. Water levels generally follow the topography and the groundwater flow direction is generally to the east in the west part of the aquifer and to the northeast in the east part of the aquifer, toward Barton Springs.

Water-level fluctuations vary throughout the aquifer. Unlike many of the aquifers in the state, such as the Ogallala aquifer, where there is a continual decline in groundwater levels in response to pumping, water levels in the Barton Springs aquifer do not show a long-term decline as a result of pumping. The Barton Springs aquifer is dynamic, and water levels generally respond to temporal variations in recharge and local areas of pumping. Although water levels decline during long periods of drought, they recover rapidly in response to recharge. Slade and others (1985) noted that maximum water-level fluctuations range from 1 to 10 ft in the west area, 10 to 50 ft in the central area, and 40 to 119 ft in the east area. Water-level fluctuations are greatest in the confined section of the aquifer.

Water levels are continuously monitored in eight wells in the study area (figs. 14, 15). A variety of factors impact the range of water levels recorded by various wells, including penetration of fractures and/or conduits and location near major pumping centers. It is difficult to compare the range in water-level fluctuations among the monitoring wells because the record lengths are quite variable. In wells with the longest monitoring record, the range in water levels was from 96 ft (58-58-123; fig. 15c) to 164 ft (58-50-216; fig. 14b). Minimal water-level fluctuations in well 58-50-411 (range 28 ft; fig. 15a) are attributed to penetration of conduits during well construction. Most of the monitoring wells demonstrate large seasonal fluctuations in water levels. Senger and Kreitler (1984) indicated that water-level fluctuations in many of the wells in the confined section of the aquifer correlated with variations in spring discharge. For example, well 58-58-301, which is just east of the bad-water line, correlated with spring discharge, indicating a hydraulic connection between the “bad-water” zone and the fresh-water aquifer. Short-term fluctuations in water levels were also recorded in several wells. Hauwert and Vickers (1994) noted that well 58-50-801 showed rises of 10 to 20 ft in response to 1- to 2-inch rainfall events in early 1992. Similarly well 58-58-123 showed an 8-ft rise in water level in

response to rain in May 1994. These large water-level fluctuations represent the movement of pressure pulses through the aquifer and indicate that the wells are hydraulically connected to the recharge area.

Rivers, Streams, Lakes, and Springs

Five major drainage basins traverse the study area (fig. 1). The drainage basins include a catchment area where the groundwater discharges to the streams and the streams are gaining. When the streams reach the outcrop area of the Edwards, they become losing streams and recharge the aquifer. The catchment area of the streams is 264 mi², whereas the recharge zone is about 90 mi². Stream flow is recorded in nine gaging stations in the study area (figs. 16 through 24). Stream-gaging stations are located upstream and downstream of the outcrop zone on Onion Creek (fig. 25). The other creeks have gaging stations on the upstream edge of the outcrop zone. Most of the streams are ephemeral and oftentimes record no flow during the summer (July, August, September) or during winter months (December, January, February) (figs. 16 through 24).

Most flow in the aquifer discharges in Barton Springs (figs. 1, 26). The mean spring discharge is 53 cfs (1917 through 1998). Discharge ranged from 13 cfs at the end of the drought in the 1950's (1956) to 106 cfs (1992). Barton Springs consists of five major springs (Senger and Kreitler, 1985). The Main Springs consists of three springs in the pool area and constitutes about 80 percent of the discharge; Concession Springs, just north of the pool, and Old Mills Springs discharge from a small pool downstream from Main Springs on the south bank of Barton Creek. Cold Springs, located northwest of Barton Springs, discharges into the Colorado River and is flooded by Town Lake.

Recharge

The primary source of recharge is provided by seepage from streams crossing the outcrop area. Flow losses from the creeks are sufficient to account for groundwater discharge in springs and through wells. Five major creeks (Barton, Williamson, Slaughter, Bear, and Onion) provide most of the recharge to this area (fig. 1, table 1). The creek watersheds can be subdivided into contributing and recharge zones. The contributing zone (264 mi²) is west of the recharge zone,

and the streams are gaining streams as they flow over low-permeability Glen Rose limestone. The recharge zone (90 mi²) coincides with the outcrop area of the Edwards aquifer, where the streams become losing streams. About 15 percent of the total recharge also occurs in interstream regions, where rainfall infiltrates the soil (Slade and others, 1985).

Calculation of stream recharge was described in detail by Barrett and Charbeneau (1996) and Slade and others (1985). Procedures developed in these earlier studies were followed in this study. Hourly flow records from gaging stations located upstream and downstream of the recharge zone were downloaded from the U.S. Geological Survey Web site (<http://tx.usgs.gov>). Recharge was calculated by subtracting daily average flow downstream of the recharge zone from that upstream of the recharge zone for Onion Creek. With the exception of Barton Creek, recharge increases linearly with flow in the upstream gaging station until a threshold flow is exceeded. These threshold values were determined by Slade and others (1985) and were used in this study (table 1). All flow in the upstream gaging station less than the threshold value was therefore assigned to recharge. Once the threshold value was reached, recharge was assumed constant at that value. Barrett and Charbeneau (1996) calculated recharge values by using data from 1979 through 1995. These recharge calculations were extended to December 31, 1998, in this study. Surface runoff from interstream areas to streams in the recharge zone was ignored in the recharge calculations because such runoff generally only occurs during very large storms, when recharge is already maximized. In the case of Barton Creek, the downstream gaging station is located within the recharge zone; therefore, recharge from this creek may be underestimated. A new gaging station was installed 110 ft upstream of Barton Springs on October 1, 1998, and a low-flow rating curve was developed for this station (Mike Dorsey, U.S. Geological Survey, personal communication, 2000). Additional data are required to develop rating curves for higher flows. Various relationships were used to assign recharge to Barton Creek. For low flows (≤ 30 cfs in Lost Creek), recharge is equal to stream loss. Between 30 and 250 cfs, a quadratic relationship developed by Barrett and Charbeneau (1996) was used. Flows greater than 250 cfs were assigned this value for recharge because this was the highest measured recharge. Average annual recharge was calculated for the 20-yr period (1979 through 1998). The percentage of total recharge represented by each creek is similar to values found by Barrett and Charbeneau (1996) (table 2). Diffuse interstream recharge was assumed to equal 15 percent of total recharge on the basis of studies conducted by Barrett and Charbeneau (1996) and is similar to the estimate provided by Slade and others (1985).

Hydraulic Properties

Although hydraulic property data from aquifer tests are not very useful in estimating zonal properties for equivalent porous media models, information on hydraulic properties from the literature was compiled to estimate the range in measured hydraulic parameters. On the basis of aquifer tests in the Edwards and associated limestones in Travis County (north of the Colorado River), Brune and Duffin (1983) reported a range of transmissivities from 400 to 300,000 gal/d/ft (53.6 to 40,200 ft²/d). Senger and Kreitler (1984) calculated transmissivity using recession-curve analyses from wells near Barton Springs. Values range from 0.1 m²/s (93,000 ft²/d) to 0.4 m²/s (372,003 ft²/d).

To determine a range of values of hydraulic properties in the BSEACD, aquifer-test reports and analyses were compiled. Aquifer tests are required as part of the application process for commercial and public water-supply wells in the Barton Springs Edwards Aquifer Conservation District. Data from 24 aquifer tests conducted within the study area from 1982 through 2001 were compiled. Several hydraulic conductivity values, or a range of values, were averaged for each aquifer test. Hydraulic conductivity values range from 0.40 to 75.3 ft/d. Hydraulic conductivity values appear to be log-normally distributed, although the limited number of data may not adequately define the distribution (fig.27). The geometric mean hydraulic conductivity is 0.6 ft/d (table 3).

Brune and Duffin (1983) estimated the range of specific yield to be 0.04 to 0.06 and specific storage to be 0.00025 to 0.00045 ft⁻¹. Senger and Kreitler (1984) estimated storativities using recession-curve analyses from wells near Barton Springs. Values range from 0.001 to 0.023. Slade and others (1985) calculated a mean specific yield of 0.017 and estimated the storativity (0.00003 to 0.00006 ft⁻¹) taken from aquifer compressibility analyses by Maclay and Small (1984). Specific yield and storativity values were estimated for 10 of the 24 aquifer tests compiled from the study area. Specific yield ranged from 0.005 to 0.06 (n=5), and storativity ranged from 1×10^{-6} to 2.9×10^{-2} ft⁻¹ (n=5).

Discharge

Groundwater discharge occurs primarily at Barton Springs, which consists of a series of springs in the Barton Springs Pool area in Barton Creek close to where it enters the Colorado River. Barton Springs discharge is calculated from a rating curve that relates water levels in well

YD-58-42-903 to spring discharge. Discharge at Barton Springs was highly erratic during the winter and spring of 1992, as a result of a large flood in December 1991. Barton Springs Pool was drained for repairs as a result of the flood (Barrett and Charbeneau, 1996). The lower water level in the pool resulted in underestimation of spring discharge because of its effect on the water level in the well used to estimate spring discharge. During the spring of 1992, several large storms caused the pool to fill, resulting in large increases in estimated spring discharge. Although a separate rating curve has been developed for periods when the pool is empty (Slade, personal communication, 2001), the reported decrease in spring discharge is questionable. Accurate discharge estimates are available from when the pool was refilled in the summer of 1992. Long-term discharge at Barton Springs is 53 cfs (1918 through 1999). Cold Springs, northwest of Barton Springs, discharges into the Colorado River but is not gaged because it is flooded by Town Lake. A limited number of flow data are available from Cold Springs. Discharge from Cold Springs of 3.7 cfs was measured on 8/10/1918 when discharge at Barton Springs was 14 to 15 cfs (N. Hauwert, BSEACD, personal communication, 2000), suggesting that discharge at Cold Springs is about 25 percent of that at Barton Springs. This value is considered the most accurate total measurement of flow at Cold Springs. Other measurements, considered partial measurements for Cold Springs, indicate that flow at Cold Springs ranges from 3 to 4 cfs when the corresponding flow at Barton Springs ranges from 14 to 84 cfs. These data suggest that discharge at Cold Springs may be as low as 4 percent of the discharge at Barton Springs.

Groundwater is also discharged through pumping wells. Monthly pumpage data are collected by the BSEACD and are available from 1989 through present. Pumpage data are also available from the Texas Water Development Board (TWDB); however, the data from the BSEACD are considered more reliable for later years because the district requires discharge reporting and meters have been installed in a number of wells, whereas the TWDB reporting is voluntary. The number of reported users ranged from 100 in 1989 to 142 in 1998 (table 4). The location of the major pumping areas is shown in fig. 28. Values for unreported pumpage were calculated from countywide estimates obtained from the TWDB and percentage of the county in the study area (~ 5%). This pumpage was uniformly distributed among all the active cells in the model. Annual pumpage ranged from 3.9 cfs (1990, 1991) to 6.3 cfs (1998). The years with lowest pumpage (1991 and 1992) correspond to years with highest precipitation. Annual pumpage ranges from 3 percent (1991, 1992) to 138 percent (1996) of recharge (table 4).

Other potential discharge areas include subsurface flow from the Edwards to other underlying aquifers (that is, the Glenrose Limestone); however, Slade and others (1985) concluded that such flow is negligible.

CONCEPTUAL MODEL OF GROUNDWATER FLOW

Development of a conceptual model of groundwater flow is a prerequisite for numerical modeling of any aquifer. This conceptual model describes our understanding of how the aquifer works. Precipitation falling on the contributing zone generally moves into streams, which recharge the aquifer as they traverse the outcrop. There are five major stream drainages in the study area. Recharge increases linearly with stream flow to a threshold stream flow and remains uniform after further increases in stream flow. Approximately 15 percent of the recharge in the study area results from infiltration of precipitation on the outcrop. Groundwater generally flows from areas of higher to lower topography (west to east) in the west part of the aquifer and then flows north in the east part of the aquifer toward Barton Springs and Cold Springs. Most of the aquifer discharges to the springs. Discharge to wells represents about 10 percent of long-term average discharge at Barton Springs. The aquifer is unconfined in the outcrop zone and in the adjacent area, where the Edwards limestone is overlain by the Del Rio Clay. Farther to the east the aquifer is confined (fig. 1). The east boundary of the region is marked by the bad-water line, where the TDS of the water exceeds 1,000 mg/L. The aquifer is dynamic and responds rapidly to recharge events. This rapid response is attributed to the high degree of karstification, as evidenced by caves. Additional evidence of karstification is provided by the results of dye tracer tests, which indicate that water travels long distances within hours. Groundwater levels fluctuate to as much as 90 ft in some areas. Because of the dynamic nature of the aquifer, it will also respond quickly to drought conditions, and flow at Barton Springs could decrease rapidly in response to severe droughts. The aquifer should recover fairly rapidly after drought, however, and cumulative effects of drought should be negligible.

MODEL DESIGN

Model design includes information on the code and processor, aquifer discretization, and model parameter assignment.

Code and Processor

MODFLOW-96 (Harbaugh and McDonald, 1996), a modular finite-difference groundwater flow code developed by the U.S. Geological Survey, was used for the simulations. This code was chosen because (1) it is the most widely used and tested code for groundwater resource evaluation, (2) it is well documented (McDonald and Harbaugh, 1988), and (3) it is in the public domain. A variety of pre- and postprocessors have been developed to facilitate data entry and allow analysis of model output. In this study we used the Processing MODFLOW for Windows (PMWIN) version 5.0.54 (Chiang and Kinzelbach, 1998). The model was run on Dell Latitude with a Pentium II Processor and 64 MB RAM running Windows NT.

Grid

The model consists of 1 layer that has 120 rows and 120 columns and a total of 14,400 cells. The cell size was chosen to be small enough to reflect the availability of input data, to provide appropriate details in the output, and to be manageable. Model rows were aligned parallel to the strike of the Edwards; the grid was therefore rotated 45° from horizontal. Rectangular cells were 1,000 ft long parallel to the strike of the faults and 500 ft wide (fig. 29). This discretization is much finer than that previously used by Slade and others (1985; minimum cell spacing was 1,500 ft). The zone of active cells was defined on the basis of the hydrologic boundaries as described previously. The north boundary is the Colorado River. The east boundary is the bad-water line that was obtained from the BSEACD. The south boundary is a hydrologic divide located along Onion Creek in the Edwards aquifer recharge zone and between the cities of Buda and Kyle in the confined part of the aquifer, as determined by Stein (1995). The west boundary is the Mount Bonnell fault, which acts as a hydrologic (no-flow) barrier (Senger and Kreitler, 1984). Cells with layer thickness of less than 20 ft were assigned as inactive. Cells outside the model area were made inactive, resulting in 7,043 active cells.

Model Parameters

Model parameters include (1) elevations of the top and bottom of the layer, (2) horizontal hydraulic conductivity, (3) specific yield, and (4) specific storage. Specific yield and specific storage are required only for the transient simulations.

The structure of the top of the aquifer was based on ground-surface elevation in the unconfined recharge zone. A digital elevation map of the ground surface was downloaded from the U.S. Geological Survey Web site. East of the outcrop zone, the top of the aquifer corresponds to the base of the Del Rio Clay. The base of the aquifer corresponds to the base of the Walnut Formation, determined from recent studies by Small and others (1996). The location of faults was also based on interpretations by Small and others (1996). The contoured structure surfaces and faults were digitized and gridded using CPS3 for input to the model. Structure surfaces were interpolated to model cell centers using GIS software (ARC/INFO).

The model layer was assigned as confined/unconfined. The model was set up to calculate transmissivity and storativity on the basis of saturated thickness. The length unit was feet, and the time unit was days for all model input. Initial head for the steady-state simulations was the top of the aquifer.

MODEL BOUNDARIES

We assigned model boundaries for (1) recharge, (2) pumping, (3) springs, and (4) initial conditions. Recharge values were assigned to stream cells on the basis of analysis of flow losses in the streams. Recharge was uniformly distributed in each stream where the stream intersects the outcrop. Interstream recharge was 15 percent of the total stream recharge and was assigned to all active cells.

Pumping was assigned to cells on the basis of the location of pumping wells reported to the BSEACD. Unreported domestic (rural) pumpage was calculated from countywide estimates and was assigned to all active cells.

We used the Drain Package of MODFLOW to represent Barton Springs and Cold Springs. The drain elevation is the spring elevation (432 ft for Barton Springs and 430 ft for Cold Springs), and a high drain conductance value was used (1,000,000 ft²/d) to allow unrestricted discharge of water.

Modeling Approach

Three basic steps were followed in modeling the aquifer: (1) a steady-state model was developed to determine the spatial distribution of hydraulic conductivity, (2) a transient model

was run for a 10-yr period (1989 through 1998) by using monthly recharge and pumpage, and (3) a predictive model was developed to evaluate effects of increased pumpage and potential future droughts on groundwater availability. The steady-state model was developed because it is much more readily calibrated (because specific yield or storage coefficient data are not required) and the simulations run much faster. The calibration process involved matching simulated and measured water levels. Water levels measured during July/August 1999 were used for the steady-state calibration because spring discharge (66 cfs) was close to average conditions (53 cfs) during this time and water levels measured during this time represent the most extensive survey conducted in the aquifer. Trial and error and automated procedures were used to estimate the zonal distribution of hydraulic conductivity during model calibration. Sensitivity analyses were conducted to assess the impact of varying recharge and hydraulic properties on the model results. We quantified the calibration, or goodness of fit between the simulated and measured water-level values, using the root mean square (RMS) error, where n is the number of calibration points, h_m is the measured hydraulic head at point i , and h_s is the simulated hydraulic head at point i .

$$RMS = \left[\frac{1}{n} \sum_{i=1}^n (h_m - h_s)_i^2 \right]^{0.5} \quad (1)$$

The framework of the steady-state model was used to develop a transient model for the years 1989 through 1998, using monthly time steps. The zonal distribution of hydraulic conductivity developed from the calibrated steady-state model was used in the transient model. Hydraulic heads simulated in the steady-state model were used as input to the transient model. The 10-yr time period was chosen because pumpage records were only available for this time period, detailed synoptic water levels were measured during this time, transient water-level monitoring records correspond to this time period, and this record includes a range of hydrologic conditions from dry (1996 drought) to wet (1991, 1992). Very little calibration was required for the transient model.

The transient model was then used to predict how water levels and spring discharge might change during the next 50 yr in response to increases in pumping and potential future droughts.

STEADY-STATE MODEL

Calibration

Measured water levels in July and August (1999) were used to evaluate the steady-state model calibration because the number of measured water levels (99) was greatest for this time and spring discharge was close to average conditions (~ 66 cfs). The spatial distribution of recharge among the streams and in the interstream settings was based on the average recharge for a 20-yr record (1979 through 1998; table 2). The total amount of recharge was reduced to equal the average spring discharge for Barton and Cold Springs of 55 cfs and pumpage for 1989 of 5 cfs. Recharge was assumed to be known and was not changed during calibration. The distribution of hydraulic conductivity was estimated using a combination of trial and error and automated inverse approaches. The trial-and-error calibration involved the following steps:

- Horizontal hydraulic conductivity was adjusted during successive steady-state runs. Initial simulations used a uniform distribution of hydraulic conductivity that ranged from 5 to 50 ft d⁻¹.
- The next set of simulations used a zonal distribution of hydraulic conductivity, with conductivities ranging from 5 to 40 ft d⁻¹ in the recharge zone and 200 ft d⁻¹ outside the recharge zone. A zone of high conductivity (~ 1,000 ft d⁻¹) was then set adjacent to Barton Springs. Either the simulations did not converge or the simulated heads were much too high.
- We then imported the spatial distribution of hydraulic conductivities used by Slade and others (1985); however, almost the entire model region went dry when these conductivity values were used.
- We simulated faults with the greatest amount of offset as horizontal flow barriers (Hsieh and Freckleton, 1993). Input data required for this module include the hydraulic conductivity divided by the aquifer thickness; values of 0.01 d⁻¹ (southwest fault) and 0.05 d⁻¹ (other faults) were used in the simulations. Three faults were used in the simulations.
- The final approach that was used to achieve a calibrated model involved increasing the complexity of the hydraulic conductivity distribution from the

simple three-zone model based on calibrated hydraulic conductivities determined by Slade and others (1985) and variations in the hydraulic gradient. Steep hydraulic gradients in the southwest part of the model suggested low hydraulic conductivities, and shallow hydraulic gradients near Barton Springs suggested high hydraulic conductivities. The structure of the base of the aquifer was adjusted in some of the steady-state simulations to achieve convergence.

The results of the trial-and-error calibration indicated that there are 10 zones of hydraulic conductivity that range from 1 to 1,000 ft/d. Monthly pumpage at 1989 rates was also included in the final steady-state model and represents approximately 6 percent of the discharge at Barton Springs. Including this amount of pumpage did not significantly alter water levels or spring discharge in the model.

The results of the trial-and-error calibration generally reproduced the spatial distribution of water levels. Comparison of measured and simulated water levels resulted in an RMS error of 35 ft. The RMS error indicates that, on average, the simulated water levels differ from the measured water levels by about 35 ft. We also evaluated the use of automated inverse modeling to estimate the zonal distribution of hydraulic conductivity. Initial attempts to use automated inverse modeling in the early stages of calibration suggested that this procedure could not be used to determine reasonable values of hydraulic conductivity. Once the trial-and-error calibration was completed, we wanted to determine whether automated procedures could further improve the calibration and reduce the RMS error. The automated inverse code UCODE (Poeter and Hill, 1998) was used for this process. The hydraulic conductivity estimates from the trial-and-error calibration were used as initial estimates of the zonal hydraulic conductivity for UCODE. Log transformation of the hydraulic conductivity was used. Initially all 10 zones were included in the automated fitting; however, best results were obtained when only 4 of the 10 zones were fitted. Use of automated inversion reduced the RMS error to 24 ft. This error represents 7 percent of the total head drop across the model. The primary difference between the trial-and-error and automated zonal hydraulic conductivity estimates was in the confined section to the southeast, where hydraulic conductivity was increased from 1 to 39 ft/d. The final distribution of hydraulic conductivity is shown in fig. 30. The steady-state model generally reproduced the potentiometric surface developed from water-level measurements in July/August 1999 (fig. 31). The scatter plot of simulated versus measured heads indicates that there is very little bias in the simulation results (fig. 32). The RMS error reflects both uncertainties in

measured and simulated hydraulic heads. The heads were measured over a 2-mo period. Synoptic water-level measurements over a 2-mo period is generally considered very short for most porous media aquifers but is fairly long for this karst aquifer, which is dynamic, and spring discharge decreased from 80 to 60 cfs during this time. Therefore, the measured heads may not reflect the average discharge of Barton Springs (~53 cfs). Most of the head data were based on well locations and elevations obtained from 1:250,000 topographic maps, whereas some head data were based on global positioning system measurements. Errors were generally low throughout the model area with the exception of the southwest area, where heads are underpredicted by up to 60 ft (fig. 33). Simulated discharge was 52 cfs at Barton Springs, 2.8 cfs at Cold Springs, and 5 cfs from pumping wells.

Sensitivity Analysis

Once the steady-state model was calibrated, the sensitivity of water levels in the model to different aquifer parameters was evaluated. Sensitivity analysis quantifies the uncertainty of the calibrated model to uncertainty in the estimates of the aquifer parameters, stresses, and boundary conditions (Anderson and Woessner, 1992, p. 246). Sensitivity analysis is used to evaluate the nonuniqueness of the calibrated model. The hydrologic parameters that have the greatest impact on simulated water levels and spring discharge can be identified through sensitivity analyses.

Sensitivity analyses were conducted on hydraulic conductivity, recharge, spring conductance, and pumpage. Each parameter was varied systematically, and the change in simulated water levels from the base case was calculated (1) at the location of the calibration wells and (2) in each active cell in the model. Any bias in the sensitivity analysis and the calibration between the calibration points and the entire model layer could be identified by comparing the results at the well locations and the active cells. The change in water levels was quantified by calculating the mean difference:

$$MD = \frac{1}{n} \sum_{i=1}^n (h_{sen} - h_{cal}) \quad (2)$$

where n is the number of points, h_{sen} is the simulated water level for the sensitivity analysis, and h_{cal} is the calibrated water level. Positive values indicate that simulated water levels are higher than calibrated values, and negative values indicate that simulated water levels are lower than calibrated values.

Simulated water levels in the model were most sensitive to recharge and hydraulic conductivity and insensitive to pumpage and drain conductance (fig. 34). The mean differences calculated at the calibration locations and at each active cell in the model are similar, indicating that the calibration points probably do not bias the sensitivity analysis and represent the aquifer well. Higher values of recharge resulted in higher simulated water levels. The model failed to converge for reductions in recharge of 25 and 50 percent of the calibrated value. Higher values of hydraulic conductivity resulted in lower simulated water levels, whereas lower values of hydraulic conductivity resulted in higher water levels. The sensitivity to hydraulic conductivity was slightly asymmetric in that the simulated water levels were more sensitive to lower than to higher hydraulic conductivities.

TRANSIENT MODEL

Simulated heads and the calibrated distribution of horizontal hydraulic conductivity from the steady-state model were used as input for the 10-yr transient model, which was from 1989 through 1998. Annual precipitation during this time ranged from 26 inches in 1989 to 52 inches in 1991 (fig. 35; table 4). Monthly stress periods were used for the transient simulations, with 12 time steps in each stress period. This setup resulted in a total of 120 stress periods for the 10-yr simulation (1989 through 1998). A stress period is a time interval in MODFLOW during which all inflow, outflow, properties, and boundary conditions are constant. Recharge and pumpage were changed for each stress period (fig. 35a, b). Recharge rates were estimated from stream-loss studies, as discussed previously. Annual recharge was highest in 1992 (169 cfs) and lowest in 1996 (4 cfs) (table 4). Monthly recharge was much more variable and ranged from 0.3 to 500 cfs (fig. 35b). Pumpage was assigned on the basis of data from the BSEACD. Annual pumpage ranged from 3.9 cfs (1990, 1991) to 6.3 cfs (1998) (table 4). Because recharge varied greatly from year to year, the percentage of recharge represented by pumpage varies from 3 percent during 1991 and 1992 to 138 percent during 1996. Initial estimates of specific yield (0.005) and specific storage ($5 \times 10^{-5} \text{ ft}^{-1}$) were based on data from Slade and others (1985).

Initial transient simulations did not converge because of cells near the west-central portion, in which the simulated hydraulic head oscillated between iterations. These cells were located in a zone where the base of the Edwards aquifer was much higher than surrounding areas. By lowering the base of some of these cells to values similar to those in adjacent areas, we

achieved convergence. This lowering assumes that the underlying Glen Rose Formation is locally permeable and connected to the Edwards aquifer.

The transient simulation was evaluated using three different criteria: (1) Simulated and measured spring discharge were compared (figs. 36, 37). (2) Simulated hydraulic heads were compared with hydrographs for eight monitoring wells (figs. 38 and 39). (3) Scatter plots were developed for simulated and measured heads during low (1994, 1996) and moderately high (1998) flow conditions (fig. 40).

Generally good agreement was obtained between measured and simulated discharge at Barton Springs (figs. 36, 37). Simulated discharge at Barton Springs was calculated by subtracting discharge at Cold Springs (6 percent of total discharge) from total discharge listed in the output file. The RMS error between measured and simulated discharge for the distributed model is 12 cfs, which represents 11 percent of the discharge fluctuations measured at Barton Springs during that time. Data from an 8-mo period, December 1991 through July 1993, were omitted from the error calculations because of uncertainties related to the measured discharge data as a result of flooding. One of the main objectives of the model is to accurately simulate low flows in Barton Springs. The scatter plot suggests that on average there is no bias in the results (fig. 37); however, this plot masks underpredictions and overpredictions at different times. Overprediction of low spring flows in 1989 and early 1990 is attributed to the initial conditions (hydraulic head from steady-state model) not being in equilibrium with the boundary conditions (recharge and discharge) for the transient simulation. Good correspondence between measured and simulated discharge was found for 1990 through 1991. Simulated spring discharge generally underestimates measured discharge during the 1994 low flow period; however, both measured and simulated discharges have the same minimum value. In contrast, simulated discharge overestimates measured discharge during the 1996 low flow period. The slope of the simulated recession is more gradual than that of the measured recession, which is U shaped, and the timing of the minimum simulated discharge is later than that of the measured data. Peak discharges are underestimated in some cases (1990 through 1991), simulated accurately in other cases (1989, 1993, 1995), and overestimated in other cases (1991 - 1992, 1997, 1998). During high flows, some of the discharge may be diverted to an ungaged spring and other smaller springs along Barton Creek, which is unaccounted for in the model.

The transient model generally reproduces water levels monitored continuously in many of the continuously monitored water levels (figs. 38, 39). Water levels in the north part of the

aquifer are reproduced more accurately than those to the south. The RMS error ranged from 3.8 ft (58-42-8TW) to 31 ft (58-50-221) in the four wells in the north, and these errors represent 16 to 63 percent of the range in water-level fluctuations. RMS errors increase in wells to the south and range from 37.5 ft (58-50-411) to 83.7 ft (58-58-123). Because well 58-50-411 is located adjacent to a cave (N. Hauwert, BSEACD, personal communication, 2000), its water levels remain fairly constant. These water levels are not reproduced in the simulation, which cannot represent flow in caves.

Scatter plots between measured and simulated water levels were developed for different times during the transient simulation (fig. 40). The scatter plot for March/April 1994 shows that the model generally simulated the water levels during low-flow conditions (fig. 40a). The RMS error of 29 ft represents 11 percent of the head drop in the model area. Comparison of measured and simulated water levels for July and August 1996 (fig. 40b) indicates that simulated water levels underestimate measured water levels by 37 ft (10 percent of the head drop across the model area) on average for this low-flow period. It is difficult to compare measured and simulated water levels during high flow periods because spring discharge is generally changing rapidly and synoptic water-level measurements over 2-mo time periods generally span large changes in spring discharge. The scatter plot for July and August 1998 generally represents the end of the transient simulation (fig. 40c). The RMS error of 64 ft (22 percent of the head drop in the model) is much higher than the other RMS errors and is attributed, in part, to the dynamic nature of the aquifer during high flow conditions. In general, the model provides reasonable simulations of water levels for different times.

Sensitivity analyses were conducted to assess the impact of varying groundwater recharge, pumpage, specific yield, and specific storage on simulated spring discharge and water levels in monitoring wells (figs. 41 through 45). In many cases, we could not evaluate the effect of reducing the various parameters by 50 percent because the simulations did not converge in most cases. Therefore, the evaluation is limited to the range of -10 to + 50 percent. Groundwater recharge had the greatest impact on spring discharge and water levels in monitoring wells. Increasing recharge by 50 percent resulted in increasing the mean spring discharge by about the same amount (table 5; fig. 41a). Increasing recharge had a greater impact on high spring flows than on low flows, and spring discharge was more variable, as shown by the range and coefficient of variation of spring discharge (table 5). Simulated water levels in monitoring wells displayed a similar response to variations in recharge as spring discharge (fig. 42). Decreasing

recharge had the opposite effect of increasing recharge. Simulated spring discharge and water levels in wells were much less sensitive to variations in pumpage, specific yield, and specific storage (figs. 41b, c, d; 43, 44, 45; table 5). Increasing pumpage by 50 percent had a negligible effect on spring discharge and water levels in wells. Increasing specific yield and specific storage by 50 percent resulted in 1.6 and 0.7 percent increase in mean spring discharge, respectively, compared with 50 percent increase in response to recharge. Uncertainties in specific storage are greater than those of specific yield; therefore, an additional simulation was conducted to evaluate the impact of varying specific storage by a factor of 10. Increasing specific storage by 10 decreased the mean spring discharge slightly but greatly reduced the range in spring discharge (table 5). The increased specific storage does not simulate the low spring discharges which are critical for groundwater management. Increasing specific storage by 10 had a similar effect on the simulated water levels in the monitoring wells, which better replicate the measured water-level fluctuations in the monitoring wells (fig. 45). However, the emphasis of the study on simulating low spring discharges over accurately simulating water levels in monitoring wells precludes using the higher specific storage in the final simulations.

PREDICTIONS

The calibrated model was used to evaluate the future availability of groundwater in the Barton Springs segment of the Edwards aquifer under average recharge and drought-of-record conditions. Senate Bill 1 requires water planning under drought-of-record conditions to ensure that future water needs are met during times of severe drought. The drought of record was evaluated for the study area.

Future Pumpage

The future simulations were initiated with pumpage data from BSEACD for 2000. Estimates of future groundwater demands were based on demand numbers from the Regional Water Planning Group (Region K). Future pumpage was estimated on the basis of projections made by the Region K Water Planning Group and the Capital Area Metropolitan Planning Organization (CAMPO). Estimates of future population and water usage have been made by these groups for cities and counties in and around the District; however, none of these

projections could be applied directly to the District. On the basis of estimated total pumpage in the District (permitted and exempt wells), a multiplier of 2.1 was used to calculate pumpage in 2050 from current pumpage (2000). This multiplier is higher than estimates for rural areas, but lower than for towns. Starting with current (year 2001) total pumpage of 6,754 acre-ft/yr (equivalent to 9.3 cfs), pumpage in 2050 was estimated to be 14,183 acre-ft/yr (19.6 cfs). Monthly pumpage used in the future simulations was linearly interpolated between 2001 and 2050. The regional planning groups included the implementation of conservation measures as a part of projected water usage but did not consider substitution of surface water for groundwater. Because we do not have any information on the seasonal distribution of pumpage, we used the monthly data from the transient simulation from 1989 through 1998 and simply multiplied by the factors required to increase the annual pumpage to the values for 2001 through 2050.

Drought of Record

A drought of record is the most severe drought during the period of record in terms of duration and lack of rainfall. The drought of record for the study area occurred between 1950 and 1956 according to the 140-yr record of precipitation (1860 through 2000) (fig. 46). Precipitation ranged from 25.8 inches in 1950 to 11.4 inches in 1954. The mean annual precipitation during the 7-yr drought period (23.1 inches) was about two-thirds of the long-term annual precipitation (33.5 inches). The mean annual precipitation during the last 3 yr of the drought (16.5 inches) was about half the long-term average precipitation.

We tried to estimate the recharge that would correspond to the 1950's drought by relating precipitation to recharge for the period of record (1989 through 1998), but the relationship was very poor. We then tried to relate recharge to Barton Springs discharge for the same period, but the scatter plot indicated very poor relationships. Comparison of the time series nevertheless suggested a much stronger relationship, with some lag between recharge and discharge. Therefore, we finally decided to assume that recharge equals discharge, although doing so may slightly overestimate recharge during low recharge conditions because it might include discharge from storage in the aquifer. Annual discharge values for Barton Springs were obtained from Slade and others (1986) for the period 1950 through 1956 (fig. 26) and were increased by 5 percent to account for discharge from Cold Springs. Recharge for normal climatic conditions was based on long-term average discharge at Barton Springs and Cold Springs of about 55 cfs. The

monthly distribution of recharge from the transient simulation (1989 through 1998) was used for the future simulations of drought conditions, and these values were reduced to average recharge of 55 cfs for the first 3 yr and reduced by the amount required to obtain the recharge for the 1950's drought for the remaining 7 yr. Future simulations of average recharge (55 cfs) with increased pumpage used evenly distributed recharge for each month of the year and not the seasonal distribution from the transient simulation from 1989 through 1998. The latter approach was used because the simulated potentiometric surfaces from future simulations with the seasonal distribution of recharge varied markedly, making it difficult to estimate drawdowns when comparing different potentiometric surfaces. The baseline potentiometric surface was developed by simulating average recharge (55 cfs) evenly distributed throughout the year and current pumpage conditions (2000) (fig. 47).

Predicted Groundwater Availability

Predictive simulations were conducted with the calibrated model: baseline run with average recharge (55 cfs) evenly distributed throughout the year and future pumpage for each 10-yr period (2001 through 2010; 2011 through 2020; 2021 through 2030; 2031 through 2040; 2041 through 2050); simulations with future pumpage and drought conditions for each 10-yr period (3 yr of average recharge followed by 7 yr of drought) (Table 6).

We calculated the water-level declines at the end of the first and last decades (2010 and 2050) by subtracting the predicted water levels at the end of these decades from the baseline water levels. The predictive simulations indicate that water-level declines in response to increased groundwater pumpage are small: ≤ 5 ft in 2010 and ≤ 35 ft in 2050 (figs. 48a, 49a). In contrast, water-level declines in response to increased pumpage and drought-of-record conditions were much greater: ≤ 200 ft in 2010 and ≤ 270 ft in 2050 (figs. 48b, 49b). These results are consistent with the sensitivity analyses for the transient simulation, which indicate that the model is much more sensitive to recharge than to pumpage.

Average discharge at Barton Springs in response to average recharge and current pumpage (9 cfs) is about 43 cfs (fig. 50a). The sum of discharge at Barton Springs (43 cfs), Cold Springs (3 cfs), and pumpage (9 cfs) equals the average recharge of 55 cfs. The model predicts that Barton Springs discharge will decrease to 41 cfs in 2010 and to 33 cfs in 2050, which is directly proportional to increased pumpage (~ 2 cfs per decade and 10 cfs over 50 yr). The model

predicts that spring discharge should decline much more in response to potential drought-of-record conditions. Predicted spring discharge at the end of 2010 is 7.5 cfs and 0 cfs in 2050 under drought-of-record conditions (fig. 50b). The results for spring discharge are similar to those for water levels and emphasize the significance of recharge and potential droughts in controlling water availability in the future.

MODEL LIMITATIONS

All numerical groundwater models are simplifications of the real system and therefore have limitations. Limitations generally result from assumptions used to develop the model, limitations in the input data, and the scale at which the model can be applied.

Use of a distributed, porous media model to simulate flow in a karst system is a simplification, and the model will not be able to simulate some aspects of flow accurately in this system, particularly the effects of conduits on groundwater flow. This simplification is not critical for water-resources management, and the study showed that the model was able to predict variations in spring flow over time, as well as fluctuations in water levels in monitoring wells. However, this model was not able to simulate very low water-level fluctuations in one of the monitoring wells that was located adjacent to a cave. The model will not be able to simulate travel times for contaminants in the system and should not be used for this purpose. The bad-water line to the east was simulated as a no-flow line. This representation may not be entirely accurate, particularly during low flow periods when low gradients may induce flow from the east. Further studies should evaluate this process. The current model did not include the underlying Glen Rose Limestone, which in some areas may be sufficiently permeable and may contribute to flow in the Edwards aquifer.

There are also limitations associated with input data. Recharge data for this model are generally considered much more accurate than are available for many other regions. Stream recharge was distributed uniformly along the outcrop areas because of lack of information on spatial focusing of recharge in particular locations. This assumption may affect flow to Cold Springs because the line of recharge along Williamson Creek generally forms a divide, minimizing flow south of this creek to Cold Springs. Future studies should spatially distribute recharge along the streams. Because recharge data are not available for the 1950's drought, we approximated recharge during this time by assuming that recharge equals discharge. More

studies should be conducted to develop better estimates of recharge during this time. Water-level data for drawing potentiometric surfaces may affect our evaluation of the goodness of fit of the model because comparisons of simulated and measured water levels are restricted to areas where water levels have been measured.

The model also predicts drying in certain zones, such as in the south-central region. Such dry zones may be an artifact of the model as a result of steep gradients in the base of the Edwards and may or may not be realized in the future. Such drying may also depend on the conductivity of the underlying Glen Rose and the hydraulic connectivity of the units at the base of the Edwards units. The model also predicted unrealistically high water levels in the western fringe of the model, particularly in the southwest region. Overestimation of water levels in this zone may result from the aquifer being very thin in this region, and future modeling studies should evaluate whether this region should be included in the model. The high water levels may also be an artifact of the uniform distribution of recharge along streams in the model. This situation should also be evaluated in future studies.

This model was developed to evaluate variations in spring discharge and aquiferwide water-level declines over the next 50 yr. The model is not considered appropriate for local issues, such as water-level declines surrounding individual wells, because of the coarse grid size (500 × 1,000 ft) and limitations described earlier.

CONCLUSIONS

The Edwards aquifer is a critical source of water to about 45,000 residents in Travis and Hays Counties. We developed a numerical groundwater flow model for the Barton Springs segment of the Edwards aquifer to predict water levels and spring discharge under future pumping and potential future drought conditions. The model has 1 layer and 7,043 active cells and incorporates recent information on the geology and hydrology of the Edwards aquifer in this region. Recharge to the system was calculated by using stream-gage data. A steady-state model was calibrated to determine the distribution of hydraulic conductivity in the model, and a transient model simulated flow for a 10-yr period from 1989 through 1998. Future simulations included various projected pumpage scenarios and 3 yr of average recharge, followed by 7 yr of drought conditions similar to that of the 1950's drought.

Good agreement was found between measured and simulated water levels for the steady-state model (RMS error is 24 ft, 7 percent of the hydraulic head drop across the study area). The steady-state model predicted that 6 percent of the discharge was through Cold Springs and the remainder through Barton Springs. The transient simulation generally reproduced measured spring discharge for 1989 through 1998. The RMS error was 12 cfs, which represents 11 percent of the discharge fluctuations measured at Barton Springs during that time.

To assess the future availability of groundwater in the Barton Springs segment of the Edwards aquifer, we used the calibrated model to predict future water levels under drought-of-record conditions using estimates of future groundwater demands that were based on demand numbers from the Regional Water Planning group. The model predicts that water-level declines in response to increased pumpage under average recharge conditions are small (≤ 35 ft), whereas water-level declines in response to increased pumpage and drought-of-record conditions are much greater (≤ 270 ft). Declines in spring discharge in response to increased pumpage are also small and proportional to the increased pumpage (~ 10 cfs in the next 50 yr), whereas the model predicts that spring discharge will decrease to 0 in response to drought-of-record conditions by as early as 2030. The extreme sensitivity of water levels and spring discharge to recharge and drought conditions indicates that aquifer management under drought conditions should consider enhanced recharge in addition to groundwater conservation.

ACKNOWLEDGMENTS

The authors would like to thank the Lower Colorado River Authority for providing the funding for this study. Staff at the BSEACD provided invaluable assistance with the study. Water level data were examined and compiled by Stefani Helmcamp and Brian Hunt. Brian Hunt conducted many of the sensitivity analyses. Pumpage data were provided by Shu Liang, and water level monitoring data were provided by Joseph Beery at the BSEACD. The authors benefited from many discussions with Nico Hauwert at the BSEACD (currently City of Austin). Ted Angle at the TWDB also provided pumpage data. Leiying digitized these contour maps, and Joseph Yeh used CPS3 to provide digital output from the model. The City of Austin provided long-term precipitation and spring discharge data. The authors benefited from many helpful discussions with Mike Barrett (Center for Research in Water Resources) and Raymond Slade

(U.S. Geological Survey) who conducted previous modeling studies of the aquifer. Figures were drafted by Jason West (BSEACD) and Pat Alfano (Bureau of Economic Geology).

REFERENCES

- Anderson, M. P., and W. W. Woessner, 1992, Applied groundwater modeling, simulation of flow and advective transport: New York, Academic Press, 381 p.
- Barrett, M. E., and Charbeneau, R. J., 1996, A parsimonious model for simulation of flow and transport in a karst aquifer: Technical Report Center for Research in Water Resources, Report No. 269, 149 p.
- Chiang, W. H., Kinzelbach, W., and others, 1998, Aquifer simulation model for Windows—groundwater flow and transport modeling, an integrated program: Berlin, Stuttgart, Gebruder Borntraeger, ISBN 3-443-01029-3.
- Collins, E. W. and Woodruff, C. M., 2001, Faults in the Austin, Texas, area—defining aspects of the local structural grain, *in* Woodruff, C. M., and Collins, E. W., trip coordinators, Austin, Texas, and beyond, geology and environment: Austin Geological Society Guidebook 21, p. 15–26.
- Collins, E. W., 1996, San Antonio relay ramp; area of stratal continuity between large-displacement barrier faults of the Edwards aquifer and Balcones Fault Zone, Central Texas: Gulf Coast Association of Geological Societies Transactions, v. 46, p. 455–456
- Ferrill, D. A., and Morris, A. P., 2001, Displacement gradient and deformation in normal fault systems: *Journal of Structural Geology*, v. 23 no. 4, p. 619–638.
- Garner, L. E., and Young, Keith, 1976, Environmental geology of the Austin area: an aide to urban planning: The University of Texas at Austin, Bureau of Economic Geology Report of Investigations No. 86, 39 p.
- Guyton, W. F., and Associates, 1958, Recharge to the Edwards reservoir between Kyle and Austin: report prepared for the City Water Board, San Antonio, Texas, 9 p.
- Hanson, J. A., and Small, T. A., 1995, Geologic framework and hydrogeologic characteristics of the Edwards aquifer outcrop, Hays County, Texas: U.S. Geological Survey, Water-Resources Investigations Report 95-4265, 10 p. (1 sheet).
- Harbaugh, A. W., and McDonald, M. G., 1996, User's documentation for MODFLOW-96, an update to the U.S. Geological Survey modular finite-difference ground-water flow model: U.S. Geological Survey Open-File Report 96-485, 56 p.
- Hauwert, Nico, Hanson, John, Small, Ted, and Liang, Shu, 1997, Geologic map of the Barton Springs segment of the Edwards aquifer: Barton Springs/Edwards Aquifer Conservation

- district in co-operation with the U.S. Geological Survey: unpublished ARC/INFO Geographic Information System database and map plot.
- Hauwert, N., and Vickers, S., 1994, Barton Springs/Edwards aquifer hydrogeology and groundwater quality: Austin, TX, Barton Springs/Edwards Aquifer Conservation District, report prepared for Texas Water Development Board under contract no. 93483-346, 92 p.
- Hovorka, S. D., 1996, High-frequency cyclicity during eustatic sea-level rise: Edwards Group of the Balcones Fault Zone: Gulf Coast Association of Geological Societies Transactions, v. 46, p. 179–184.
- Hovorka, S. D., Mace, R. E., and Collins, E. W., 1998, Permeability structure of the Edwards aquifer, South Texas—implications for aquifer management: The University of Texas at Austin, Bureau of Economic Geology Report of Investigations No. 250, 55 p.
- Hsieh, P. A., and Freckleton, J. R., 1993, Documentation of a computer program to simulate horizontal-flow barriers using the U.S. Geological Survey's modular three-dimensional finite-difference ground-water flow model U.S. Geological Survey, Open-File Report 92-477, 32 p.
- Immenhauser, Adriana, and Scott, R. W., 1999, Global correlation of Middle Cretaceous sea-level events: *Geology*, v. 27, no. 6, p. 551–554.
- Larkin, T. J., and Bomar, G. W., 1983, Climatic atlas of Texas: Austin, Texas, Department of Water Resources, 151 p.
- Mace, R. E., Chowdhury, A. H., Anaya, R., and Way, S. C., 2000, Groundwater availability of the Trinity Aquifer, Hill Country Area, Texas: numerical simulations through 2050: Texas Water Development Board Report 353, 117 p.
- Maclay, R. W., and Small, T. A., 1976, Progress report on geology of the Edwards aquifer, San Antonio area, Texas, and preliminary interpretation of borehole geophysical and laboratory data on carbonate rocks: U.S. Geological Survey Open-File Report 76-627, 65 p.
- McDonald, M. G., and Harbaugh, A. W., 1988, A modular three-dimensional finite-difference ground-water flow model: U.S. Geological Survey, Techniques of Water Resources Investigations, Book 6, Chapter A1.
- Moore, C. H., 1996, Anatomy of a sequence boundary—Lower Cretaceous Glen Rose/Fredericksburg, Central Texas Platform: Gulf Coast Association of Geological Societies Transactions, v. 46, p. 313–320.

- Poeter, E. P., and Hill, M. C., 1998, Documentation of UCODE, a computer code for universal inverse modeling: U.S. Geological Survey Water-Resources Investigations Report 98-4080, 116 p.
- Rose, P. R., 1972, Edwards Group, surface and subsurface, Central Texas: The University of Texas at Austin, Bureau of Economic Geology Report of Investigations No. 74, 198 p.
- Senger, R. K., and Kreitler, C. W., 1984, Hydrogeology of the Edwards aquifer, Austin area, Central Texas: The University of Texas at Austin, Bureau of Economic Geology Report of Investigations No. 141, 35 p.
- Slade, R. M., Jr., Dorsey, M. E., and others, 1986, Hydrology and water quality of the Edwards aquifer associated with Barton Springs in the Austin area, Texas: U.S. Geological Survey, Water-Resources Investigations Report 86-4036, 96 p.
- Slade, R. M., Ruiz, L., and others, 1985, Simulation of the flow system of Barton Springs and associated Edwards aquifer in the Austin area, Texas: U.S. Geological Survey, Water Resources Investigations Report 85-4299, 49 p.
- Small, T. A., Hanson, J. A., and Hauwert, N. M., 1996, Geologic framework and hydrogeologic characteristics of the Edwards aquifer outcrop (Barton Springs segment), northeastern Hays and southwestern Travis Counties, Texas: U.S. Geological Survey, Water-Resources Investigations WRI 96-4306, 15 p. (1 sheet).
- Stein, W. G., 1995, Edwards aquifer ground-water divides assessment, San Antonio region, Texas: Edwards Underground Water District Report 95-01 prepared by LBG-Guyton Associates, variously paginated.
- Trescott, P. C., Pinder, G. F., and others, 1976, Finite-difference model for aquifer simulation in two dimensions with results of numerical experiments: U.S. Geological Survey, Techniques of Water Resources Investigations, Book 7, Chapter C1, 116 p.

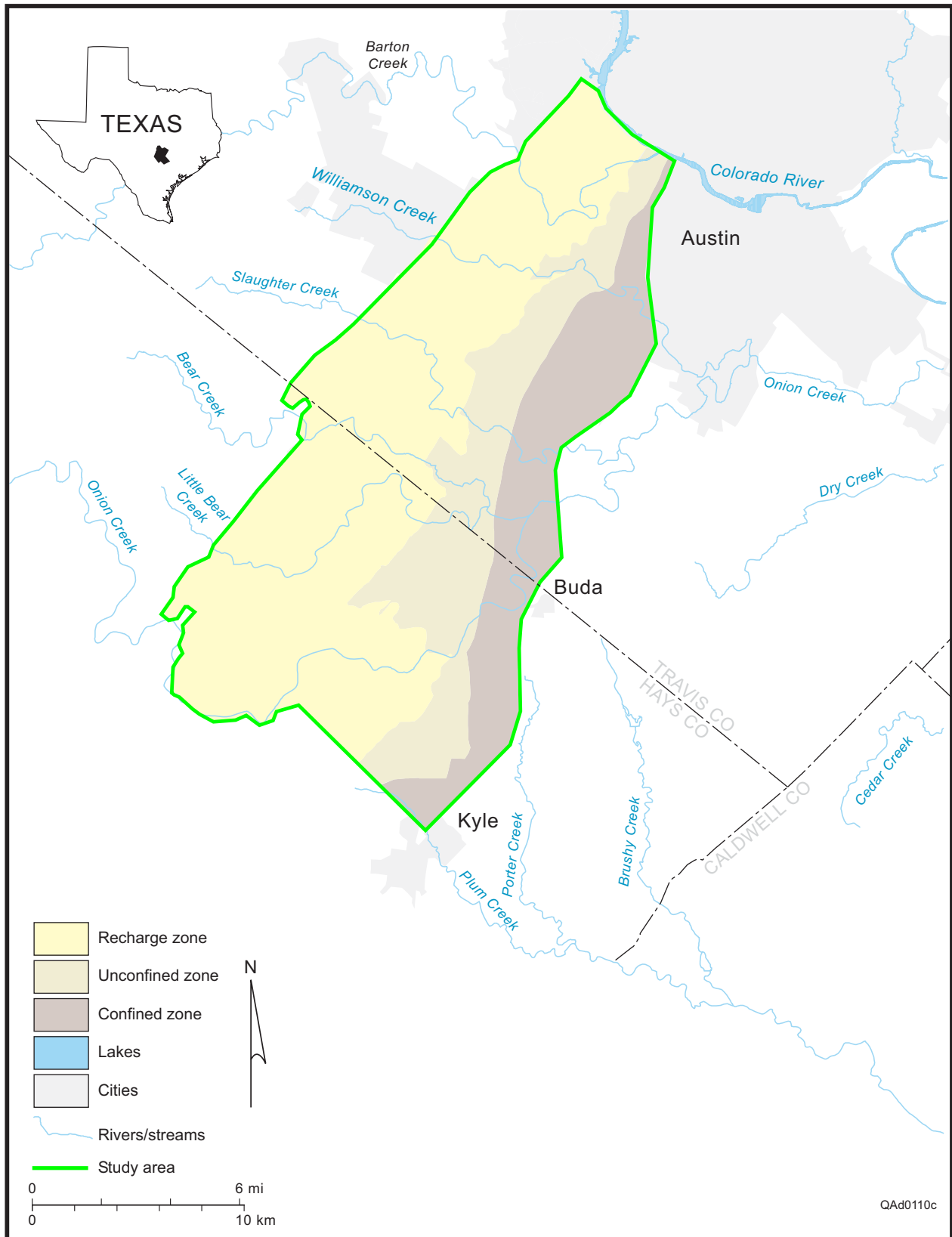


Figure 1. Location of the study area relative to cities, towns, roads, and rivers.

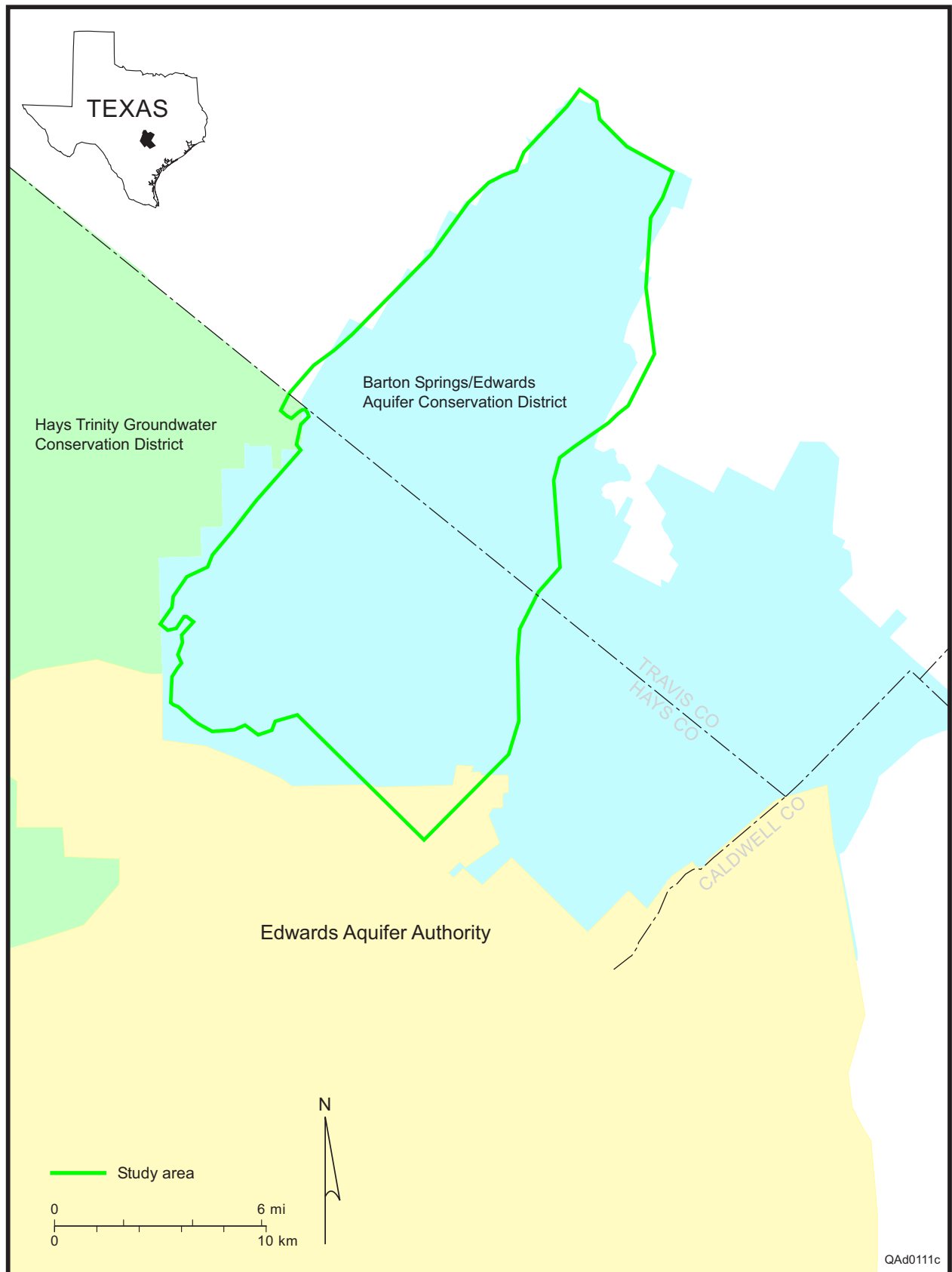


Figure 2. Location of Groundwater Conservation Districts in the study area.

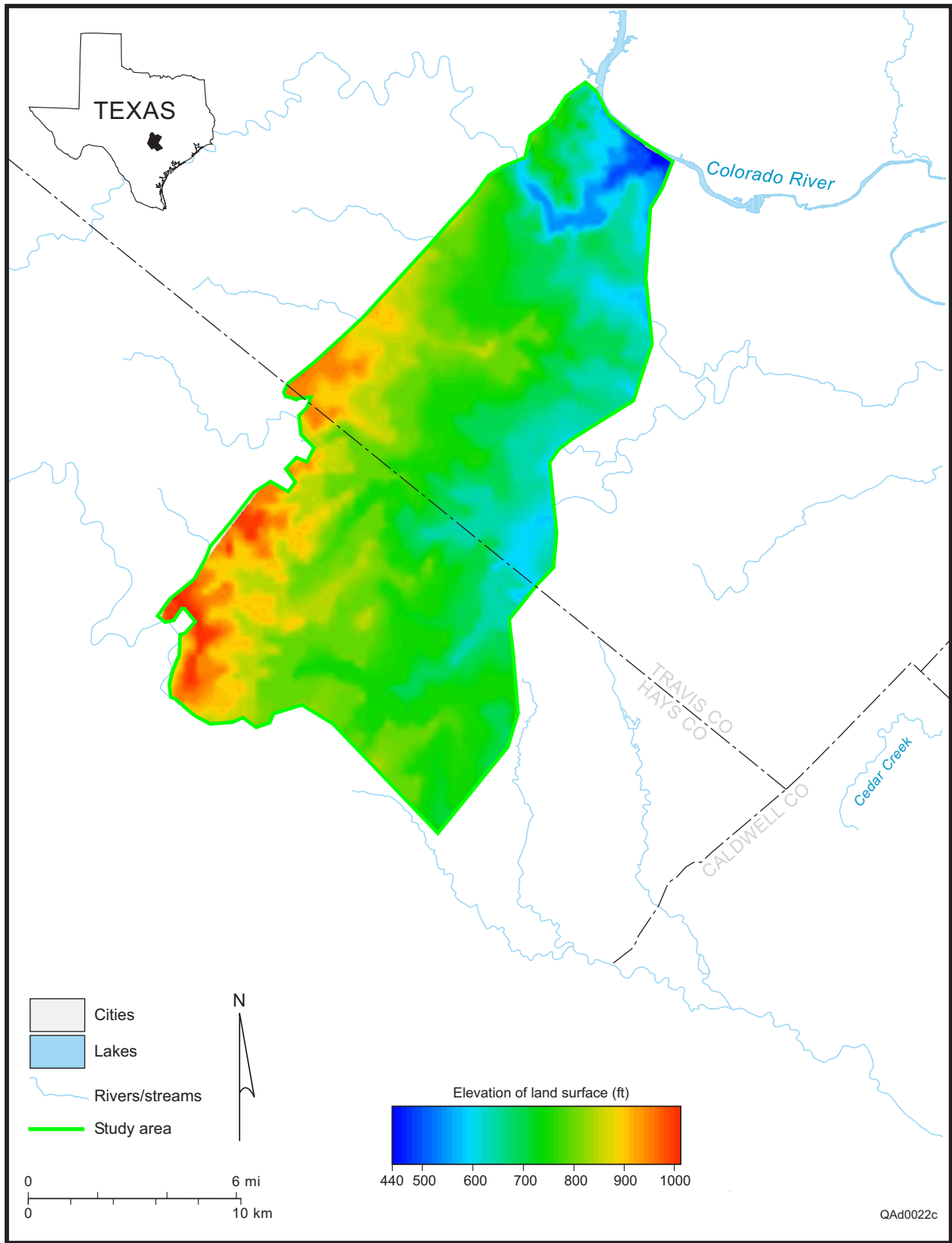


Figure 3. Land-surface elevation in the study area.

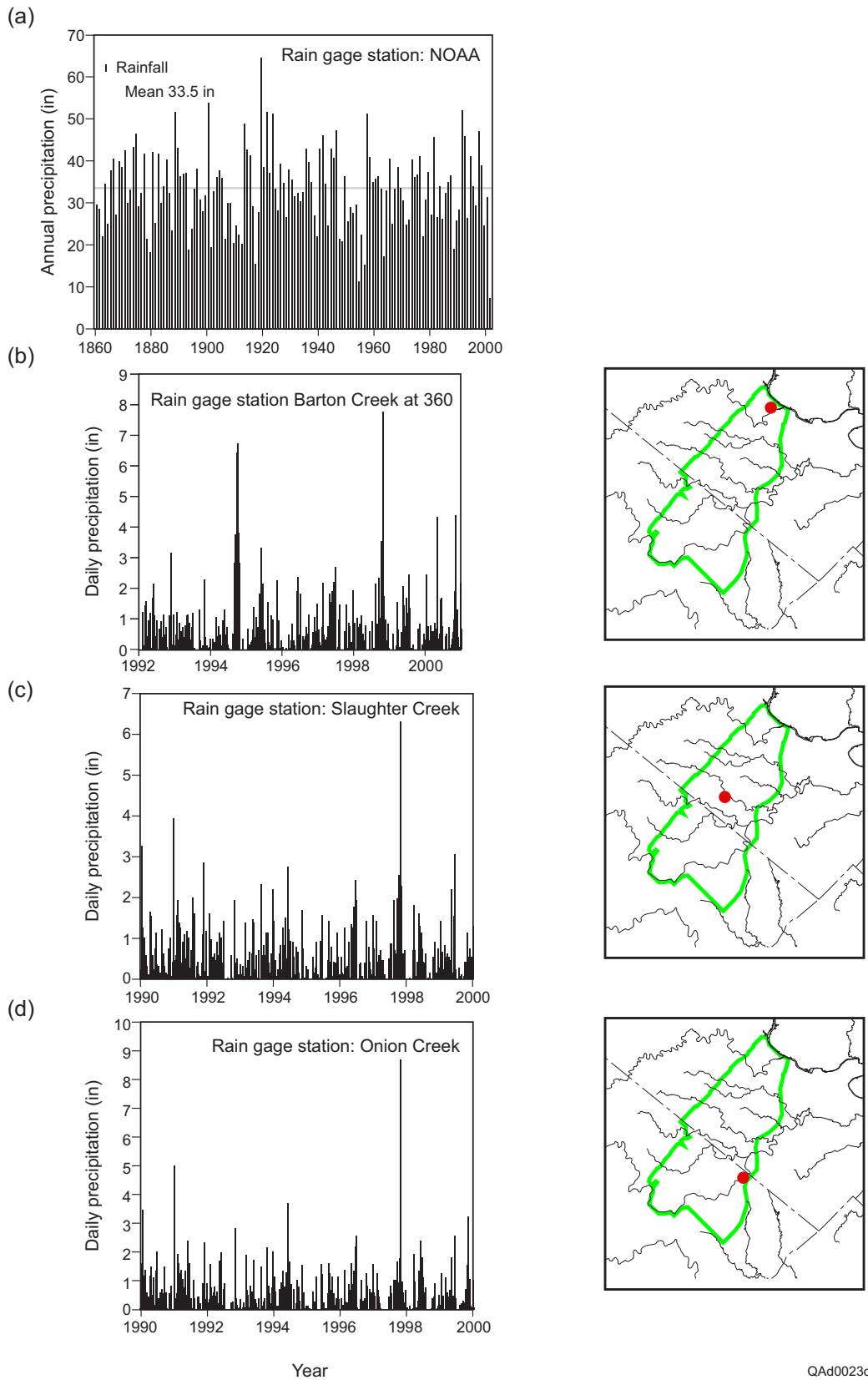
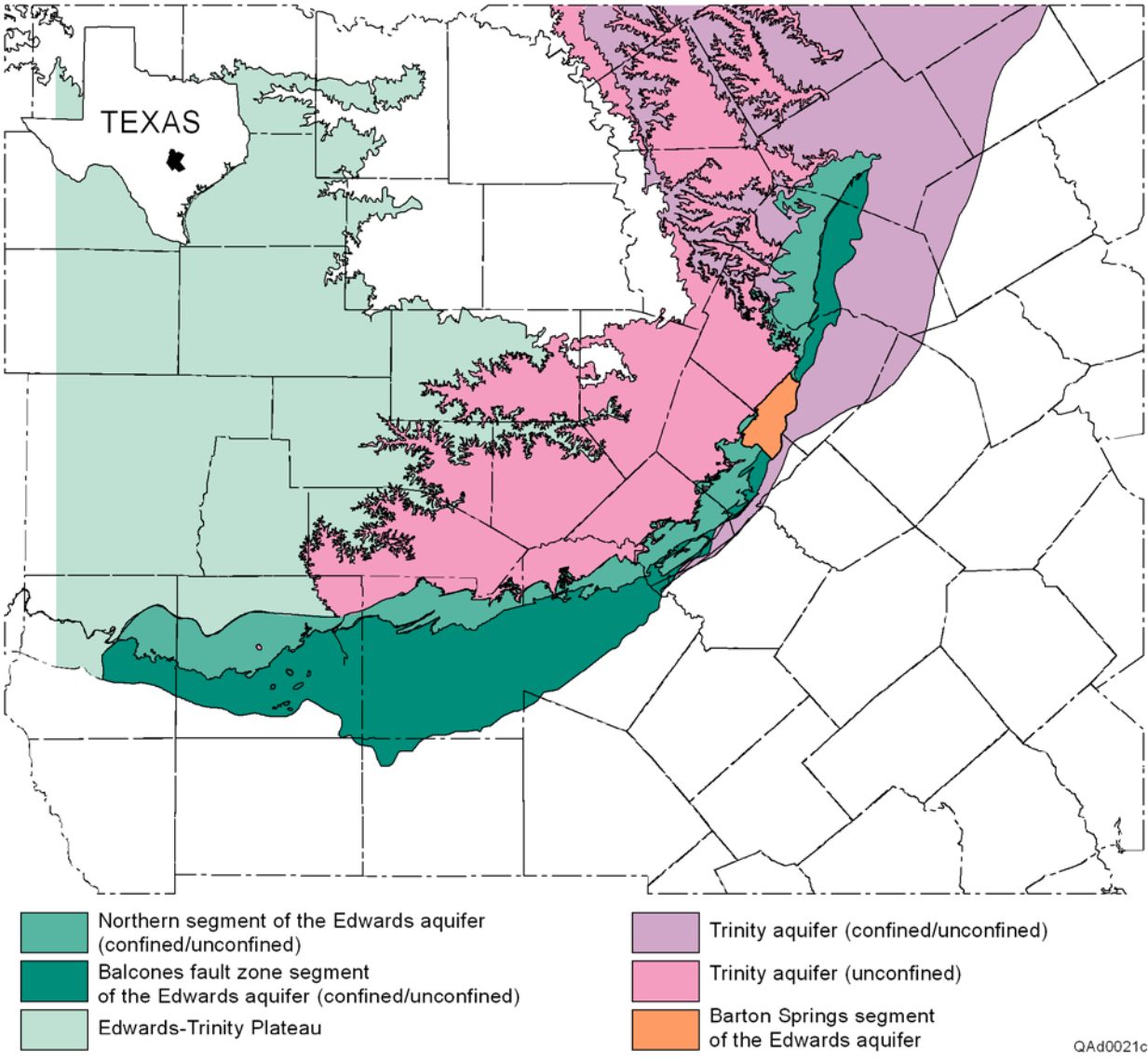


Figure 4. Historical annual precipitation for rain-gage stations at (a) Camp Mabry and Mueller Airport (NOAA station), (b) Barton Creek, (c) Slaughter Creek, and (d) Onion Creek.



QAd0021c

Fig. 5. Geologic setting of the Barton Springs segment of the Edwards aquifer.

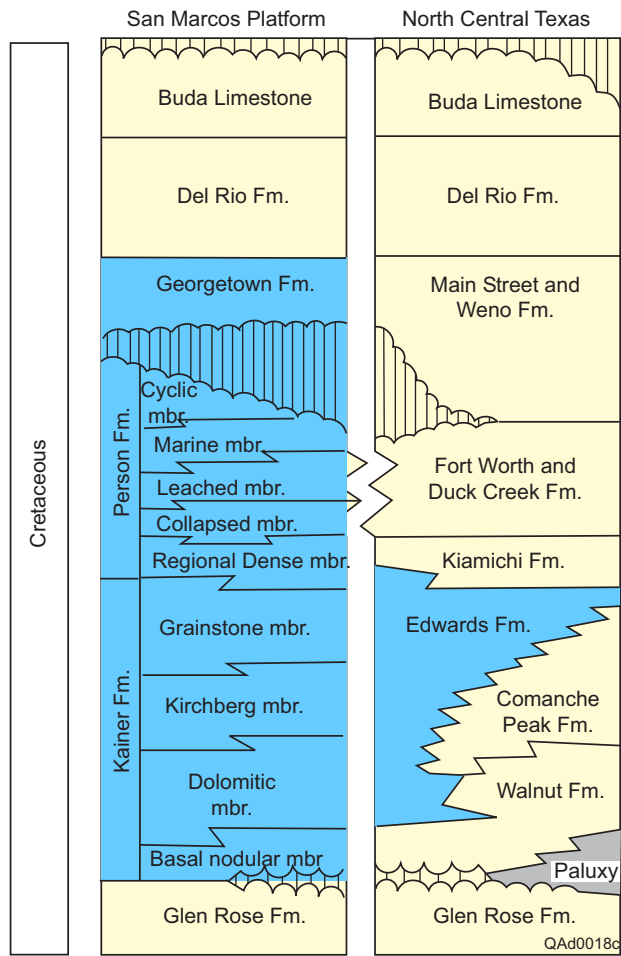


Fig. 6. Stratigraphic and hydrostratigraphic section of the study area.

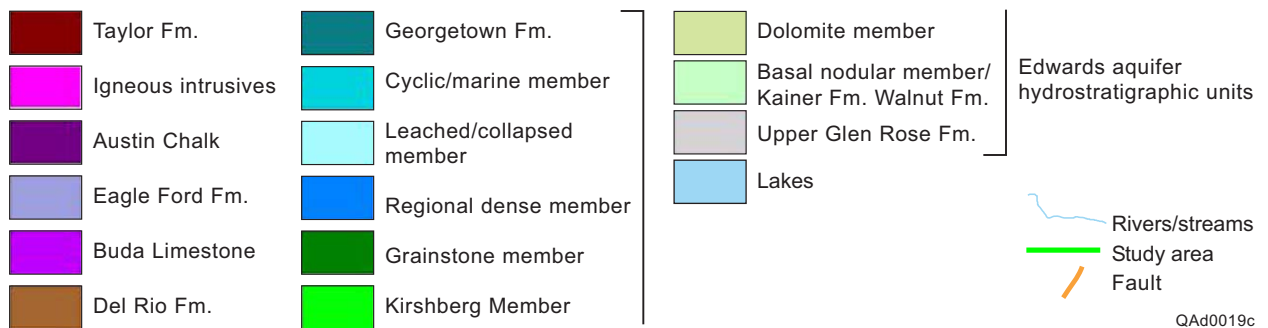
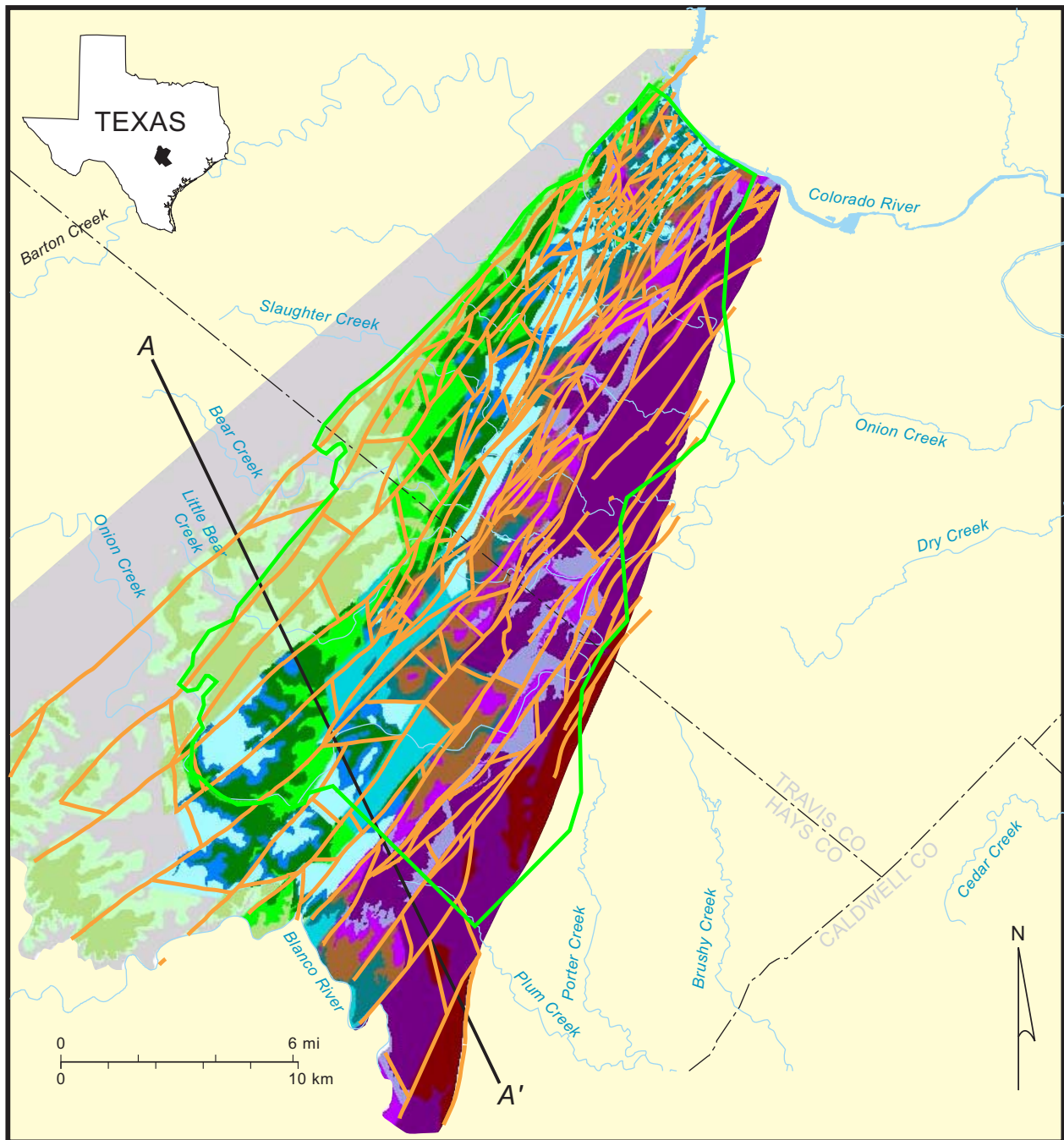


Fig. 7. Surface geology in the study area.

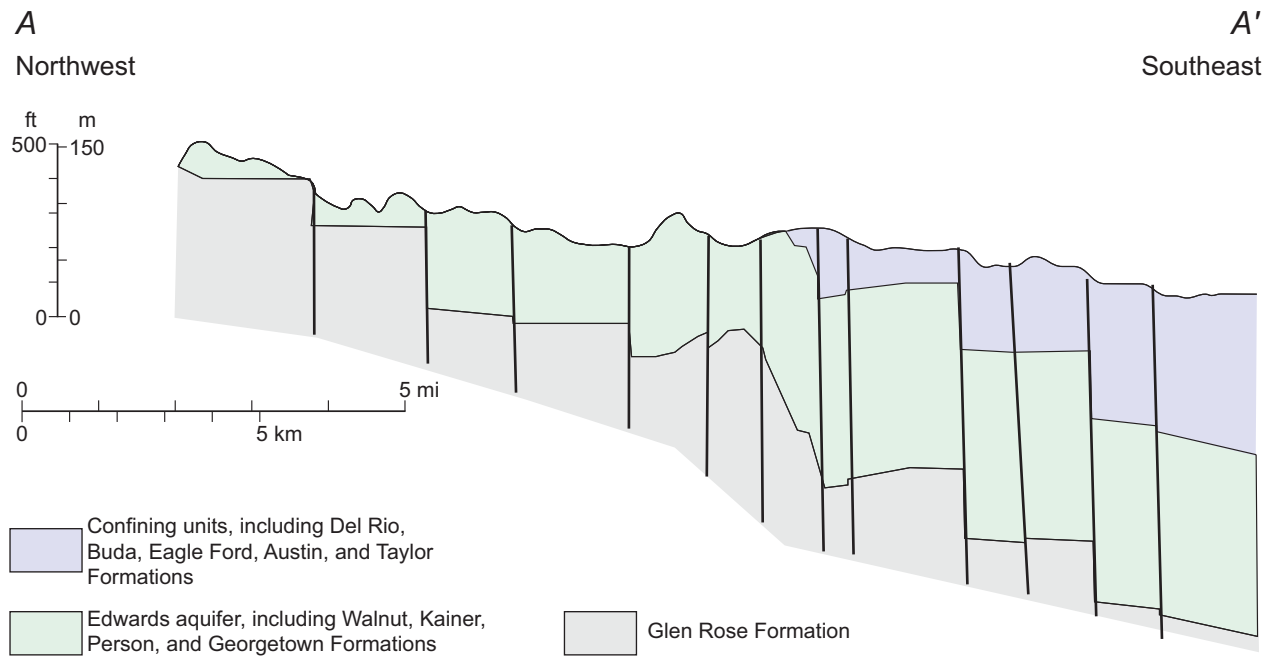


Fig. 8. Geologic cross section of the study area. Location of cross section shown in figure 7.

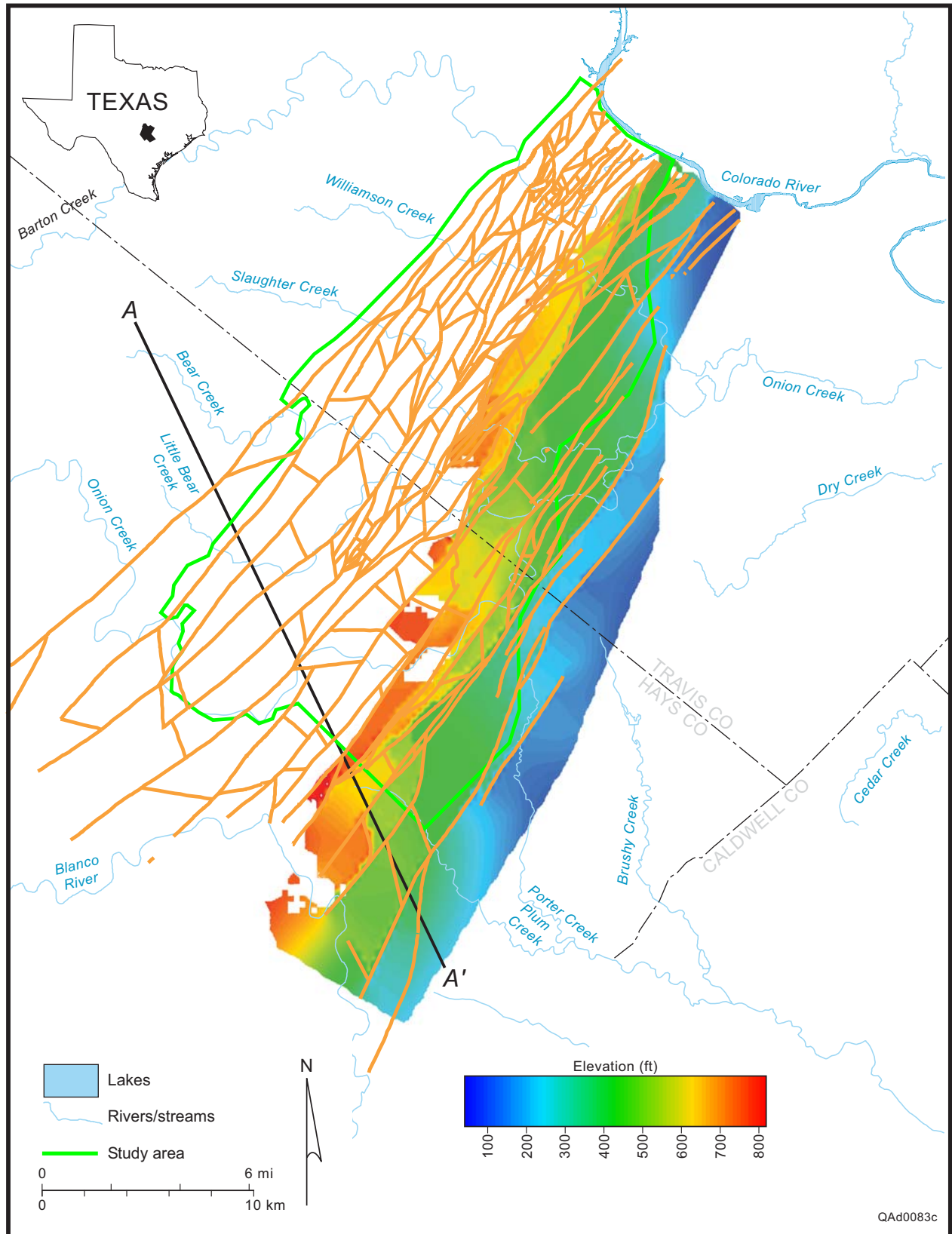


Fig. 9. Elevation of the top of the Edwards aquifer (which corresponds to the base of the Del Rio Formation). Figure 12 shows the location of the control points.

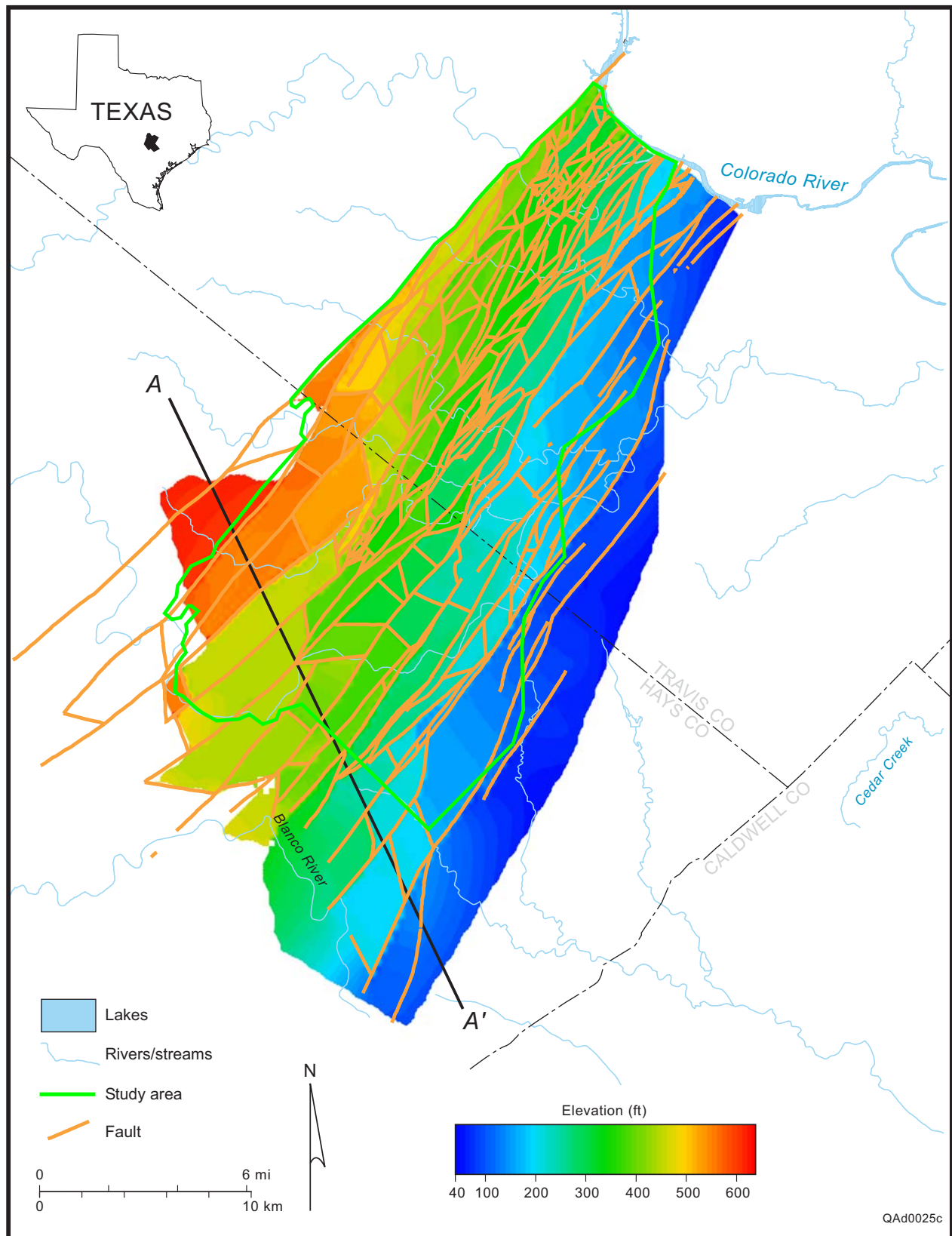


Fig. 10. Elevation of the base of the Edwards aquifer (which corresponds to the top Glen Rose Formation). Figure 12 shows the location of the control points.

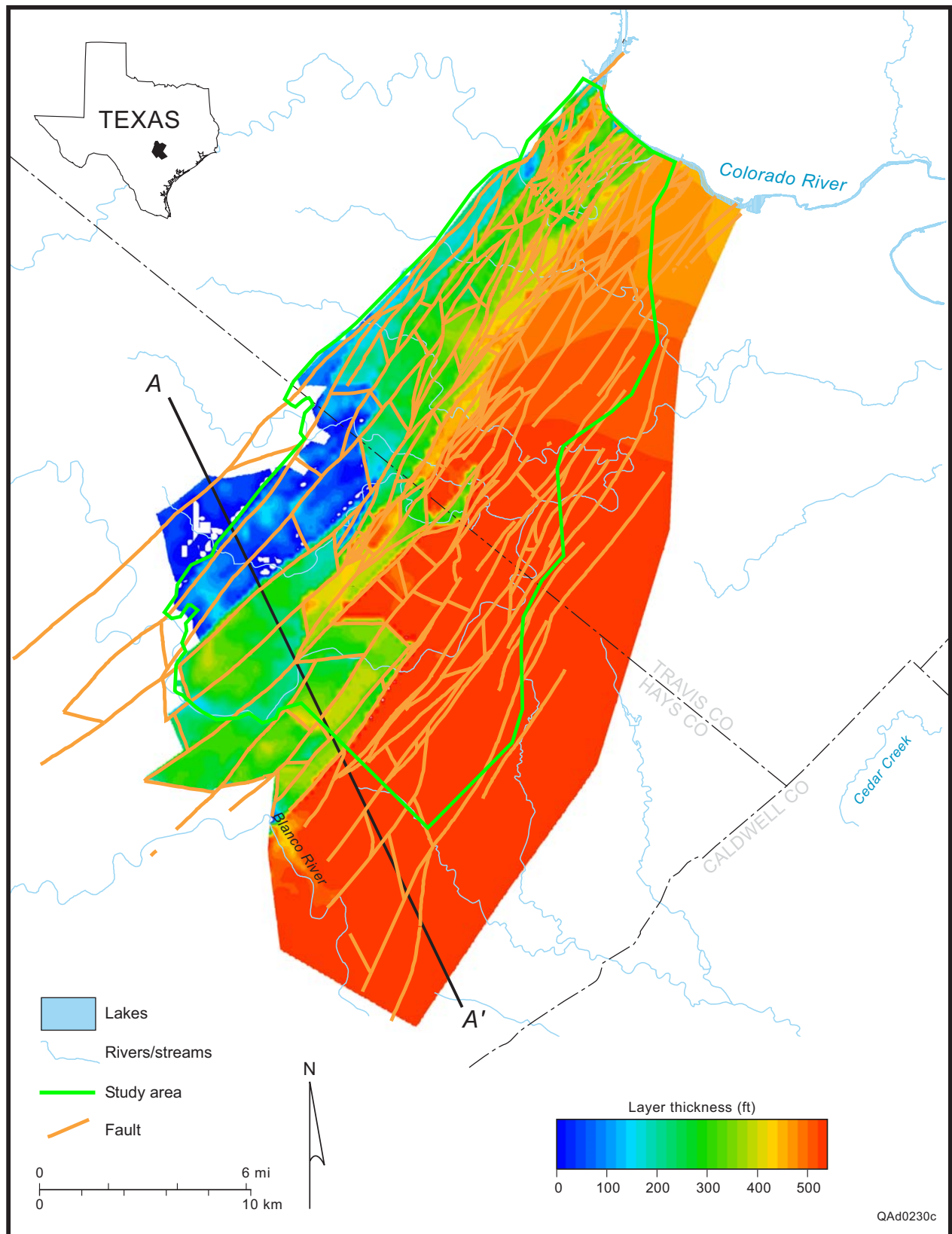


Fig. 11. Approximate thickness of the Edwards aquifer.

QAAd0230c

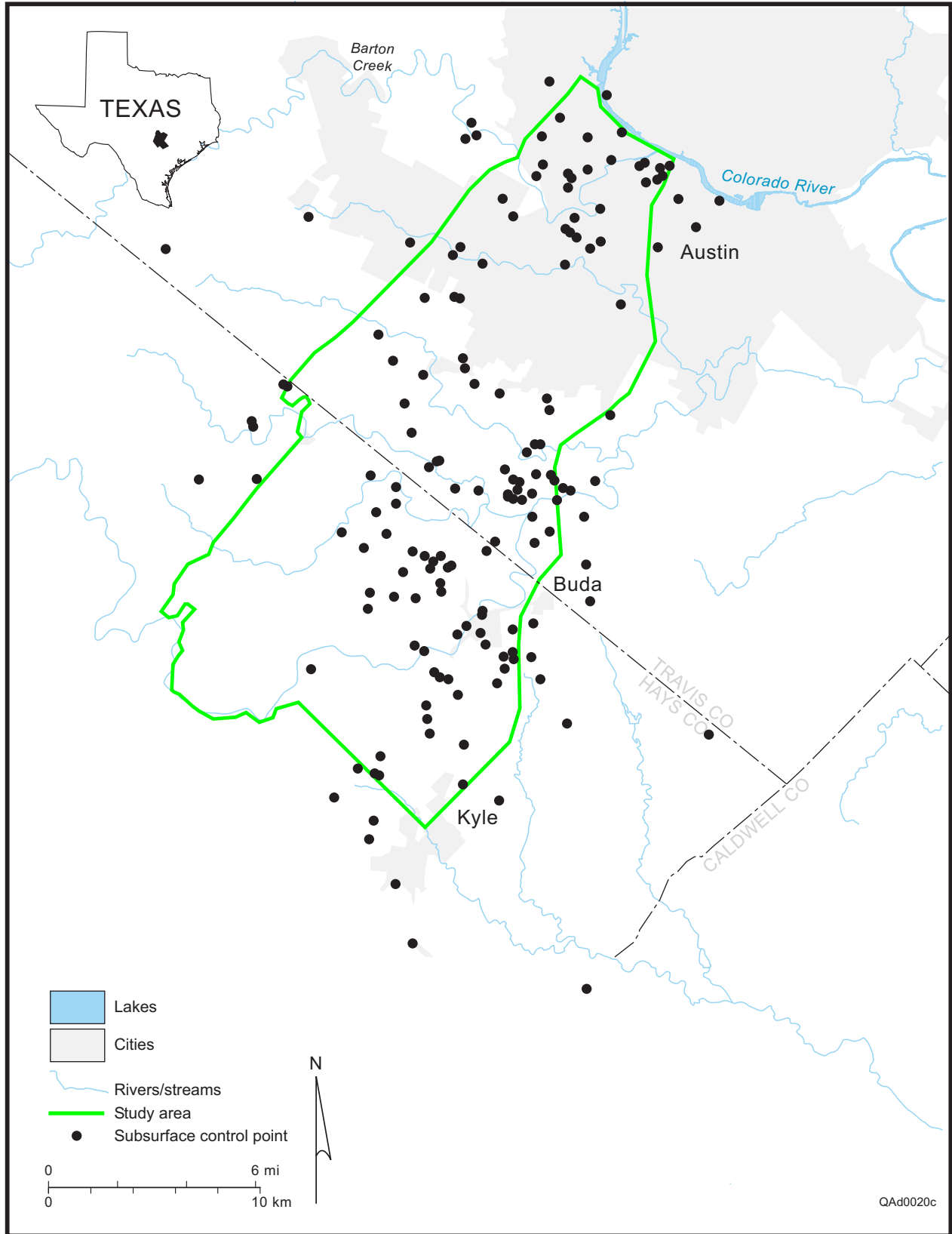


Fig. 12. Control points for the elevation of the top and the base of the Edwards aquifer.

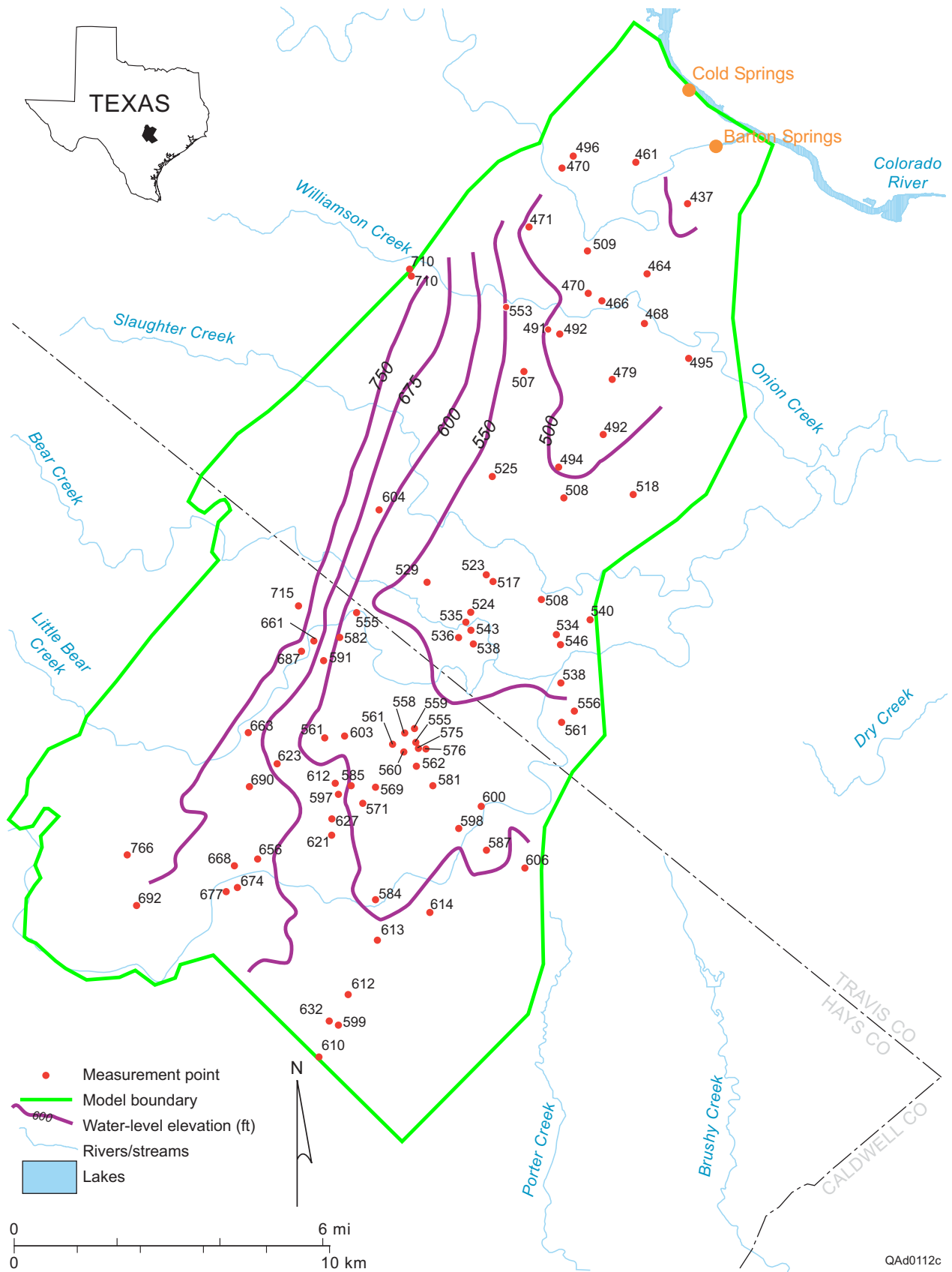


Figure 13. Water-level elevations in the aquifer (include water-level measurements in July and August 1999).

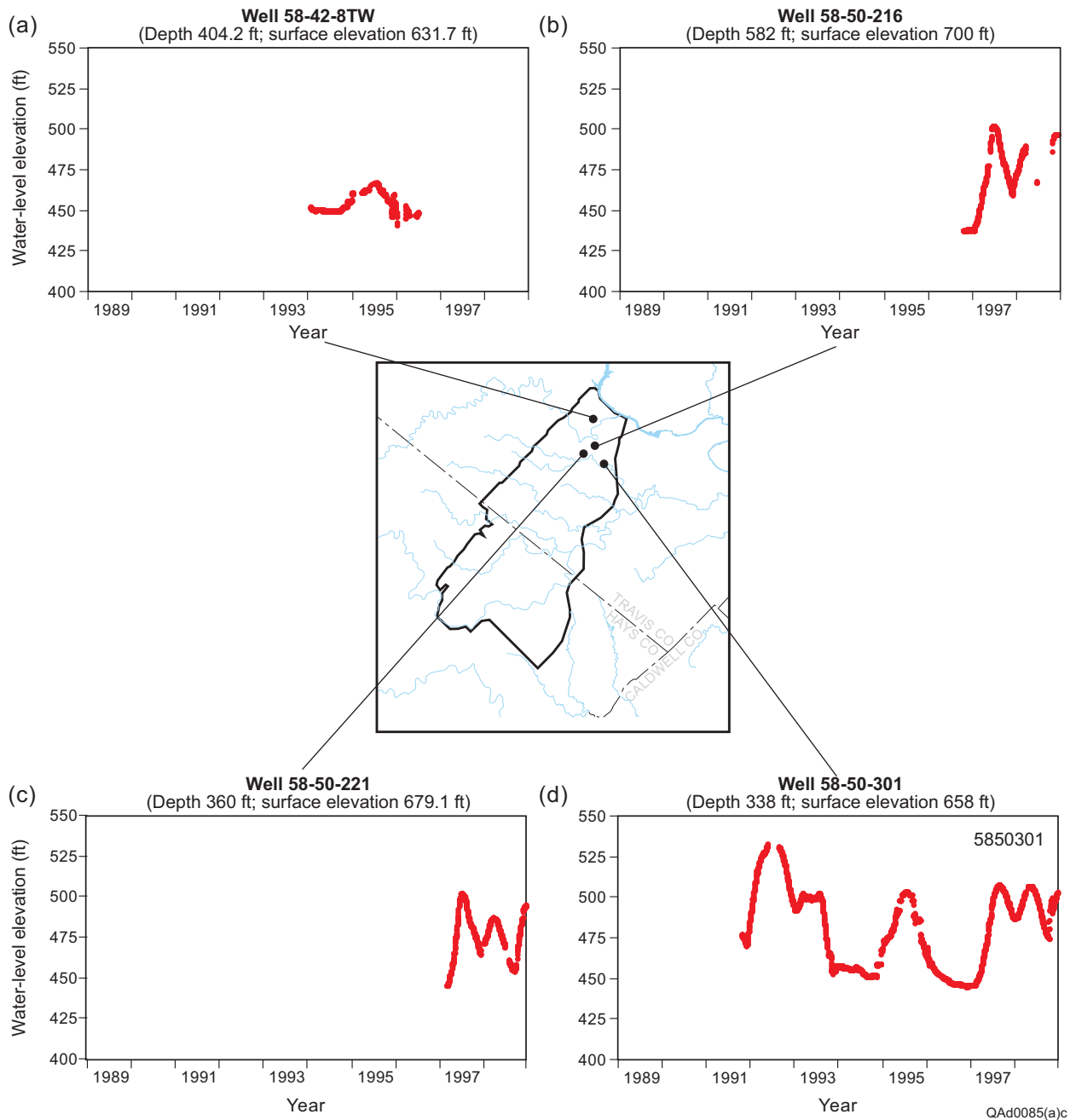


Figure 14. Hydrographs for wells (a) 58-42-8TW, (b) 58-50-216, (c) 58-50-221, and (d) 58-50-301.

QAd0085(a)c

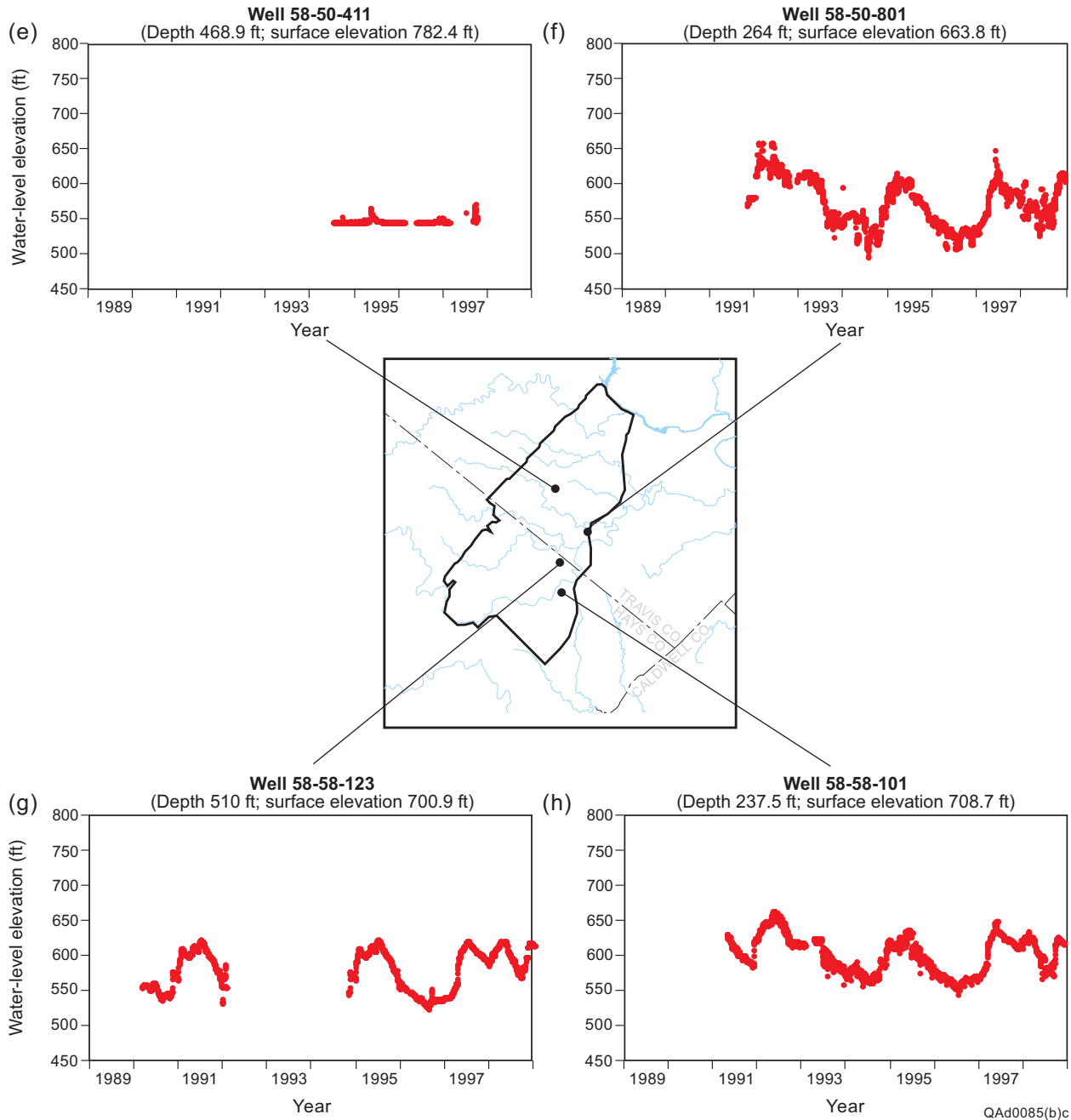


Figure 15. Hydrographs for wells (e) 58-50-411, (f) 58-50-801, (g) 58-58-123, and (h) 58-58-101.

QAAd0085(b)c

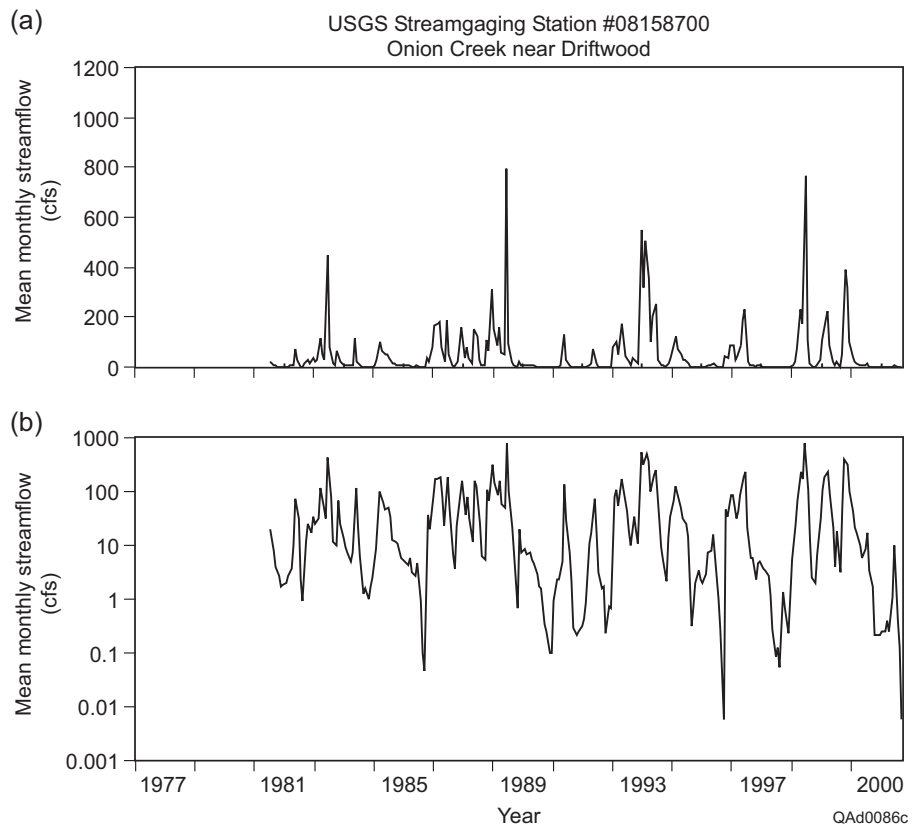


Figure 16. Mean monthly streamflow for USGS gaging station 08158700 on Onion Creek near Driftwood for (a) linear and (b) logarithmic scales. Figure 25 shows the location of the stream gage.

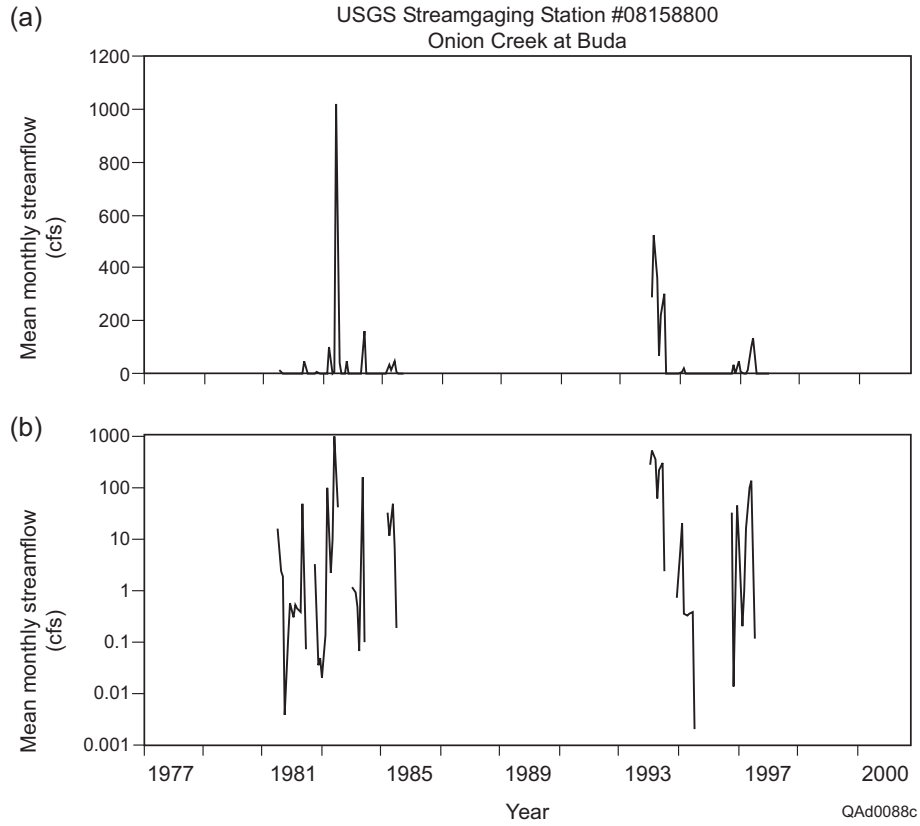


Figure 17. Mean monthly streamflow for USGS gaging station 08158800 on Onion Creek at Buda for (a) linear and (b) logarithmic scales. Figure 25 shows the location of the stream gage.

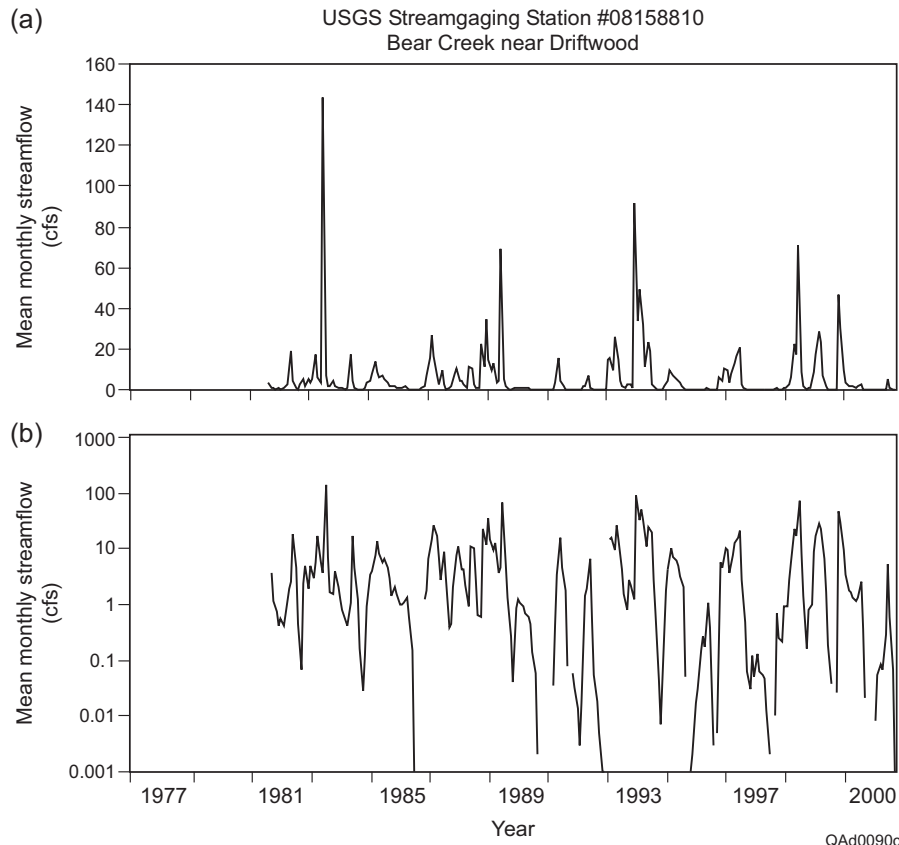


Figure 18. Mean monthly streamflow for USGS gaging station 08158810 on Bear Creek near Driftwood for (a) linear and (b) logarithmic scales. Figure 25 shows the location of the stream gage.

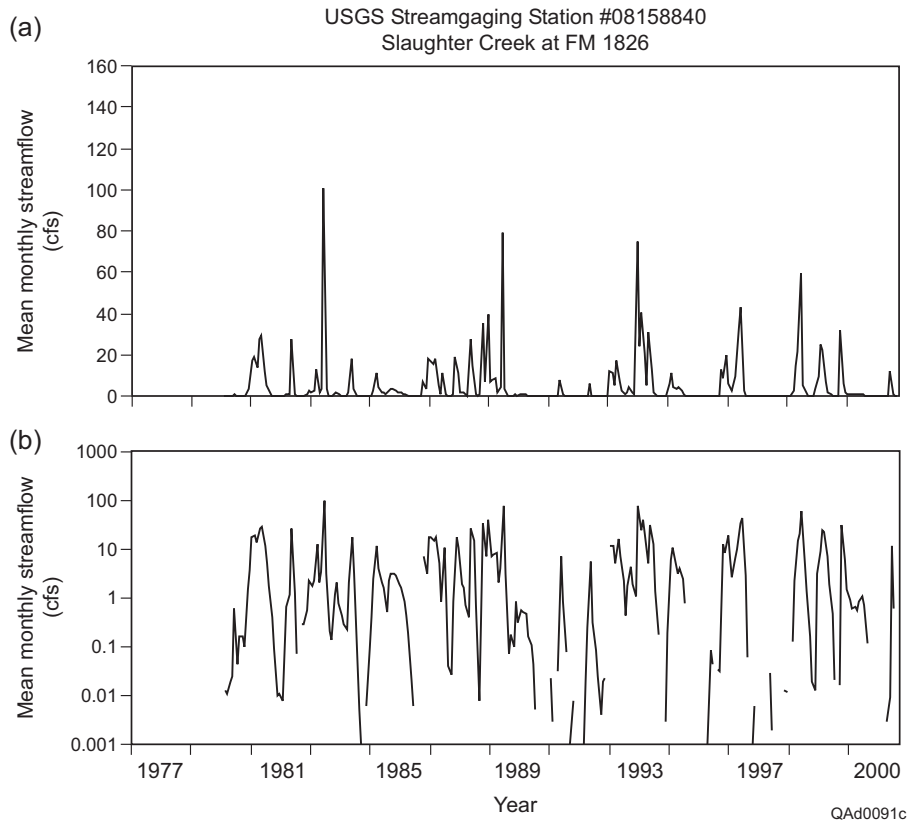


Figure 19. Mean monthly streamflow for USGS gaging station 08158840 on Slaughter Creek at FM 1826 for (a) linear and (b) logarithmic scales. Figure 25 shows the location of the stream gage.

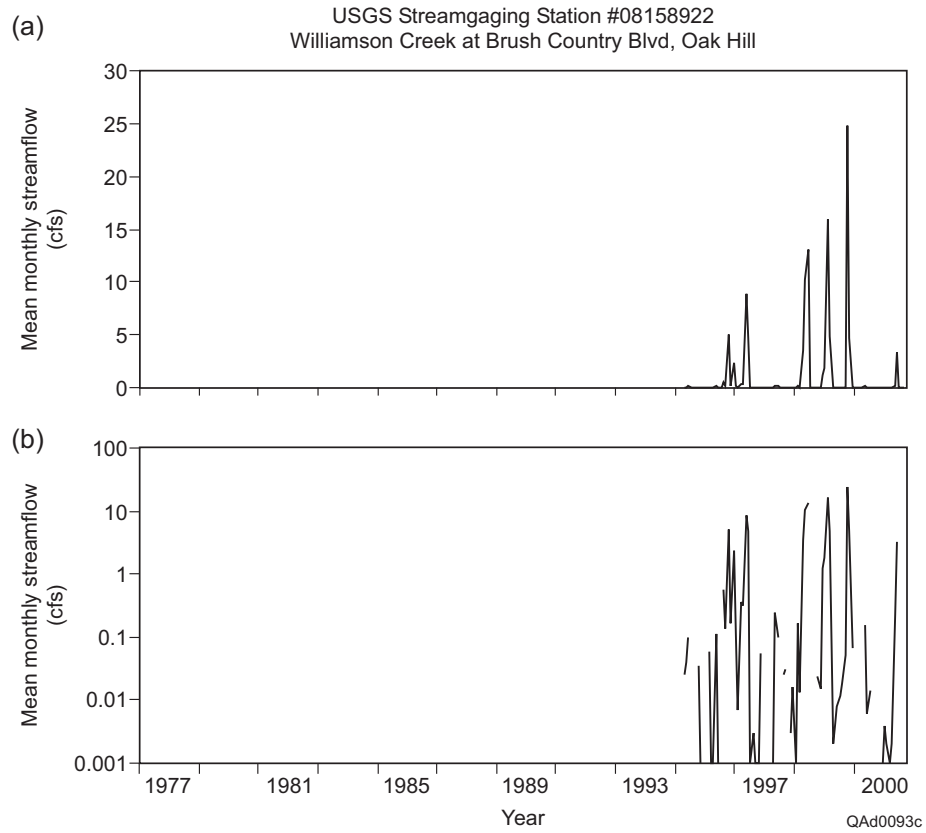


Figure 20. Mean monthly streamflow for USGS gaging station 08158922 on Williamson Creek at Brush Country Blvd., Oak Hill, for (a) linear and (b) logarithmic scales. Figure 25 shows the location of the stream gage.

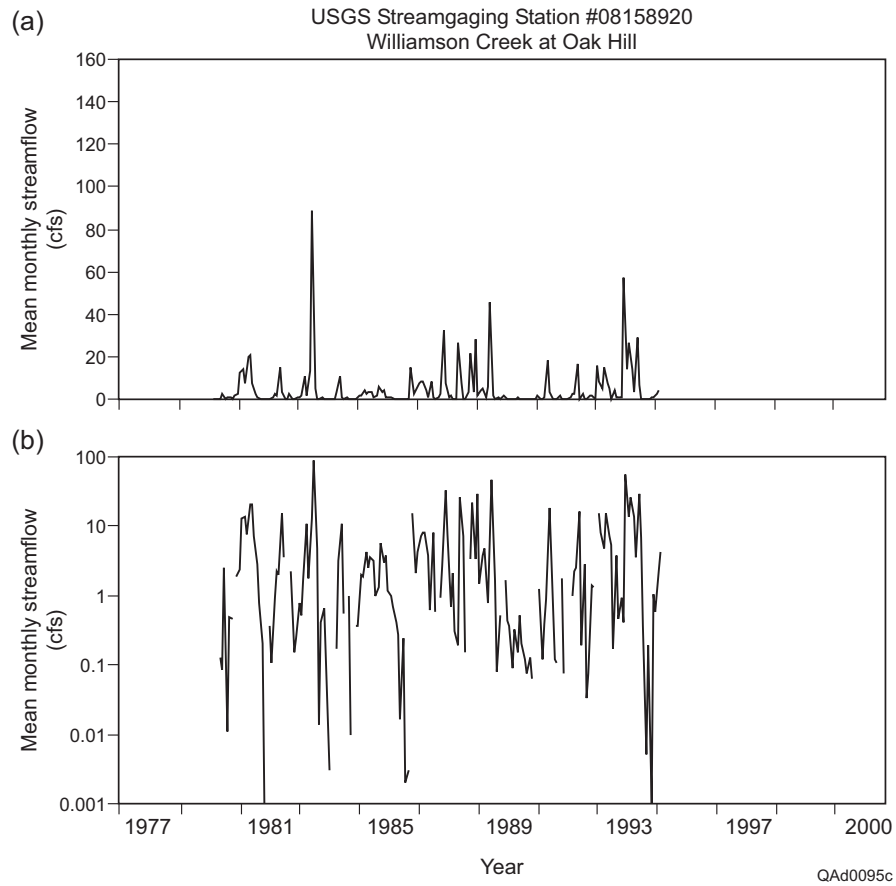


Figure 21. Mean monthly streamflow for USGS gaging station 08158920 on Williamson Creek at Oak Hill for (a) linear and (b) logarithmic scales. Figure 25 shows the location of the stream gage.

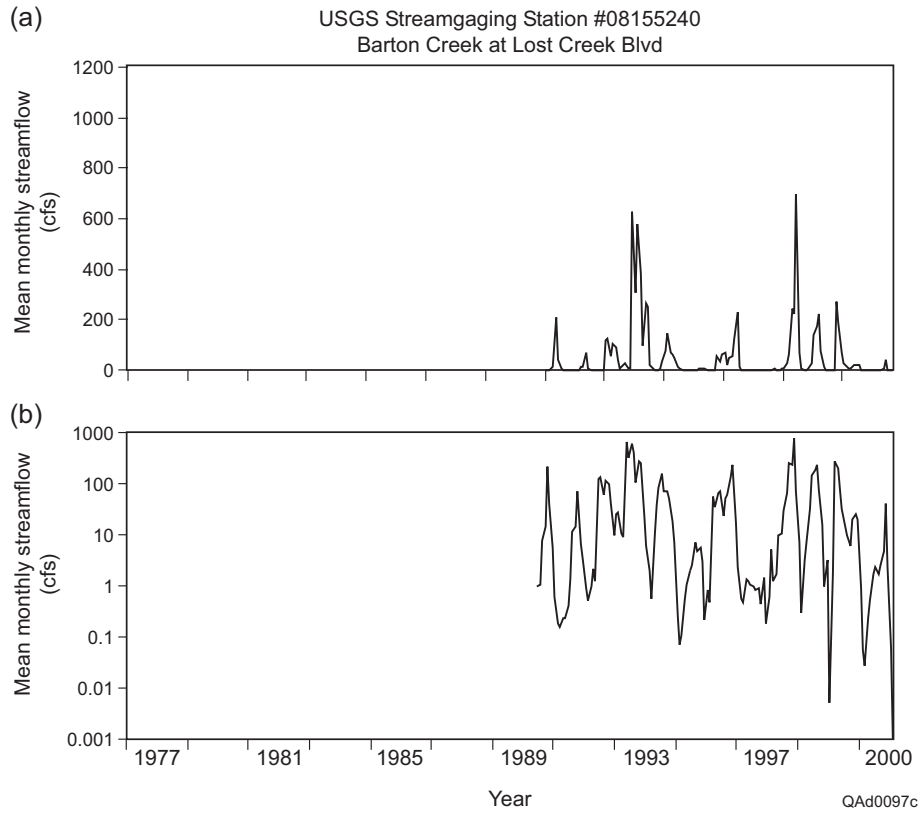


Figure 22. Mean monthly streamflow for USGS gaging station 08155240 on Barton Creek at Lost Creek Blvd. for (a) linear and (b) logarithmic scales. Figure 25 shows the location of the stream gage.

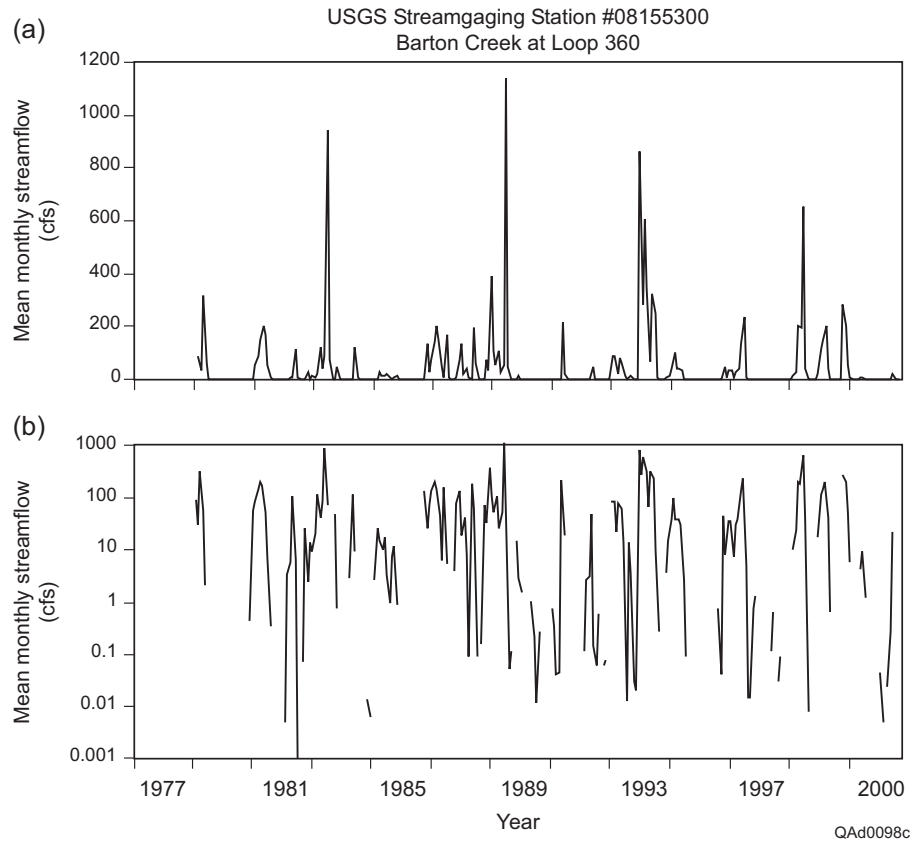


Figure 23. Mean monthly streamflow for USGS gaging station 08155300 on Barton Creek at Loop 360 for (a) linear and (b) logarithmic scales. Figure 25 shows the location of the stream gage.

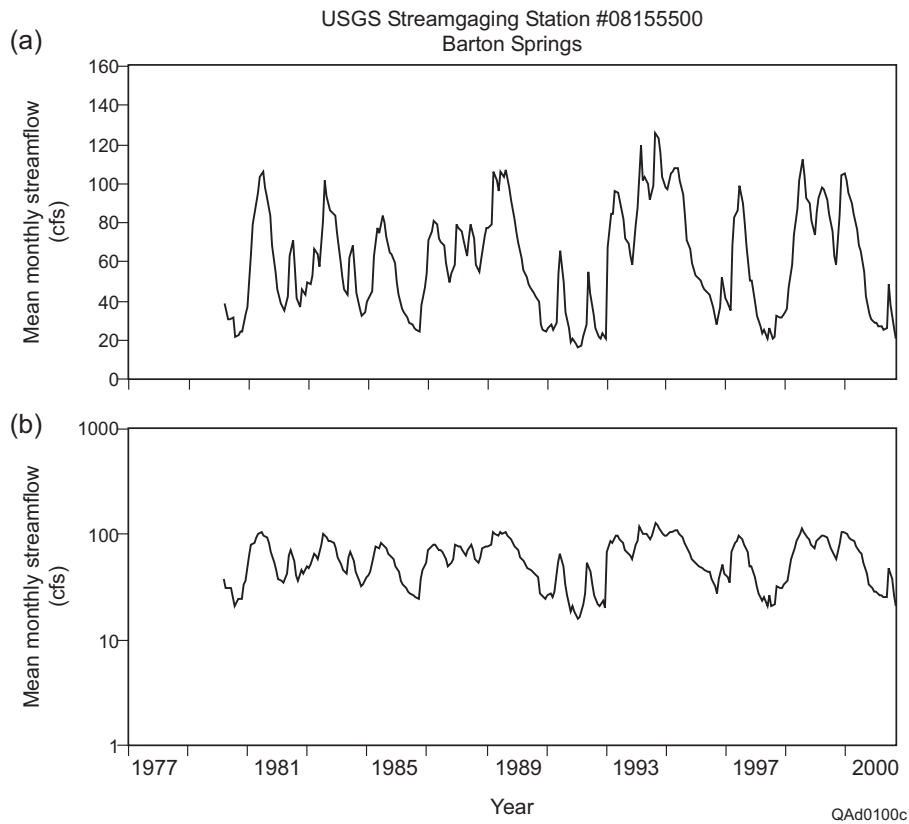


Figure 24. Mean monthly streamflow for USGS gaging station 08155500 at Barton Springs for (a) linear and (b) logarithmic scales. Figure 25 shows the location of the stream gage.

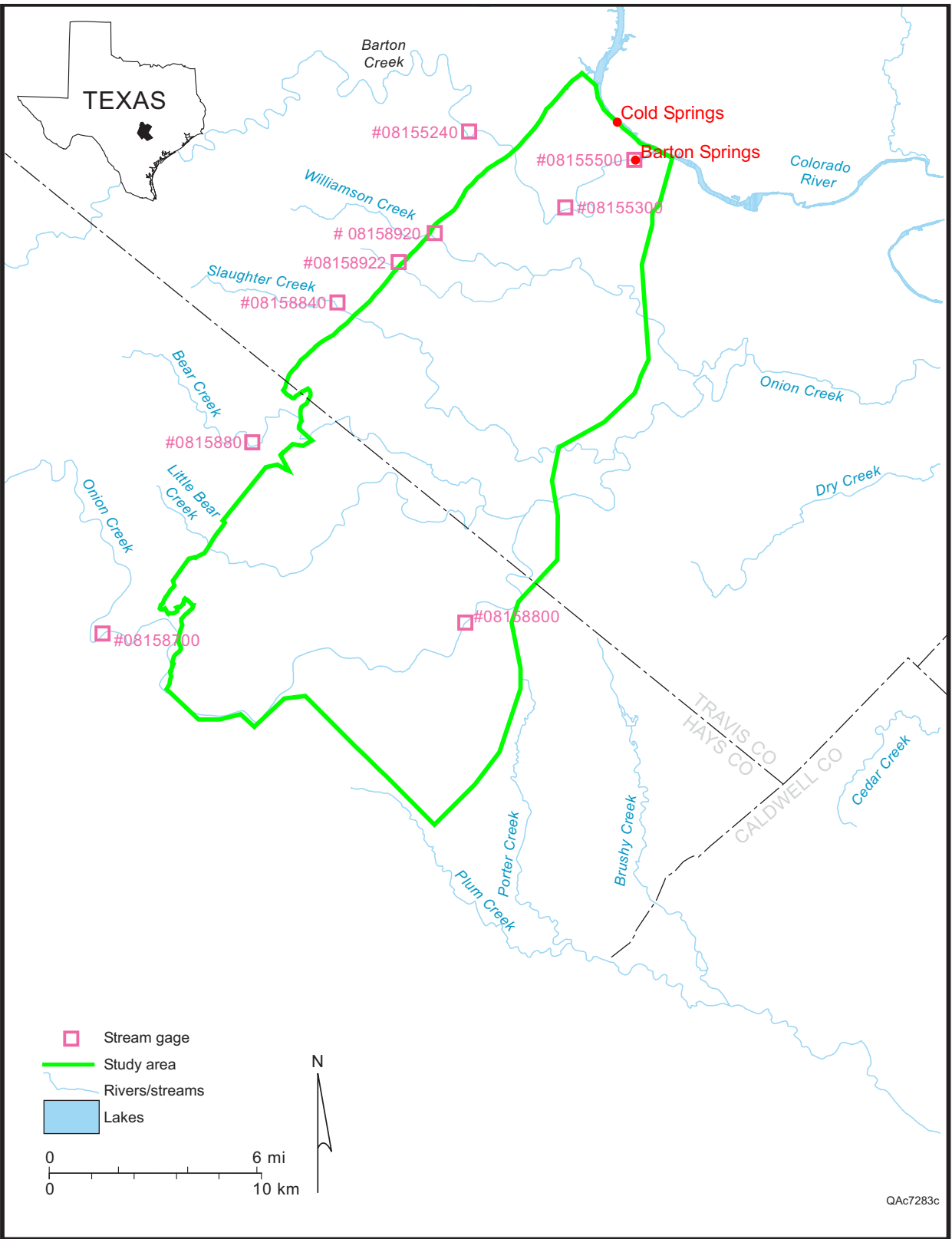


Figure 25. Location of the stream gages for the stream-flow hydrographs shown in figures 16 through 24.

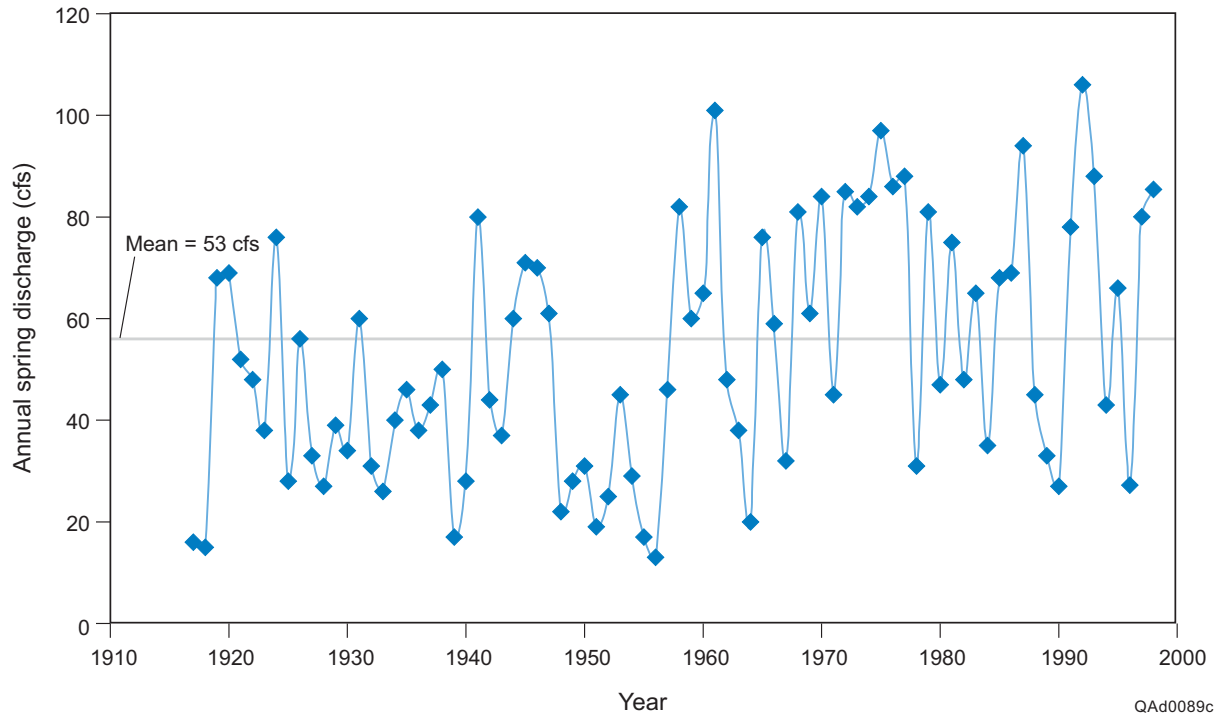


Figure 26. Discharge at Barton Springs.

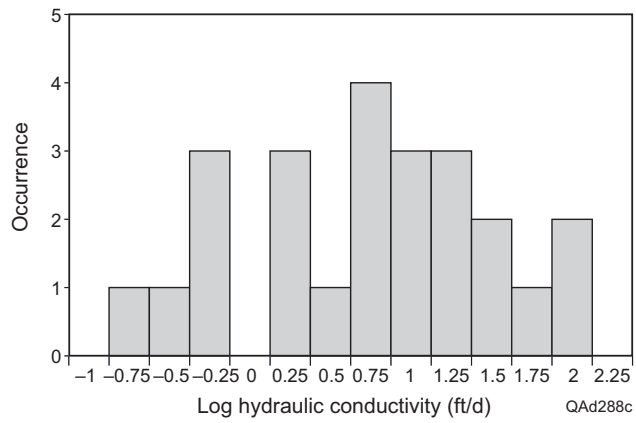


Figure 27. Histogram of hydraulic conductivity from aquifer tests.

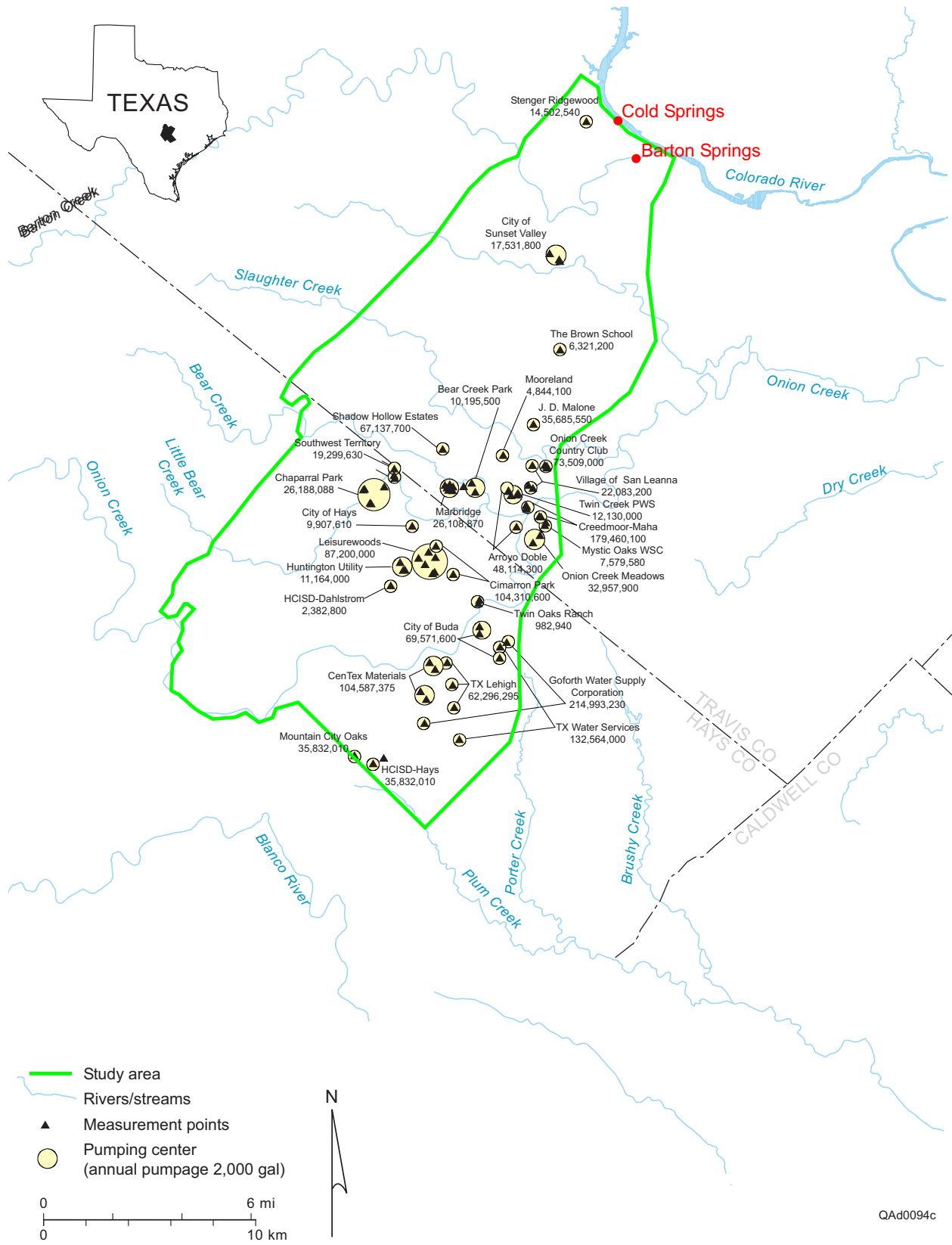
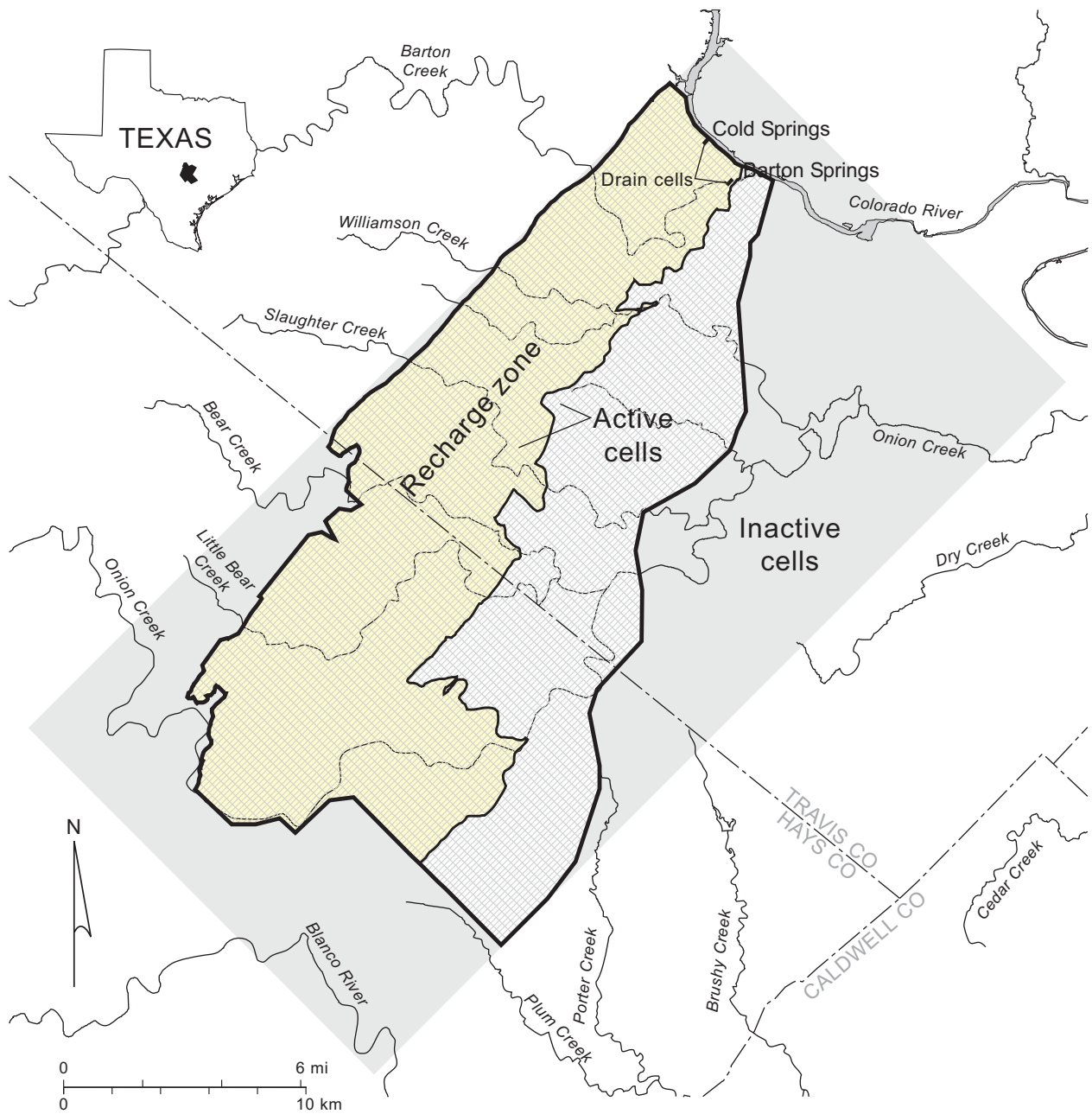


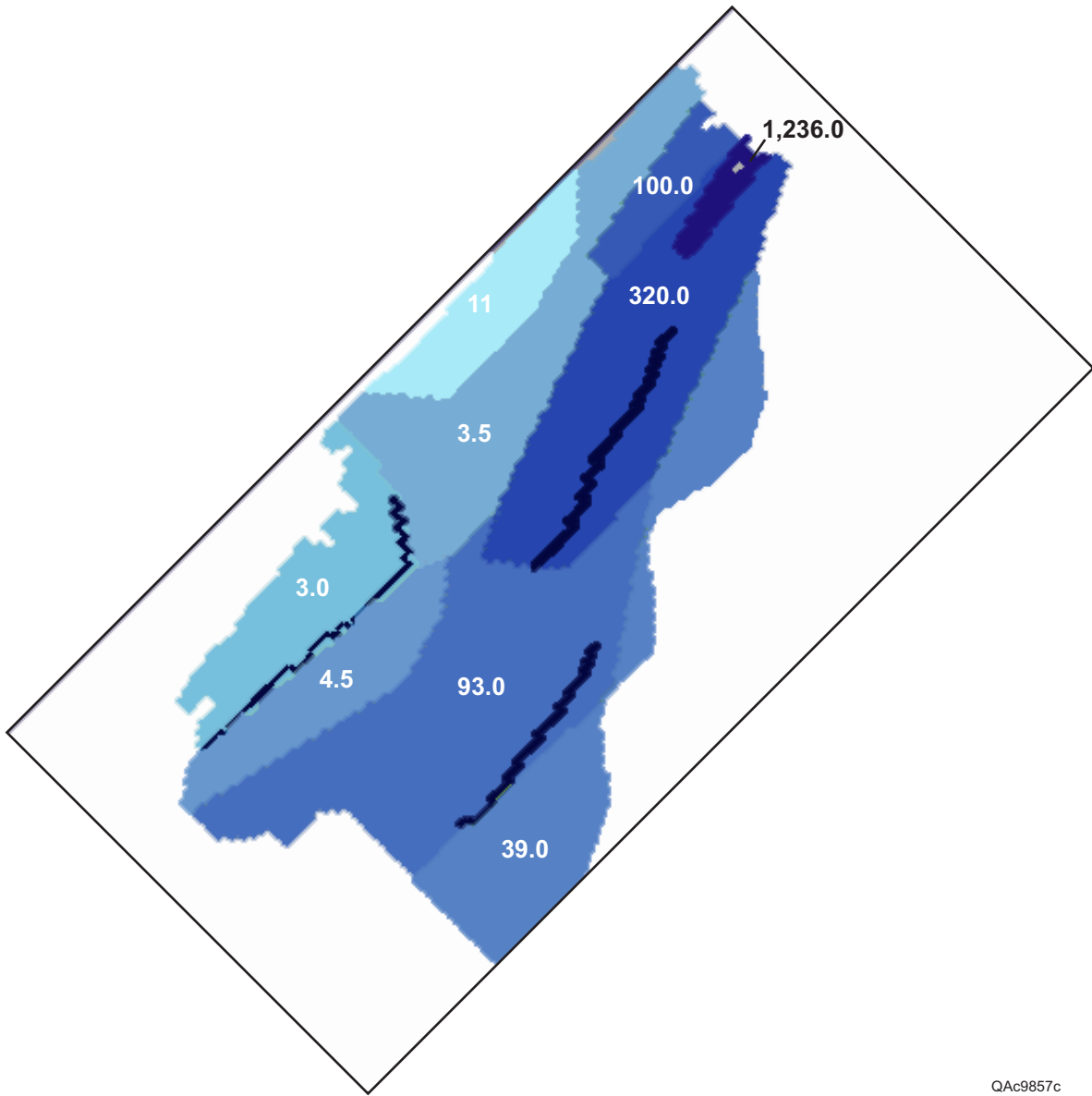
Figure 28. Spatial distribution of pumping in the aquifer.



— Model boundary ~ Rivers/streams

QAd0096c

Fig. 29. Model grid, consisting of 120 cells 120 cells (14,400 cells) that are 1,000 ft long 500 ft wide. The active zone of the model is shown by the solid line and consists of 7,043 cells.



QA9857c

Figure 30. Zonal distribution of hydraulic conductivity resulting from calibration of the steady-state model.

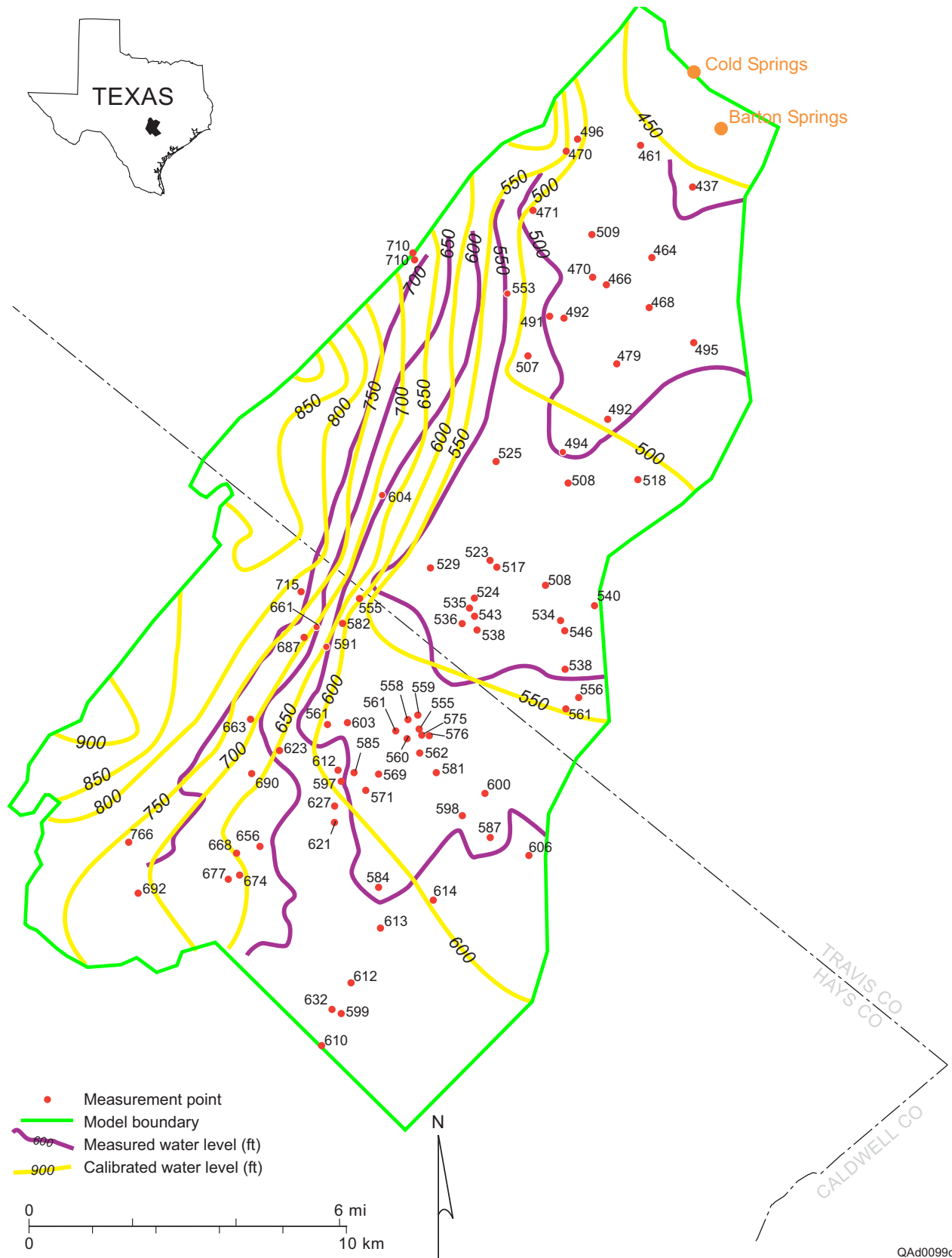


Figure 31. Comparison of simulated and measured (July/August 1999) water-level contours for the steady-state model.

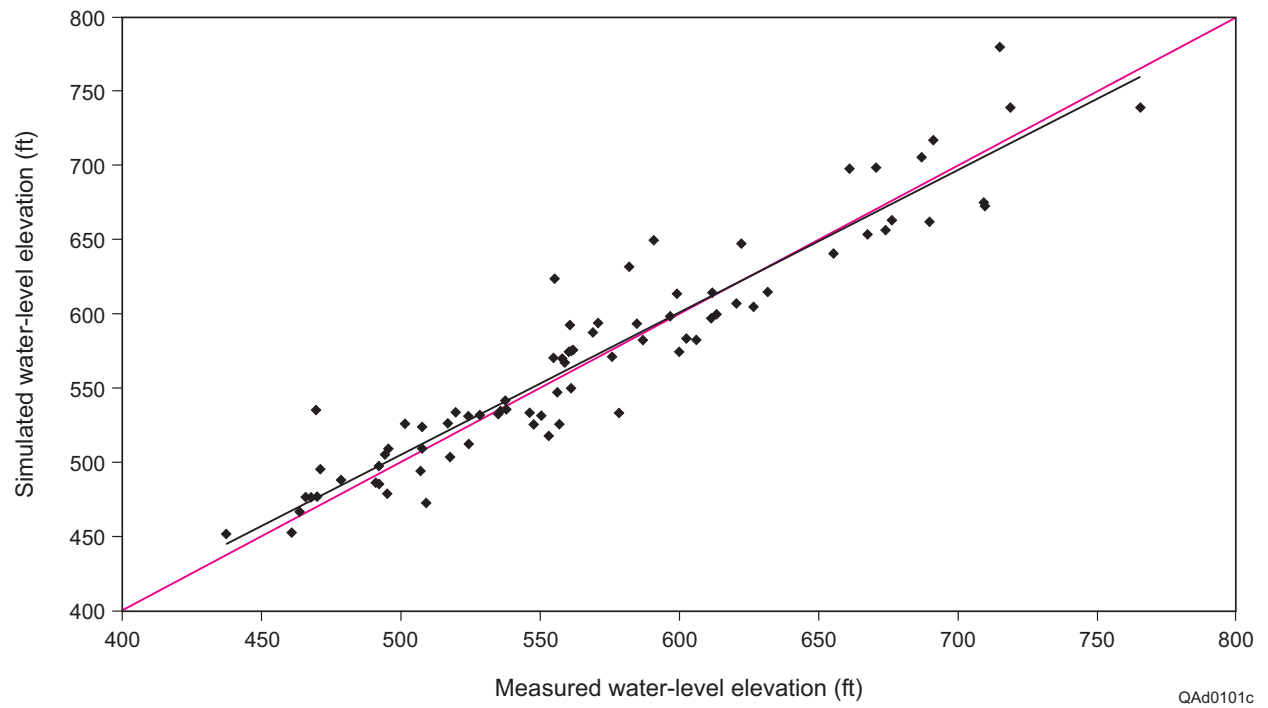


Figure 32. Scatter plot of simulated and measured (July/August 1999) water levels for the steady-state model.

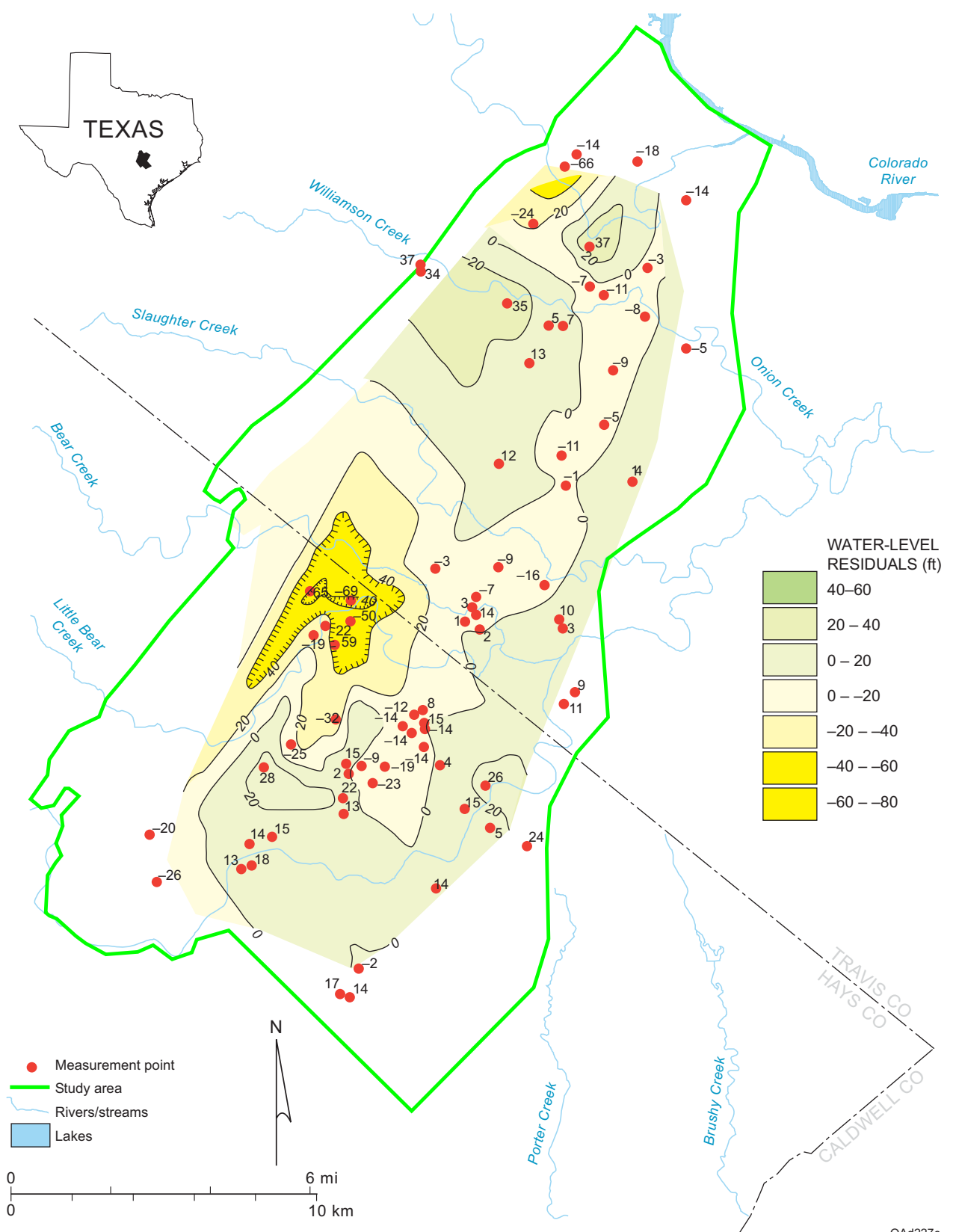


Figure 33. Water-level residuals (difference between measured and simulated water-level elevations) for the calibrated steady-state model.

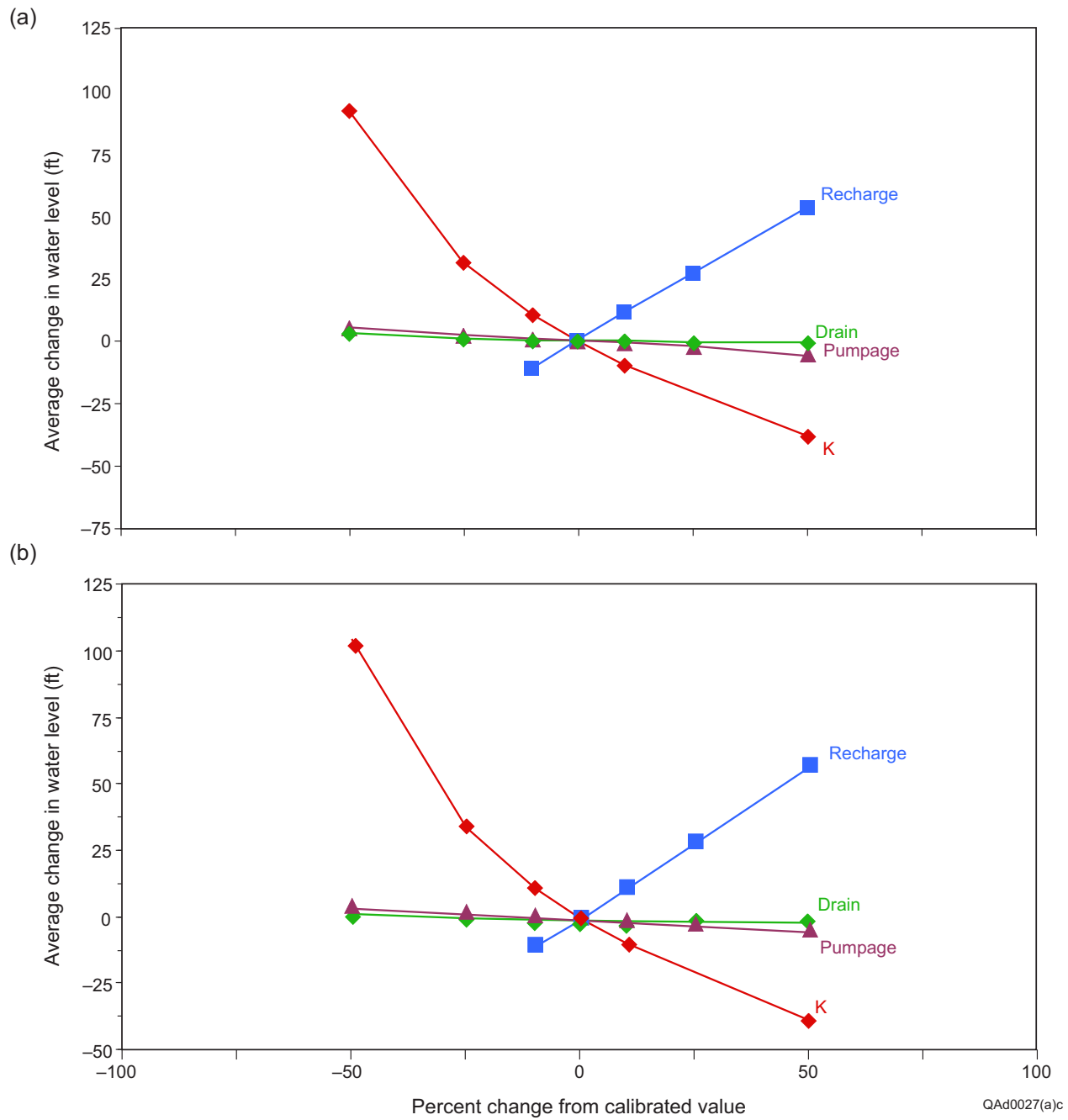


Figure 34. Sensitivity of the numerically predicted water levels of the steady-state model to changes in model parameters at (a) calibration wells and (b) each active cell in the model.

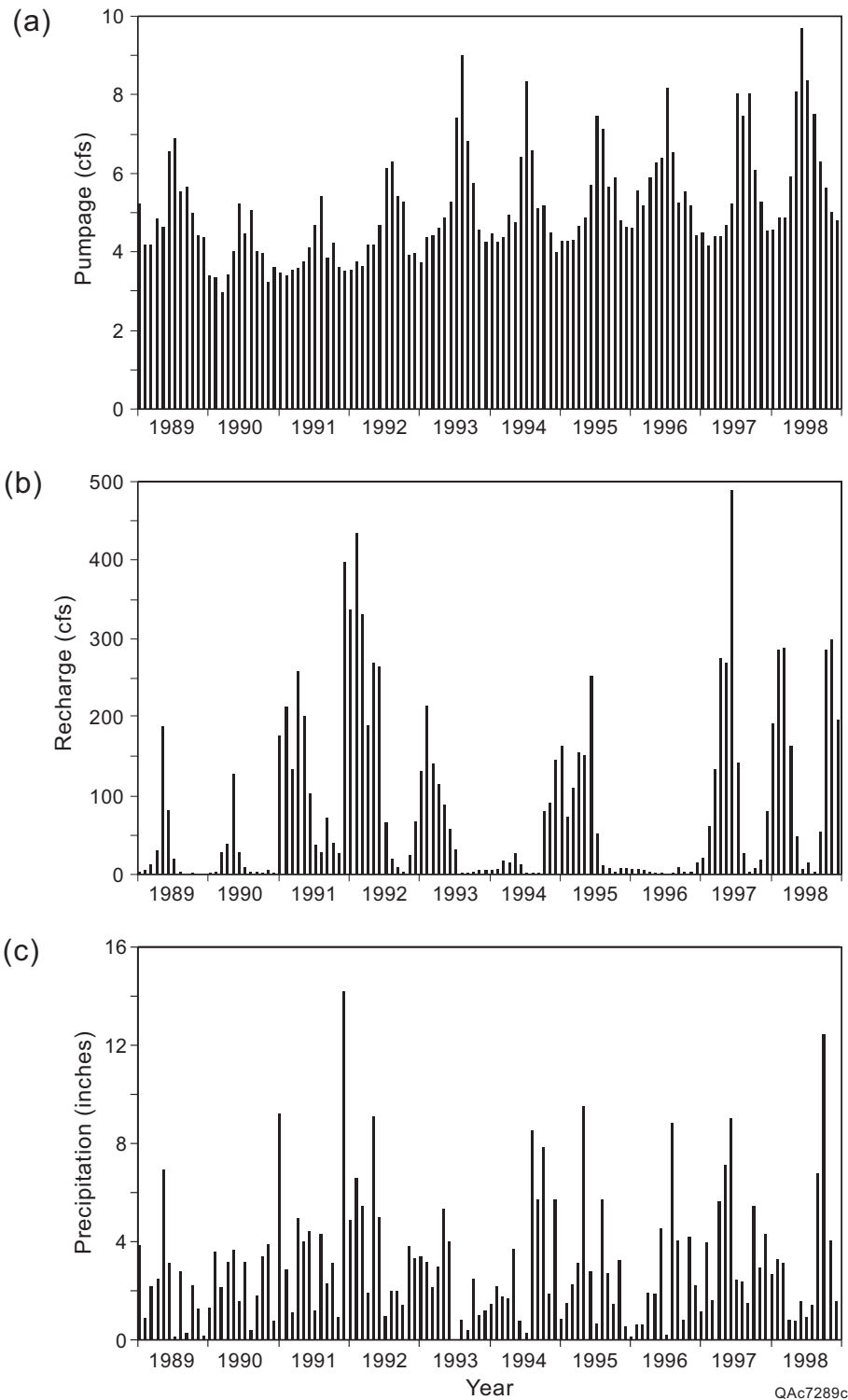


Figure 35. (a) Monthly pumpage, (b) recharge, and (c) precipitation for the transient model (1989 through 1998).

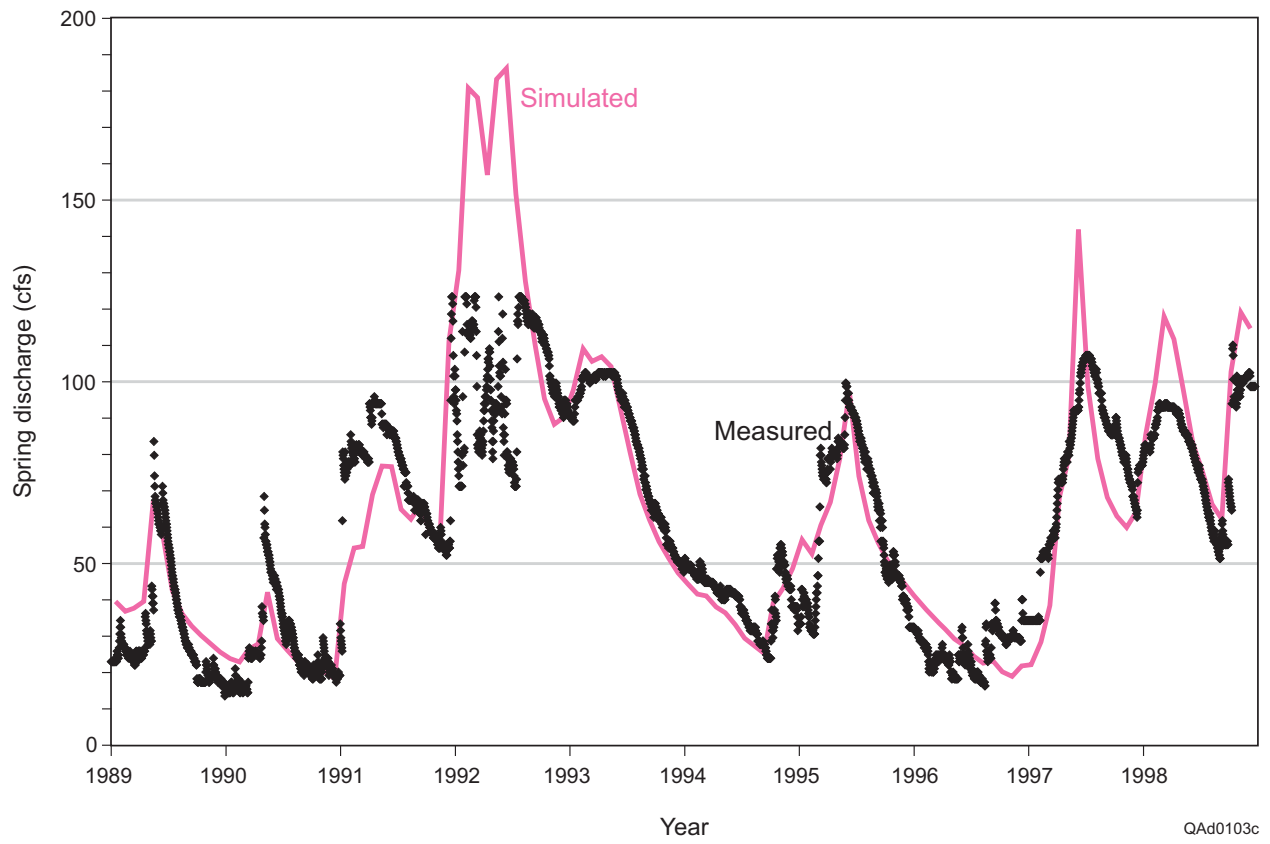


Figure 36. Comparison of simulated and measured discharge at Barton Springs for 1989 through 1998.

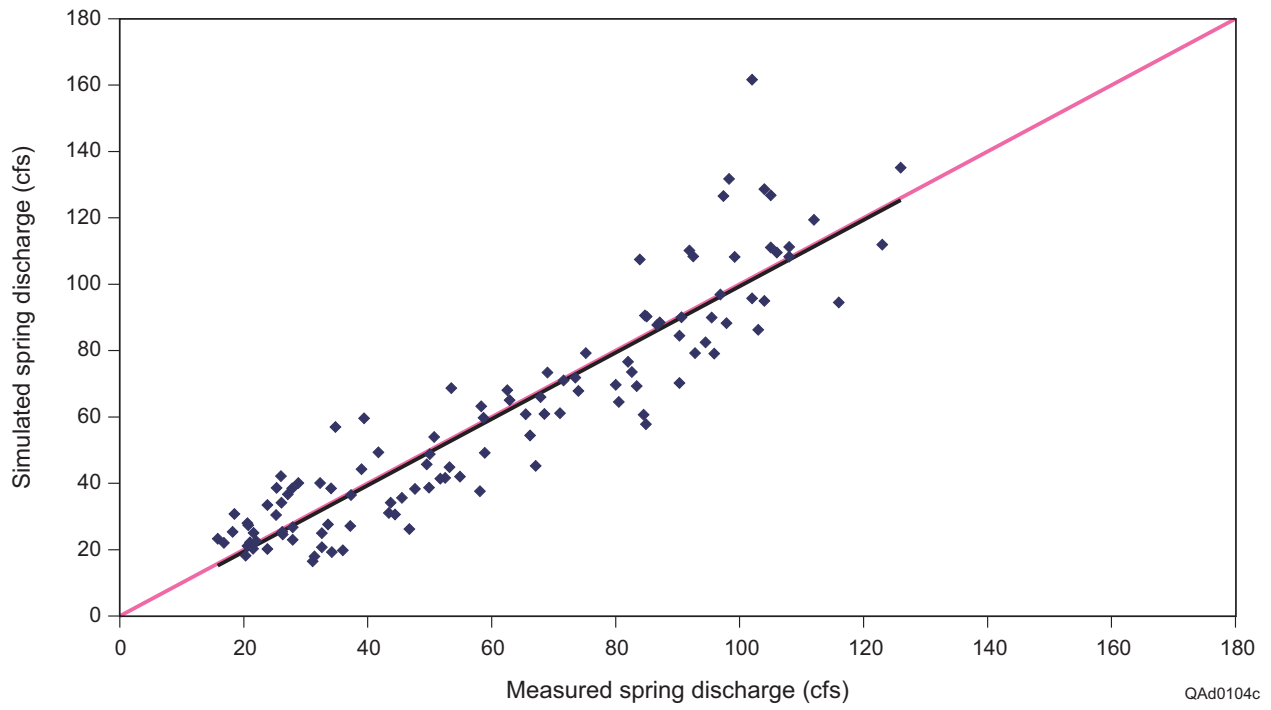


Figure 37. Scatter plot of simulated versus measured spring discharge for 1989 through 1998.

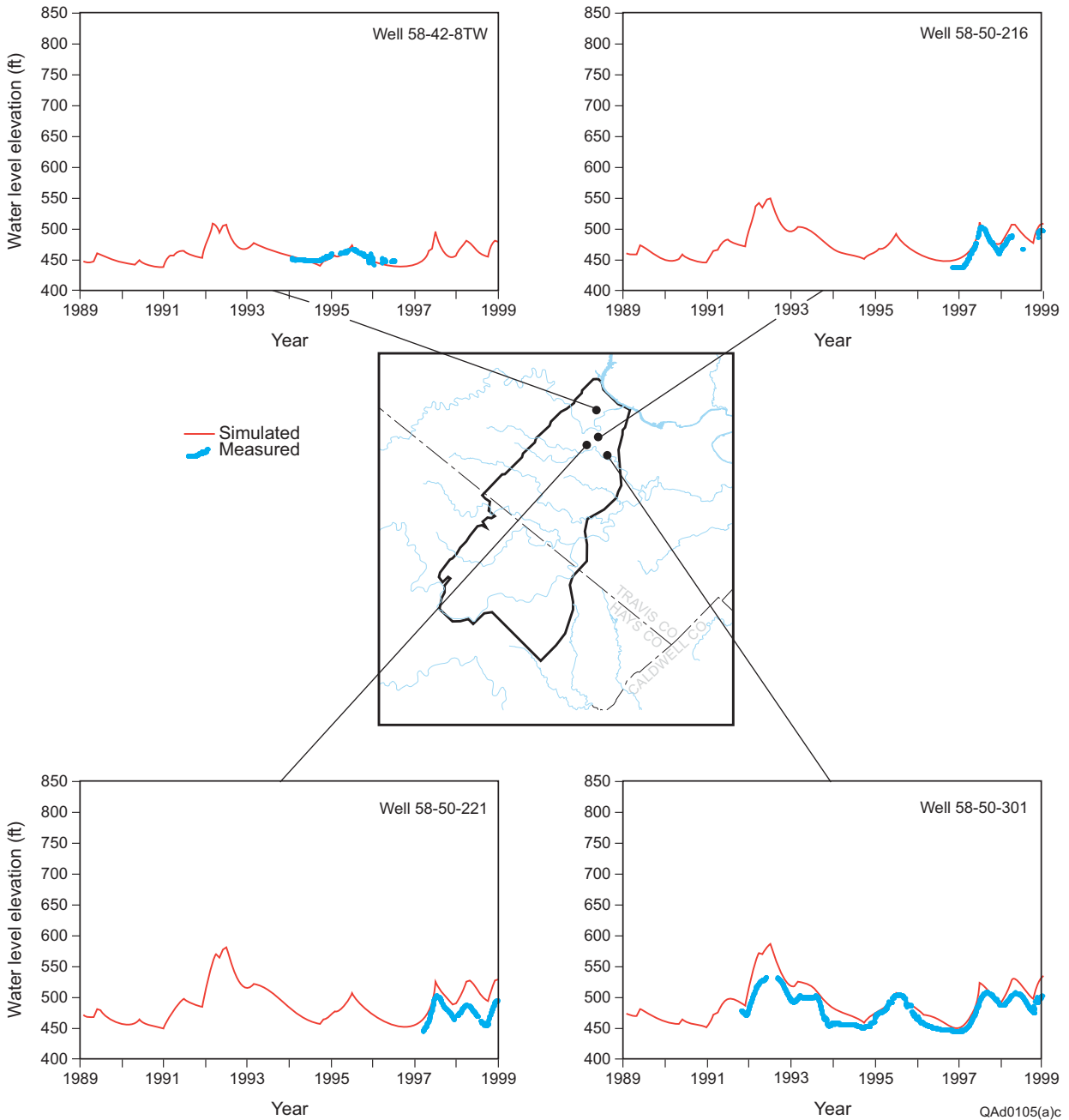


Figure 38. Comparison of simulated and measured water-level elevation hydrographs in four monitoring wells, northern study area.

QAd0105(a)c

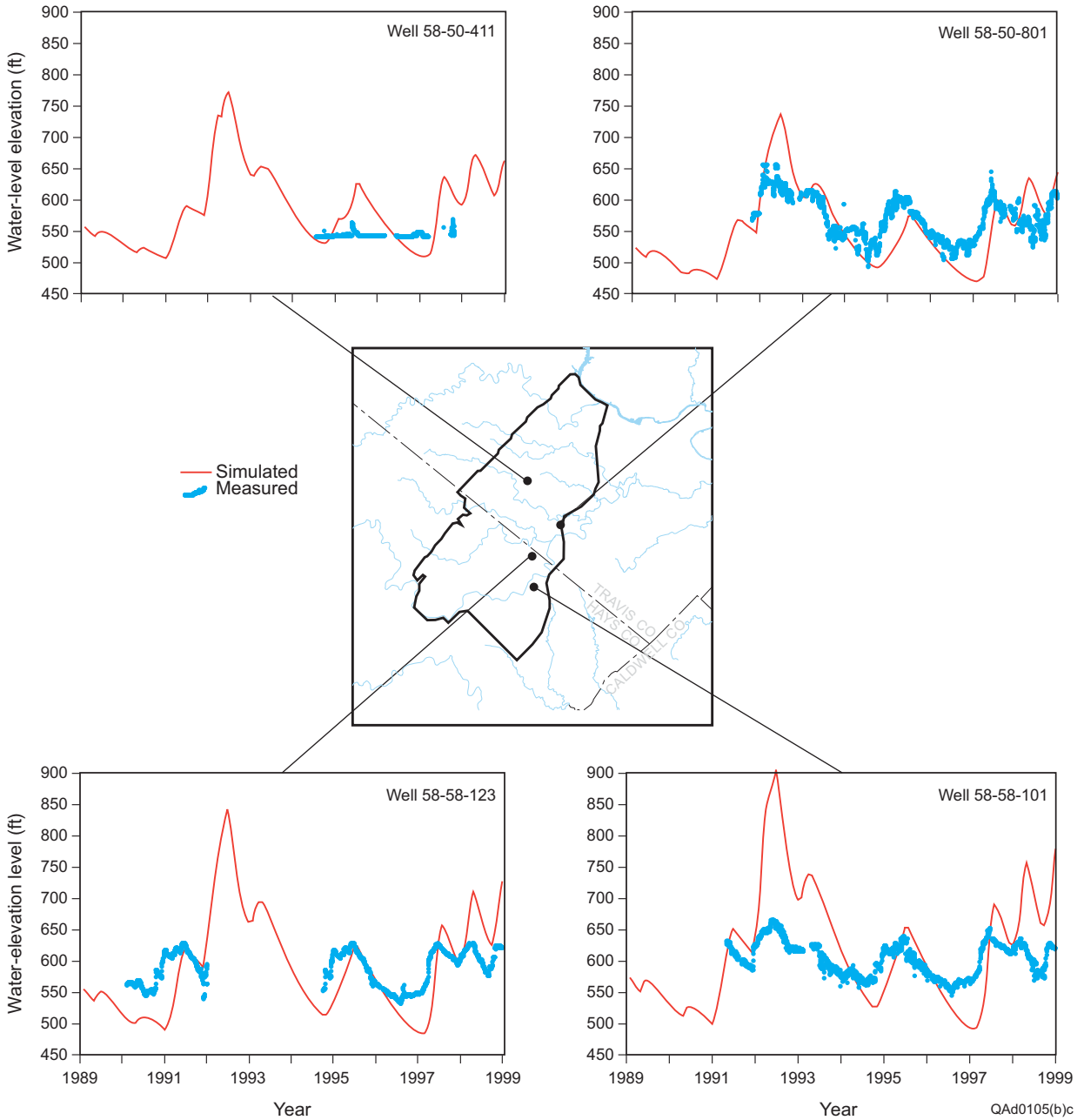


Figure 39. Comparison of simulated and measured water-level elevation hydrographs in four monitoring wells, central and southern study area.

QAd0105(b)c

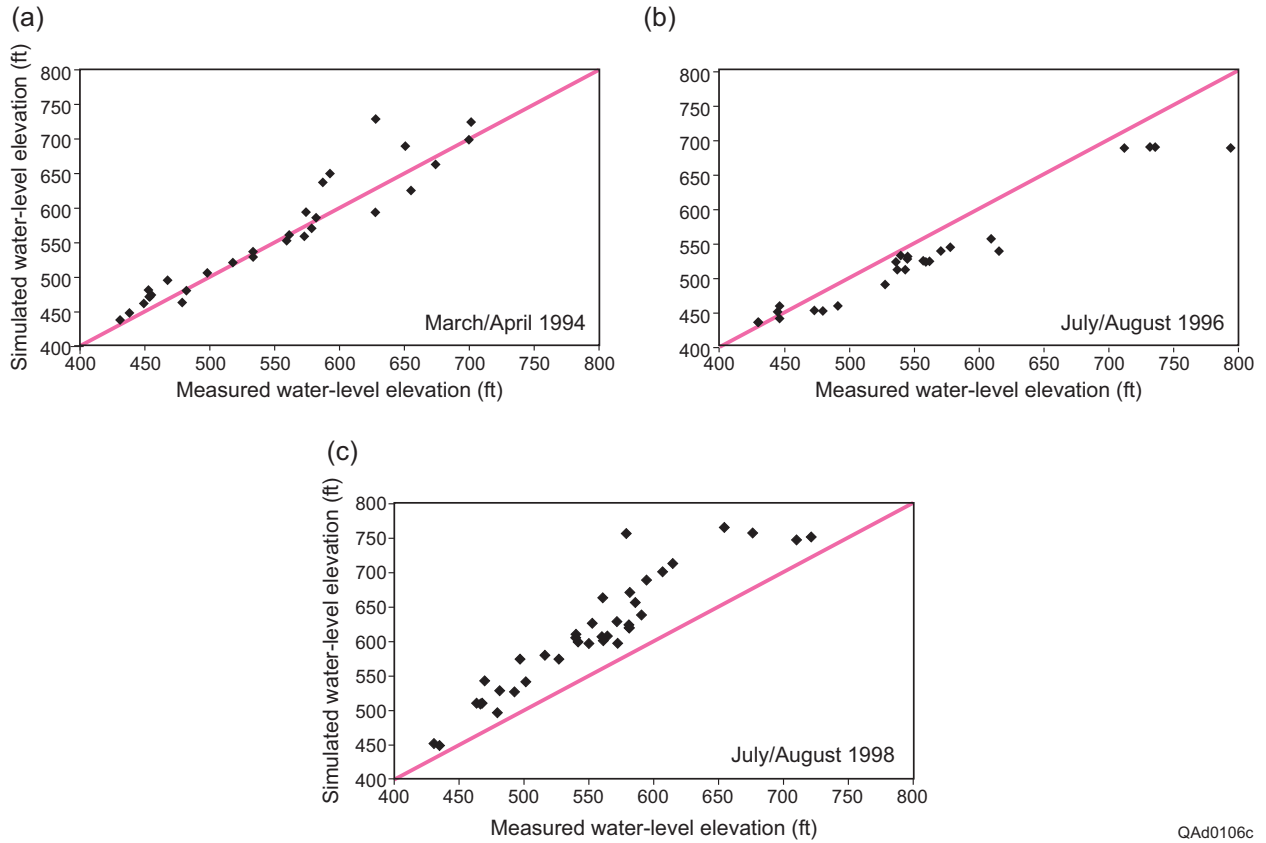


Fig. 40. Scatter plots of simulated versus measured water-level elevations for the transient simulations (a) March/April 1994, (b) July/August 1996, and (c) July/August 1998.

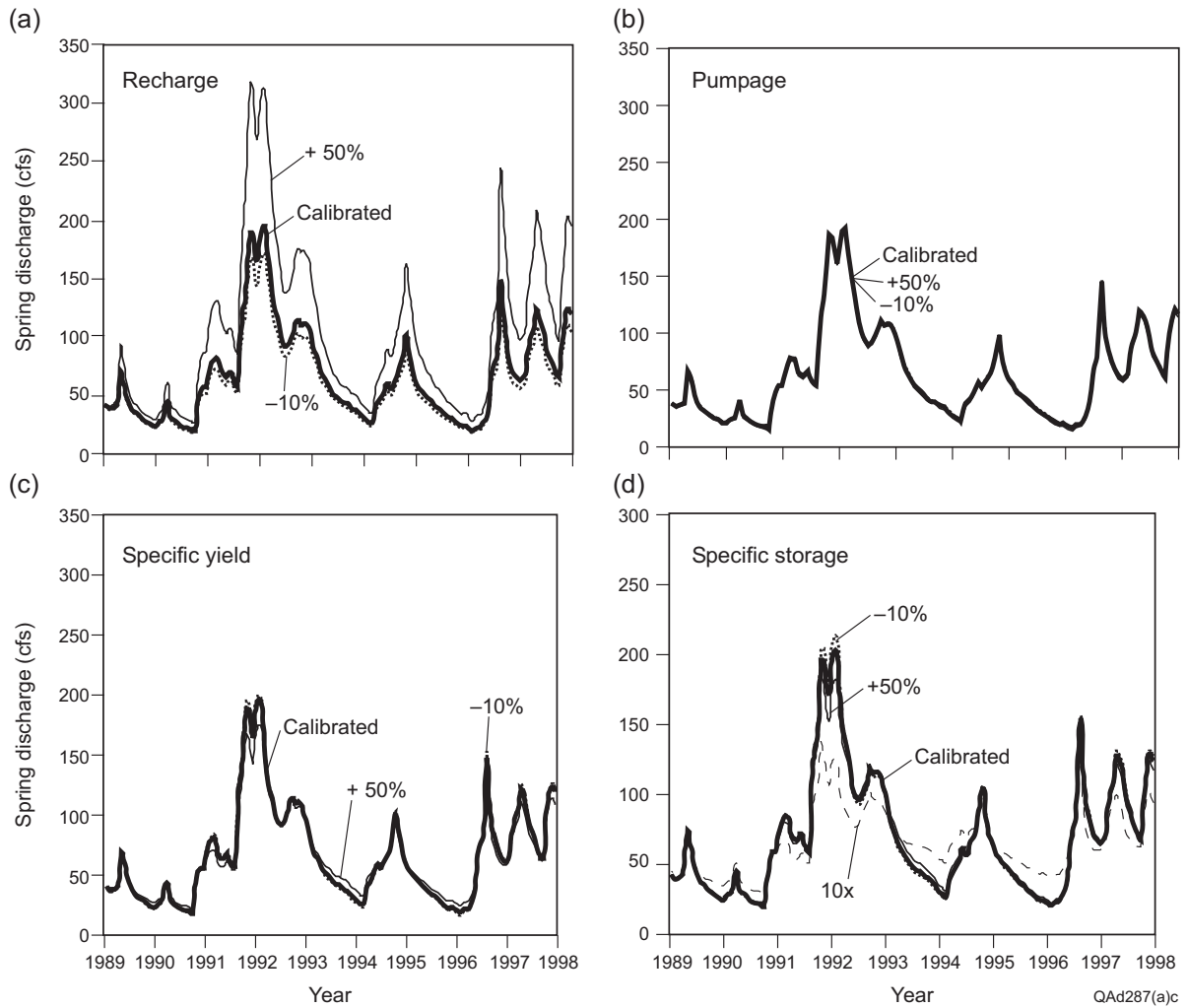


Figure 41. Sensitivity of the transient simulated spring discharge to (a) recharge, (b) pumpage, (c) specific yield, and (d) specific storage.

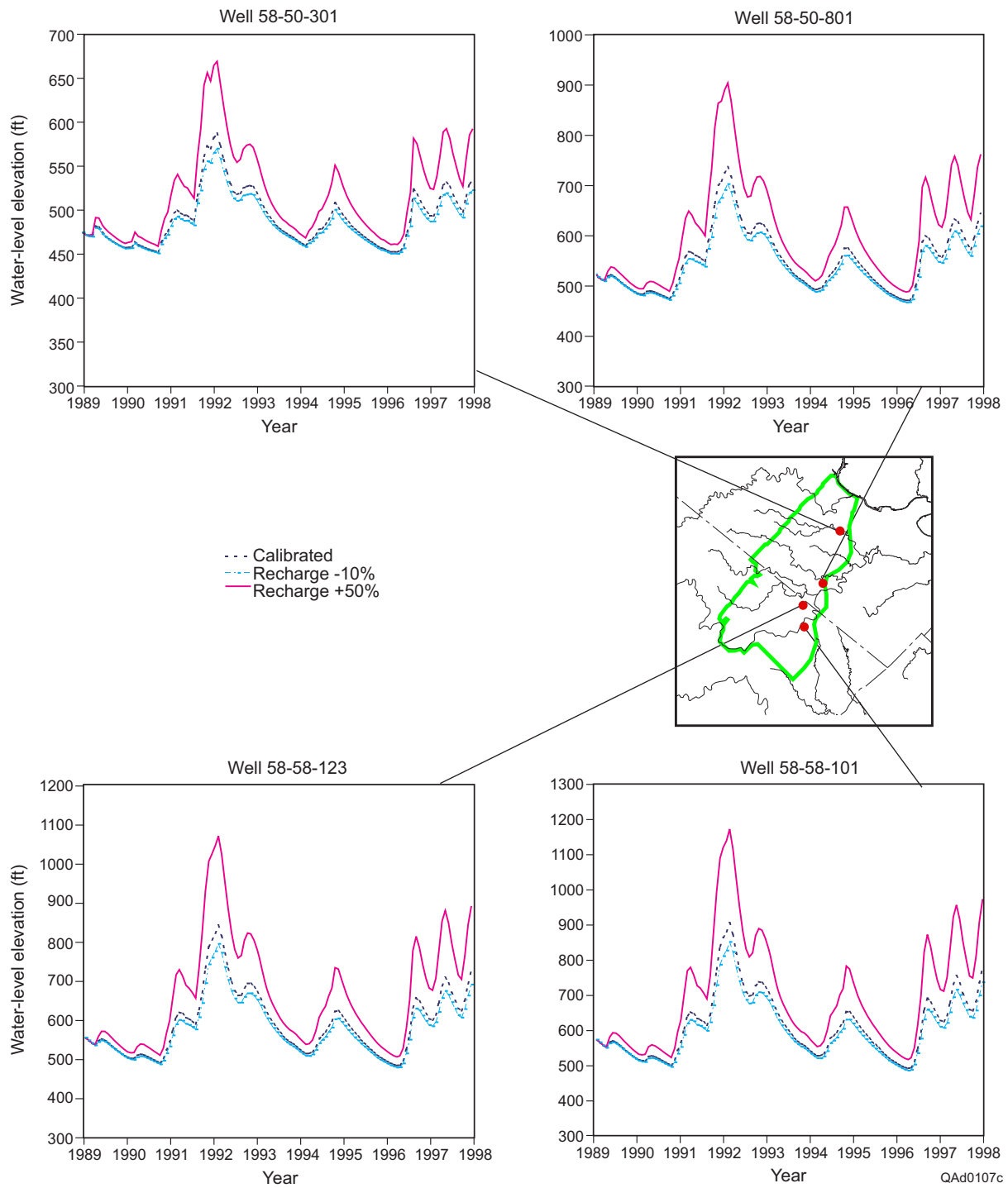


Figure 42. Sensitivity of the transient simulated water levels to recharge.

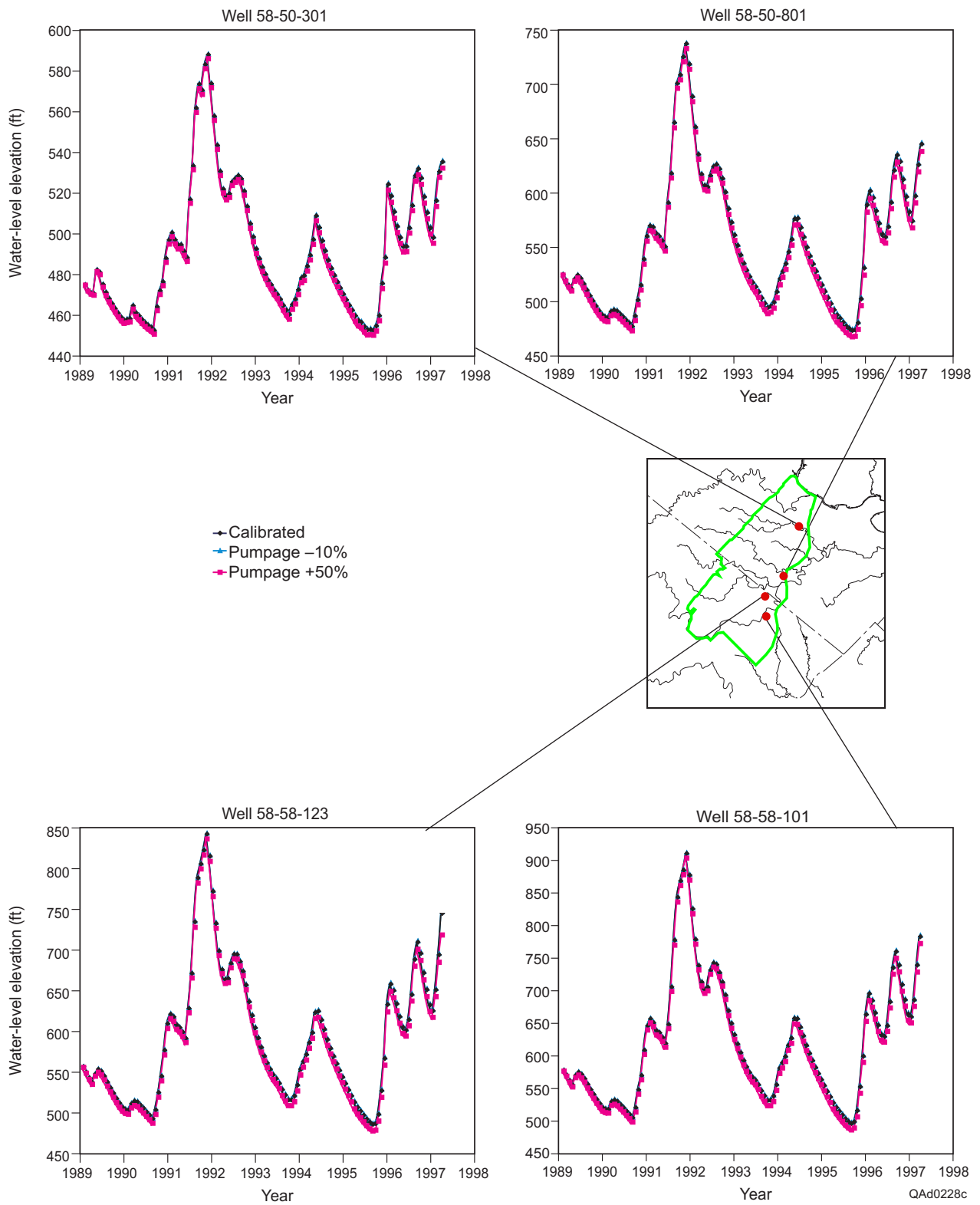


Figure 43. Sensitivity of the transient simulated water levels to pumpage.

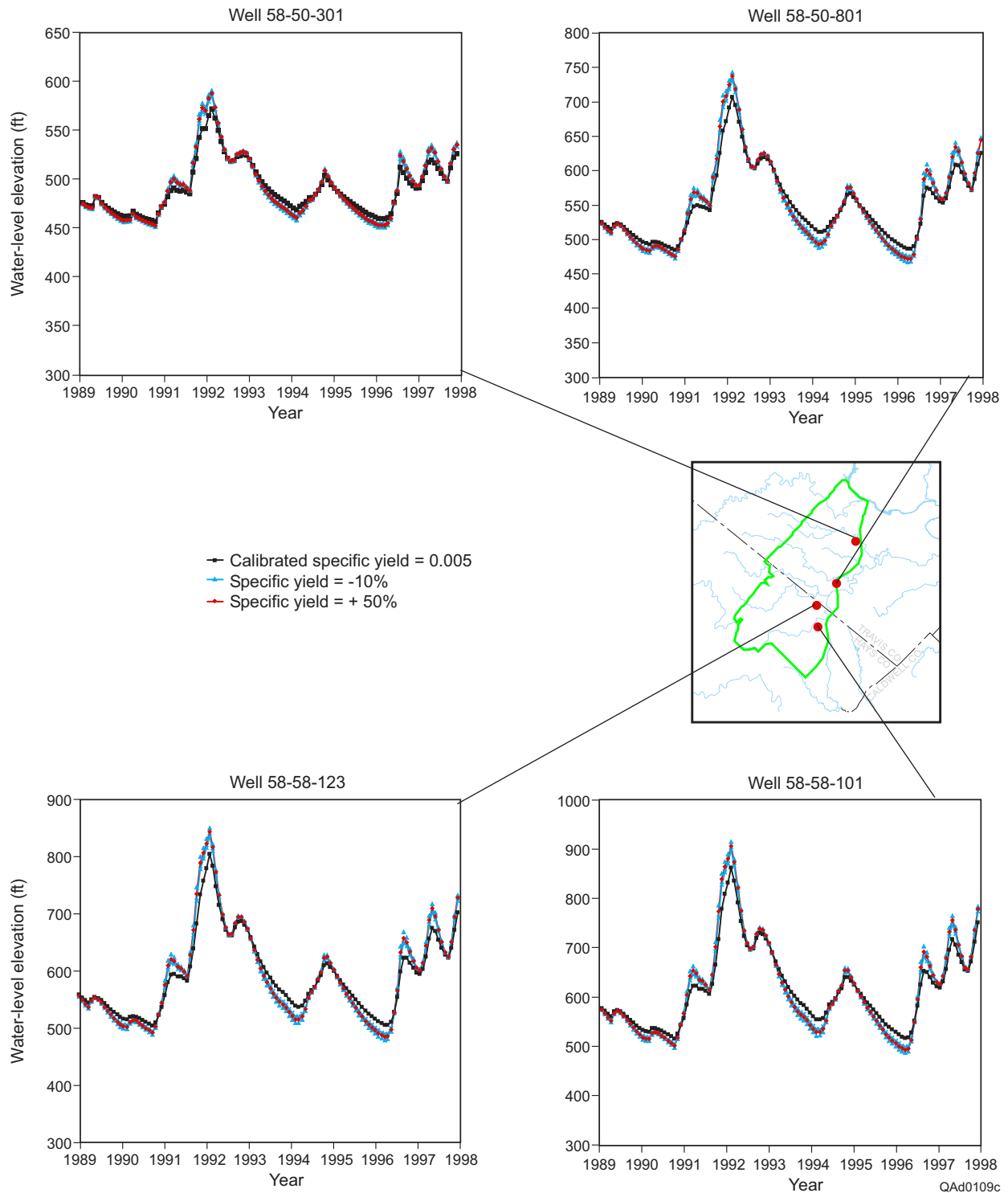


Figure 44. Sensitivity of the transient simulated water levels to specific yield.

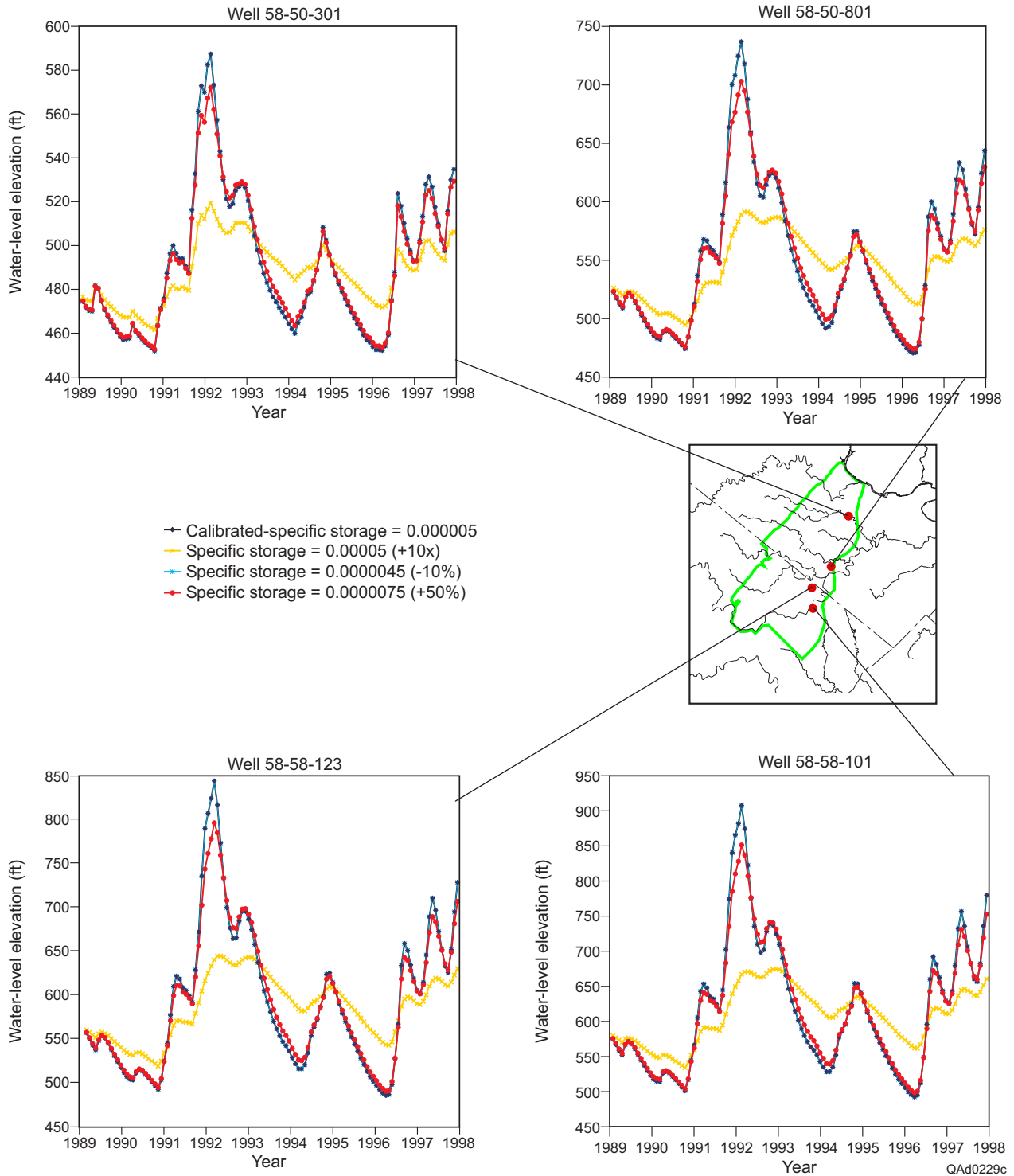


Figure 45. Sensitivity of the transient calibration water levels to specific storage.

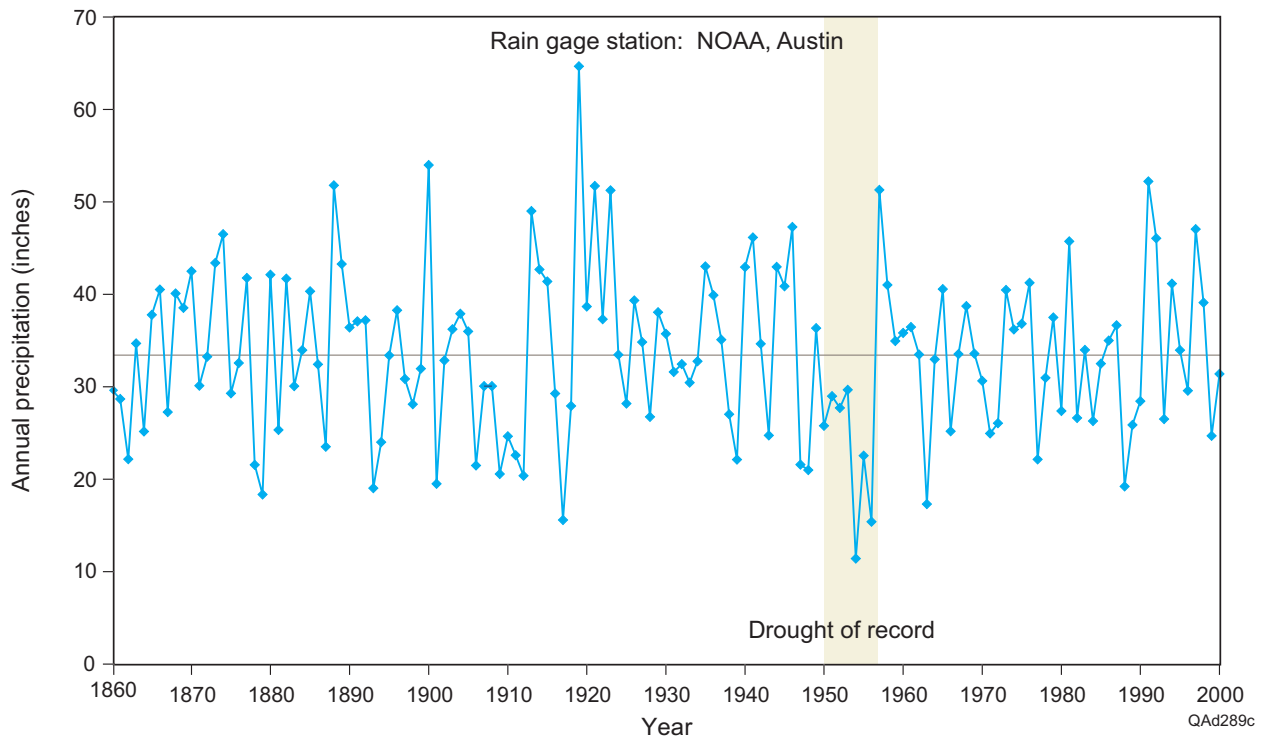


Figure 46. Precipitation from 1860 through 2000 measured at the rainfall gaging station in Camp Mabry and Mueller Airport in Austin (NOAA), showing the drought of record during the 1950's.

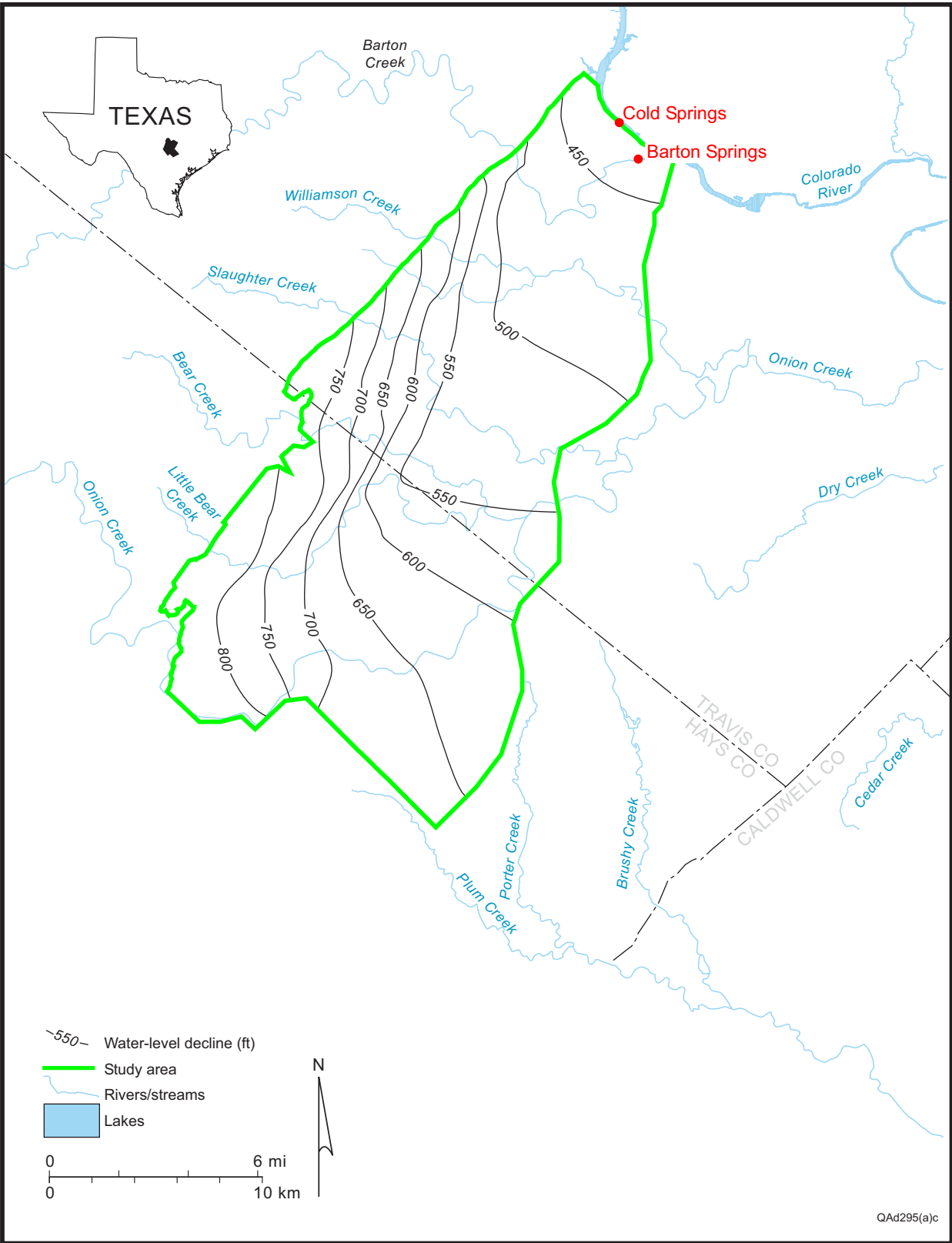


Figure 47. Baseline water levels based on average recharge (55 cfs) and current pumpage (2000) at the end of a 10-yr simulation for comparison with future simulations.

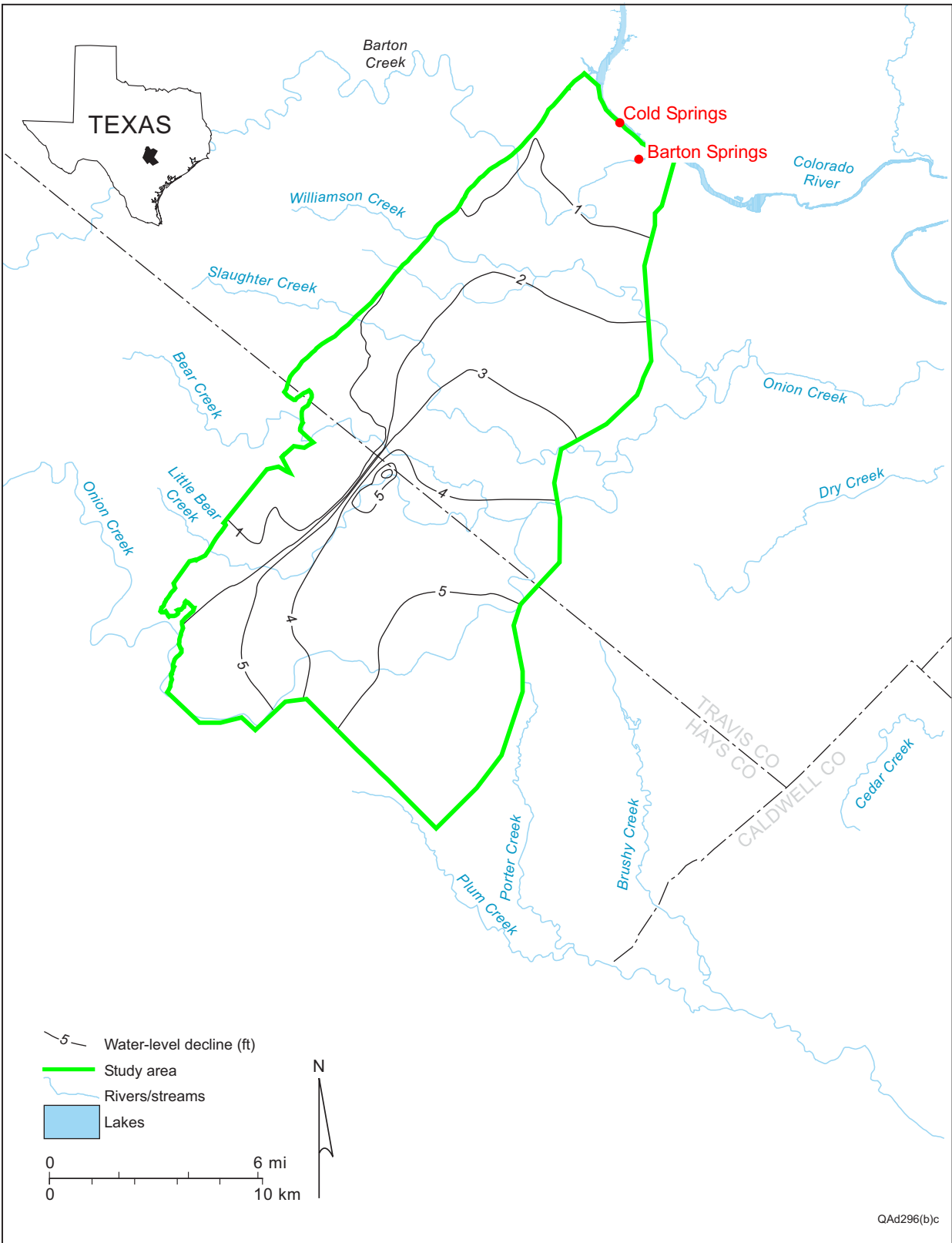


Figure 48(a). Simulated water-level declines in 2010 (relative to baseline water levels (Fig. 47)) using average recharge conditions through 2010.

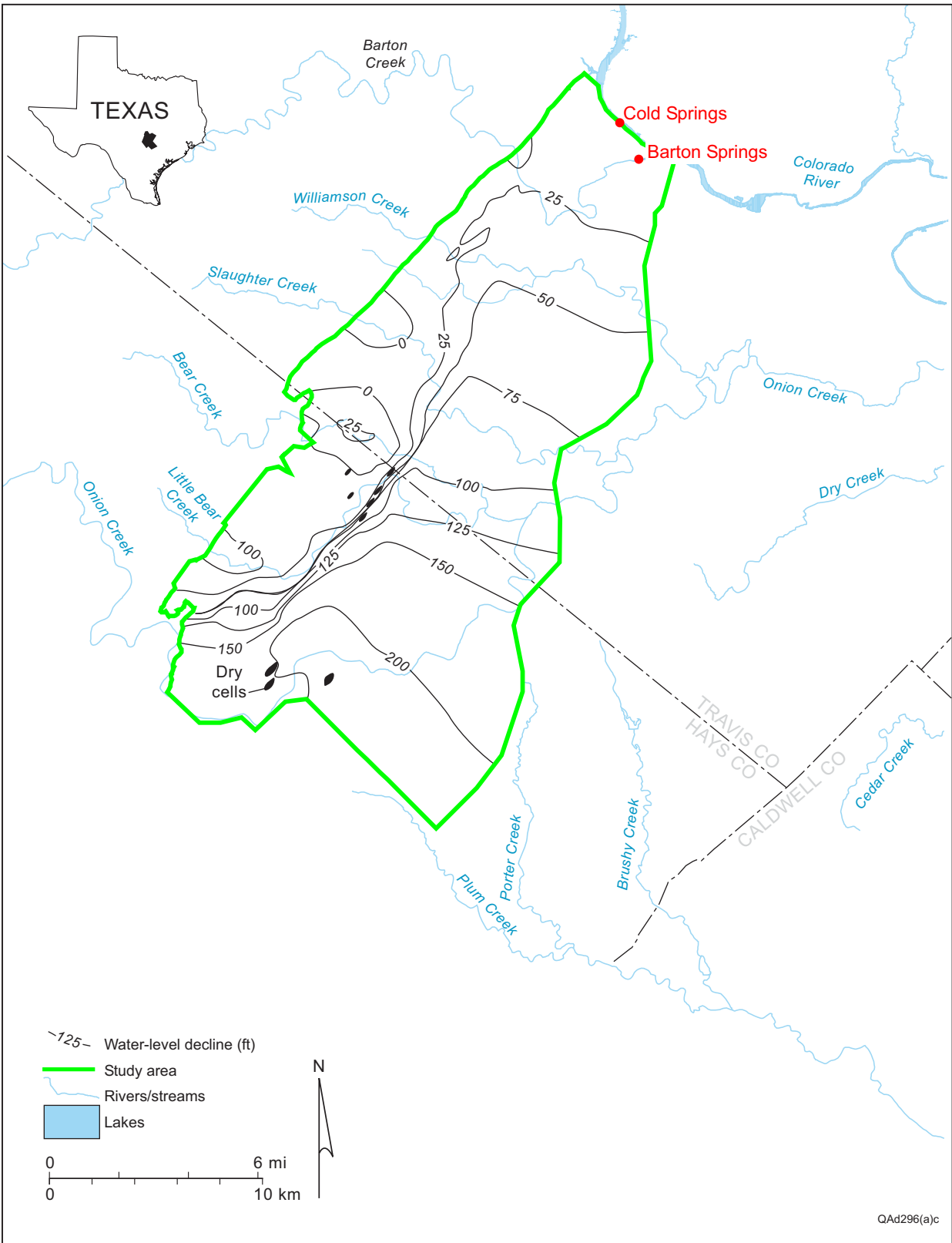


Figure 48(b). Simulated water-level declines in 2010 (relative to baseline water levels (Fig. 47)) using average recharge conditions through 2003 and drought-of-record recharge conditions from 2004 to 2010.

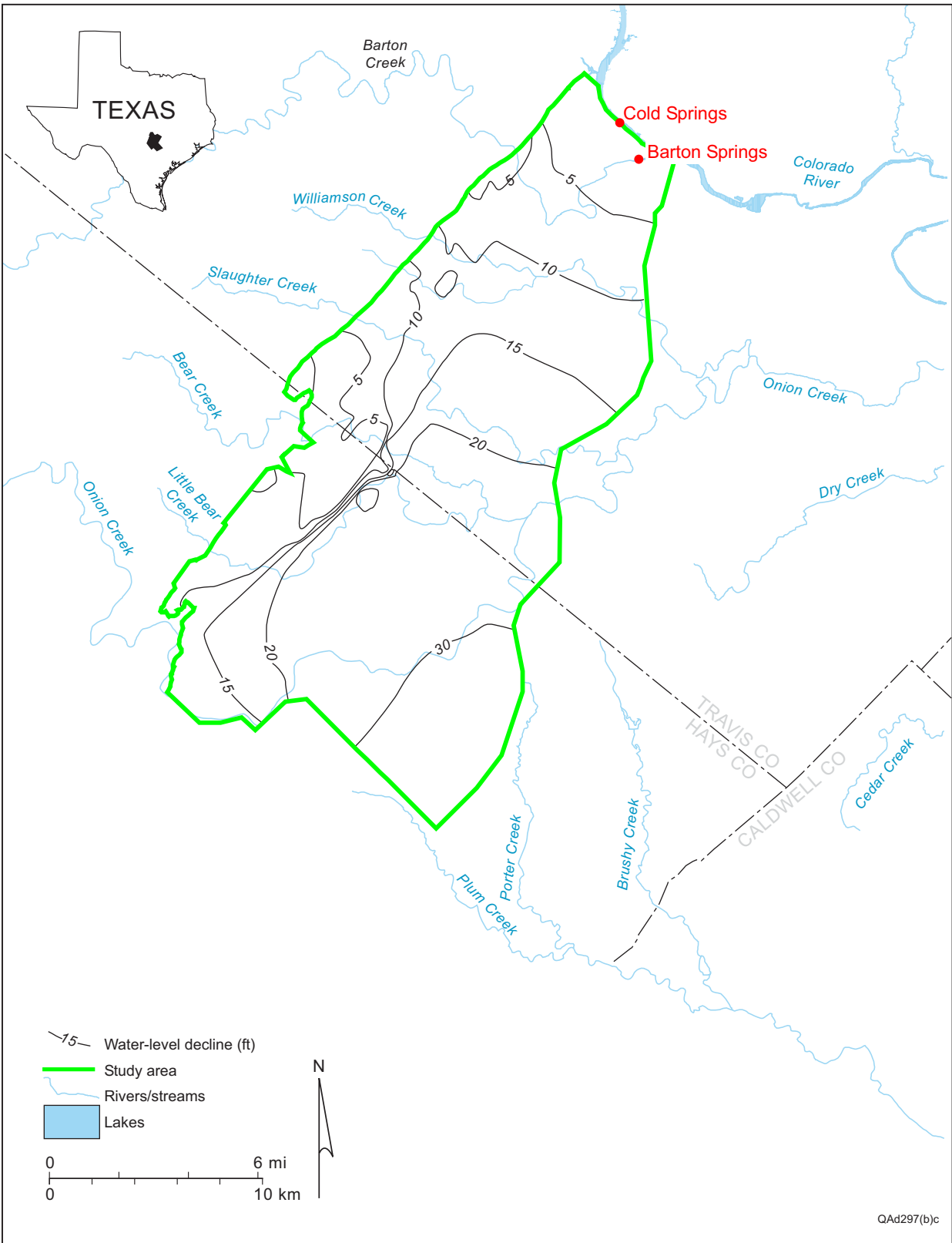
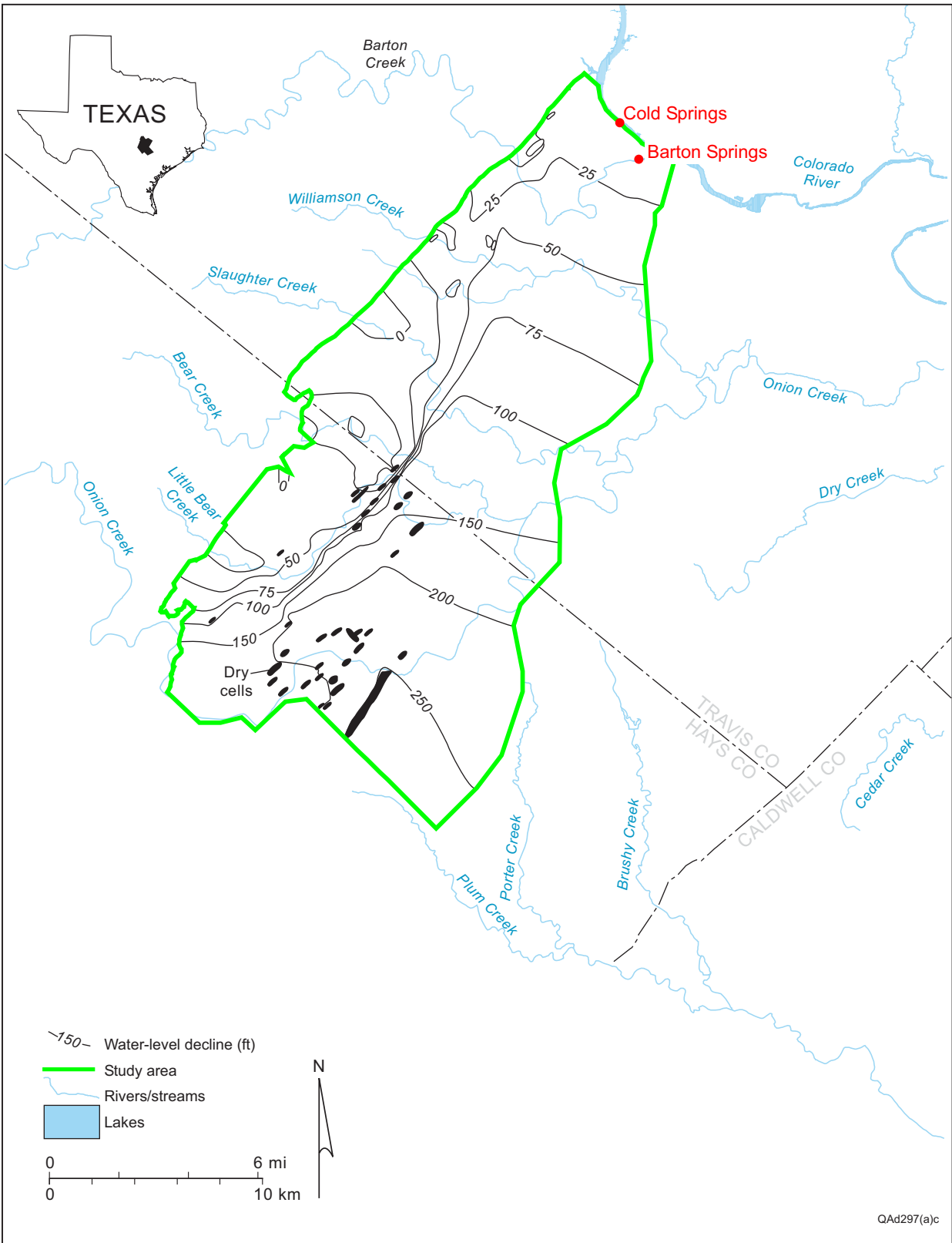


Figure 49(a). Simulated water-level declines in 2050 (relative to baseline water levels (Fig. 47)) using average recharge conditions through 2050.



QAd297(a)c

Figure 49(b). Simulated water-level declines in 2050 (relative to baseline water levels (Fig. 47)) using average recharge conditions through 2043 and drought-of-record recharge conditions from 2043 to 2050.

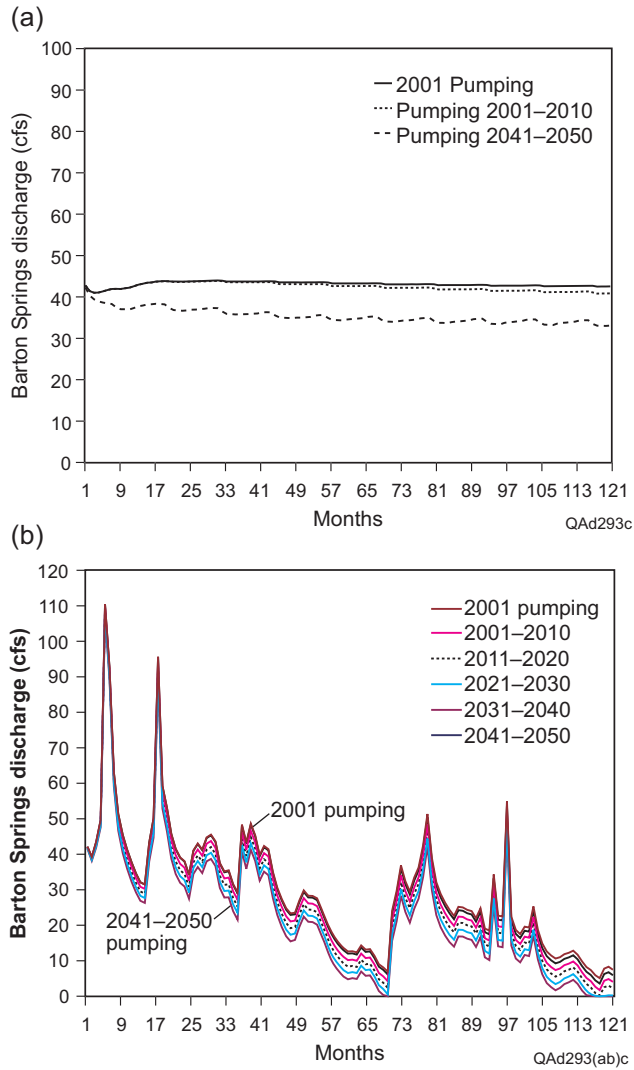


Figure 50. Simulated spring discharge for 10-yr periods using (a) average recharge conditions through 2050 and (b) average recharge conditions for the first three years and drought of record for the last seven years of each 10-yr period. The order in the legend reflects the vertical order in the line graphs.

Table 1. Stream-gauge data, including location, length of record, and maximum recharge.

Creek name	Station no.	Latitude/longitude	Upstream/downstream	Length of gauging record	Maximum recharge (ft ³ /s)
Barton (Lost Creek)	8155240	301626,0975040	Upstream	12/28/88–9/30/98	250
Barton (Loop 360)	8155300	301440, 0974807	Downstream	2/1/77–12/29/98	
Williamson Creek	8158920	301406, 975136	Upstream	12/29/93	13
Williamson Creek	8158922	301334,0975228	Upstream	3/1/93–12/29/98	
Slaughter Creek	8158840	301232,0975411		1/1/78–12/29/98	52
Bear Creek	8158810	300919,09752623		7/1/79–12/29/98	66
Onion Creek (Drift)	8158700	300458,0980027	Upstream	7/1/79–12/29/98	120
Onion Creek (Buda)	8158800	300509,975052	Downstream	7/1/79–9/30/83	

Table 2. Distribution of recharge among creeks calculated from daily data from 1/1/1980 through 12/31/1998.

	Recharge (ft ³ /yr)	Total creek recharge (%)
Barton Creek	6.35E+08	29
Williamson Creek	4.95E+07	2
Slaughter Creek	1.22E+08	5
Bear and Little Bear Creeks	4.19E+08	19
Onion Creek	1.00E+09	45
Total	2.23E+09	100

Table 3. Statistical summary of hydraulic conductivity values for the Barton Springs segment of the Edwards aquifer.

n	p ₂₅	p ₅₀	p ₇₅	x _g	x _{g+s}	x _{g-s}	s ²
24	1.3	4.9	13.8	0.6	1.4	-0.2	0.6

n—number of points

p₂₅— 25th percentile (medial) (ft/d)

p₅₀—50th percentile (median) (ft/d)

p₇₅—75th percentile (median) (ft/d)

x_g—geometric mean

x_{g-s}—geometric mean minus a standard deviation (ft/d)

x_{g+s}—geometric mean plus a standard deviation

s²—variance (log[ft/d])²

Standard deviations are calculated from the log-normal distribution.

Table 4. Annual precipitation, recharge, pumpage, and number of reported users for the transient simulation (1989 through 1998) and predicted recharge for average conditions (2041 through 2043) and potential future drought (2044 through 2050) estimated from the 1950's drought for the future simulations.

Time (yr)	Precipitation (inches)	Recharge (cfs)	Pumpage (reported + domestic) (cfs)	Pumpage as % of recharge	Number of users
1989	25.87	28.84	5.11	18	100
1990	28.44	20.91	3.88	19	103
1991	52.21	140.98	3.92	3	116
1992	46.05	168.56	4.57	3	126
1993	26.5	66.07	5.41	8	129
1994	41.16	33.38	5.23	16	131
1995	33.97	82.86	5.29	6	136
1996	29.58	4.15	5.73	138	139
1997	47.06	127.39	5.56	4	140
1998	39.11	153.45	6.29	4	142

Table 5. Sensitivity of transient spring discharge to variations in recharge, pumpage, specific yield, and specific storage.

	Mean (cfs)	Minimum (cfs)	Maximum (cfs)	Range (cfs)	Coefficient of variation
Calibrated value	67.6	19	196	177	0.61
Recharge (-10%)	60.8	18	172	154	0.59
Recharge (50%)	102.7	26	319	293	0.68
Pumpage (-10%)	68.1	20	197	178	0.61
Pumpage (+50%)	65.4	17	194	177	0.63
Specific yield (-10%)	67.9	18	200	182	0.63
Specific yield (+50%)	66.5	23	177	154	0.52
Specific storage (-10%)	67.8	19	207	188	0.63
Specific storage (+50%)	67.1	20	178	158	0.56
Specific storage (10x)	64.2	28	133	105	0.35

Table 6. Water budget for the calibrated steady-state, transient, and predictive runs. All values are in cubic feet per second (cfs).

Model Run	Recharge	Wells	Springs	Storage
	cfs	cfs	cfs	cfs
Steady State	60.0	-5.1	-54.8	NA
Transient 89-98	82.7	-5.1	-71.9	5.7
2010	13.5	-11.2	-7.6	-5.3
2020	13.5	-13.2	-5.8	-5.5
2030	13.5	-15.3	-4.1	-5.9
2040	13.5	-17.3	-2.3	-6.1
2050	13.5	-19.4	-1.5	-7.4
2010 (no drought)	55.0	-11.2	-41.1	2.7
2050 (no drought)	55.0	-19.4	-33.7	1.9

To convert cfs to acre-ft/yr, multiply by 723.97

A positive sign indicates additions to the water budget and negative signs indicate removals.

Numbers represent fluxes for the year listed. The transient calibration model represents the average flux for 1989 – 1998.

ATTACHMENT 1

TEXAS WATER DEVELOPMENT BOARD

Review of the draft Final Report: Contract No. 2001-483-399

“Groundwater Availability of the Barton Springs Segment of the Edwards Aquifer,
Texas: Numerical Simulations through 2050:

Board staff offers the following comments:

1. Report is well written and easy to read and understand
2. Cover page, need to note that Brian Smith is with BSEACD.

Brian Smith’s affiliation has been noted on the cover page.

3. Page 2, 1st and 3rd sentence: It would be clearer if Barton Springs pool was defined and then described.

Sentences reordered to clarify meaning.

4. Page 2, paragraph 2: “in a computer” does not seem like correct terminology, perhaps “using” or some other word would be more appropriate.

Changed in a computer to using a computer.

5. Page 2, paragraph 2, 2nd sentence: Calibrated is introduced here but it is unclear what it means.

Model calibration is a standard process in modeling and is explained in detail in the Methods section

6. Page 3, paragraph 1, 1st sentence: The statement “(1,000 x 500 versus a minimum of 1,500 ft)” does not seem to be parallel and is hard to understand. Whether it means 500,000 vs 1500 or 1000 versus 1500 or something else entirely is not clear.

Changed sentence to indicate that minimum cell spacing of 500 ft versus 1,500 ft.

7. Page 4, geology section (and many places afterward): Comment on aquifer nomenclature. TWDB calls the aquifer the Edwards (Balcones Fault Zone) aquifer. This aquifer consists of three segments: the San Antonio segment, the Barton Springs segment, and the northern segment. In the report, you refer to the San Antonio segment as the Balcones Fault Zone segment.

Balcones Fault Zone segment renamed the San Antonio segment throughout.

8. Page 10, paragraph 4: This statement seems to compare a description “stratigraphic thickness” to a process “thinning as a result of normal faulting” to each other and is hard to understand.

Changed thinning to reduction in thickness.

9. Page 21, paragraph 1, equation 1: The m in hm needs to be a subscript. The i in hi should be a subscript s according to the equation.

Changes made.

10. Page 21, RMS equation: Explanation of terms in the text is inconsistent with the equation 1.

Explanation corrected to correspond to equation.

11. Page 26, paragraph 1: The use of the word recession here is confusing. Perhaps a definition should be included.

The term recession is replaced with low-flow period.

12. Page 29, Drought of Record: “1960 through 2000’ should be 1860 through 2000’.

Change made.

13. Figures difficult to impossible to read without being in color. Impossible to address now, but will need to be looked at in Final Report.

Color figures included in report where it was difficult to decipher material in black and white.

14. Please include a budget table in the Final Report

Table included.

APPENDIX B

SENSITIVITY ANALYSIS OF SOUTHERN GROUNDWATER DIVIDE

The 2001 GAM (Scanlon et al., 2001, Appendix A) and the recalibrated GAM, described in this report, simulate the groundwater divide between the Barton Springs segment and the San Antonio segment of the Edwards Aquifer as a no-flow boundary. Groundwater divides are commonly simulated in numerical models as no-flow boundaries (Chiang and Kinzelbach, 2001; Cleary et al., 2001). To test the assumption that a no-flow boundary adequately simulates this aquifer, a sensitivity analysis was conducted by comparing the recalibrated GAM with a no-flow boundary to the recalibrated GAM with constant-head and general-head boundaries. The influence of these different boundary conditions and pumping rates on water levels was evaluated in this sensitivity analysis. Results of this analysis show that water levels will either increase or decrease, relative to the results of the recalibrated GAM, depending on water levels and hydraulic conductivity values set at the boundary. The most realistic scenario tested, which uses a general-head boundary, indicates that the increase in water levels is small compared with water levels from the recalibrated GAM with a no-flow boundary. Conditions simulated by the general-head boundary are more realistic than the constant-head boundary. Using a flow boundary for the southern boundary of the model could marginally improve the model, but additional data, such as pumping rates, water levels, and hydraulic conductivity, from the northern part of the San Antonio aquifer are needed to incorporate into the recalibrated GAM.

Boundary Changes

Scenarios were run with various conditions for the southern boundary of the model area. Figure B1 shows the part of the boundary that was modified for the sensitivity analysis. The no-flow boundary used in the 2001 GAM (Scanlon et al., 2001, Appendix A) and the recalibrated GAM was changed to constant-head and general-head boundaries for this analysis.

Constant-Head Boundary Conditions

Constant-head boundaries are used in numerical models to simulate a boundary at which water levels remain constant throughout the model run, allowing water to flow into or out of the model area, depending on relative water levels within the model area. A constant-head boundary provides an inexhaustible supply or sink of water (Chiang and Kinzelbach, 2001). Table B1

summarizes changes that were made to the recalibrated model to test the sensitivity of the groundwater divide to various boundary conditions. A constant-head boundary was set for model simulations Mod1 and Mod3 using water levels set to low levels of the 1950's drought (Slade et al., 1986).

General-Head Boundary Conditions

General-head boundaries allow flow to take place across the boundary, but the amount of flow is regulated by the water level that is set for a point or boundary at some distance outside the model area and by the conductance that is set for the area between the actual model boundary and the distant point or boundary. A general-head boundary was used in Mod2 and Mod4 with a water level of 574 ft above mean sea level (msl), which represents the elevation of the lake at San Marcos Springs. A conductance value of 112 ft²/day was used for the general-head boundary on the basis of the distance of 80,000 ft from the model boundary to San Marcos Springs, the cross-sectional area of a model cell of 225,000 ft², and hydraulic conductivity of 40 ft/day. The formula to calculate conductance is:

$$C = K A / L$$

where

C = conductance of general-head boundary

K = hydraulic conductivity

A = cross-sectional area of a cell

L = distance of actual boundary to domain boundary

(Cleary et al., 2001)

Pumping Scenarios

Constant-head and general-head boundary model runs were made using low- and high-pumping scenarios to determine effects of flow and no-flow boundaries on water levels on the southeastern part of the model area.

Brune and Duffin (1983) estimated that pumping from the aquifer was about 0.66 cfs during the 1950's drought of record. To test the sensitivity of the southern model boundary to 1950's drought conditions, two scenarios (Mod1 and Mod2) were run with a pumping rate of 0.66 cfs.

The District estimates that permitted groundwater pumping plus exempt well pumping in 2004 is 10.8 cfs. To test the sensitivity of the southern model boundary to current pumping conditions, two scenarios (Mod3 and Mod4) were run with a pumping rate of 10 cfs.

Results of Sensitivity Analysis

Six model runs were made for the sensitivity analysis of the southern groundwater divide (Table B1). Water-level values from the recalibrated GAM were compared with water levels from the different boundary and pumping scenarios.

To determine the relative impacts of modified boundary conditions on water levels, water-level values from the recalibrated GAM were subtracted from water levels simulated in the scenarios with modified boundary conditions. Table B1 shows water-level differences for selected cells along a southwest-northeast transect (Figure B1) of the southern model area. Two cross sections (Figures B2 and B3) show water-level differences for each cell along this transect. The magnitude of water-level changes decreases away from the modified boundary. Water-level changes are less than 1 ft in the cells within 1,000 ft of Barton Springs.

At a low pumping rate (0.66 cfs), water levels from the constant-head and general-head boundary scenarios are slightly lower than water levels from the recalibrated GAM (Figure B2). At cell 32,77, water levels are 10 ft and 25 ft lower in Mod1 and Mod2, respectively, than in the recalibrated GAM.

At a high pumping rate (10 cfs), water levels from the constant-head and general-head boundary scenarios are greater than in the recalibrated GAM (Figure B3). At cell 32,77, water levels are 22 ft and 90 ft higher in Mod4 and Mod3, respectively, than in the recalibrated GAM.

Discussion of Results

As shown in Table B1 and Figures B2 and B3, water-level changes are small in scenarios with low rates of pumping (Mod1, and Mod2) compared with the scenario with a high rate of pumping (Mod3). Water-level changes in Mod4 are small compared with Mod3.

Mod3, with a constant-head boundary, simulates 1950's drought conditions north and south of the divide, but does not consider drawdown from pumping south of the divide, and therefore is unrealistic. Mod4 is the most realistic of all the scenarios tested as part of this sensitivity analysis. Mod4, with a general-head boundary set to the elevation of San Marcos Springs, allows for water levels to vary at the boundary, which can occur owing to pumping of wells south of the divide, discharge to San Marcos Springs, and climatic conditions.

Judging from the well-impact evaluation described in Section 4 of this report, increases in water level of 22 ft (as simulated in Mod4) are unlikely to significantly reduce the number of wells that might be impacted by pumping and drought-of-record conditions.

Summary

Mod4, which incorporates current (2004) rates of pumping with drought-of-record conditions and a general-head boundary at the southern boundary of the model area, is the most realistic of the tested scenarios. Results of this simulation suggest that if the recalibrated GAM, currently being used by the District, was modified with a general-head boundary across a part of the southern model boundary, the potential for flow across the boundary could be addressed. Because of the small changes in water levels between Mod4 and the recalibrated GAM, model results for water levels in the model area would not improve significantly. Therefore, the recalibrated GAM, with a no-flow boundary, is an adequate model for simulating the Barton Springs aquifer. Future modeling of the Barton Springs aquifer should consider using a time-varying specified-head boundary for the southern boundary in addition to collection of hydrogeologic data near the groundwater divide. Water-level data from the USGS model for the San Antonio segment of the Edwards Aquifer (currently undergoing review) could be used to set water levels along the southern boundary.

REFERENCES

- Brune, Gunnar and Duffin, Gail, 1983, Occurrence, Availability, and Quality of Ground Water in Travis County, Texas: Texas Department of Water Resources, Report 276, 219 p.
- Chiang, W. H., and Kinzelbach, W., 2001, 3D-groundwater modeling with PMWIN: New York, Springer, 346 p.
- Cleary, R. W., Franz, T., and Guiguer, N., 2001, The MODFLOW Course: National Ground Water Association, November 6–8, Orlando, FL.
- Scanlon, B., Mace, R., Smith, B., Hovorka, S., Dutton, A., and Reedy, R., 2001, Groundwater Availability of the Barton Springs Segment of the Edwards Aquifer, Texas—Numerical Simulations through 2050: The University of Texas at Austin, Bureau of Economic Geology, final report prepared for the Lower Colorado River Authority, under contract no. UTA99-0, 36 p. + figs., tables, attachment.

Slade, Raymond, Jr., Dorsey, Michael, and Stewart, Sheree, 1986, Hydrology and Water Quality of the Edwards Aquifer Associated with Barton Springs in the Austin Area, Texas: U.S. Geological Survey Water-Resources Investigations, Report 86-4036, 117 p.

Table B1. Results of sensitivity analysis

Model version	Boundary type	Water levels at boundary	Pumping (cfs)	Barton Springs flow (cfs)	Water-level changes*		
					Cell 32,77	Cell 50,77	Cell 67,77
Recalibrated GAM	No flow	2001 GAM initial conditions	0.66	11.3			
Mod1	CHB	D-O-R conditions	0.66	9.7	-10	-14	-11
Mod2	GHB	San Marcos Springs	0.66	9.6	-25	-22	-14
Mod3	CHB	D-O-R conditions	10	5.6	+82	+57	+30
Mod4	GHB	San Marcos Springs	10	3.5	+22	+15	+7
Recalibrated GAM	No flow	2001 GAM initial conditions	10	1.1			

* Water-level changes are relative to corresponding results of recalibrated GAM (0.66 or 10 cfs of pumping) with a no-flow boundary.

D-O-R- Drought of record

CHB- Constant-head boundary; GHB- General-head boundary

Spring flow and water-level values are from Stress Period 117, which represents the lowest flows and water levels of the drought of record.

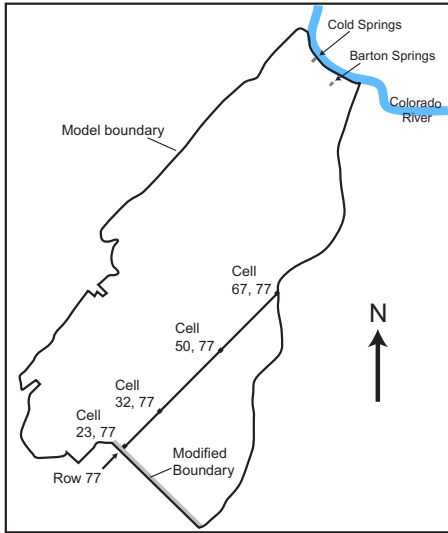


Figure B-1. Model area of the Barton Springs aquifer.

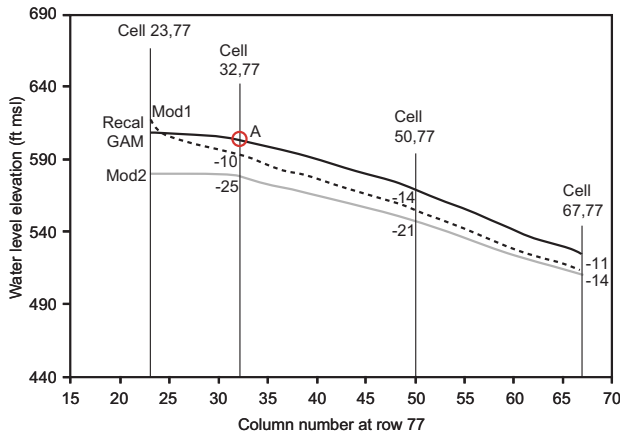


Figure B-2. Cross section of southeast model area with 0.66 cfs pumping scenarios. Head values are from stress period 117, time step 12.

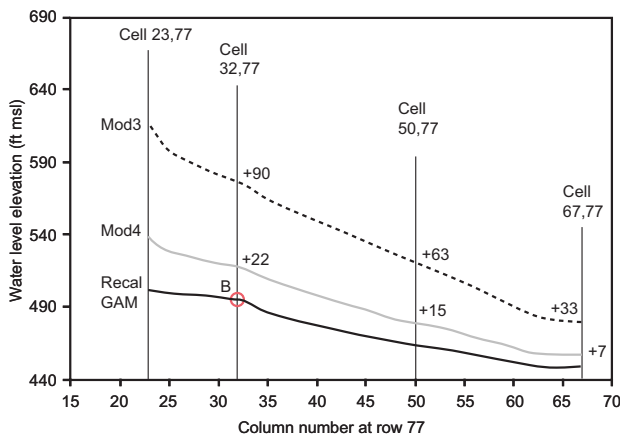


Figure B-3. Cross section of southeast model area with 10 cfs pumping scenarios. Head values are from stress period 117, time step 12.

APPENDIX C

LIST OF PARTICIPANTS AND AFFILIATIONS AT SUSTAINABLE YIELD MEETINGS AT THE BSEACD

September 10, 2003

Suzanne Pierce, UT Graduate Student	Robert Mace, TWDB
Larry Land, HDR Engineering	Nico Hauwert, City of Austin WPDRD
Rene Barker, USGS	David Johns, City of Austin, WPDRD
Rick Lindgren, USGS	Steve Musick, TCEQ
Raymond Slade, Consulting Hydrologist	Randy Williams, TC&B
Joe Vickers, Wellspec Co.	Ken Manning, LCRA
James Beach, LBG-Guyton Assoc.	Nadira Kabir, LCRA
Clarence Littlefield, Southwest Eng.	Ned Troshanov, EAA
Kaveh Khorzad, Wet Rock Groundwater	Marshall Jennings, EARDC
John Mikels, Geos Consulting	Lendon E. Gilpin, EARDC
Shirley Wade, TWDB	Bridget Scanlon, UTBEG

March 24, 2004

John Mikels, Geos Consulting	Ned Troshanov, EAA
Frank Del Castillo, PBS&J	Hugo Elizondo, Jr., Cuatro Consulting
Tricia Sebes, HDR Engineering	Nadira Kabir, LCRA
Larry Land, HDR Engineering	Brent Covert, LCRA
Joe Vickers, Wellspec Co.	Raymond Slade, Consulting Hydrologist
Roberto Anaya, TWDB	Suzanne Pierce, UT Graduate Student
Ian Jones, TWDB	Ron Green, CNWRA/SWRI
Andrew Backus, HTGCD	Robert Mace, TWDB
Randy Goss, LCRA	John Littlefield, Southwest Eng.
Phil Savoy, Murfee Engineering	Lauren Ross, Greater Edw. Aq. Alliance